DSWA-TR-97-66

Technical Report

COMBAT WEATHER SYSTEM MODEL SELECTION

Approved for public release; distribution is unlimited.

July 2000

Prepared for:
Defense Threat Reduction Agency
45045 Aviation Drive
Dulles, VA 20166-7517

DNA001-94-C-0096

Bruce L. Bauer, et. al,

Prepared by: Mission Research Corporation
6703 Odyssey Drive, Suite 101
Huntsville, AL 35806-3301

DESTRUCTION NOTICE:

Destroy this report when it is no longer needed. Do not return to sender.

PLEASE NOTIFY THE DEFENSE THREAT REDUCTION AGENCY, ATTN: ADM, 45045 AVIATION DRIVE, DULLES, VA 20166-7517, IF YOUR ADDRESS IS INCORRECT, IF YOU WISH IT DELETED FROM THE DISTRIBUTION LIST, OR IF THE ADDRESSEE IS NO LONGER EMPLOYED BY YOUR ORGANIZATION.

CUT HERE AND RETURN

DISTRIBUTION LIST UPDATE

This mailer is provided to enable DTRA to maintain current distribution lists for reports. (We would appreciate you providing the requested information.)

- ☐ Add the individual listed to your distribution list.
- ☐ Delete the cited organization/individual.
- ☐ Change of address.

Note:
Please return the mailing label from the document so that any additions, changes, corrections or deletions can be made easily. For distribution cancellation or more information call DTRA/ADM (703) 325-1036.

NAME: _____

ORGANIZATION: _____

OLD ADDRESS	NEW ADDRESS
_____	_____
_____	_____
_____	_____

TELEPHONE NUMBER: ( ) _____

DTRA PUBLICATION NUMBER/TITLE	CHANGES/DELETIONS/ADDITIONS, etc.) *(Attach Sheet if more Space is Required)*
_____	_____
_____	_____
_____	_____

DTRA or other GOVERNMENT CONTRACT NUMBER: _____

CERTIFICATION of NEED-TO-KNOW BY GOVERNMENT SPONSOR (if other than DTRA):

SPONSORING ORGANIZATION: _____

CONTRACTING OFFICER or REPRESENTATIVE: _____

SIGNATURE: _____

DEFENSE THREAT REDUCTION AGENCY
ATTN: ADM
45045 AVIATION DRIVE
DULLES, VA 20156-7517

DEFENSE THREAT REDUCTION AGENCY
ATTN: ADM
6801 TELEGRAPH ROAD
ALEXANDRIA, VA 22310-3398

REPORT DOCUMENTATION PAGE

Form Approved
OMB NO. 0704.0188

1. AGENCY USE ONLY *(Leave Blank)*	2. REPORT DATE	3. REPORT TYPE AND DATES COVERED
		Technical 940725 - 970724

4. TITLE AND SUBTITLE
Combat Weather System Model Selection

5. FUNDING NUMBERS
C - DNA001-94-C-0096
PE – 62715H
PR – AC
TA – BA
WU – DH00113

6. AUTHOR(s):
Bruce L. Bauer, Craig J. Tremback, Michael J. Weissbluth, Thomas M. Myers, Jeffrey A. Shorter, Precilia C. Ip, Theresa Campbell (MRC) and Hershel A. Rabitz (PU)

7. PERFORMING ORGANIZATION NAME(S) AND ADDRESS(ES)
Mission Research Corporation
6703 Odyssey Drive, Suite 101
Huntsville, AL 35806

8. PERFORMING ORGANIZATION REPORT NUMBER
MRC-HSV-97-R-003

9. SPONSORING/MONITORING AGENCY NAME(S) AND ADDRESS(ES)
Defense Threat Reduction Agency
45045 Aviation Drive
Dulles, VA 20166-7517

CPWT/Smith

10. SPONSORING/MONITORING AGENCY REPORT NUMBER
DSWA-TR-97-66

11. SUPPLEMENTARY NOTES
This work was sponsored by the Defense Special Weapons Agency under RDT&E RMC Code B 4662 D BA 00113 4400 A AC 25904 D.

12a. DISTRIBUTION/AVAILABILITY STATEMENT
Approved for public release; distribution is unlimited.

12b. DISTRIBUTION CODE

13. ABSTRACT *(Maximum 200 words)*

This report documents the effort to identify a candidate numerical weather prediction model, suitable for theater use, from currently available off-the-shelf mesoscale models. The candidate models were the Mesoscale Model Version 5 (MM5), the Navy Operational Regional Atmospheric Prediction System Version 6 (NORAPS6), and the Regional Atmospheric Modeling System (RAMS). The Air Force (AF) regional forecast model, the Relocatable Window Model (RWM) was the baseline against which the other models were evaluated. Based on the model comparison, DSWA chose to use RAMS to provide high resolution meteorological forecasts for its transport and diffusion program. The report also describes the subsequent adaptation and application of this model to actual field tests. This report is divided into three parts to document this process. Part 1 describes the model comparison. Part 2 describes our efforts to reduce the execution time required for a given forecast and enhance the forecast accuracy in complex terrain. Part 3 documents the use of RAMS during numerous field tests at White Sands Missile Range in support of the transport and diffusion tests.

14. SUBJECT TERMS
Computer Models; Weather Forecasting; Meteorology; Hazard Prediction; Mesoscale Model 5; Relocatable Window Model; Regional Atmospheric Modeling System; Navy Operational Regional Atmospheric Prediction Version 6

15. NUMBER OF PAGES

16. PRICE CODE

17. SECURITY CLASSIFICATION OF REPORT	18. SECURITY CLASSIFICATION OF THIS PAGE	19. SECURITY CLASSIFICATION OF ABSTRACT	20. LIMITATION OF ABSTRACT
UNCLASSIFIED	UNCLASSIFIED	UNCLASSIFIED	SAR

CLASSIFIED BY: N/A since Unclassified

DECLASSIFY ON: N/A since Unclassified

7. Performing Organization Name(s) and Address(es) (Continued)
Princeton University
129 Frick Lab
Princeton, NJ 08544

SUMMARY

This report documents the effort to identify a candidate numerical weather prediction model, suitable for theater use, from currently available off-the-shelf mesoscale models. The candidate models were the Mesoscale Model Version 5 (MM5), the Navy Operational Regional Atmospheric Prediction System Version 6 (NORAPS6), and the Regional Atmospheric Modeling System (RAMS). The Air Force (AF) regional forecast model, the Relocatable Window Model (RWM) was the baseline against which the other models were evaluated. Based on the model comparison, DSWA chose to use RAMS to provide high resolution meteorological forecasts for its transport and diffusion program. The report also describes the subsequent adaptation and application of this model to actual field tests. This report is functionally divided into three parts to document this process.

The first part of the report (Sections 1-5) describes, in detail, the model comparison process. It begins with a description of the requirements that were used to develop the comparison criteria. As the forecast model was to be used in the field this consisted of a set of parameters such as run time goals, grid size, and spacing that were to be used. In addition, a number of test cases were defined to exercise the models in a number of different situations. Specifically, the model comparison included two data sets in Alaska, Central America, the Middle East, and Korea. The initial comparison case was located in the Continental United States (CONUS). The meteorological data sets were obtained from the National Center for Atmospheric Research (NCAR) and from the Air Force Global Weather Central (AFGWC). The comparison of the performance of the models was accomplished through a number of statistical measures. The ranking of the models was consistent. RAMS was first, followed closely by MM5. -

The next part (Section 6) reports on efforts to adapt the RAMS model to operational forecasting. The primary goal of the effort described in this portion of the report was to reduce the execution time required for a given forecast. Major reductions in run-time were accomplished by using the new parallel computer systems such as the IBM SP-2 or HP Exemplar. This adaptation built on earlier work using parallel clusters of independent workstations and resulted in significant run-time reductions. In addition, the possibility of using a technique called the Fully Equivalent Operational Model (FEOM) was explored as a potential means of improving model performance without laborious recoding. The proof of concept used the radiative transport module from RAMS in one configuration. The FEOM equivalent ran a thousand times faster with an accuracy difference of less than one tenth of a percent. Finally, this section describes the exploration of a new scheme for computation of gradients in models using a terrain following coordinate system. The use of this code improved the forecast of plume dispersion from the test at WSMR.

The final part (Section 7) documents the use of RAMS during numerous field tests at White Sands Missile Range in support of the transport and diffusion tests. The support for these tests resulted in a better user interface and the integration of RAMS output with DSWA's SCIPUFF dispersion model.

CONVERSION TABLE

Conversion Factors for U.S. Customary to Metric (SI) Units of Measurement		
MULTIPLY → TO GET ←	BY → BY ←	TO GET DIVIDE
angstrom	1.000 000 X E-10	meters (m)
atmosphere (normal)	1.013 25 X E+2	kilo pascal (kPa)
bar	1.000 000 X E+2	kilo pascal (kPa)
barn	1.000 000 X E-28	meter^2 (m^2)
British thermal unit (thermochemical)	1.054 350 X E+3	joule (J)
calorie (thermochemical)	4.184 000	joule (J)
cal (thermochemical)/cm^2	4.184 000 X E-2	mega joule/m^2 (MJ/m^2)
curie	3.700 000 X E+1	giga becquerel (GBq)*
degree (angle)	1.745 329 X E-2	radian (rad)
degree Fahrenheit	$t_K = (t^oF+459.67)/1.8$	degree kelvin (K)
electron volt	1.602 19 X E-19	joule (J)
erg	1.000 000 X E-7	joule (J)
erg/second	1.000 000 X E-7	watt (W)
foot	3.048 000 X E-1	meter (m)
foot-pound-force	1.355 8818	joule (J)
gallon (U.S. liquid)	3.785 412 X E-3	meter3 (m^3)
inch	2.540 000 X E-2	meter (m)
jerk	1.000 000 X E+9	joule (J)
joule/kilogram (J/kg) (radiation dose absorbed)	1.000 000	Gray (Gy)
kilotons	4.183	terajoules
kip (1000 lbf)	4.448 222 X E+3	newton (N)
kip/inch^2 (ksi)	6.894 757 X E+3	kilo pascal (kPa)
ktap	1.000 000 X E+2	newton-second/m^2 (N-s/m^2)
micron	1.000 000 X E-6	meter (m)
mil	2.540 000 X E-5	meter (m)
mile (international)	1.609 344 X E+3	meter (m)
ounce	2.834 952 X E-2	kilogram (kg)
pound-force (lbs avoirdupois)	4.448 222	newton (N)
pound-force inch	1.129 848 X E-1	newton-meter (N-m)
pound-force/inch	1.751 268 X E+2	newton/meter (N/m)
pound-force/foot^2	4.788 026 X E-2	kilo pascal (kPa)
pound-force/inch^2 (psi)	6.894 757	kilo pascal (kPa)
pound-mass (lbm avoirdupois)	4.535 924 X E-1	kilogram (kg)
pound-mass-foot^2 (moment of inertia)	4.214 011 X E-2	kilogram-meter^2 (kg-m^2)
pound-mass-foot^3	1.601 846 X E+1	kilogram/meter^3 (kg/m^3)
rad (radiation dose absorbed)	1.000 000 X E-2	Gray (Gy)**
roentgen	2.579 760 X E-4	coulomb/kilogram (C/kg)
shake	1.000 000 X E-8	second (s)
slug	1.459 390 X E+1	kilogram (kg)
torr (mmHg, 0°C)	1.333 22 X E-1	kilo pascal (kPa)

* The becquerel (Bq) is the SI unit of radioactivity; 1 Bq = 1 event/s.
** The Gray (Gy) is the SI unit of absorbed radiation.

TABLE OF CONTENTS

TABLE OF CONTENTS (Continued)

FIGURES

FIGURES (Continued)

FIGURES (Continued)

TABLES

TABLES (Continued)

SECTION 1
MODEL COMPARISON

1.1 INTRODUCTION AND OVERVIEW.

Air Force Weather (AFW) identified a deficiency in producing timely and accurate theater forecasts. To overcome this deficiency, AFW and the Defense Special Weapons Agency (DSWA), formerly the Defense Nuclear Agency (DNA), sponsored the development of the Theater Forecast Model (TFM). There were two main objectives of the TFM development effort. The first objective was to identify a candidate numerical weather prediction model, suitable for theater use, from currently available models. Once the best model was selected, it was to be adapted to meet the needs of deployed forces on the battlefield.

The actual model selection process began with Air Weather Service's (AWS) "Combat Weather System Technical Alternatives Study." This study, conducted by Dynamic Research Corporation in 1993, reviewed over 100 different numerical weather prediction models, and compared and ranked their capabilities. The ranking was based on an integrated set of customer requirements and relied on published and developer provided information on the models.

The second phase of the selection process was the detailed performance comparisons of three of the top ranked models. Performance in this phase of the evaluation was defined as how well the model could forecast the observed weather. The emphasis of the performance evaluation was on statistical measures of model performance rather than subjective measures. The ability of the models to operate on a workstation was also evaluated by actually making forecasts on a representative workstation. This performance evaluation is documented in section one of this report, and was extracted from an informal report prepared to support the TFM decision (Bauer et al., 1995).

The baseline was the performance of the current AF model operating at Air Force Global Weather Central (AFGWC), the Relocatable Window Model (RWM). The three candidates are the Pennsylvania State University (PSU)/National Center for Atmospheric Research (NCAR) Mesoscale Model Version 5 (MM5), the Navy Operational Regional Atmospheric Prediction System Version 6 (NORAPS6) model, and the Colorado State University (CSU) Regional Atmospheric Modeling System (RAMS). To insure the model evaluation was not biased to a particular region or climate type, test forecasts were accomplished in five regions of the world. These regions were the Continental United States (CONUS), Alaska, Korea, Central America, and the Middle East

1.2 OVERVIEW.

A previous comparison study focused on the ability of mesoscale prediction models to make accurate forecasts (Pielke and Pearce, 1994). As noted in that study "modelers were free to decide their own initialization and data assimilation procedures so that, inevitably, the results represent differing levels of sophistication of external forcing. Some modelers were able to carry out a series of experiments to determine the most appropriate values of some assigned model parameters . . ." (Busch et al., 1994).

The guiding principal behind the current study was to perform a pseudo-operational comparison under standard conditions using identical data. Expected field operational constraints on forecast area, resolution, and data available were imposed. Once the models were set up, no changes were made in

their configuration, and they remained the same for all forecasts, independent of the geographical region. The models used were obtained from the sponsors of the models and reflect the "standard" model available at the time the study began. Since many of the parameterizations used in the models were scale dependent, careful selection of model options was required. The models' authors, to insure that the correct options had been selected, reviewed these selections and the output from the first case. Two of the models, MM5 and RAMS, were under active development and new algorithms and capabilities were being added as they were completed and tested. Since the focus of this study was to operate the models as if they were operational, no attempt was made to access these research capabilities during the evaluation of the models. The infusion of new technology into operations would require further extensive testing and evaluation.

1.3 REQUIREMENTS.

The Combat Weather System (CWS) development was cancelled by the Air Force (AF) shortly after this effort was initiated. However, AWS reaffirmed the requirement for a TFM model capable of providing theater forecasts in the field. The requirements for this model were those developed for the CWS forecast module plus additional requirements that reflected AFGWC's role in producing theater forecasts. Section 2 reviews all the requirements for the forecast model and develops an integrated set of requirements.

1.4 TEST PROCESS.

The models were configured to use the "best" parametric options available, to use identical sets of input data, and to generate forecasts that could be directly compared. The requirements provided a challenging set of criteria to evaluate in a single program.

To meet the AF requirements, each model must ultimately be able to operate correctly on a workstation. However, most of the models were developed on some version of a mainframe CRAY computer and would operate on that platform with minimal changes. After obtaining the models, we attempted to install all but RWM on DSWA's UNIX based CRAY and an RS/6000 (Figure 1-1.). RWM normally operates on a CRAY XMP with data input support from the mainframe computers and databases at AFGWC. The model had been ported and validated on a Unix RS/6000 workstation at AFGWC and this version was used. RWM was run only on the workstation since no validated version for a Unix-based CRAY exists. A convenient and available workstation, the IBM RS/6000, was used as the test workstation for all forecasts. The RS/6000 is a RISC-based machine made by IBM that is in the middle- to high-performance category today, but will probably represent the medium- to low-end capability when the Theater Forecast Model (TFM) is operational. The configuration of models and input data sets were the same on both the workstation and the CRAY.

The models, options selected, and their run performance will be described, in detail, in Section 3. Each model has one or more data ingestion programs or routines associated with it. These ingestion routines often manipulate the data and boundary conditions to reduce startup generated "noise." For this reason, each model's native data ingestion routine was used to construct the initial forecast fields from the observations and boundary conditions supplied by the global circulation models. Since data from both National Center for Atmospheric Research (NCAR) and AFGWC were used to initialize the various forecast runs, we translated the data into a standard data format and modified each data ingestion routine to accept the standard format.

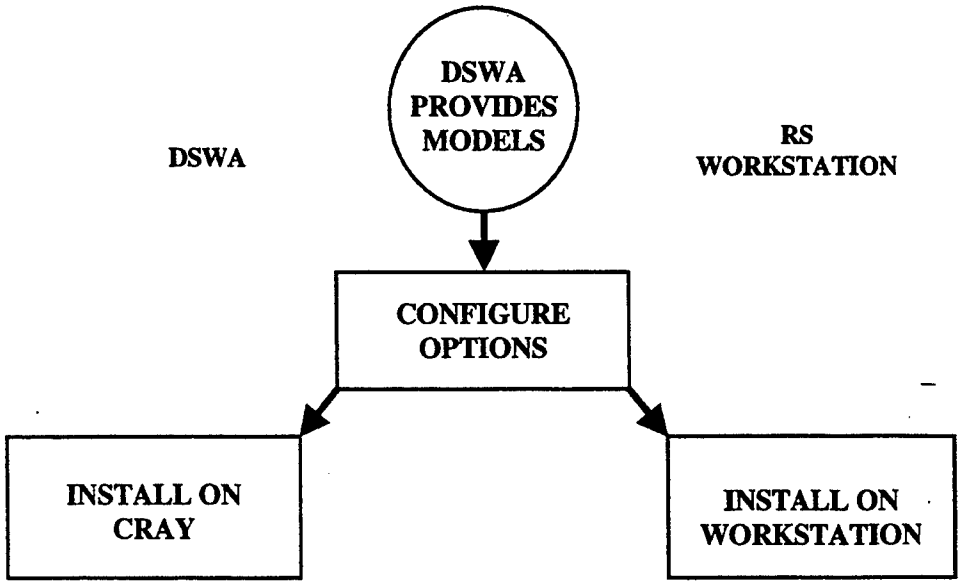

Figure 1-1. Initial steps.

The basic forecast modules were used, to the extent possible, as received (Figure 1-2.). The only changes made were to read the standard data format and to remove any smoothing of the output. The elimination of smoothing was done to insure that the forecast ability and not display capability was measured. Each test consisted of an independent 36 hour forecast. This forecast period was selected to reduce the amount of run time required for testing while allowing the models adequate time to "spin-up." "Spin-up" refers to the time required for the model to overcome "noise" resulting from the initial conditions. For the basic or benchmark tests, data was obtained for a three-day period.

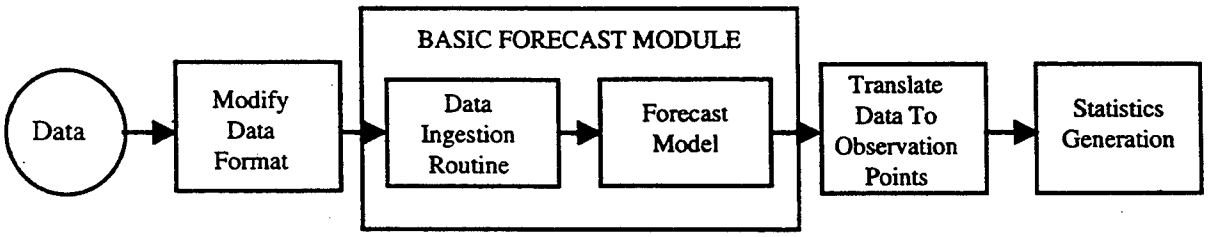

Figure 1-2. Forecast flow.

Once a forecast was accomplished, the computed data was interpolated to the observation points. Forecast data was compared to observed data using a program called REVU, which we designed to produce the required statistical data. This program and the quantities it compares are discussed in Section 3.6. Figure 1-3 indicates that we accomplished two independent forecasts during each three day period. One forecast was initialized at the beginning of the three days and the second initialized midway through the data period. Forecasts were made at the times indicated to allow comparison with surface and upper air observations.

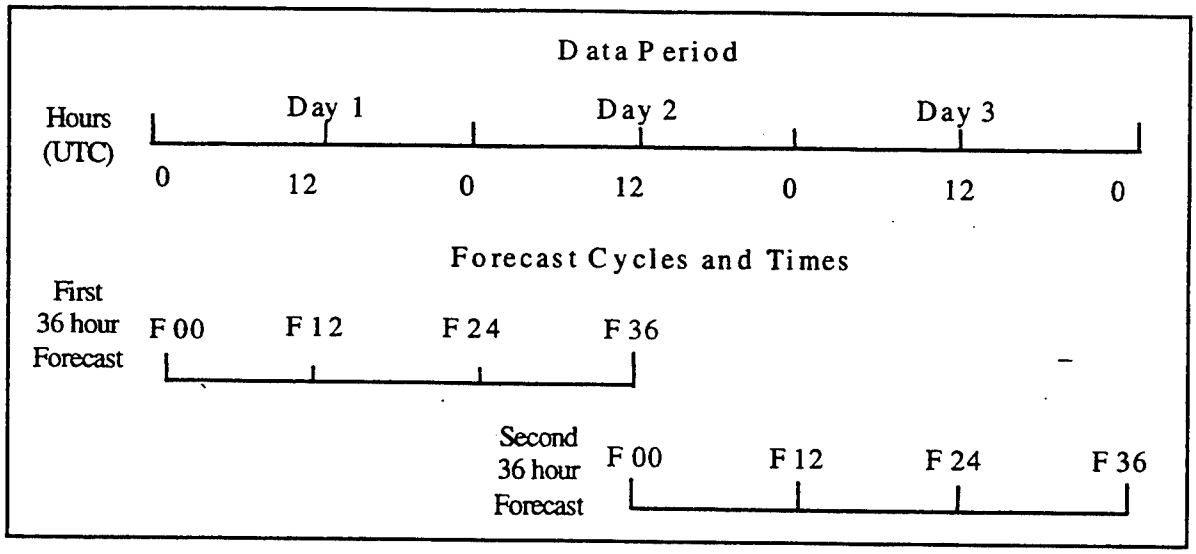

Figure 1-3. Forecast periods and production times.

The test series focused on the ability of the models to perform at the minimum or threshold TFM level. Two excursions were also examined. First, the model's performance was evaluated in a theater where portions of the observations were not available, perhaps due to enemy actions or simple communications failure. Second, the potential improvements due to the higher resolution inherent in the objective TFM requirements were examined.

1.4.1 Threshold Forecasts.

Table 1-1 summarizes the threshold tests. We began by running a well reported set of data corresponding to the Atmospheric Variability Experiment—Severe Environmental Storms and Mesoscale Experiment (SESAME) 1 Test which took place in CONUS during April 10-11, 1979.

Our test forecasts were based on and compared to data extracted from NCAR archives corresponding to the days April 9-11. With the RWM exception noted, we intended to duplicate the forecasts on the CRAY and the workstation. This exercise was to provide specific information about code portability, any performance degradation on a workstation, and the integrity of each model—whether it produces the same results on the workstation as on the supercomputer. We were able to accomplish this for all the candidate models except MM5. Each of the models that were able to run on both platforms produced forecasts that were independent of the platform used. We were unable to get the original version of MM5 to operate on the workstation. This was entirely due to problems encountered with the data ingestion routines. We obtained what was described as a workstation version, but found that workstation compatible data ingestion routines do not exist for MM5. The workstation version of MM5 exhibited a large number of changes from the CRAY version. Rewriting the ingestion routines was started but was quickly determined to be beyond the scope of this effort. A hybrid approach was considered, e.g. running the data ingestion routines on the CRAY and transferring their output to the workstation. However, MM5 uses binary transfer files, and data conversion and validation would have significantly delayed testing. As a result of these problems, we restricted MM5 to the CRAY. The workstation forecast module was tested on the CRAY by comparing its forecast to that produced by the

CRAY version using identical input data created by the CRAY ingestion routines. Even with the substantive rewrite evident in the workstation version, both versions gave the same results. The data for SESAME are presented in Section 4.1.1.

Table 1-1. Threshold forecast cases.

Test	Benchmark	Benchmark	Benchmark	Data Denied
Data Source	NCAR April 79	NCAR August 94	AFGWC November 94	NCAR September 93
Theater				
CONUS	SESAME			
Alaska		Summer	Winter	
Central America		Wet	Winter	
Middle East		Summer	Winter	
Korea		Monsoon	Winter	Fall

Once we completed the SESAME comparisons, we began the remaining benchmark tests. SESAME allowed comparison of the model's performance in the CONUS and between platforms. The next tests used August 1994 data from NCAR but were accomplished for Alaska, Korea, Central America, and the Middle East. The final tests in this series looked at simulated operational data from AFGWC. AFGWC personnel downloaded this data in November 1994. The data corresponds to the operational time AFGWC would have initialized the TFM. The intent was to reproduce the environment in which the TFM would need to operate. Late reporting stations were not included. In all of these post-SESAME tests, NORAPS6 and MM5 were used on the CRAY, and RWM and RAMS on the workstation. All of the data from the August tests are discussed in detail in Section 4.1.2 and the November tests in Section 4.1.3.

1.4.2 Data Denied Forecast.

In addition to basic threshold forecasts, each model's ability to produce realistic forecasts in areas where data is denied needed to be accomplished. These were conducted using surface and upper air data obtained from NCAR for September 1993 in the Korean theater. Three sets of forecasts were produced. In the first set, a basis of comparison was established and all available data was used to initialize the predictions. In the second set, only a single station (at Seoul, assumed to be the location of the TFM) was used. This situation might occur on a battlefield due to enemy action or to a communications failure caused by any number of factors. The third forecast was accomplished with the surface and upper air data from China and North Korea eliminated. Military operations will not cease and there is a need to provide a credible forecast in this situation. The single station initialization results were of minimal value for all models. In the case where stations in North Korea and China were eliminated, all the models did surprisingly well. This is discussed in more detail in Section 4.2.

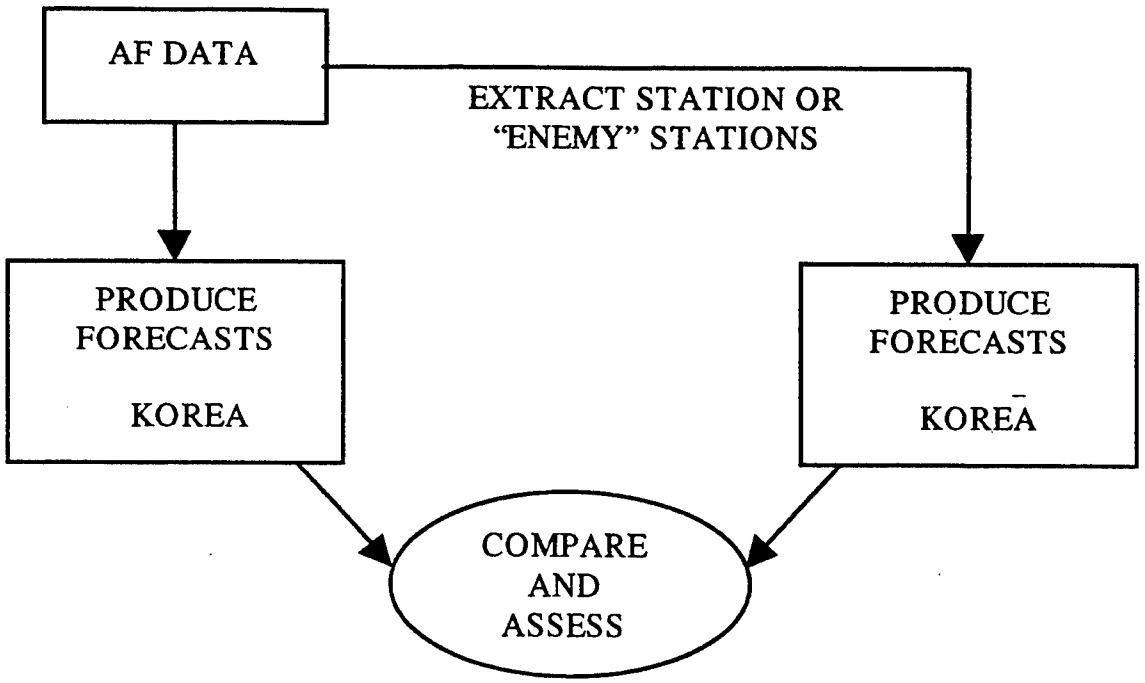

Figure 1-4. Data Denied Flow.

1.4.3 Objective Requirements and Enhanced Forecast.

The AF has established a set of objective requirements that they ultimately want to meet. These conditions correspond to an enhanced resolution, with grid size reduced from 25 nmi to 6 nmi. This increased resolution will emphasize non-hydrostatic terms in physical models and parameterizations. RAMS and MM5 both include options to use non-hydrostatic equations, whereas NORAPS6 can only use a hydrostatic approximation. This difference will have a bearing on code selection, as the model should be viable at the objective resolution to provide for required future growth. It could also be required to support a cloud model that might supplement the theater forecast model. We attempted to replicate the Central American and Middle East theater forecasts with these tests using the nested grid option where available. MM5, NORAPS6, and RAMS claim to be able to develop the smaller more finely resolved grids that interact with a larger more coarsely resolved grid. There is no AF requirement for an ability to generate these nested grids and the capability was used here only to look at the effect of enhanced resolution. Central America and the Middle East provide an interesting contrast for this evaluation. The increased resolution was expected to improve the forecast for Central America but have less impact on the Middle East. Again, the data ingestion routines for MM5 proved to be a formidable obstacle. We were unable to initialize these forecasts for MM5. Comparisons for NORAPS6 and RAMS are provided in Section 4.3.

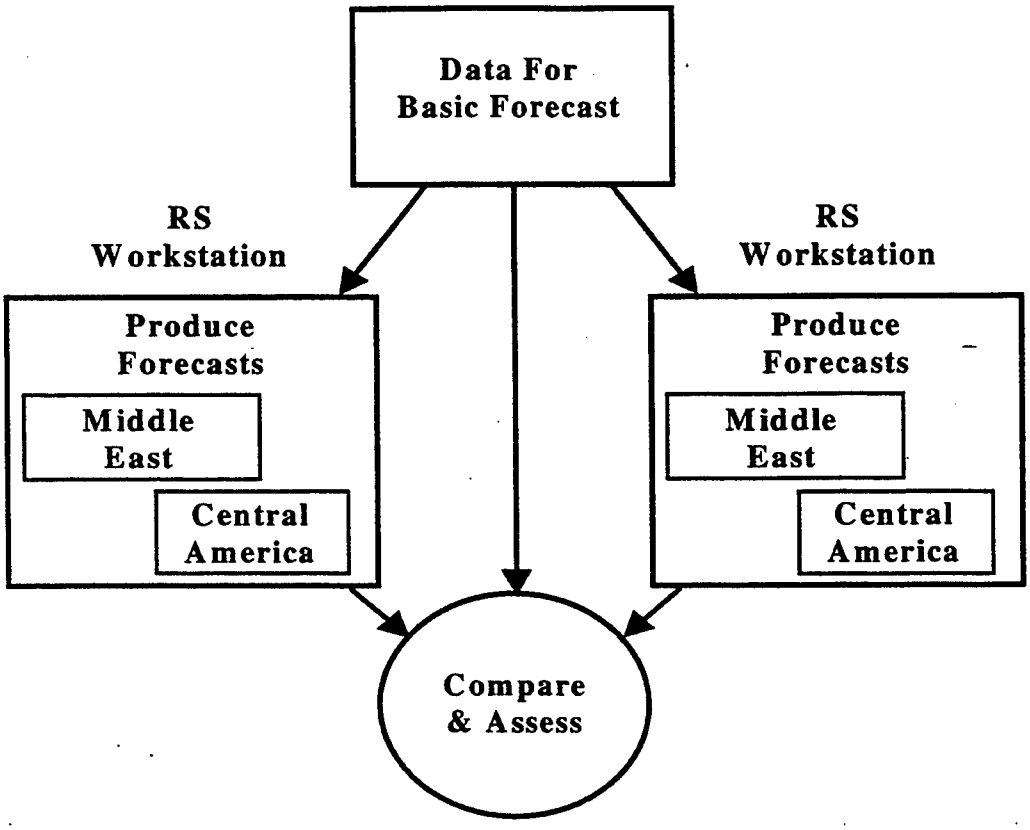

Figure 1-5. Objective Test Flow.

SECTION 2
TEST CRITERIA

This section described the test criteria that were used in evaluating the models. The test criteria were derived from diverse Department of Defense and AF requirements defined at the start of the study. In addition, requirements were developed jointly by DSWA and the AF in anticipation of changes in the published requirements. As these requirements have continued to evolve since this study began, this section documents the requirement baseline at the time the study was conducted. The following describes and traces these requirements and the resulting test criteria.

2.1 MODEL CAPABILITIES VS. WEATHER FORECASTING AND OBSERVING CAPABILITIES.

Hydrodynamic models attempt to describe the future state of the atmosphere from a set of initial conditions. As computational capabilities have improved, models have improved their resolution, model physics, and ability to use diverse input. Their goal has been to improve temporal and spatial resolution of predicted weather features using the best science available within the limits imposed by computational and hardware constraints. Judging the utility of a hydrodynamic model based solely on results for a few output parameters (such as wind speed and direction, temperatures, pressure values, humidity within a set range of error bars) can be misleading. Models must be judged both by statistical comparisons of forecast and observed parameters and by their ability to produce coherent descriptions of the three-dimensional structure of tropospheric weather and the global, synoptic, and mesoscale features that drive the weather. Accuracy is desired, but a model's forecast does not need to be perfect, if its biases can be quantified.

2.2 MODEL OUTPUTS VS. CUSTOMER REQUIREMENTS.

Forecast models are usually judged by their ability to forecast the development, location, temporal and spatial resolution of major global, synoptic, and mesoscale features and atmospheric structure, rather than their ability to predict specific parameters. AWS customer requirements for weather support typically are based on go/no-go criteria for a particular operation or on the known weather sensitivities of a particular weapon system. These criteria are presented in various weather support documents as Requirement Correlation Matrices (RCMs). While useful for defining goals for weather support systems, these criteria may be unrealistic forecast model goals because weather observing platforms cannot measure some of these quantities, much less forecast them. For models, the goal is to build the best atmospheric model, so the best possible estimate of specific required parameters will be produced.

2.3 TRACEABILITY AND PRIORITY OF REQUIREMENTS.

The test criteria were traceable to weather support requirements. Collectively, the test criteria ensure that the model chosen met the broadest possible spectrum of weather support needs.

2.4 TYPES OF REQUIREMENTS.

In establishing reasonable test criteria, we considered various types of requirements and several different requirement sources. We also considered both objective and subjective model evaluation criteria.

2.4.1 Objective Evaluation Criteria.

Objective test criteria compare a model's output parameters and characteristics to a desired standard. Each standard is derived from or traceable to a user requirement or quantifiable test criteria based on the

ORD, the SOW, or other meteorological support studies. Examples of objective test criteria are the model verification statistics produced by the Mission Research Corporation (MRC)-ASTeR model comparison software, REVU that is described in Section 3.6. Verification statistics produced by each candidate model are cross-compared to identify which model produces the best estimate of various atmospheric parameters as a function of forecast lead-time. Key subclasses of quantitative test criteria are discussed in the following paragraphs.

2.4.1.1 Meteorological Parameters. The primary atmospheric parameters output by dynamic models in the United States Air Force (USAF) Electronic System Center (ESC) study (4-2) are: wind components (u, v, w), potential temperature, specific humidity (q), and pressure. These parameters were judged using the data generated by the REVU software that compared model output to the RAOBS and surface data.

2.4.1.2 Customer Support Requirements. Many of the applications and weather support requirements for the TFM are summarized in RCM matrices in the ORD, the Weather 2000 Study, and a previous study, Combat Weather Systems Technical Alternative Study Interim Report, by ESC in 1993. While these specify the accuracy of meteorological parameters that are required to support a mission or weapon system, many of these stated values were really requirements for meteorological observations, and were not the accuracy required from a tactical weather forecast model.

2.4.2 Subjective Evaluation Criteria.

Subjective criteria involve assessing model performance or characteristics based on extensive experience. For example, a model that provides superior forecast results may not be transportable to a workstation environment, or cannot be maintained without being thoroughly rewritten in another programming language. Other examples include models that require excessive run-time, do not perform well in data-sparse regions, or do not degrade gracefully when part of the forecast grid becomes data-denied. Subjective criteria include comparisons to other meteorological information, which is not subject to statistical evaluation. This includes, for example, the correct placement and intensity of a low-pressure center. Subjective model selection criteria are as important as objective criteria and must also be traceable to ORD requirements, support requirements, or support studies such as the Weather 2000 report.

2.5 REQUIREMENTS OVERVIEW.

This section briefly reviews all documented test requirements. These requirements were either explicit or implied. Derived requirements are summarized in Section 2.6. The documents considered, shown in Table 2-1, include both primary and secondary sources.

Table 2-1. Documents from which requirements are derived.

DOCUMENT	SECTION
Operational Requirements Document Version 3	2.5.1.
Statement of Need, Tactical Weather Observing System	2.5.2.
Statement of Need, Tactical Forecast System	2.5.3.
DNA Statement of Work, TFM	2.5.4.
DNA Test Requirements Letter	2.5.5.
Army Manual FM34-81/AFM 105-4	2.5.6.
CWS Technical Alternative Interim Report	2.5.7.

2.5.1 Operational Requirements Document (ORD) Version 3.

The ORD (Operational Requirements Document-Combat Weather System, 1992) was a key source document driving the need to upgrade weather support systems for theater applications and to upgrade AFGWC theater support models to the state-of-the-art. The ORD stated that the TFM must support combat and support forces from initial deployment through sustained theater operations. The ORD identified the mission areas listed in Table 2-2 as needing improved mesoscale modeling weather support.

Table 2-2. ORD mission support areas.

Air Force	Army
Counter Air	Aviation
Strategic Attack	Air Defense
Interdiction	Close Combat
Close Air Support	Land Combat Engineering Support
Strategic Airlift	Special Operations
Operational Support	Fire Support
Base Operability and Defense	Biological and Chemical
Logistics	

The goal of the TFM system was to integrate highly capable automated weather observing and forecasting systems with combat planning and execution systems. Theaters forecast support must integrate observations, generate tailored forecast information quickly, and distribute it to the Theater Battle Management (TBM) Command, Control, Communication, Computers, and Intelligence (C4I) systems. The TFM, as the primary forecast function embedded within a tactical weather support system, must respond to single points of failure both within and outside the theater and should degrade gracefully to a point where observations only, or single station analyses are produced.

The TFM was to produce the most accurate analysis and forecast fields that technology could provide. The requirements for "forecast fields" indicated that not only were accurate analyses of synoptic and

mesoscale weather features required but gridded fields of specific weather parameters were also required. Many forecast functions at AFGWC require gridded analysis fields of multiple parameters at multiple mesh resolutions. The TFM needed to meet this requirement if it was to replace the RWM at AFGWC. The TFM, as part of a tactical weather support center, was to provide a theater-scale analysis and forecast model capability. This use made model run-time and user interface a key selection criterion.

Under the description of existing weather support components, the ORD described the Combat Air Forces Weather Software Package (CAFWSP) as one of the key interfaces to produce weather support products for the C4I system. The model selected as the TFM would have generated output and analysis fields that were compatible with the CAFWSP.

Additional specific operational requirements for the TFM are listed starting on page 17 of the ORD:

- The TFM must use standard terrain databases, AFGWC supplied boundary values, climatological data bases, and theater weather observations (here the term "theater" was presumed to be synoptic scale to mesoscale).
- The Model must execute a theater scale weather analysis and forecast that cover an area at least 1500 nmi by 1500 nmi with an objective coverage area of 3200 by 3200 nmi.
- The theater scale weather analysis and forecast model should have forecast outputs every 3 hours out to 72 hours.
- Model run-time for the above requirements should be 1 hour or less. The model should produce uniform gridded data fields of the same parameters forecast by the comparable model used at AFGWC (RWM). Examples of these parameters are: temperature, pressure, u,v,w, relative humidity and specific humidity.
- Based on available data, the model should gracefully degrade to produce the best possible analysis and forecast fields as data becomes sparse or denied.
- Horizontal resolution must be 25 nmi with an objective of 6 nmi to produce databases and inputs to support requirements such as tactical decision aids and support to precision guided munitions, as well as CBW and fallout predictions.
- Software engineering requirements are discussed on page 22 of the ORD. They are summarized as follows:

  (1) The TFM must be developed in an open systems environment to enhance portability and interoperability;
  (2) Existing DOD and COTS software shall be used to the extent possible;
  (3) Reasonable software configuration management methods and tools shall be used; and
  (4) The system shall interface with existing AFGWC and C4I systems.

The ORD also summarizes key model requirements in a Requirements Correlation Matrix (RCM) that should be considered in development of the model selection criteria.

2.5.2 Statement of Need (SON) for Tactical Weather Observing Systems (TWOS) (USAF 211-89).

This document was a SON for weather observing systems, not for the forecast system. It stated requirements for high vertical, horizontal, and temporal resolution for weather parameters to support the full spectrum of battlefield operations. These requirements implied a corresponding need for fine-scale,

high resolution weather forecast products that could not be met with the 25 nmi resolution model output that had been proposed as a requirement, but is currently being provided to front line commanders. The SON stated: *"Theater Army, Tactical Air Forces, and Special Operations Forces planners require detailed weather observations across the depth of the battlefield to determine mission tactics and to manage combat resources. For example, electro-optical sights and guidance systems, laser designators, and night vision goggles can give forces a significant advantage. However, these 'force-multipliers' can be significantly limited or completely neutralized by battlefield induced haze and smoke and atmospheric conditions such as fog, heavy rainfall, and cloud cover. Detailed knowledge of the existence of these elements is essential for mission planners to manage these limited electro-optical assets"* (page 1, par. 1(b) 1). These types of weather support requirements could not be met with 25 nmi resolution. Paragraph 2a(1) of the SON cited deficiencies in current tactical weather observing capabilities. It stated that 1) tactical combat forces require weather observations of more weather elements, with increased observation frequency, and from a denser network of locations to provide an enhanced current picture of the environment, and 2) there is a corresponding need to improve forecasts. In 2a(1)(b), the SON noted that AWS could provide hourly tactical weather observations from a limited number of airfields and command posts within a theater of operations. The primary deficiency of this observing network was its observation frequency and the locations were often too coarse to be used in detailed tactical applications. This again implied the need for weather products with more spatial and temporal resolution than specified in the ORD or the DNA-AFGWC model verification requirements letter (discussed later).

2.5.3 Statement of Need (SON) for Tactical Forecast System (TFS) (USAF 212-89).

The SON (paragraph 2) stated that AWS must provide more environmental information with finer resolution in shorter periods of time to theater war fighting elements. With existing or programmed capabilities, AWS was not at that time able to meet this requirement. To accomplish the support required, AWS needed a portable, stand-alone capability with greater employment flexibility to produce and disseminate weather products. At the time this document was written, tactical weather support was forced to rely on a single CONUS-based source — AFGWC —for most required weather data, which left it vulnerable to a single point of failure. The support structure also had potential single points of failure in its communications system, the Automated Weather Net (AWN). The TFS was needed to eliminate complete dependency on AFGWC and the AWN and provide a mobile, survivable theater capability to rapidly develop and transfer environmental information to Air-Land Battle components.

Under "current capabilities" in section 3, the SON stated that AFGWC had the RWM with 25 nmi resolution for use in contingency support. It also noted that the Mesoscale Weather Prediction and Analysis System (MPAS) was a software development effort that was needed to provide theater-wide, short-range, fine-scale forecasting. The MPAS software was required to run on transportable or tactical computers. These requirements implied that a 25 nmi grid scale was not sufficient for sustained support within theater, and they support the stated requirement for a mesoscale model with better than 25 nmi resolution running in theater.

Table 2-3. ORD Theater Forecast Model requirements RCM.

System Characteristics	ORD 1 Threshold	ORD 1 Objective	ORD 3 Threshold	ORD 3 Objective
a.1 Source			GFE	
a.2 Coverage	1500 sq nmi	1500 sq nmi	3200 sq nmi	3200 sq nmi
b. Init GWC Model	yes		yes	
c. Init Climo	yes		yes	
d. Use Terrain DB	yes		yes	
e. Theater OBS	yes		yes	
f. Forecast Times		3 hr out to 72 hr	3 hr out to 72 hr	3 hr out to 72 hr
g. Model Run-time		1 hour	1 hour	1 hour
h. Graceful Degrade		yes		yes
i. Forecast Parameters:				
Horizontal Resolution		1/8 Mesh(25 nmi)		6 nmi
Vertical Resolution		Variable		

Section 4 of the SON listed needed operational capabilities that are key to the selection of a tactical forecast model. These are listed below:

- The TFS must be able to receive and process all available weather data automatically. This implies a requirement for the TFM to have Four Dimensional Data Assimilation (FDDA).
- The TFS will prepare, quality control, and analyze data using an automated capability that ensures all relevant information will be considered for weather analyses and forecasts. The TFS should run limited area analysis and forecast models that use standard digital terrain data. The models will use boundary values from large scale analyses and forecast fields and will incorporate theater observations on a continuous basis. Based on available data—either a complete, partial, or single station data set—an automated capability will select appropriate models to produce forecasts and ensure graceful degradation of forecast support as sources of weather data are lost. The TFS models will be capable of providing limited area, high-resolution forecasts out to 96 hours. This section is the basis for the TFM using AFGWC terrain and other databases for initialization. It is also the basis for the requirement that the TFM degrade gracefully when experiencing data-dropout or data-denial.
- For future requirements, the TFS will be capable of adding new forecast techniques and algorithms in a modular fashion. The TFM, as part of the TFS, must also be modular. Table 2-4. is extracted from the SON RCM and summarizes TFS requirements that are related to or imply TFM model selection test and selection criteria.

2.5.4 Theater Forecast Model (TFM) Statement Of Work (SOW) (1994).

The following are excerpts from the SOW that relate to or imply model test requirements.

Ref. SOW Task 2, Model Analysis and Selection: The Contractor shall investigate, analyze, and develop methods for evaluation and analysis of the candidate models for in-theater weather prediction use at the operational unit. Simultaneously, the Contractor shall determine the computer workstation environment

that best meets the requirements of the system. This implies the need to document model memory, storage and run-time requirements during the testing and model comparisons.

Table 2-4. SON TFS requirements.

Parameter	Requirement	Accuracy
1. Initialize with AFGWC inputs	Yes	
2. Area Coverage	1500x1500 km	
3. Low Level Temp SFC to 3km	2 km Horizontal 0.2 km Vertical	±5C at 48 hours
4. Low Level Wind SFC to 3 km	2 km Horizontal 0.2 km Vertical	±8 kts at 48 (r)and 96 hrs(g) ± 15 degs at 48 (r) and 96 hrs(g)
5. Low Level Moisture SFC to 3 km	2 km Horizontal 0.2 km Vertical	± 2 gm/m^3
6. Precip (Rate)	2 km Horizontal	± 10 mm/hr
7. Precip (Total)	2 km Horizontal	± 15 mm
8. Severe Weather	2 km Horizontal	Probability of detection • 80%
9. Upper Air Winds	2 km Horizontal 0.2 km Vertical	± 10 kts at 48 (r) and 96 hrs(g) ± 15 degs at 48 (r) and 96 hrs(g)
10. Pressure	2 km Horizontal for Standard Levels	± 1 mb
11. Model Processing Time	All Parameters for full theater 96 hour forecast	1 hour (r) 0.5 hour (g)

(r) = requirement (g) = goal

Ref. SOW Subtask 2.1, Analyze TFM Model Requirements: The Contractor shall perform a detailed requirements review of the TFM candidate models, make assessments of how each model would perform in a workstation environment, and detail what, if any, model performance capabilities would be degraded by operating the model on a workstation. The assessment will be combined with the benchmark statistics and presented in both briefing and technical report forms. This implies the need to include model performance on a workstation as a test criterion. Much of the initial comparison work will be done on a supercomputer platform. Model run-times will be carefully tracked on the CRAY and used to estimate the models' performance on workstations. NCAR did this type of analysis for the NCAR Global Climate Model (GCM) on various platforms, as shown in Table 2-5. This type of comparison will be derived from the initial model comparison runs done on the CRAY.

Ref. SOW Subtask 2.2, Benchmark Candidate Models: For benchmark testing each model shall be considered to consist of preprocessing (data analysis), processing (initialization and computation), and post processing functions (data analysis and displays). This requires test and comparison of the three primary subfunctions of each model.

This section of the SOW also stated that both objective and subjective tests should be performed. Examples of such tests are 1) statistical comparisons of model-generated fields with ground truth observations and 2) model predictions of pressure center locations. Tests would be performed on all required weather parameters outlined in the TFM requirement documents. Those parameters include air

temperature and dew point depression within 2 degrees Celsius, wind speed within 2 knots at speeds less than 20 knots and within 5 knots at speeds greater than 20 knots, wind direction within 30 degrees, and surface pressure within 1.7 millibars. These criteria, while quantitative, are really aimed at each model's ability to predict pressure fields and resultant winds. Together, these parameters provide an indication of the model's ability to forecast the development and location of overall synoptic and mesoscale features.

Table 2-5. (Haack, 1993). CCM1 run performance vs platform.

Platform	Performance
CRAY YMP	126%
CRAY-XMP	100%
IBM RS 6000/550	12%
SUN 4/260	1.6%
DEC VAX 8800	1.4%

Ref. SOW Subtask 2.3, Computer Technology and Hardware Selection: Although this section discussed the work platform requirements to host the TFM, it also implied a requirement to consider the structure, size, and input/output of each model to make sure it can be ported to a workstation environment. This section also levied a requirement to assess model performance when processing regions that are data-sparse, data-denied, or data-void. The SOW called for these assessments to be made to simulate model operation, assimilation of data, production of a forecast, and using the forecast to initialize the next model run. The production cycle for this test criterion is 5 days. The SOW further required that this simulation cycle allow time to examine the effects of varying data densities.

Ref. SOW Task 3, Model Adaptation, Testing, and Validation: The TFM objective goal for model resolution is a horizontal resolution of 10 nmi and a vertical resolution of 30 feet below 3000 feet altitude and 1000 feet above that.

Ref. SOW Subtask 3.2, Test and Validation: This section required that the system/model verification procedure 1) prove that the system/model implementation meets specifications in the ORD and 2) show that the forecast model produces an accurate representation of the atmosphere. It must also ensure that the adapted model accurately represents the original model. This requirement implied a subjective criterion of accurately describing the atmosphere and a selection requirement that the initial, Government Furnished Equipment (GFE)-supplied model is sufficiently well documented to allow downsizing and restructuring to run on the workstation platform selected to host the TFM.

2.5.5 DSWA Test Requirements, DNA Letter dated 21 June 1994.

Requirements that were derived from this document (DNA, 1994) are as follows.

2.5.5.1 DSWA Desired Model Characteristics. The model selected will be required to run both at AFGWC and on a workstation. This implied a requirement that it be coded to allow the maximum degree of portability. Thus the subjective selection criteria, model structure, documentation, and portability (programming language) needed to be considered. This letter also required that the selected model must exceed the current capability of the AFGWC RWM. Table 2-6 lists desired characteristics of the selected model.

Table 2-6. DSWA and AFGWC desired TFM model characteristics.

Model Characteristic	Required	Goal
Window Size	1500 x 1500 nmi	3200 x 3200 nmi
Horizontal Resolution	25 nmi	6 nmi
Vertical Layers	20	none stated
Run-time/Cycle	1 hour from ingest	none stated
Forecast Cycles	2 per day	8 per day

These required or desired characteristics for the TFM were translated into subjective model selection criteria. Each candidate model was evaluated regarding its current ability to meet these requirements and the ability of future upgrades to meet future operational goals. These characteristics also implied model run-time and selection criteria that consider the ability to increase the grid size and number of time steps while still keeping the model run-time at one hour or less.

2.5.5.2 DSWA Desired Model Test Parameters. The DNA letter includes a brief TFM evaluation plan developed at a joint DSWA-AFGWC Technical Interchange Meeting (TIM) and lists grid, boundary, initialization, and output parameters for the model comparisons. These are broken down into the following categories:

- Model Configuration:
  These requirements cover the initialization and timing requirements for the model comparisons, as shown in Table 2-7.

Table 2-7. DSWA–AFGWC configuration.

Criteria	Value/Description
Horizontal grid spacing	25 nmi
Computational Domain Grid Points	71 x 71
Verification Domain Grid Points	61 x 61 (1500 x 1500 nmi)
Vertical Levels	Not to Exceed 20
Nested Grids	None

- Model Run Options:

  Model run options listed in the evaluation plan are:

  — AFGWC will provide observations and first-guess fields for initial conditions and lateral boundary conditions for comparison tests;

  — Each model will use whichever observation types/variables it can incorporate into its analysis scheme;

  — Model options will be determined by a model expert for each model and listed in the test plan. A model expert is a person from the supplying agency who is familiar with the model and its optimization to produce its best results.

- Theater Weather Regimes for Model Test Runs

  Theater and model test run criteria are:

  — Models will be tested in five theaters that represent different climatic and data density regimes. These theaters are Alaska, Central America, the Middle East, Korea, and CONUS.

  — Each model will be run for the 00Z and 12Z cycles for each season, with data saves for 3 days to cover the model verification period.

  — AFGWC RWM will be used as the baseline for comparison of each model in each weather regime and theater. A TFM candidate must outperform the RWM to be considered viable.

- Verification Criteria:

  Model verification criteria agreed to at the TIM are listed in Table 2-8.

If there are conflicts among the various sources of model requirements and test criteria, those of the DSWA-AFGWC TIM were given preference.

Table 2-8. DSWA-AFGWC model verification criteria.

Criteria	Value/Description
Forecast Times	F00, F06, F12, F24, F36 hours
Output variables	q, u, v, t, slp, rh
Levels	SFC(2m) + mandatory levels: 1000, 925, 850, 700, 500, 400, 300, 200, 150, and 100 mbs
Measures of accuracy (Quantitative)	RMSE and RMSVE from available RAOBS, Mean absolute error, Relative error, Bias.
Measures of accuracy (Subjective)	Standard Map sets for same time periods to include the following levels: slp, 850, 700, 500, 300 mb
Map Evaluation	Review by AWS Personnel
Timing Statistics	Recorded for all model runs
Technology Transition and Insertion into each model	Subjective criteria Review by AWS/DSWA

2.5.6 Weather Support for Army Tactical Operations (FM 34-81/AFM 105-4, 1989).

This Training and Doctrine Command (TRADOC) field manual described weather support concepts and detailed weather support requirements for a full spectrum of Air-Land Battle operations. Several key aspects of weather support related to the TFM have been extracted and listed below. Key among these are those that imply the need for as fine a mesh as practical and the need to produce longer range forecasts. The following requirements are listed to ensure that Army requirements are considered in the development of the TFM test and selection criteria.

- Area of Operations:
  This manual foresees that Central Europe, the Middle East, and Korea are likely regions in which tactical forces may be employed in the foreseeable future (page ii). This provides a good fit for the proposed test regions selected by DSWA and AFGWC.

- Forecast Length:
  Forecasts of up to 72 hours (pages 1-8) are needed to plan and manage the engagement of forces. Forecasts of 96 hours are needed at the Corps level to assess the effects of weather on planning, tactics, and predicting the effects of weather on enemy operations.

- Mesh and Boundary Layer Requirements:
  The manual notes (pages 1-9) the requirement for wind inputs into the Tactical Fire Direction Computer System to support artillery operations, and notes the need for wind forecasts to support chemical and nuclear dispersion forecasting. It also indicates a need for accurate modeling of planetary boundary layer conditions. This implies the need for as fine a mesh as is practical (nesting) within an Area of Operations.

- Model Robustness to Data Sparseness:
  On page 2-1, the manual discusses the problem of denial of weather data and data sparseness in the area of operations. This implies a need for a TFM weather model to be robust and degrade gracefully when these conditions are encountered.

- Need for In-Theater Model Support:
  Page 3-1 discusses disadvantages of centralized support because of possible loss of communications to forecast centers. It also discusses past use of coarse-grid global-scale forecast model output provided by forecast centers.

- Chemical Warfare Operations:
  In a summary of staff weather officer support roles on pages 3-7, the manual discusses the need for weather forecast support to chemical warfare operations, including prediction of low level inversions, wind shears, wind shifts, and diurnal weather changes within the boundary layer. Micro-scale terrain effects on these types of operations also must be accounted for in forecast model support. This implies the need for a fine mesh (nesting) and a model that can produce reasonable forecasts of the planetary boundary layer.

2.5.7 CWS Technical Alternatives Interim Report, ESC/XRC, (1993).

The purposes of this study by ESC were to determine analysis and forecast model outputs needed for tactical weather support, to review existing and planned mesoscale/microscale meteorological modeling efforts and their suitability for use in tactical forecasting, and to determine additional software and models needed to meet battlefield requirements. The following are key points of this study germane to this effort.

- Operations Concept:

  The operations concept for theater weather support is for AFGWC to provide initial forecasts while weather support teams arrive and set up their operations in-theater. After a theater weather forecast support function is established, forecast support will transition to a mesoscale model run at the Theater Forecast Unit for the battlefield Area of Operations. The tactical forecast mesoscale model will be driven by surface observations taken in-theater and any remotely sensed data, as might be available from platforms such as Defense Meteorological Satellite Program (DMSP).

- Source of Stated Forecast Requirements:

  Requirements for forecast and analysis support stated in the ORD, the Weather 2000 Study, and the HQ TAC Plan for Automated Support are based on needs for the observation of each environmental element, not as a specific forecast parameter produced by a model. Therefore, model requirements tend to be overstated regarding a model's ability to produce particular forecast parameters desired for operational support.

- Model Outputs:

  As part of their discussion of a notional forecast model, the ESC study notes that all numerical weather prediction models typically provide the same (or closely related) set of basic output variables: horizontal components of the wind (u and v); the vertical component of the wind (w); potential temperature (Θ); specific humidity (q); and pressure (p). Other desired atmospheric elements can be derived from this set of variables. Close comparisons of these parameters using the MRC-ASTeR model verification software will be one of the primary set of test criteria. The types of statistics produced by the MRC-ASTeR REVU verification software are discussed in Section 4.6.

- Model Outputs vs. Model Capabilities:

  Attachments 4 and 5 of the ESC study tabulate present numerical model capabilities and tactical forecast model essential Elements. An excerpt from these tables, shown in Table 2-9, provides a brief summary of known model capabilities and the types of outputs deemed essential for a theater forecast model. These provide insight into the final determination of reasonable selection criteria for the TFM comparison testing by showing what the most important customer support requirements are in priority order and by indicating how each desired parameter is produced (either directly or indirectly by the forecast model).

Table 2-9. Forecast model output vs. priority and model capability. [from ESC study, (1993)].

Forecast Product/Element	Wx 2000 Priority	Model Code*
Temperature: (Low Level Potential)	1	1
Temperature (Runway)	1	3
Temperature (Freezing Level)	1	3
Wind (Low Level Speed and Direction)	2	1
Thermal Stress (Wind Chill - Heat Stress)	2	3
Low Level Wind Shear	2	3

Table 2-9. Forecast model output vs. priority and model capability. [from ESC study, (1993)]. (Continued).

Forecast Product/Element	Wx 2000 Priority	Model Code*
Low Level Wind (Drop Zone Mean Wind)	2	3
Low Level Moisture (Specific Humidity)	3	1
Low Level Moisture (Absolute Humidity, Dew Point, RH)	3	3
Low Level Temperature (Surface)	3	3
Temperature (Upper Air)	4	1
Upper Air Temperature (Trop Ht, Inversion Ht, Mixing Depth, Freezing Level, Vertical Profile, Gradients(Vertical & Horizontal), D Values)	4	3
Upper Air Wind (Direction and Speed)	5	1
Upper Air Wind (Vertical and Horizontal Gradients, Wind shear, Turbulence)	5	3
Upper Air Moisture (Specific Humidity)	6	1
Upper Air Moisture (Condensation Pressure Spread, Absolute Humidity, Dewpoint, RH)	6	3
Precipitation Phase (Type)	7	2
Precipitation Rate	8	1
Present Weather (Type and Intensity)	8	4
Severe Weather (Stability Index)	9	3
Severe Weather (Snow >6 ins, moderate snow)	9	4
Severe Weather (Winds Greater than 30, 35, 40, 50 kts)	9	4
Severe Weather (Freezing Precip)	9	4
Severe Weather (Hail)	9	4
Severe Weather (Thunderstorms, Lightning, Tornadoes, Thunderstorm Tops)	9	5
Cloud Cover	10	2
Sea State	17	4
Wave Height	18	4
State of Surface (Wet, Dry, Frozen)	19	4
Low Level Temperature (Inversion Height)	20	2
Low Level Temperature (Vertical Profile)	20	3
Low Level Temperature (Horizontal & Vertical Gradients)	20	3
Refractive Index	21	4
Cloud Phase	22	2
Cloud LWC	23	2
State of Surface (Snow Cover-Depth, Age, Character)	24	2
Cloud Amount	25	2

* Model Capability Codes
  1 = Forecast element is directly forecast by numerical models
  2 = Some but not all models produce this parameter directly
  3 = Forecast element is derived from model output via some simple relationship
  4 = Derived from model output via algorithm with accurate results
  5 = Derived from model output via algorithm, but results not reliable or contain some uncertainty

2.6 REQUIREMENTS STUDY.

Based on the review of the documents cited, a matrix of recommended test requirements was developed. This matrix is shown in Table 2-10 and has the test and selection criteria sorted into three classes.

- Class 1 Criteria:

These consist of model comparison criteria that can be compared to a quantifiable standard. The order of consideration is first to compare basic model output parameters (t, p, u, v, w, q) to rawinsonde and surface data using the REVU model performance software. This will provide insight on each model's ability to correctly forecast basic output parameters at a given geographic location. Next, model analyses will be compared to a standard meteorological package to assess how well the model predicts the actual location and development of major synoptic and mesoscale features.

- Class 2 Criteria:

  These criteria are subjective and compare model functionality and adaptability issues. Model characteristics such as robustness to data sparsity, adaptation to use AFGWC input databases, ability to produce analysis fields to support AFGWC operations, and initialization options are areas where the models must be assessed subjectively and compared to the AFGWC RWM.

- Class 3 Criteria:

  These subjective criteria cover areas such as software management issues, model adaptation to a work station environment, and the test scenarios that have been selected to test the models against each other and the RWM. One of the key issues is to complete a synoptic description of all weather data sets that will be used as test inputs. This is required in order to fully understand the behavior of the models that are based on the actual weather conditions input.

Table 2-10. Recommended model test and selection requirements matrix.

Type of Criteria	Measurement	Compare to	CLS	Source
OBJECTIVE Basic Model Outputs	t, p, u, v, w, q RMSE, RMSVE, mean absolute Errors	RAWINS Metsat soundings(data sparse) REVU comparison software	1	DNA SOW ORD
OBJECTIVE Derived Analysis Fields	Cloud Cover Winds Pressure Temperature	Observed analysis charts Nephanalysis/Metsat Constant level charts sfc, 850, 700, 500, 300 mbs	1	DNA
OBJECTIVE Forecast Times	Forecast to 72 hours	Observations (sfc and U/A) Compare against RWM	1	DNA ORD FM 34-81 TFS-SON
SUBJECTIVE Atmospheric State	Synoptic and Mesoscale feature location and description(timing)	Surface charts Metsat Surface and U/A Data	1	DNA
SUBJECTIVE Model Traits and Subfunctions	•Science/Physics •Robustness to Lack of Inputs	Cross compare each model and compare to RWM as the baseline	2 2	DNA ORD
SUBJECTIVE Initialization	Area Coverage Boundary Condition Options FDDA Available	Subjective review of each model and cross compare to RWM	2	DNA
OBJECTIVE Basic Model Outputs	t, p, u, v, w, q RMSE, RMSVE, mean absolute Errors	RAWINS Metsat soundings(data sparse) REVU comparison software	1	DNA SOW ORD

Table 2-10. Recommended model test and selection requirements matrix. (Continued).

Type of Criteria	Measurement	Compare to	CLS	Source
OBJECTIVE Derived Analysis Fields	Cloud Cover Winds Pressure Temperature	Observed analysis charts Nephanalysis/Metsat Constant level charts sfc, 850, 700, 500, 300 mbs	1	DNA
OBJECTIVE Forecast Times	Forecast to 72 hours	Observations (sfc and U/A) Compare against RWM	1	DNA ORD FM 34-81 TFS-SON
SUBJECTIVE Atmospheric State	Synoptic and Mesoscale feature location and description(timing)	Surface charts Metsat Surface and U/A Data	1	DNA
SUBJECTIVE Model Traits and Subfunctions	•Science/Physics •Robustness to Lack of Inputs	Cross compare each model and compare to RWM as the baseline	2 2	DNA ORD
SUBJECTIVE Initialization	Area Coverage Boundary Condition Options FDDA Available	Subjective review of each model and cross compare to RWM	2	DNA
SUBJECTIVE Software Characteristics	Documentation Portability & upgradability Analysis package I/O and interface to AFGWC Models and C4I	Subjective review of each model and cross compare to RWM	3 3 3 3 3	ORD SOW DNA
SUBJECTIVE Implementation Factors	Memory Requirements Run-time I/O	Cross compare models and compare to RWM with same vertical levels and grid spacing	3	ORD
SUBJECTIVE Model Input Requirements	AFGWC DATA BASES •GSM to initialize •GWC sfc and UA and terrain databases •Metsat (DMSP ingest)	•Determine how well model interfaces to use of AFGWC databases. •Impacts of AFGWC input databases (scale, etc.) on model performance	2 2	DNA
SUBJECTIVE Test Data Weather Scenarios Impacts on Model Performance and Model Comparisons.	Required Test Scenarios Weather Regimes are: • Alaska • Central America • Middle East • Korea • CONUS	•determine and document effects of test scenarios on overall model performance. •provide a complete synoptic analysis of the overall weather regime for each test •Compare to RWM	3 3	DNA

SECTION 3
TEST ITEM DESCRIPTIONS AND RUN PERFORMANCE

This section describes the models tested, their configuration during the tests, and their run performance on the CRAY and workstation.

3.1 SOFTWARE MODELS AND CONFIGURATION.

Each model was configured using the "best" selection of physical parameters available, our a priori assumption being that this would produce the best forecast. Candidate models can be grouped by their use. NORAPS6 and RWM were used in operational settings and have few switches to select different physical models. Their options are more related to types of data output available. MM5 and RAMS have more of a research background and have numerous physical model switches. In addition, they have many of the same types of options for data assimilation and output. The four candidate models have existed for some time, or are new upgrades of existing models. RAMS and its immediate predecessors have a history dating back to the mid-1970s. MM5 and NORAPS6 have similar lineages that provide a track record of what they can and cannot do and how well they can do it.

RAMS, MM5, and NORAPS6 have much in common: they are all 3-D, primitive equation, relocatable, regional mesoscale models; they can all use staggered gridding, terrain-following vertical coordinates, and four dimensional data assimilation using nudging; and they include many similar parameterizations for sub-grid mixing, cumulus, and radiation. There are some differences, particularly between NORAPS6 and the other two models.

The NORAPS series of codes has been developed by the Navy for their own operational use and are optimized for ocean area forecasts; MM5 and RAMS are not. This distinction is easily seen by noting that NORAPS6 models sea ice, but RAMS and MM5 do not. RAMS and MM5 both model numerous types of land use, which can significantly affect local weather, but NORAPS6 has no land use model.

Two of the models that were tested (NORAPS6 and RWM) do not have options for a non-hydrostatic equation set. A non-hydrostatic model is critical in the simulation of a variety of buoyancy-driven atmospheric features. For the grid scales used in this study (46 km), neither buoyancy-driven or the oscillatory circulations would be resolved. A large thunderstorm may only be 10-20 km in diameter, and since an NWP model needs to have a circulation defined by at least four grid spaces to be handled adequately, even runs with a grid spacing of about 10 km will not be sufficiently fine to resolve these circulations. A lee wave train (an example of an oscillatory circulation) usually has a horizontal wavelength of about 20 km, so these will not be resolved well either. At the resolution used, the potential advantages of a non-hydrostatic model will be minimized.

However, as computers get faster, the spacing of the objective domain will be able to have a finer grid spacing. Once the grid spacing is reduced below the 6 nmi, a non-hydrostatic model will become necessary.

3.1.1 Grid Configuration.

The objective of these tests was to compare predicted forecasts produced by the various models. To accomplish these comparisons the computational domains were made to be as similar as possible. There is no common map projection available for all the models, so we chose projections that are appropriate for each theater and as similar as possible. RAMS uses a rotated polar-stereographic projection which

"rotates" the pole point of the projection to the center of the computational domain. This allows the use of the same projection with a minimum of distortion. MM5, NORAPS6, and RWM do not use a rotated projection; therefore, two projections had to be used in an attempt to minimize distortion. The three models used a Mercator projection for the Central America domain and a Lambert-Conformal projection for the remaining areas. The Mercator projections differed slightly, as MM5 and NORAPS6 are hardwired to use the equator as the standard latitude, and RWM uses 22.5°N.

The same computational domain or grid was used in all the tests except the objective resolutions tests. A 71 x 71 grid with nominal 46.3 km spacing was used. The gridded regions are displayed below (Figures 3-1 through 3-5). The two gridded regions for the objective tests with the nested finer resolution grids are also displayed (Figures 3-6 and 3-7). The finer grid spacing is approximately the 6 nmi objective. RAMS allows for a user-selectable spacing ratio between the grids, so it would be possible to take the coarse grid as the 25 nmi grid used in the threshold tests and use a 4-1 grid space ratio. However, both MM5 and NORAPS6 allow only a 3-1 grid space ratio. Therefore, we reconfigured the coarse grid domain with an 18 nmi spacing and ran all models with a nested grid at a 3-1 grid space ratio. Because of the finer spacing, we used 98 x 98 grid points on the coarse grid to cover the 1500 x 1500 nmi domain. Nested grids will be run with 71 x 71 grid points.

Vertical structures also differ. RAMS uses a terrain-following height coordinate and the others use a terrain-following pressure coordinate. However, even with these differences, we closely matched the "effective" resolutions of the models. Approximately twenty layers were used for each model. Some of the models may have been designed (or work better) with more levels than the target of 20. NORAPS6 is run operationally with 36. The target number of levels, while adequate in some cases, should be greater to allow for increased resolution near the ground and additional levels in the stratosphere.

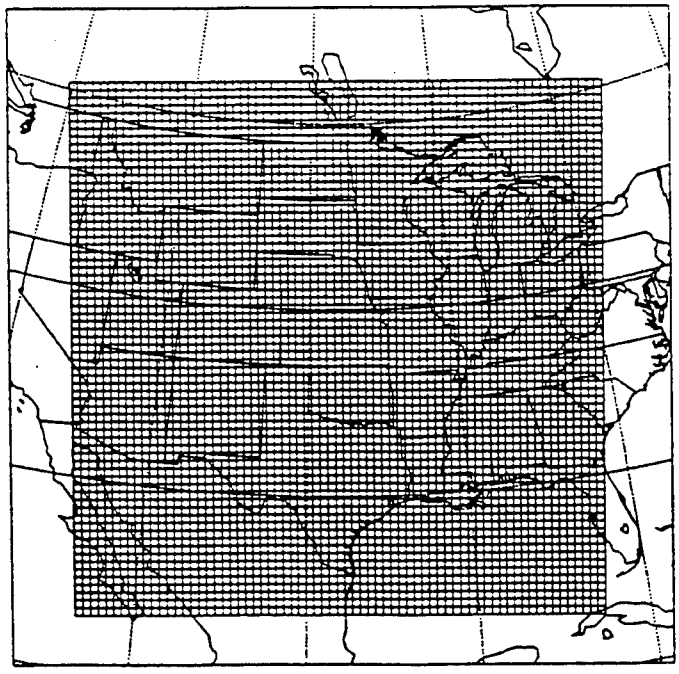

Figure 3-1. CONUS grid centered at 38 N and 98 W.

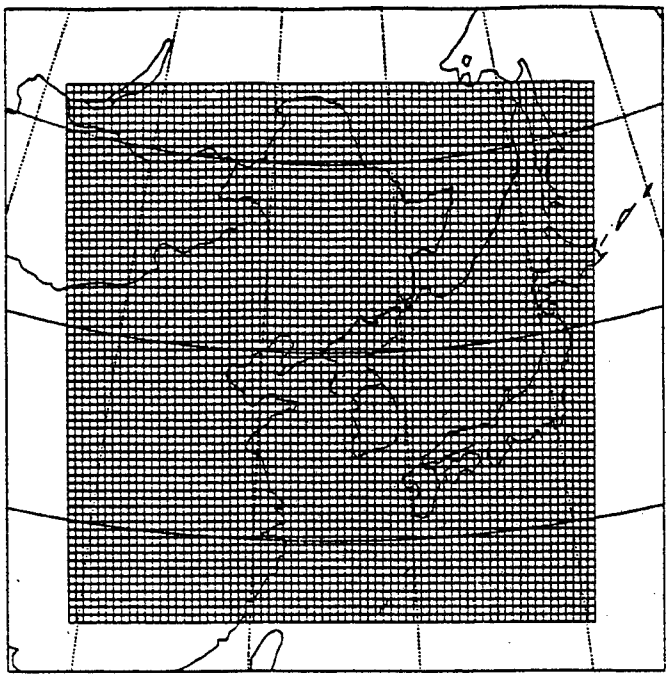

Figure 3-2. Korean grid centered at 40 N and 125 E.

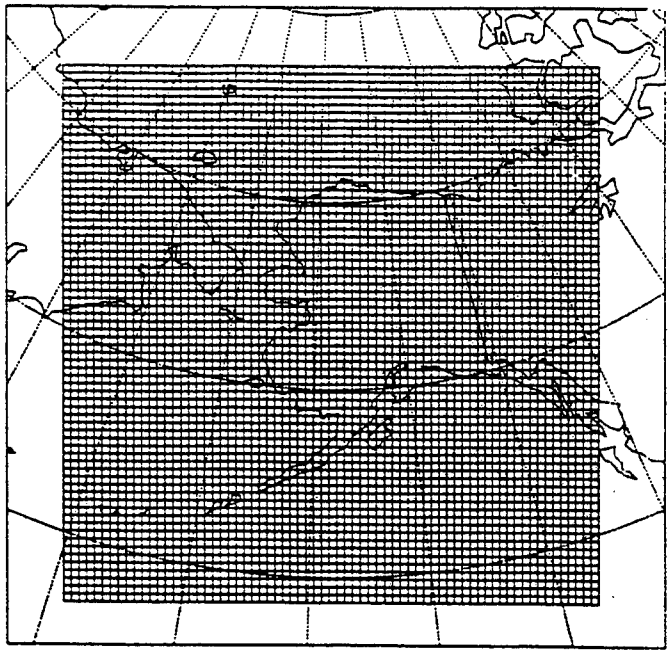

Figure 3-3. Alaskan grid centered at 63 N and 158 W.

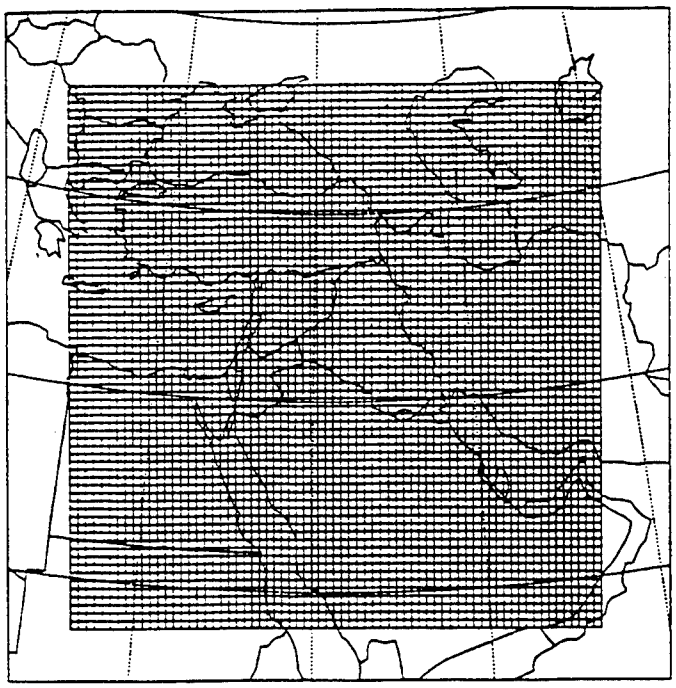

Figure 3-4. Middle Eastern grid centered at 32.5 N and 41.5 E.

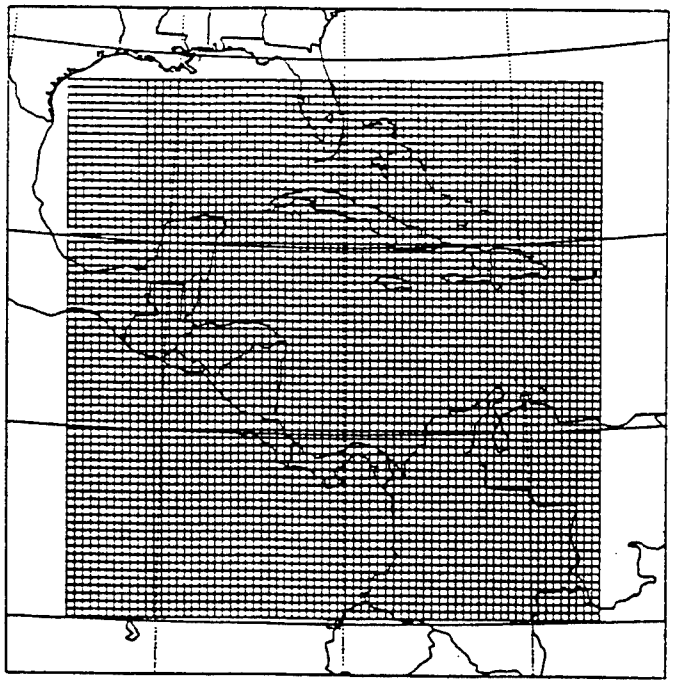

Figure 3-5. Central American grid centered at 14.6 N and 80.5 W.

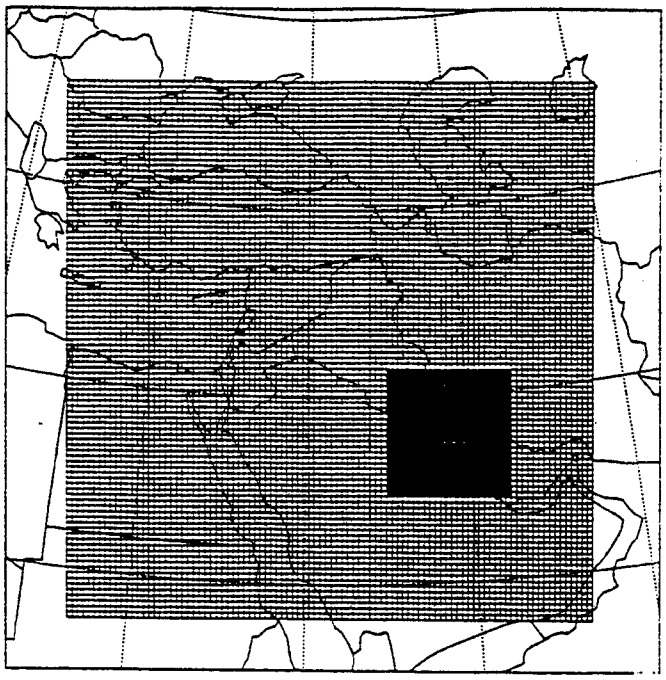

Figure 3-6. Middle Eastern grid with nested objective grid.

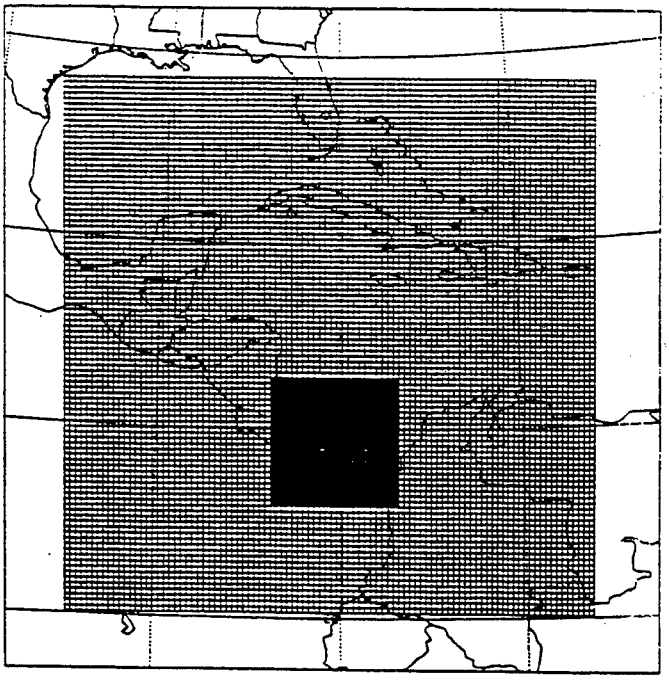

Figure 3-7. Central American grid with nested objective grid.

3.1.2 Configuration of "Physics" Parameters.

The candidate forecast models could be operated in a number of different configurations—hydrostatic, non-hydrostatic, sponge boundary, transmitive boundary, etc. The "best" and most appropriate options were selected. Since these tests were more concerned with capability than with speed, we used the most sophisticated level of parameterization available in each of the models which is consistent with the tests, tactical applications and the developer's recommendations (the model configurations were reviewed by R. Hodur (NORAPS6), S. Chen (MM5), and Captain Crasner (RWM)). Although four-dimensional data assimilation was an available option for RAMS and MM5, it was not used in the benchmark comparison tests, because the AF baseline, RWM, does not include four-dimensional data assimilation. Each model will be described briefly below.

3.2 FIFTH-GENERATION PSU/NCAR MESOSCALE MODEL (MM5).

MM5 is a regional-scale primitive equation model that can be configured hydrostatically or non-hydrostatically. It uses a terrain-following coordinate in pressure and solves its finite-difference equations with a time-split scheme using the leapfrog operator. Multiple, moving, overlapping nesting capability exists with two-way interactivity and predefined nest ratios of 3:1. Its boundary-layer physics package can be either a simple bulk aerodynamic parameterization or a more detailed scheme based upon a revised version of Blackadar's PBL model (Zhang and Anthes, 1982). The atmospheric radiation option provides longwave and shortwave schemes that interact with the atmosphere, including cloud and precipitation fields, as well as with the surface (Dudhia, 1989).

Large-scale and convective precipitation modules are included in the model, and large-scale processes are treated explicitly. Marshall-Palmer size distributions are assumed for rain and snow and solid and liquid water are allowed to co-exist. Options for deep cumulus convection include parameterizations based on Kuo (1974), and a modified Arakawa-Schubert (1974) scheme that includes moist convective-scale down draft (Grell, 1991).

3.2.1 MM5 Configuration.

Grid Projection and Vertical Levels

MM5 has polar-stereographic, Lambert conformal, and Mercator projection options. We used the Lambert conformal projection for the CONUS, Korea, Middle East, and Alaska domains and the Mercator projection for the Central America region. MM5 permits any number of vertical levels to be used. We have used 23 layers for these tests. The vertical levels selected are σ_p: 1.00, 0.99, 0.98, 0.96, 0.93, 0.89, 0.85, 0.8, 0.75, 0.7, 0.65, 0.6, 0.55, 0.5, 0.45, 0.4, 0.35, 0.3, 0.25, 0.2, 0.15, 0.1, 0.05, and 0.0.

Computational or "Physics" Options

Table 3-1. gives the physics and numeric features that are available as options in the standard version and those that we chose to activate for the tests.

Table 3-1. MM5 options.

MODEL PARAMETER	OPTIONS	USED
BASIC EQUATIONS	Hydrostatic	
	Non hydrostatic	✓
DIMENSIONALITY	3-Dimensional	
GRID	Stagger-Arakawa B-grid horizontal and vertical	✓
Spacing	Nesting-up to 10, 3:1 space ratio	
	Movable nested grids	
	Horizontal spacings used-variable-1km to 300 km	✓
INITIALIZATION	Cressman objective analysis on pressure surfaces	✓
NUMERICS		
Time differencing:	Leapfrog	✓
Advection:	2nd order leapfrog	✓
	4th order leapfrog	
COORDINATE SYSTEM		
Horizontal:	Mercator projection	✓
	Lambert-conformal	✓
	Polar stereographic	
Vertical:	Terrain-following pressure	✓
LATERAL BOUNDARY CONDITIONS	Fixed	
	Time dependent	
	Time dependent and inflow/outflow dependent	✓
	Sponge	
	Relaxation	

Table 3-1. MM5 options (Continued).

MODEL PARAMETER	OPTIONS	USED
TOP BOUNDARY CONDITIONS	Rigid	✓
	Free surface	
	Sponge	
SURFACE PARAMETERIZATIONS	Bulk PBL	
	High-resolution Blackadar PBL	✓
	BATS vegetation parameterization	✓
SUBGRID DIFFUSION PARAMETERIZATIONS	Vertical mixing in conjunction with PBL parameterization only	✓
DEEP CONVECTION PARAMETERIZATIONS	Anthes-Kuo	
	Arakawa-Schubert	
	Fritsch-Chappell	
	Kane-Fritsch	
	Grell	✓
RADIATION PARAMETERIZATIONS	Long and shortwave scheme with cloud effects	✓
	Longwave scheme with atmospheric tendencies	✓
RESOLVED CONDENSATION PARAMETERIZATIONS	Bulk microphysics parameterization with liquid and 2 ice species	✓

3.2.2 MM5 Model Source.

Two versions of MM5 were obtained: the CRAY source code from National Center for Atmospheric Research (info.ucar.edu) (downloaded August, 1994); and the workstation source code from the National Center for Atmospheric Research (info.ucar.edu) (downloaded September, 1994).

3.2.3 Execution Speed.

Because the MM5 observational data "pre-processors" had not been ported to a workstation platform when the study was conducted, all MM5 runs were made on the CRAY Y-MP's at Los Alamos. The

execution speed on the "gamma" machine averaged about 12,600 seconds, with the pre-processors taking another 1400 seconds. Assuming that the ratio between the CRAY and workstation performance on NORAPS6 (ratio = 5.17) was the same for MM5, the model run would have taken about 65,000 seconds. The possibility exists that although MM5 was developed exclusively for a CRAY, that NORAPS6 has been better optimized for a vector machine. Therefore, the workstation performance of MM5 may be better than the 65,000-second estimate.

3.2.4 Attributes Noted.

MM5 has a long history dating back to the mid-1970s at PSU and continuing through the present with development at NCAR, PSU, and other places. Some of the code have not been modified for a long time and was written in the FORTRAN 66 style of programming. This is especially true of the "pre-processors". No code existed for these data ingestion routines that allowed them to work on a workstation. At the time of the comparison study, NCAR indicated they were developing such code and a full workstation capable version should now exist. Our attempts to get the same routines to initialize the multiple grids for the objective tests were also unsuccessful. The pre-processors distributed with MM5 that accomplish the data ingestion were, at the time of the study, incapable of supporting the TFM.

From a capability standpoint, MM5 is a fairly complete model and has been run extensively over the years at the threshold resolutions.

- Weak points include :
    1. simplistic parameterization of the boundary layer does not allow elevated mixed layers,
    2. simplistic microphysics parameterization,
    3. the non-hydrostatic options are very new and have not been tested thoroughly,
    4. data analysis uses a very simple Cressman technique on pressure surfaces.

3.2.5 Model Support and Maintenance.

MM5 is copyrighted by the University Corporation for Atmospheric Research (UCAR) and is distributed by NCAR without license fees. A minimal level of support is given by NCAR if their time allows. To our knowledge, commercial support is not available.

3.3 NAVY OPERATIONAL REGIONAL ATMOSPHERIC PREDICTION SYSTEM VERSION 6 (NORAPS6).

NORAPS6 is a regional-scale, primitive equation, hydrostatic model that uses a split, explicit time integration scheme to predict dynamic and thermodynamic variables. Its grids use a terrain-following vertical pressure coordinate system. Leapfrog time and space differencing is used with a fourth-order advection scheme. Surface fluxes are modeled according to Deardorff (1972). The planetary boundary layer (PBL) is assumed to be well-mixed, so all model levels within the PBL are replaced by average values through the PBL each time the model physics routines are called; presently, the model physics routines are called every nine dynamic time steps.

Large-scale and convective precipitation modules are included in the model, and evaporation of falling precipitation is allowed to occur. Its deep cumulus convection scheme is based on the Kuo scheme, which allows deep moist convection to occur when the moisture convergence exceeds some arbitrarily specified threshold. Cloud temperatures and mixing ratios follow a moist adiabat and, so, represent a non-entraining cloud (Hodur, 1987).

3.3.1 NORAPS6 Configuration.

Projection and Vertical Levels

NORAPS6 uses polar-stereographic, Lambert conformal, Mercator, spherical, and Cartesian projection options. We used the Lambert conformal projection for the CONUS, Korea, Middle East, and Alaska domains and the Mercator projection for the Central America region. The model currently uses 36 vertical levels in its operational calculations, although the Navy previously used 21. These 21 levels guided the selection of the levels used for these tests (Hodur, personal communication). The vertical levels selected are (σ_p): 1.00, 0.98, 0.95, 0.915, 0.875, 0.825, 0.775, 0.725, 0.675, 0.625, 0.55, 0.44, 0.33, 0.22, 0.145, 0.095, 0.065, 0.035, 0.015, 0.005, and 0.000.

Computational or "Physics" Options

Table 3-2. gives the physics and numeric features available as options in the standard version and those that we chose to activate for the tests. Because NORAPS6 was developed as an operational model, there are very few options in the input data controlling the physics.

Relationship between CRAY and Workstation Version

No significant changes were required to the code as received. All components of the model compiled and ran on the workstation after acquisition of a FORTRAN 90 compiler. Minor changes in the data ingestion program were required to ingest data in our format and to remove Navy-unique data queries.

Table 3-2. NORAPS6 options.

MODEL PARAMETER	OPTIONS	USED
BASIC EQUATIONS	Hydrostatic	✓
DIMENSIONALITY	3-Dimensional	✓
GRID	Stagger-Arakawa C-grid horizontal and vertical	✓
	Nesting-1 nest, 3:1 space ratio	
	Movable nested grid	
Spacing:	Horizontal spacings used-variable-20km and greater	✓
INITIALIZATION	Multivariate optimum interpolation	✓
NUMERICS		
Time differencing:	Leapfrog	✓
Advection:	2nd order leapfrog	✓
	4th order leapfrog	
COORDINATE SYSTEM		
Horizontal:	Mercator projection	
	Lambert-conformal Polar stereographic	✓
	Spherical	
Vertical:	Terrain following pressure	✓
LATERAL BOUNDARY CONDITIONS	Fixed	
	Sponge	✓

Table 3-2. NORAPS6 options. (Continued)

MODEL PARAMETER	OPTIONS	USED
TOP BOUNDARY CONDITIONS	Rigid	✓
SURFACE PARAMETERIZATIONS	Bulk PBL parameterization	✓
	Shallow cumulus parameterization	✓
SUBGRID DIFFUSION PARAMETERIZATIONS	First or 1.5 order closure in PBL	✓
DEEP CONVECTION PARAMETERIZATIONS	Modified Kuo	✓
RADIATION PARAMETERIZATIONS	Long and shortwave scheme with cloud effects and with atmospheric tendencies	✓
RESOLVED CONDENSATION PARAMETERIZATIONS	Precipitation if relative humidity exceeds a threshold	✓

3.3.2. NORAPS6 Model Source.

Source code was received from Richard Hodur, Naval Research Laboratory, Monterey on 27 December 1994.

3.3.3 Execution Speed.

NORAPS6 was primarily run on the "gamma" CRAY Y-MP at Los Alamos National Laboratories (LANL). Comparative runs were made on the IBM RS/6000 workstation for the SESAME test cases. It took 2900 seconds for the data pre-preprocessing and 15,550 seconds for the actual forecast model run on the workstation and 1174 and 3007 seconds on the CRAY.

3.3.4 Attributes Noted.

The final version of NORAPS6 that we received was well written and had very good internal documentation, although the external documentation was dated. Because of the liberal use of CRAY FORTRAN extensions, NORAPS6 required the use of either a CRAY or a FORTRAN 90 compiler. The port to a UNIX workstation was easily accomplished.

- Weak points include :
  1. simplistic parameterization of the boundary layer, does not allow for elevated mixed layers,
  2. no microphysics parameterization; water above saturation falls to next level and evaporates,
  3. no non-hydrostatic option, and
  4. data analysis does not use moisture observations, only interpolation from large scale field.

3.3.5 Model Support and Maintenance.

NORAPS6 was developed by the Navy and is being replaced by the Coupled Ocean Atmosphere Mesoscale Prediction System (COAMPS) model development. Commercial support is unavailable.

3.4 REGIONAL ATMOSPHERIC MODELING SYSTEM (RAMS).

RAMS is a regional-scale primitive equation model that can be configured hydrostatically or non-hydrostatically. The model uses a terrain-following coordinate in height, and its finite-difference equations are solved with a time-split scheme using an optional hybrid time-differencing operator. This allows desirable characteristics of the leapfrog operator to be used on velocity and pressure variables, while reserving the "forward-in-time" operator for all other variables. Multiple, moving, two-way grid nesting capability exists with two-way interactivity.

RAMS's boundary-layer physics package is based on similarity theory. Its atmospheric radiation option provides longwave and shortwave schemes that interact with the atmosphere including cloud and precipitation fields, as well as with the surface.

Large-scale and convective precipitation modules are included in the model, and large-scale processes are treated explicitly. A range of options exists when specifying how the microphysics are modeled, and mixed-phase microphysics is allowed. There are also two options for the deep cumulus convection scheme.

3.4.1 RAMS Configuration.

Projection and Vertical Levels

RAMS has rotated polar-stereographic and Cartesian options. We used the rotated polar stereographic projection which rotates the "pole" point of the polar-stereographic projection to any point on the globe, typically the center of the model domain, to minimize distortion anywhere on the Earth without having to deal with many different projections. The required vertical zoning was achieved. The vertical levels selected are shown in Table 3-3.

Table 3-3. RAMS vertical levels.

z (m)	p (Pa)
46.7	100586.7
160.7	99260.7
309.0	97561.8
501.7	95393.4
752.2	92641.7
1077.8	89175.5
1501.1	84849.2
2051.5	79509.9
2766.9	73018.0
3706.2	65185.9
4852.7	56561.3
6061.9	48468.1

Table 3-3. RAMS vertical levels.

7261.9	41359.2
8461.9	35088.5
9661.9	29591.3
10861.9	24812.6
12061.9	20690.3
13261.9	17159.4
14461.9	14167.1
15661.9	11653.5
16861.9	9554.6

Computational or "Physics" Options

Table 3-4 gives the physics and numeric features available as options in the standard version and those that we chose to activate for the tests.

Table 3-4. RAMS options.

MODEL PARAMETER	OPTIONS	USED
BASIC EQUATIONS	Hydrostatic time-split	
	Non-Hydrostatic time-split	✓
DIMENSIONALITY	3-Dimensional	✓
	2-Dimensional	
	1-Dimensional	
GRID	Stagger-Arakawa C-grid horizontal and vertical	✓
	Nesting-any number, any integer space and timestep ratio	
	Movable nested grids	
Spacing:	Horizontal spacings used-variable-2cm to 300km	✓
INITIALIZATION	Single sounding	
	Hybrid isentropic/terrain-following objective analysis package	✓
NUMERICS		
Time differencing:	Forward-backward	
	Leapfrog	
	Hybrid (combination of leapfrog and forward-backward	✓
Advection:	2nd order leapfrog	✓
	4th order leapfrog	
	2nd order forward	✓
	6th order forward	

Table 3-4. RAMS options (Continued).

MODEL PARAMETER	OPTIONS	USED
NUMERICS		
Time differencing:	Forward-backward	
	Leapfrog	
	Hybrid (combination of leapfrog and forward-backward	✓
Advection:	2nd order leapfrog	✓
	4th order leapfrog	
	2nd order forward	✓
	6th order forward	
COORDINATE SYSTEM		
Horizontal:	Cartesian	
	Rotated polar stereographic	✓
Vertical:	Cartesian	
	Terrain-following height	✓
LATERAL BOUNDARY CONDITIONS		
Radiative conditions	Orlanski	
	Klemp-Lilly	
	Klemp-Wilhelmson	✓
Nudging conditions:	Davies	✓
TOP BOUNDARY CONDITIONS	Klemp-Durran gravity wave radiative	
	Damping layer (Rayleigh friction)	
	Nudging layer	✓
SURFACE PARAMETERIZATIONS	Similarity theory surface layer	✓
	Multi-layer (usually 5-12) soil temperature / moisture	✓
	Vegetation	✓
SUBGRID DIFFUSION PARAMETERIZATIONS	Mellor-Yamada turbulent kinetic energy closure	✓
	Deardorff turbulent kinetic energy closure	
	Deformation/stability-based closure	
DEEP CONVECTION PARAMETERIZATIONS	Modified Kuo	✓
	Modified Fritsch-Chappell	
	Weissbluth	
RADIATION PARAMETERIZATIONS	Long and shortwave scheme with cloud effects and with atmospheric tendencies	✓
	Long and shortwave scheme without cloud effects and with atmospheric tendencies	

Table 3-4. RAMS options (Continued).

MODEL PARAMETER	OPTIONS	USED
RESOLVED CONDENSATION PARAMETERIZATIONS	Bulk microphysics parameterization with liquid and up to 5 ice species	✓
	Bin-resolving microphysics with 32 size bins for liquid	

Relationship between CRAY and Workstation Version

RAMS is highly portable. The same version was tested and used on both platforms, although most runs were performed on the workstation.

3.4.2 RAMS Model Source.

RAMS Version 3B was obtained from the ASTeR Division of MRC, in September 1994.

3.4.3 Execution Speed.

Because of the level of physics used, RAMS averaged about 31,500 CPU seconds on the IBM RS/6000 Model 370 workstation for a 36 hour forecast run (about 24.3% of real time). The data analysis and initialization took an additional 35 minutes.

3.4.4 Attributes Noted.

RAMS development dates back to the early 1970s, but the vast majority of the code has been kept up to date, with a re-write started in 1986.

- Weak points include :
  1. longer execution times than RWM and NORAPS6 due to more complex physical parameterizations,
  2. simple Barnes analysis used for data analysis, although performed on isentropic and terrain-following coordinates.

3.4.5 Model Support and Maintenance.

RAMS is copyrighted by CSU, who have licensed MRC as the exclusive distributor. The model is supported and maintained by MRC.

3.5 RELOCATABLE WINDOW MODEL (RWM).

The RWM is a regional-scale primitive equation model that uses a quasi-Lagrangian advection scheme to predict u and v wind components, potential temperature, surface pressure and specific humidity. It employs a single, unstaggered horizontal grid and uses a terrain-following vertical coordinate system.

RWM uses a basic boundary-layer physics package in which bulk transfers of sensible and latent heat are allowed over the ocean when the sea surface temperature is greater than the air temperature and surface

friction is modeled with a terrain-dependent drag coefficient. Large-scale and convective precipitation modules are included in the model, and evaporation of falling precipitation is allowed to occur. Its deep cumulus convection scheme is based on the Kuo scheme, which allows deep moist convection to occur when a saturated parcel originating in the lower atmosphere can rise through at least two contiguous vertical layers above the Lifting Condensation Level (LCL). RWM did not account for land surface processes, diagnosed cloud fraction and solar/terrestrial radiative processes until recently with the inclusion of the Swedish physics package.

3.5.1 RWM Configuration.

Projection and Vertical Zoning

RWM has polar-stereographic, Lambert conformal, and Mercator projections available. We used the Lambert conformal projection for the CONUS, Korea, Middle East, and Alaska domains and the Mercator projection for the Central America region. The vertical levels selected are (σ_p): 1.00, 0.98, 0.95, 0.915, 0.875, 0.825, 0.775, 0.725, 0.675, 0.625, 0.55, 0.44, 0.33, 0.22, 0.145, 0.095, 0.065, 0.035, 0.015, 0.005, and 0.000.

Computational or "Physics" Options

Table 3-5. gives the physics and numeric features available in RWM. The model is an operational model with no user options.

Table 3-5. RWM options.

MODEL PARAMETER	**OPTIONS**	**USED**
BASIC EQUATIONS	Hydrostatic	✓
DIMENSIONALITY	3-Dimensional	✓
GRID	Stagger-none	✓
	Nesting-none	
Spacing:	Horizontal spacings used-variable-40km and greater	✓
INITIALIZATION	Optimum interpolation	✓
NUMERICS		
Time differencing:	Leapfrog	✓
Advection	2nd order leapfrog	✓
COORDINATE SYSTEM		
Horizontal	Mercator projection	✓
	Lambert conformal	✓
	Polar stereographic	
Vertical:	Terrain following pressure	✓
LATERAL BOUNDARY CONDITIONS	Relaxation	✓
TOP BOUNDARY CONDITIONS	Rigid	✓
SURFACE PARAMETERIZATIONS	Multi-level PBL parameterizations	✓
SUBGRID DIFFUSION PARAMETERIZATIONS	Deformation-based closure	✓

Table 3-5. RWM options. (Continued)

MODEL PARAMETER	OPTIONS	USED
DEEP CONVECTION PARAMETERIZATIONS	Kuo	✓
RADIATION PARAMETERIZATIONS	Long and shortwave scheme with cloud effects and with atmospheric tendencies	✓
RESOLVED CONDENSATION PARAMETERIZATIONS	Precipitation if relative humidity exceeds a threshold	✓

Computational Flow and Relationship between CRAY and Workstation Version

The model was run only on the workstation. However, not all data ingestion routines operate on this platform and AF personnel and AFGWC accomplished this data preparation. These routines are associated with grid dependent quantities and not the meteorological data.

3.5.2 RWM Model Source.

Source code for RS/6000 was received September 1994 on tape from AFGWC with sample run for 25 April 1994.

The Matthews' Vegetation Data was obtained from the National Center for Atmospheric Research (ftp.ucar.edu, ds765.0) and was downloaded August 1994.

The Soil Data was obtained from the National Center for Atmospheric Research (ftp.ucar.edu, ds776.0) and was downloaded August 1994.

3.5.3 Execution Speed.

The execution speed for RWM on the IBM RS/6000 Model 370 workstation was about 9,900 CPU seconds for each 36 hour forecast (7.6% of real time). The data analysis took an additional 10 minutes.

3.5.4 Attributes Noted.

RWM is a modified version of the QNGM model developed by M. Mathor (Mathor, 1983) at National Meteorological Center (NMC) in the late 1970s and early 1980s. There were two versions developed. One with and one without the ability to add a nested grid. RWM is the version without this capability. Only recently (within the last two years) has a diurnal cycle and surface physical parameterizations been included in the model. Several of the model initialization routines only run on a CRAY running the COS operating system and have not been ported to any other platform.

- Weak points include :
  1. simplistic parameterization of the boundary layer, does not allow for elevated mixed layers,
  2. no microphysics parameterization,
  3. no non-hydrostatic option.

3.5.5 Model Support and Maintenance.

RWM was developed originally by the National Meteorological Center as the QNGM, but was subsequently abandoned by NMC. AFGWC is the only user and developer of this code. Commercial support is unavailable.

3.6 RAMS EVALUATION AND VERIFICATION UTILITIES (REVU).

The statistical package we used for model intercomparison incorporated software and routines that are part of REVU, making the assessment of each atmospheric model's performance possible. REVU was modified to incorporate the various mean quantities required at each pressure level and to develop a histogram distribution of the errors.

3.6.1 Mean Errors.

A series of six statistical parameters was calculated. These quantities measured the error in the predicted field at an observation point. The quantities were summed over all observations at a specific vertical level. The ten vertical levels used are surface, 1000 mb, 850 mb, 700 mb, 500 mb, 400 mb, 300 mb, 250 mb, 200 mb, 150 mb, and 100 mb.

Statistics were generated at initialization and at all forecast times (00, 12, 24, and 36 hours). The statistical parameters calculated were:

Root Mean Square Error (RMSE)

$$\left[\sum_{i=1}^{n}\frac{\left(\Phi_p^i-\Phi_o^i\right)^2}{n}\right]^{1/2} \tag{3.1}$$

Mean Absolute Error

$$\frac{\sum_{i=1}^{n}\left|\Phi_p^i-\Phi_o^i\right|}{n} \tag{3.2}$$

Mean Relative Error

$$\frac{\sum_{i=1}^{n}\left(\Phi_p^i-\Phi_o^i\right)}{n} \tag{3.3}$$

Bias (Mean Normalized Bias)

$$\frac{\sum_{i=1}^{n}\left[\left(\Phi_p^i - \Phi_o^i\right) \Big/ \Phi_o^i\right]}{n} \tag{3.4}$$

Correlation Coefficient

$$\frac{\sum_{i=1}^{n}\left[\left(\Phi_p^i - \overline{\Phi}_p\right)\left(\Phi_o^i - \overline{\Phi}_o\right)\right]}{\left\{\left[\sum_{i=1}^{n}\left(\Phi_p^i - \overline{\Phi}_p\right)^2\right]\left[\sum_{i=1}^{n}\left(\Phi_o^i - \overline{\Phi}_o\right)\right]^2\right\}^{1/2}} \tag{3.5}$$

Root Mean Square Vector Error (RMSVE)

$$\left\{\sum_{i=1}^{n}\frac{\left[\left(u_p^i - u_o^i\right)^2 + \left(v_p^i - v_o^i\right)^2\right]}{n}\right\}^{1/2} \tag{3.6}$$

where Φ is a scalar variable, u and v are wind components, n is the total number of i observations, subscript p = predicted, subscript o = observed, and a bar indicates the arithmetic average of the quantity.

These five statistics were calculated for each model for each of seven model-predicted variables. These seven variables were:

- Specific Humidity (q)
- Zonal Wind Component (u)
- Meridional Wind Component (v)
- Temperature (t)
- Sea Level Pressure (slp)
- Geopotential height (z)
- Relative Humidity (rh)

The amount of data generated with this routine is huge and will be available from DSWA on magnetic media.

3.6.2 Distribution Histogram.

The mean data generated in the previously described part of REVU emphasize the pressure levels and not the number of observations. The mean quantities also do not indicate how often the required computational accuracy is achieved. To provide this data, REVU was modified to generate error distribution for the following variables: temperature, surface pressure, dew point depression, wind speed under 20 knots, wind speed over 20 knots, and wind direction. Each of these quantities has an established criterion. They are "air temperature and dew point depression within 2 degrees, wind speed within 2 knots at speeds less than 20 knots and within 5 knots at speeds greater than 20 knots, wind direction within 30 degrees, and surface pressure within 1.7 millibars" (SOW, see section 2.5.4.). These criteria were used to establish the central bin boundaries. Observation-prediction pairs in the central bin met the AF criteria. These histograms are based on the total number of observations available in a given set of runs. Both 36 hour forecasts were merged as were all forecast times. The dominance of surface observations was precluded by generating two sets of histograms, one for the surface and one for all the pressure levels.

3.7 HARDWARE.

All testing was conducted on one of two platforms, the DSWA CRAY at Los Alamos and an IBM, RS/6000 workstation located at MRC, Fort Collins. Personnel from MRC, Santa Barbara, performed the tests run on the CRAY. The following is a description of the hardware/compiler and procedures we used for these platforms.

3.7.1 CRAY.

The DSWA CRAY supercomputer used for the majority of the calculations was LANL machine "gamma," or specifically gamma.lanl.gov. This machine is a CRAY Y-MP with an extraordinary two gigawords of memory. During testing this computer was subjected to extreme loads and the alternative LANL machine "rho" was used for some runs. It is a CRAY Y-MP M64 and runs ~20-33 percent faster than gamma.

While the candidate CWS models are written in FORTRAN, some adhere to more standard syntax rules than others. The RAMS-3b code used is entirely f77 code; the NORAPS6 code, on the other hand, contains some f90 extensions. The "cf77" compiler on the LANL CRAY, has a sufficient number of f90 extensions to compile all of the candidate CWS models and was used.

The execution time or CPU provided by the DSWA facility includes a term that is related to the amount of job swapping that the machine must perform. A job run when the machine is nearly idle would take less CPU time than the same job run when the machine is busy. The reported CPU times are average execution times.

3.7.2 IBM RS/6000 Workstation.

The workstation used for these tests is an IBM RS/6000 Model 370 with 128 Mb of central memory and 4 Gb of attached disk storage. The operating system is IBM's UNIX variant, AIX, at revision level 3.2.5. Since both NORAPS6 and MM5 use various CRAY-specific, FORTRAN constructs, version 3.2 of the AIX FORTRAN compiler was needed to minimize the number of code changes. This compiler is a full FORTRAN 90 implementation. Fortunately, many of the non-standard CRAY extensions to FORTRAN

77 have been included in the FORTRAN 90 standard. The one extension that would have caused the most code modifications to NORAPS6 and MM5 was the concept of "automatic" arrays. These are arrays that are local to a routine (not a routine argument) that are dimensioned by arguments passed to the routine. The arrays are automatically dynamically allocated upon entrance to the routine and deallocated upon exit from the routine. Since FORTRAN 77 had no concept of dynamic allocation, modification of the codes for a FORTRAN 77 compiler would have been difficult.

SECTION 4
TESTS RESULTS

In this section, the results of the various threshold tests, the data denied tests, and the objective tests are presented. The amount of available data required that only a fraction of the tests could be presented. In general, the forecast maps were compared at 24 hours and significant differences noted in the phenomenology results. Maps for some of the differences noted are provided for illustration. The histograms of errors are provided for each of the threshold forecast test sets.

4.1 THRESHOLD TESTS AND RESULTS.

4.1.1 SESAME 1 – CONUS.

4.1.1.1 Objective. This test was used to verify correct operation of the models on both the CRAY and the workstation and measure model performance in the CONUS.

4.1.1.2 Description. AVE-SESAME I (Atmospheric Variability Experiment—Severe Environmental Storms and Mesoscale Experiment) took place on 10-11 April 1979. A vigorous shortwave over Colorado induced strong cyclogenesis centered over eastern Colorado. The resultant strong surface warm air advection over the lower Midwest, combined with cold air advection aloft and a favorable wind shear pattern, spawned a major tornado outbreak in Texas and Oklahoma. General thunderstorm activity was also observed over the Midwest. The three day period selected was 9 Apr 79 1200 UTC through 12 Apr 79 1200 UTC.

4.1.1.3 Data Source. NMC gridded data are contained within the NCAR data archives in ds082.0, tape K6838K. The rawinsonde data are in ds353.4, tape K1101K while the surface observations at 0 UTC and 12 UTC are in ds464.0, tape K0712K.

4.1.1.4 Phenomenological Results – SESAME. Phenomenology results 24 hours into the first forecast period (10 Apr 79 – 1200 UTC).

Surface

At 24 hours into the forecast, the surface front had progressed down to the Gulf coast. NORAPS6 had predicted the front in a good position at the coast, but with a steeper gradient than was observed. It also had similar gradients along the boundary in central Mexico. RWM and MM5 predicted good location and strength compared to the data analysis. However, RWM produced an area of anomalous strong heating on the lee of the Rockies in western Nebraska. The RAMS frontal gradient was well located, but was more diffuse through Texas and Oklahoma than observed.

RWM, RAMS, and MM5 all produced widespread fog and low-level clouds over the central plains, which was moister than observed. NORAPS6 hit a maximum of about 88 percent relative humidity.

A surface low of 988 mb was located over western Colorado at this time. RAMS had the low well placed with a central pressure of 982 mb, with the discrepancy possibly due to differences in sea level pressure reduction differences. MM5 had its low center in northwestern Wyoming at 986 mb. RWM

also had a 986 mb low center, but in central Colorado. Its center was much more diffuse than observed. NORAPS6 had a 999 mb low pressure center well north over the Wyoming/Montana border. Its entire sea level pressure field demonstrated a high bias of several millibars. Figures 4-1(a - e) show the analysis and model results for the surface pressure.

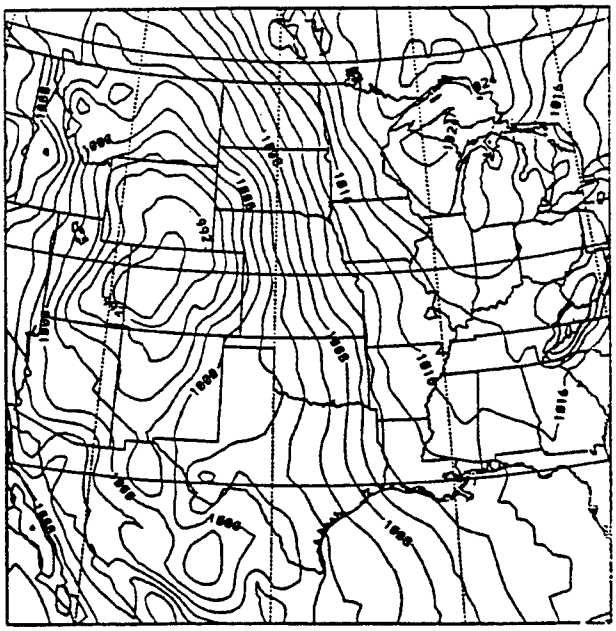

sea level pressure (mb)

(a) Analysis at 24 hours

Figure 4-1. Surface Pressure.

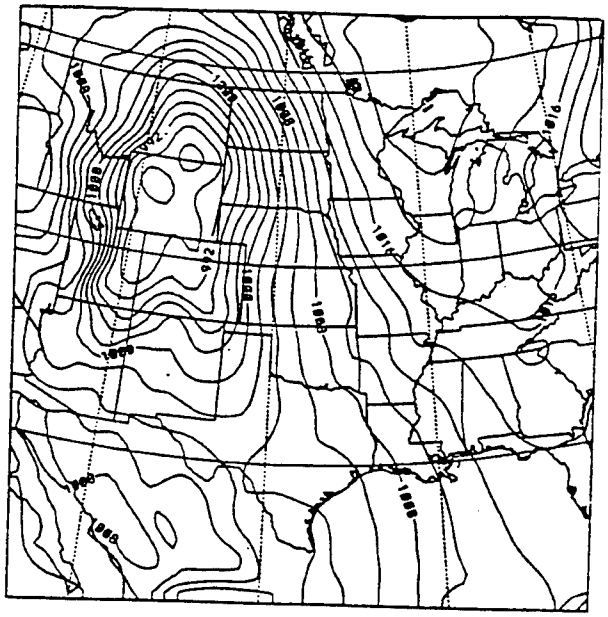

(b) MM5 - 24 hour forecast

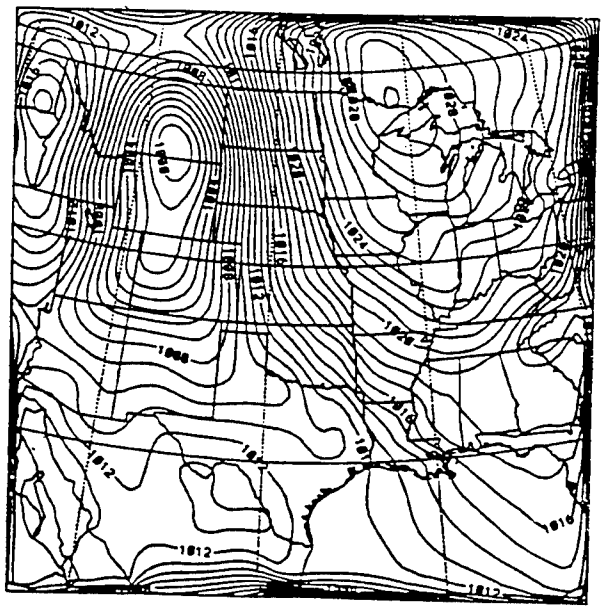

(c) NORAPS6 - 24 hour forecast

Figure 4-1. Surface Pressure. (Continued)

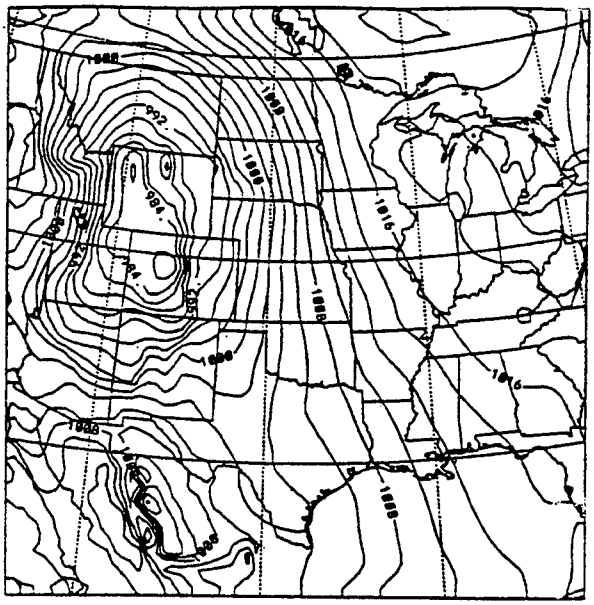

(d) RAMS - 24 hour forecast

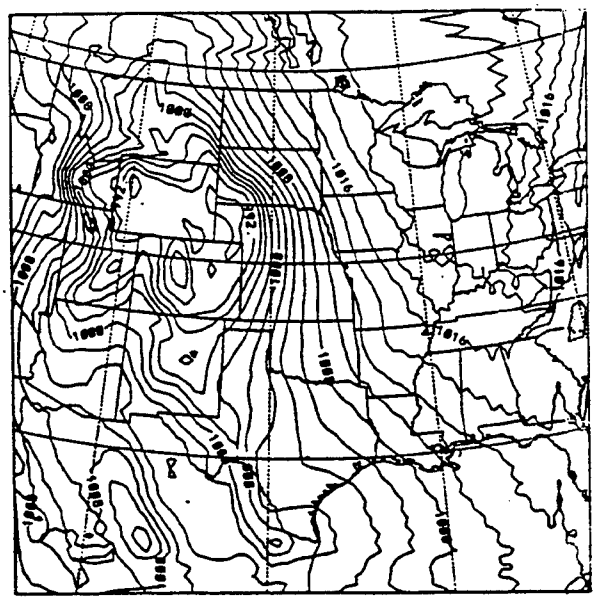

(e) RWM - 24 hour forecast

Figure 4-1. Surface Pressure. (Continued)

Upper Air

At 24 hours and 500 mb, the observed jet streak with a core of about 28 m/s was over northeastern Texas and southeastern Oklahoma at 1200 UTC. RAMS predicted the location of the core at a good location with strength of 26 m/s. MM5 predicted a "noisier" streak, probably due to vertical momentum transport in the convective parameterization. RWM under-predicted the streak with no well-defined core and strength of 22 m/s in the same area. NORAPS6 over-predicted the streak with a maximum strength of 34 m/s and a location too far to the south over southeastern Texas. Figures 4-2(a - e) show the analysis and calculated velocity fields at 500 mb.

Associated with this jet streak was a shortwave trough with an axis WNW to ESE over the central plains.

MM5 did a good job with the location and amplitude of the trough. RAMS and RWM under-predicted the trough while NORAPS6 over-predicted amplitude and had a slower movement of the trough than observed. The entire geopotential field of NORAPS6 also exhibited a high bias.

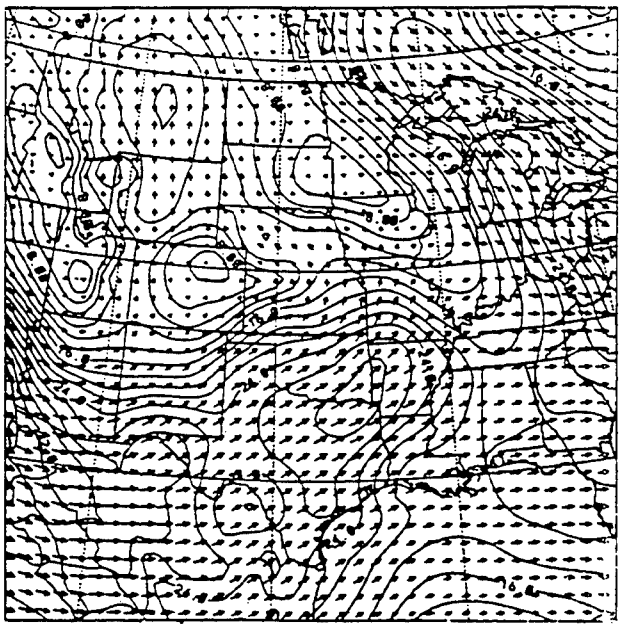

(a) Analysis at 24 hours

Figure 4-2. 500mb wind velocity.

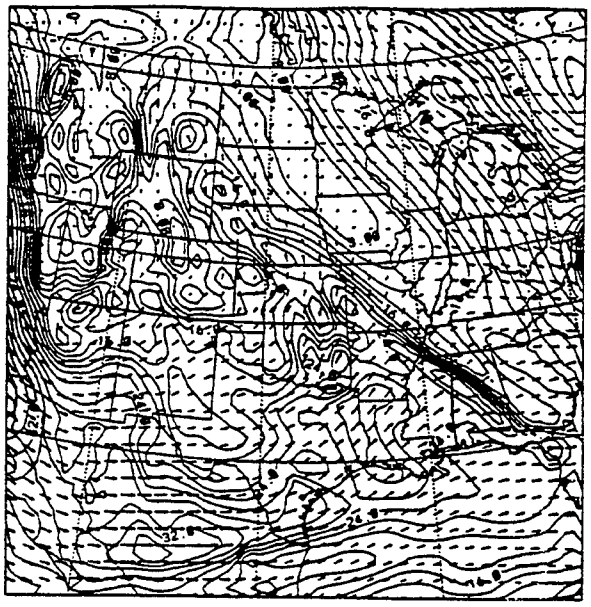

(b) MM5 - 24 hour forecast

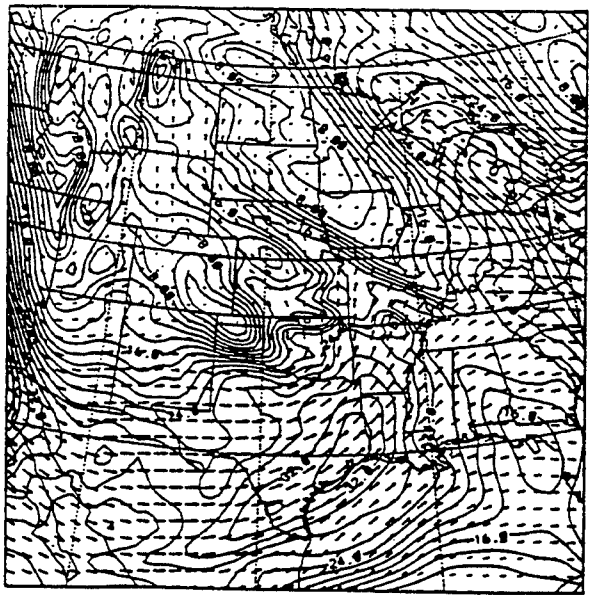

(c) NORAPS6 - 24 hour forecast

Figure 4-2. 500mb wind velocity. (Continued)

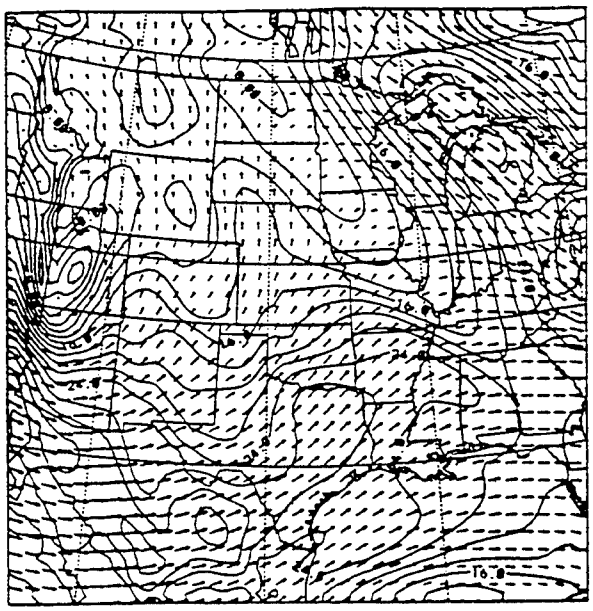

(d) RAMS – 24 hour forecast

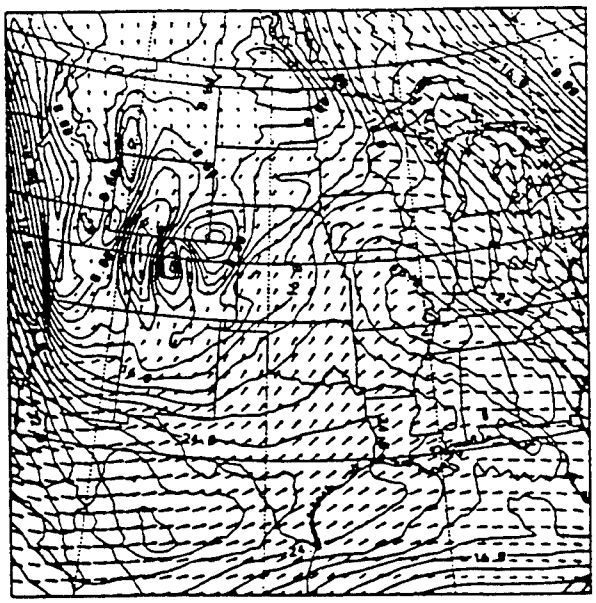

(e) RWM - 24 hour forecast

Figure 4-2. 500mb wind velocity. (Continued)

Phenomenology results 24 hours into the second forecast period (12 Apr 79 – 0000 UTC).

Surface

At 0000 UTC on 12 April, the main gradient of the surface front was located in central plains, extending from Indiana through Illinois, Iowa, and into Nebraska. All models did a relatively good job in the location and strength of the front. To the north of the front, RWM, NORAPS6, and MM5 all produced low level clouds, while RAMS showed a moist region, but not quite saturated, in the same location. The main difference produced by the models was in their handling of a "dry line" in the southern plains, extending north to south through Oklahoma and Texas. Dry lines are favored locations for convective development. The observed dry line had a strong moisture gradient with relative humilities of 20 percent in central Texas to 80 percent in eastern Texas. RWM did not predict the dry air to the west, producing a gradient of 72 percent to 96 percent through Texas. NORAPS6 produced a rather diffuse dry line of 45 percent to 72 percent through the area. MM5 predicted a good location with a gradient of 40 percent to 90 percent. RAMS produced both good location and strength with a gradient of 25 percent to 70 percent. Figures 4-3(a - e) show the analysis and computed relative humidity fields on the surface.

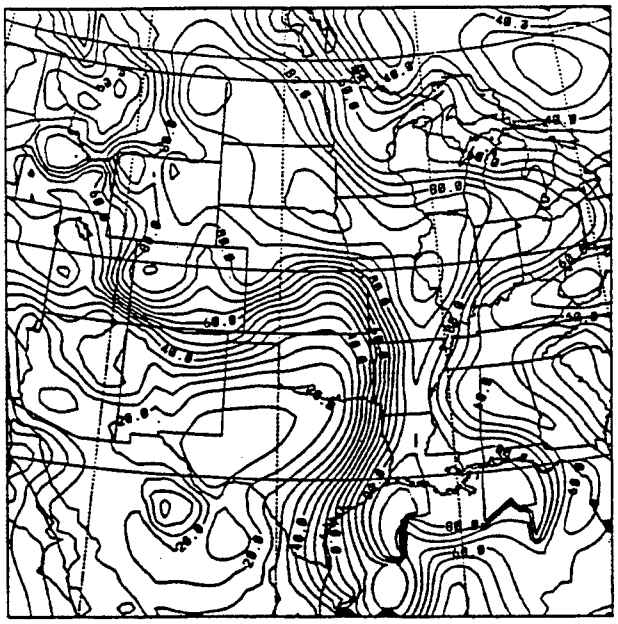

(a) Analysis at 24 hours

Figure 4-3. Surface relative humidity.

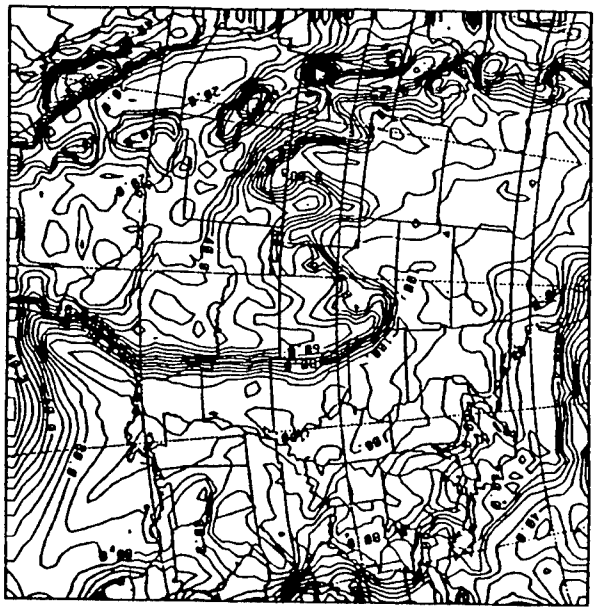

(b) MM5 - 24 hour forecast

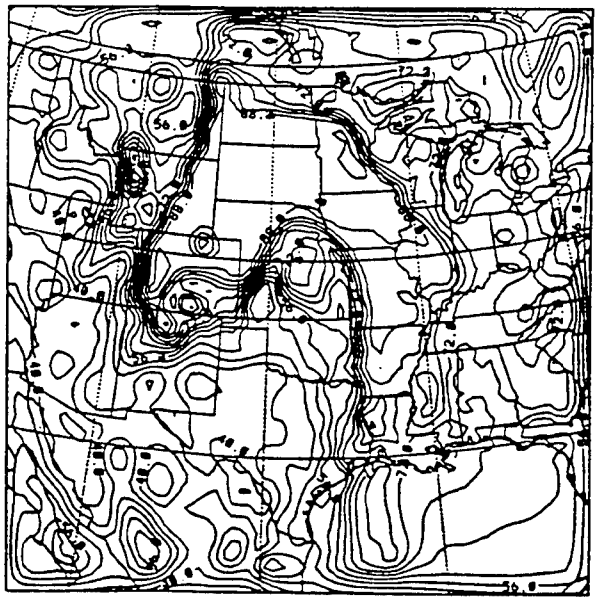

(c) NORAPS6 - 24 hour forecast

Figure 4-3. Surface relative humidity. (Continued)

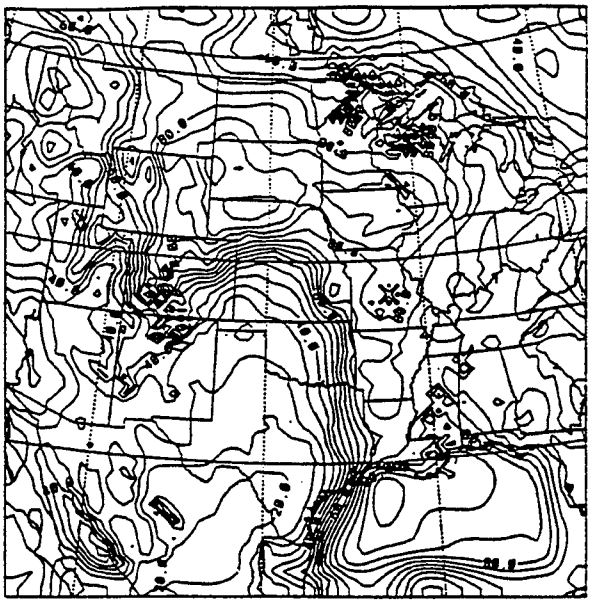

(d) RAMS – 24 hour forecast

(e) RWM - 24 hour forecast

Figure 4-3. Surface relative humidity. (Continued)

The surface synoptic flow was dominated by a large low-pressure system with an observed center of 986 mb in central Kansas. All models were slow in movement of the center, with the locations in western Kansas and eastern Colorado. NORAPS6, as with the previous 36-hour period, produced a field that had a high bias with a low center of 992 mb. RWM produced a numerically "noisy" field with a center of 986 mb. Both RAMS and MM5 had central pressures of 981 mb.

Upper Air

The main feature in the upper level flow was a closed cutoff low center over western Nebraska and northeastern Colorado with a central geopotential height of 5370 m. All models generally predicted a good location. RWM and MM5 predicted too low a central height, 5340 and 5310, respectively, with RWM, again, producing a noisy field. NORAPS6 and RAMS predictions were not as low as the observed height, both were at approximately 5400m.

4.1.1.5 Statistical Results. Error frequency distributions were generated for temperature, surface pressure, dew point depression, wind speed below 20 knots, wind speed above 20 knots, and wind direction. Data from all forecast times, and where appropriate, levels were merged. The central column corresponds to the desired error bounds. Two sets of figures were developed to describe the forecast results. One is a surface set that includes the large number of surface observations and the other is an upper air set that includes the more sparse upper air observations. Figures 4-4(a - f) are the surface results and Figures 4-5(a - e) are the upper air results.

4.1.2 August 1994 - Alaska, Korea, Central America, Middle East Theaters.

4.1.2.1 Objective. To compare the 36 hour forecasts from the candidate models in a number of representative regions or theaters, data will be obtained from the historical files at NCAR for August of 1994. Four regions or theaters will be computed: Alaska, Central America, Korea, and the Middle East.

4.1.2.2 Description. The period from 0 UTC 16 August 1994 to 0 UTC 19 August 1994 was selected. From the 500 mb hemispheric maps, a shortwave trough crossed over the Korean peninsula by 0 UTC 18 August and a separate shortwave passed over and exited Alaska by 0 UTC 19 August. These upper level shortwaves should have surface frontal systems and other interesting weather effects associated with them. The same period was used for the Middle East and Central America. No preferred days were noted for these regions as all the days were meteorologically similar. A more interesting period (10-12 August), with similar but stronger shortwaves, was not selected because NMC lost the gridded data for this period.

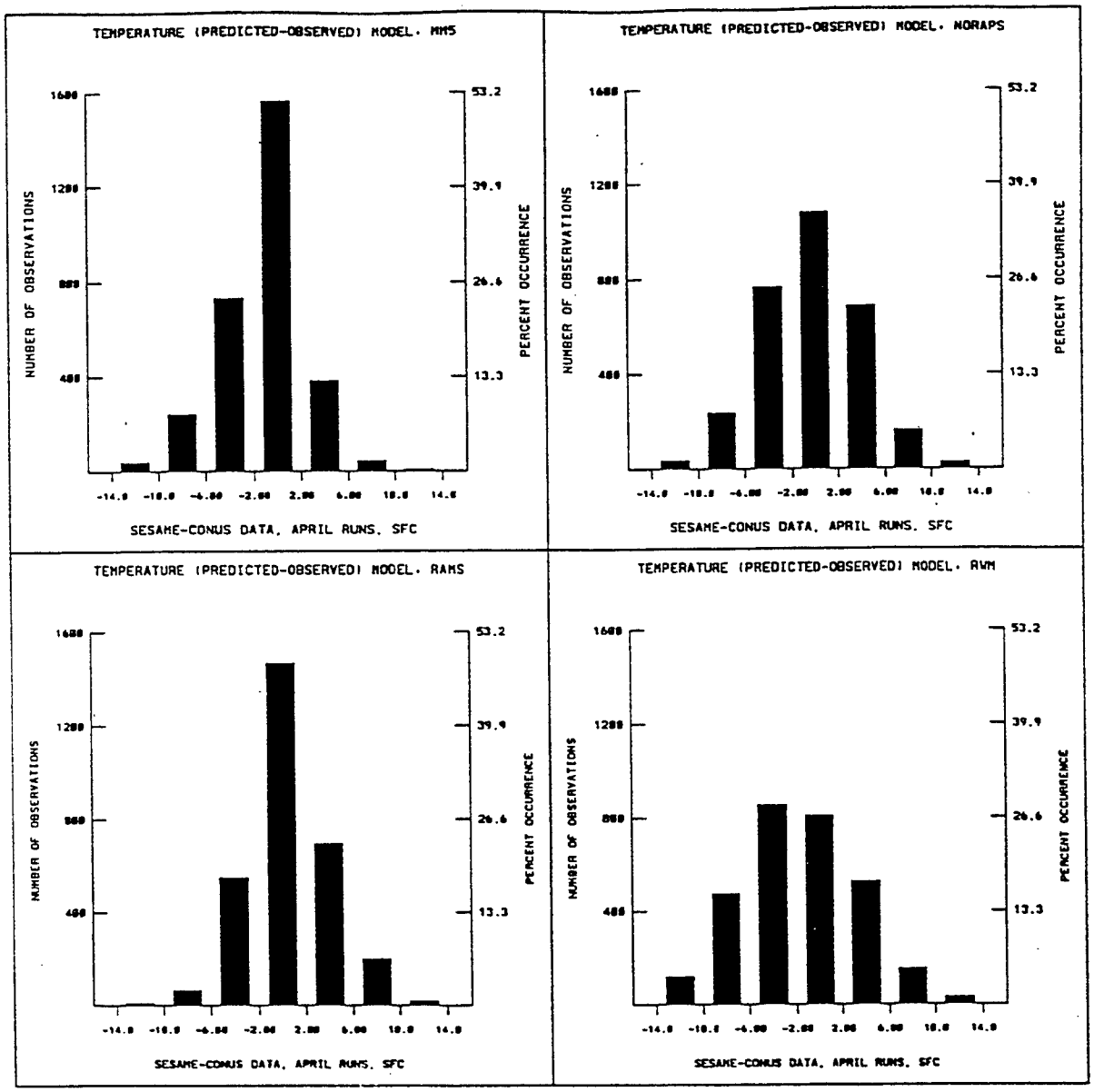

(a) CONUS temperature

Figure 4-4. Surface error statistics.

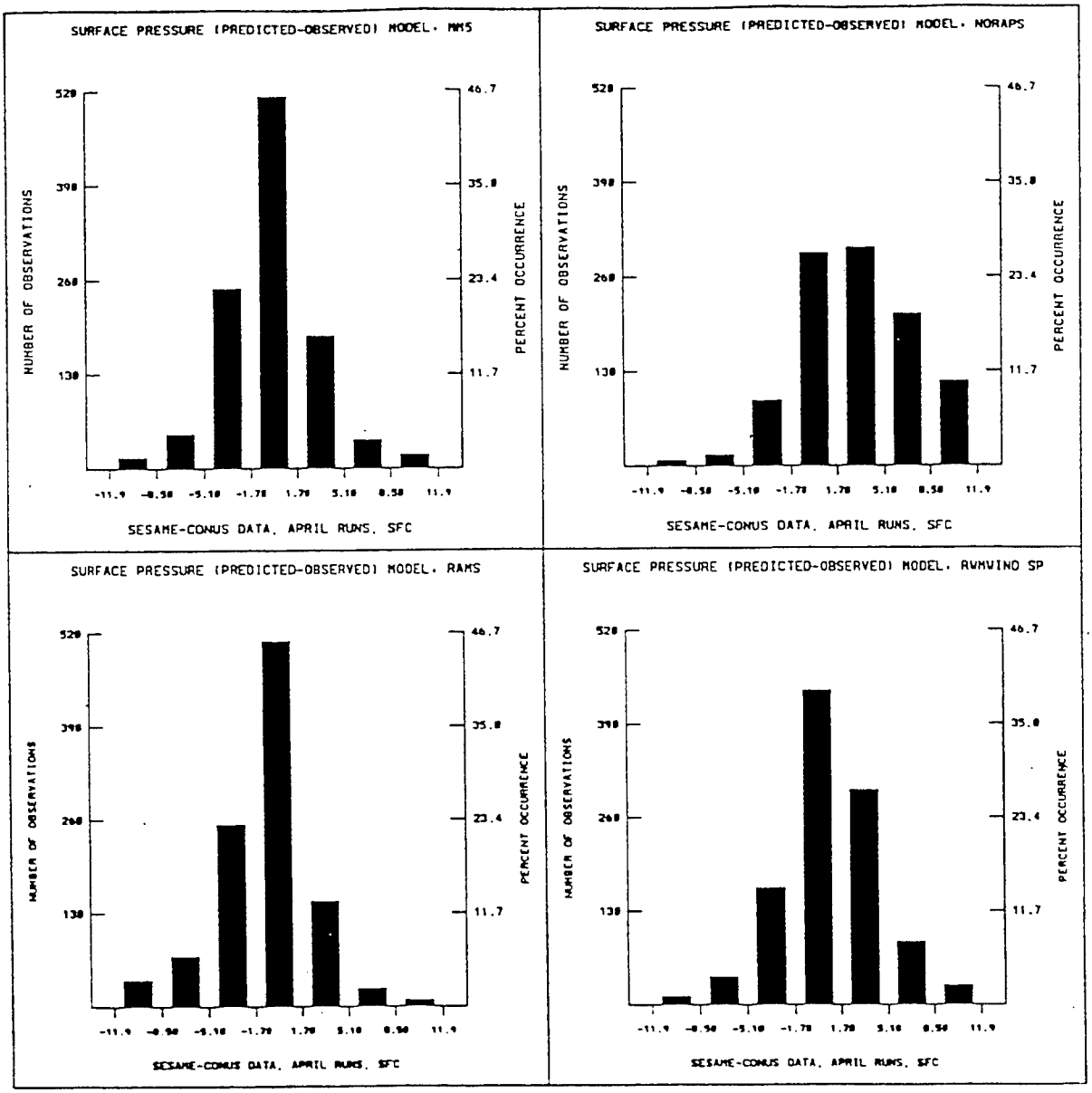

(b) CONUS pressure

Figure 4-4. Surface error statistics. (Continued)

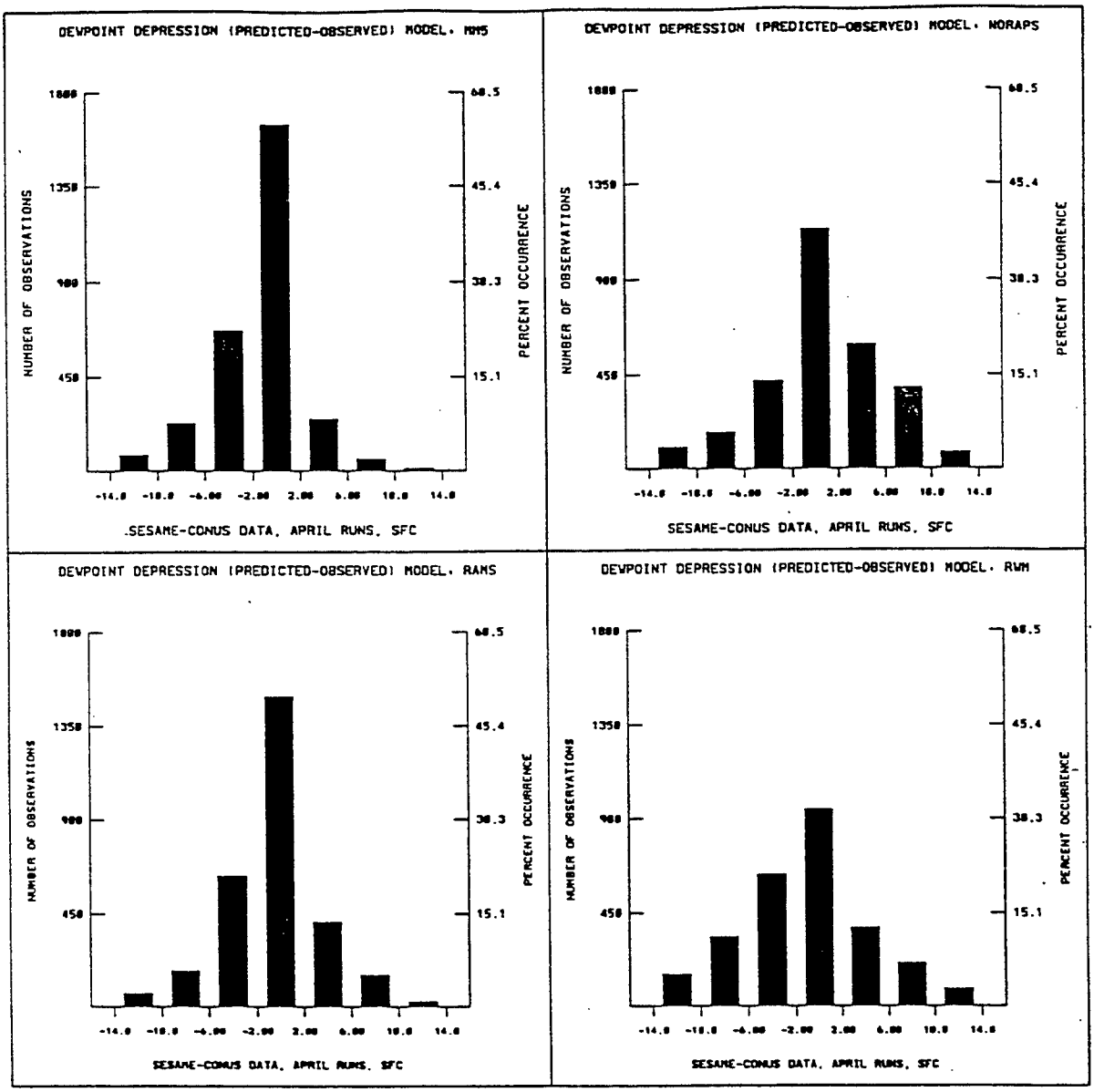

(c) CONUS dew point depression

Figure 4-4. Surface error statistics. (Continued)

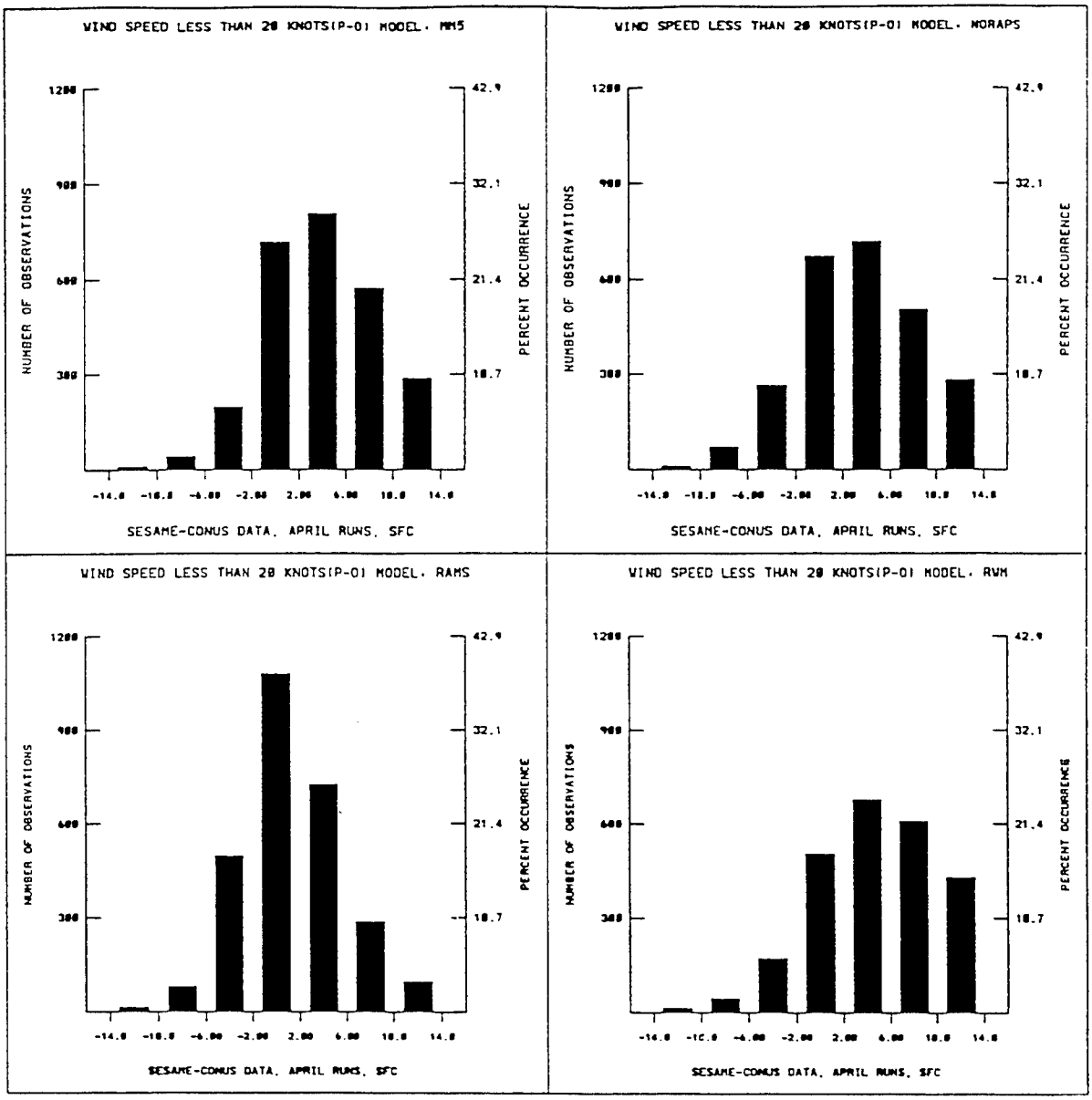

(d) CONUS wind speed < 20 Knots

Figure 4-4. Surface error statistics. (Continued)

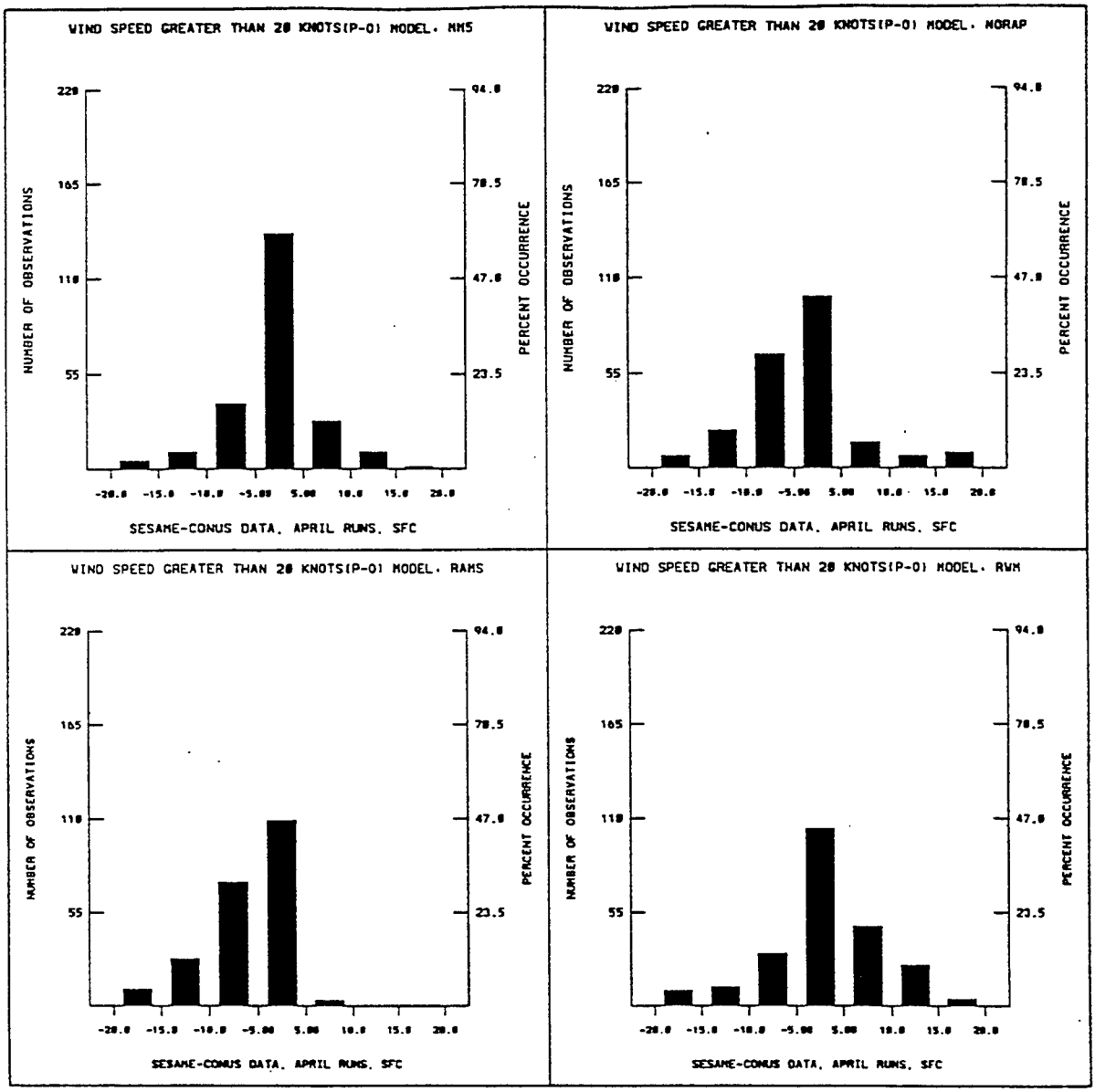

(e) CONUS wind speed > 20 Knots

Figure 4-4. Surface error statistics. (Continued)

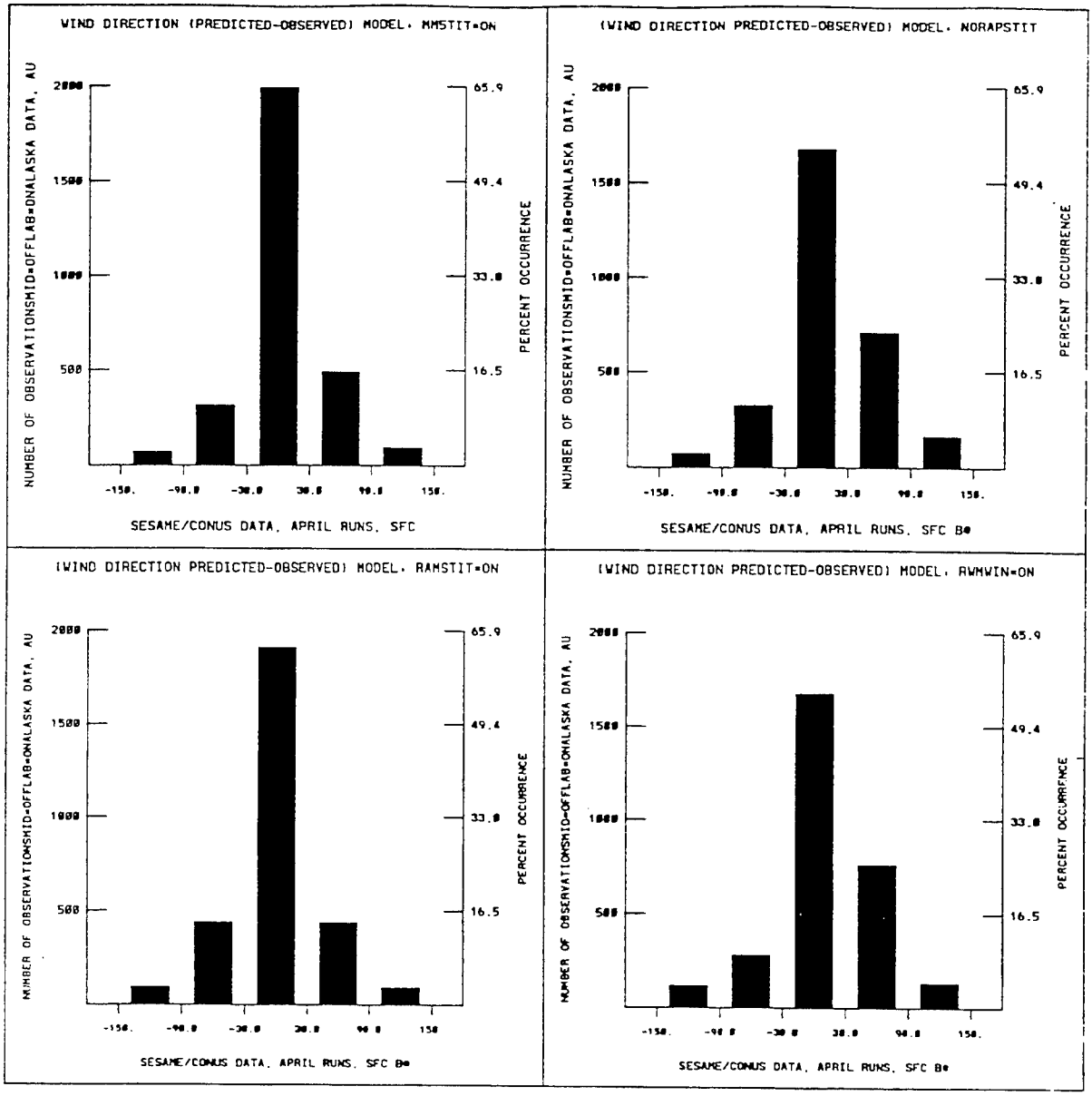

(f) CONUS wind direction

Figure 4-4. Surface error statistics. (Continued)

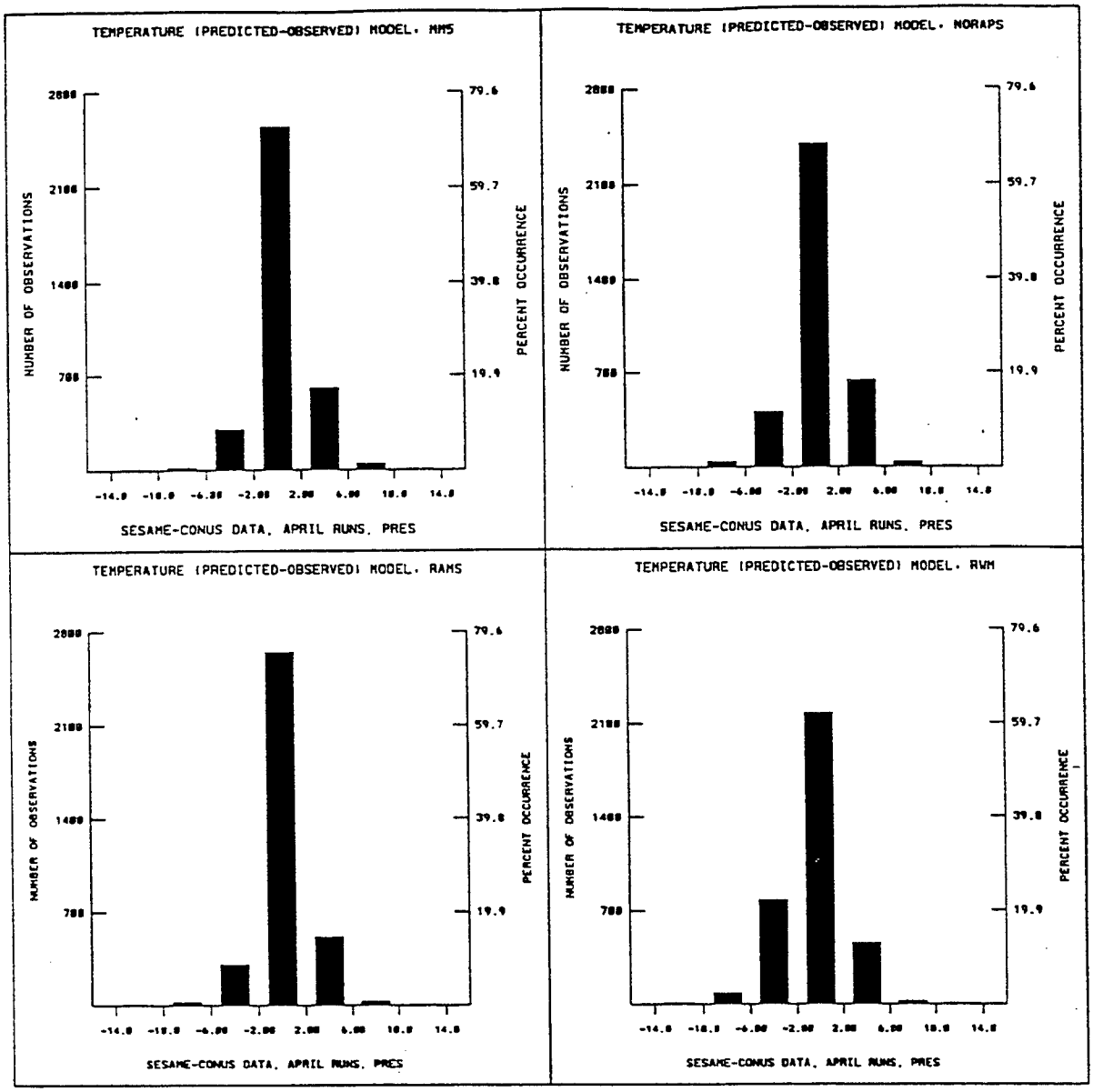

(a) CONUS temperature

Figure 4-5. Upper air error statistics.

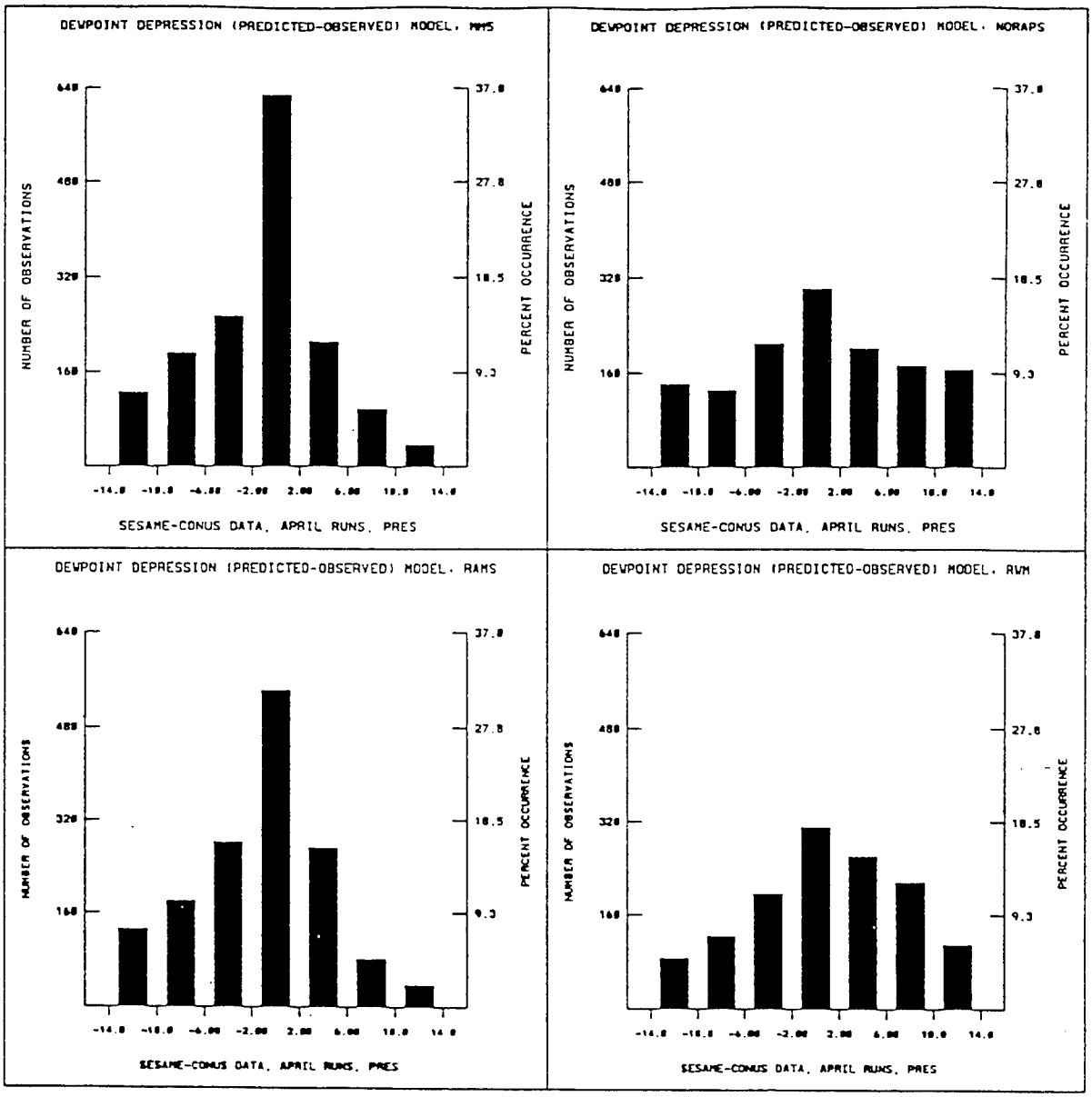

(b) CONUS dew point depression

Figure 4-5. Upper air error statistics. (Continued)

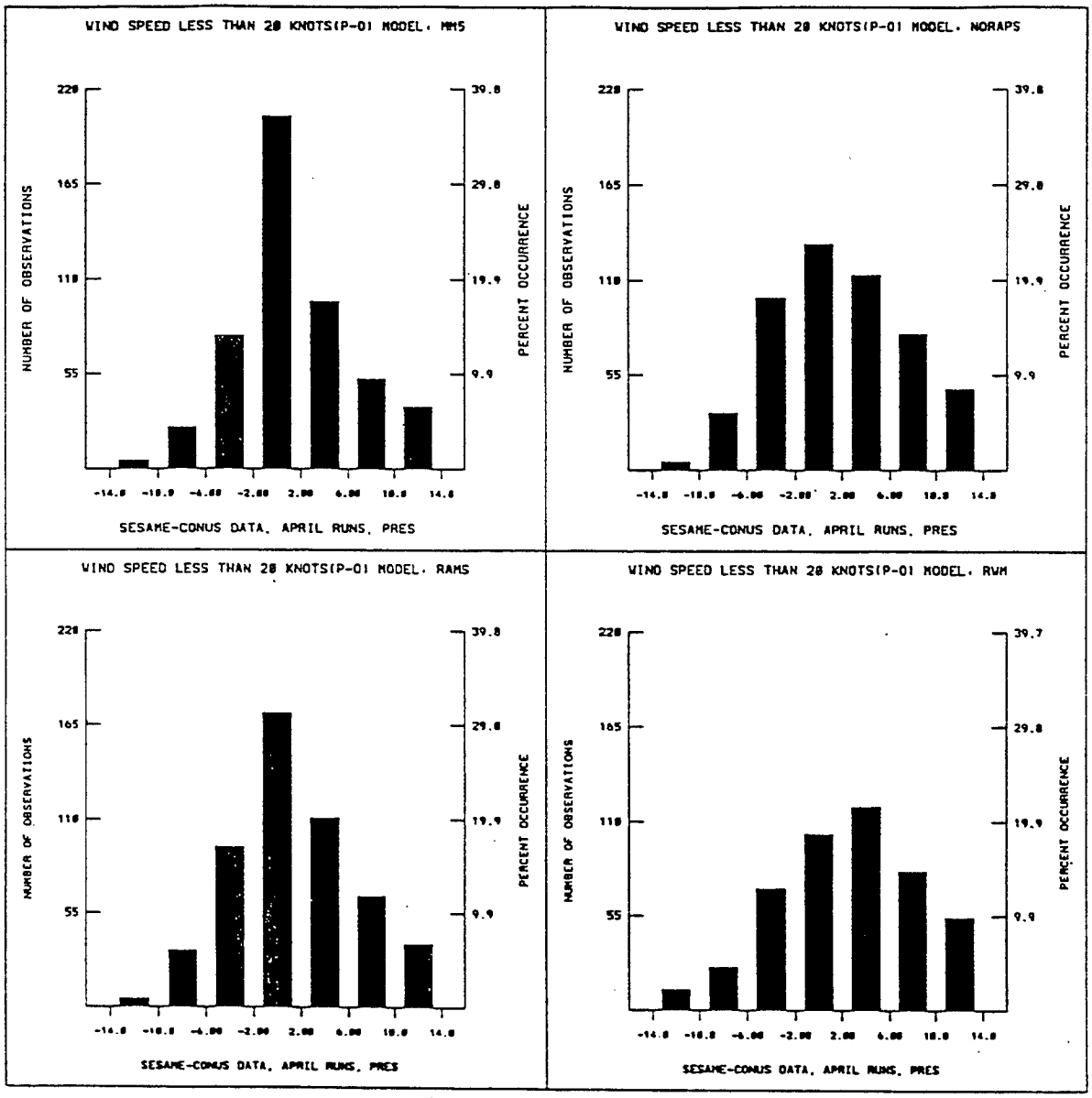

(c) CONUS wind speed < 20 Knots

Figure 4-5. Upper air error statistics. (Continued)

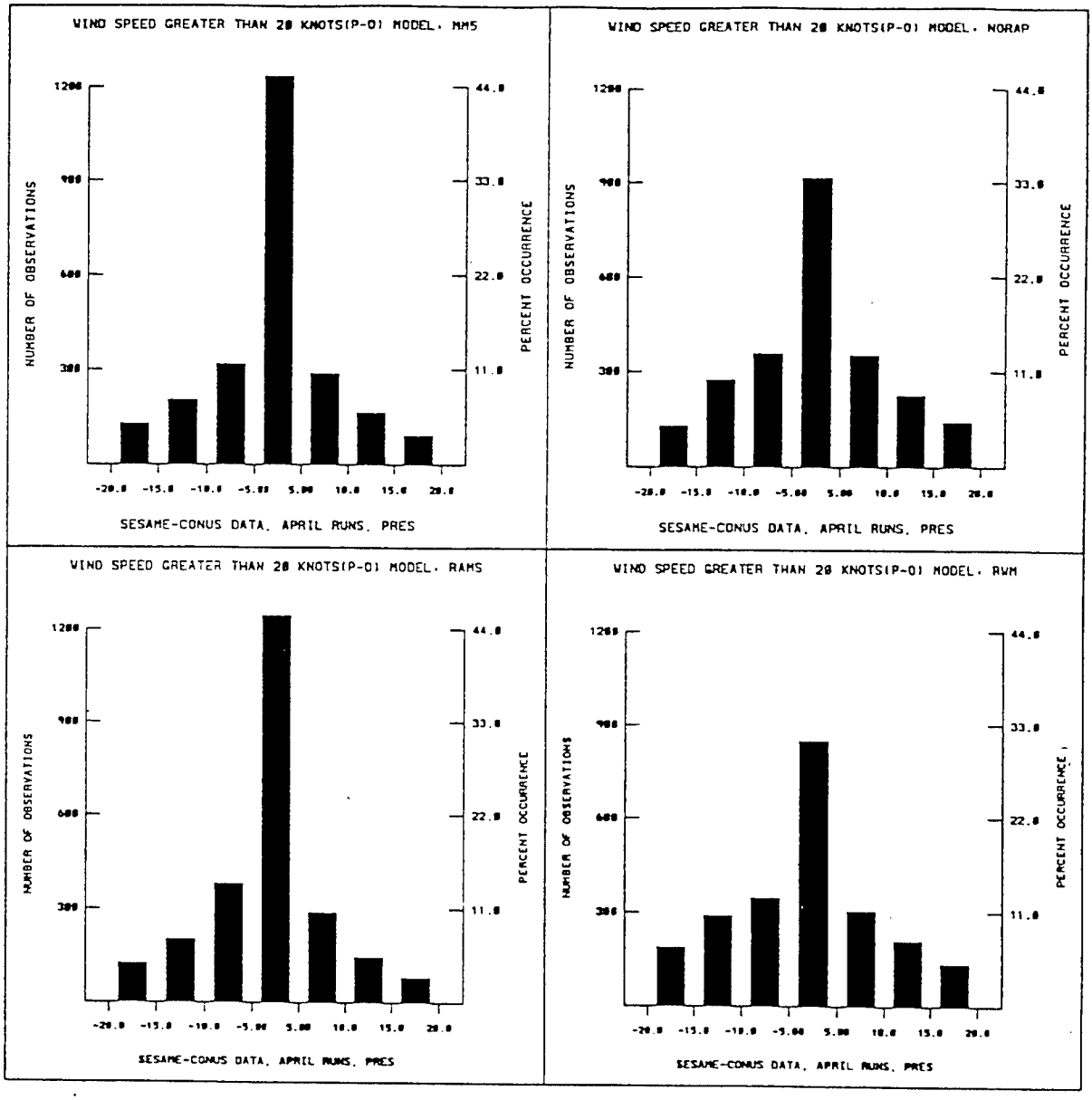

(d) CONUS wind speed > 20 Knots

Figure 4-5. Upper air error statistics. (Continued)

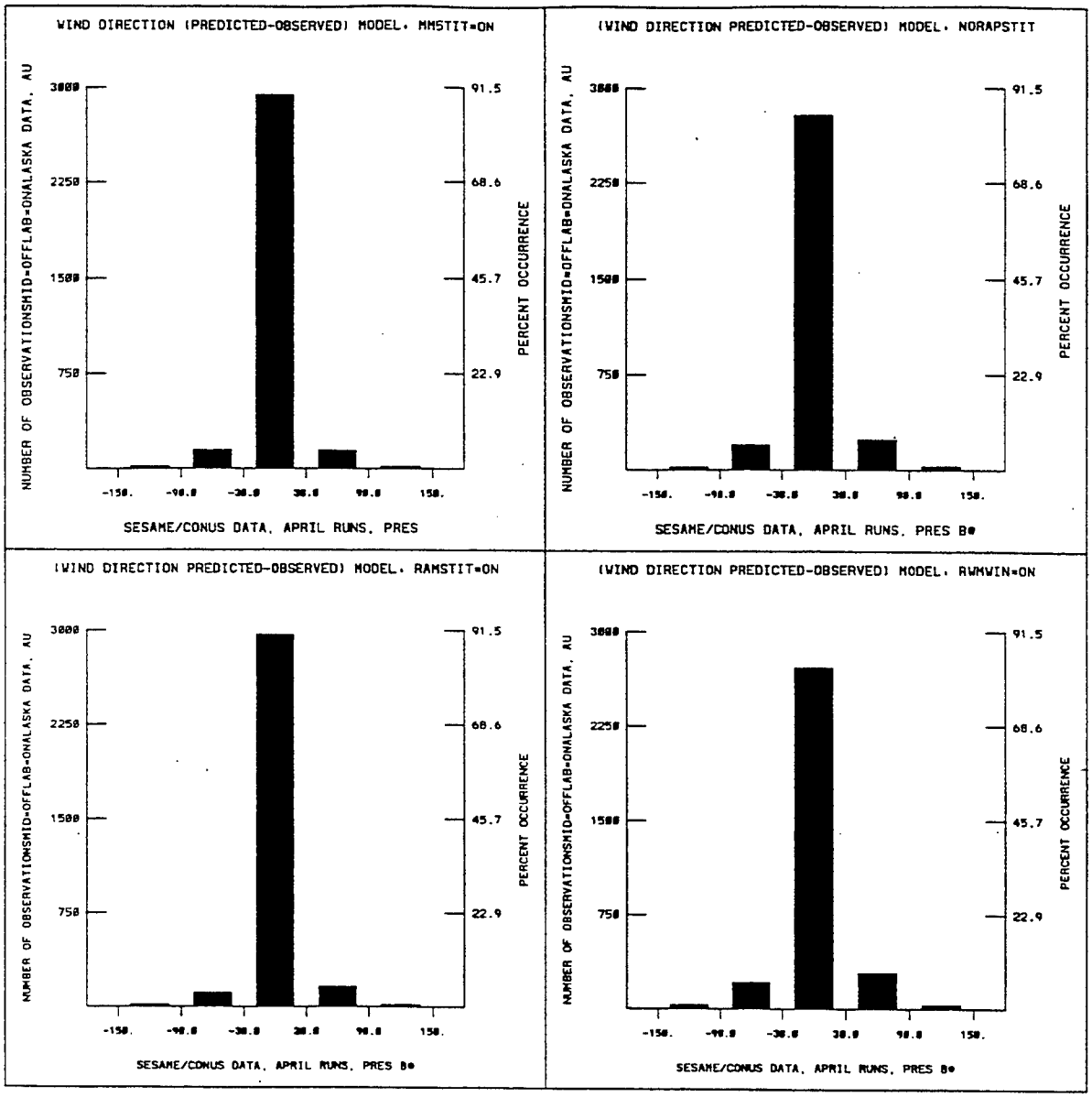

(e) CONUS wind direction

Figure 4-5. Upper air error statistics. (Continued)

The data analysis is not as clear and definitive as it was in the CONUS case, since the analysis is a mixture of heavily smoothed global fields and observations where available. These result from the large data-void regions of the four theaters. Therefore, interpretation of the analysis and the comparison with the model results will be, by necessity, somewhat less conclusive than in the CONUS case.

4.1.2.3 Data Source. The NMC gridded data are contained within the NCAR data archives in ds082.0, tape 21810. The rawinsonde data are in ds353.1, tape Y22553 and the surface observations at 0 UTC and 12 UTC are in ds464.0, tape Y22551.

4.1.2.4 Phenomenological Results – Alaska. Phenomenology results at 24 hours into the first forecast period (17 Aug 94 – 0000 UTC).

Surface

The surface wind field showed a low-level jet in advance of a surface low, centered in the western part of the domain. The analyzed jet maximum was up to 17 m/s off the western Alaska coast.

RAMS and MM5 predicted good speed of the jet and showed a slowing of the wind over land as the analysis because of vegetation parameterizations. RWM over-predicted the speed (up to 23 m/s), while NORAPS6 under-predicted the intensity at 15 m/s and showed no velocity gradients at the coastline since it does not include a land-use parameterization.

RAMS and NORAPS6 generally predicted a good temperature field. RWM generated a strong front in the north Pacific that was not in the data analysis, while MM5 generated a rather strange localized perturbation on the Aleutian peninsula. The analysis was very moist at the surface over most ocean areas. RAMS and MM5 predicted saturated conditions over most water (which could be interpreted as low stratus clouds). NORAPS6 generated some saturated regions west and north of Alaska, but showed significant boundary problems, as NORAPS6 does not use the humidity observations to initialize the forecast. RWM suffered from a bad initial analysis, and did not recover. Figures 4-6(a - e) depict the surface winds at 24 hours.

The surface low was located west of Alaska at this time in the analysis with a central pressure of 996 mb. All models predicted a good location. RAMS and RWM under-predicted the pressure at 992 mb, with RWM continuing its feature of producing noisy pressure and geopotential fields. MM5 predicted the low center at 996 mb and NORAPS6 predicted 998 mb.

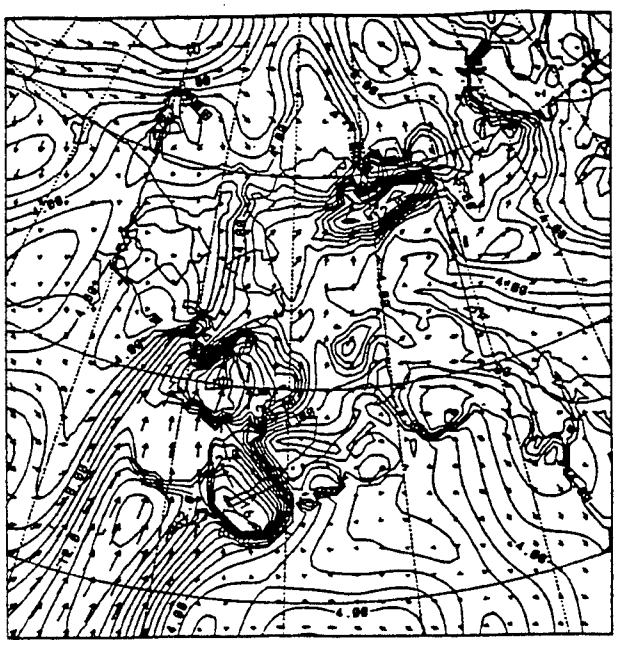

(a) Analysis at 17 Aug 94 - 0000 UTC

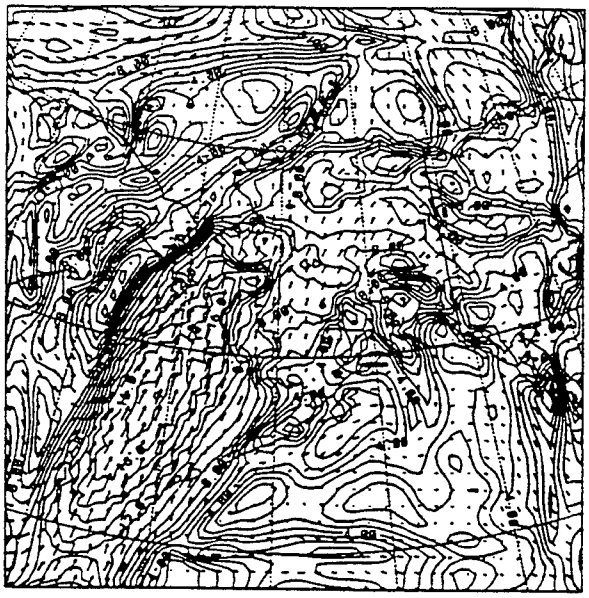

(b) MM5 - 17 Aug 94 - 0000 UTC forecast

Figure 4-6. Surface winds - Alaska.

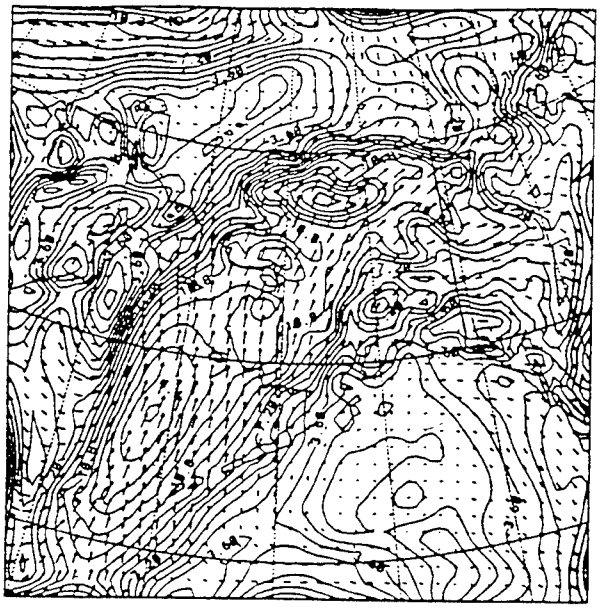

(c) NORAPS6 - 17 Aug 94 - 0000 UTC forecast

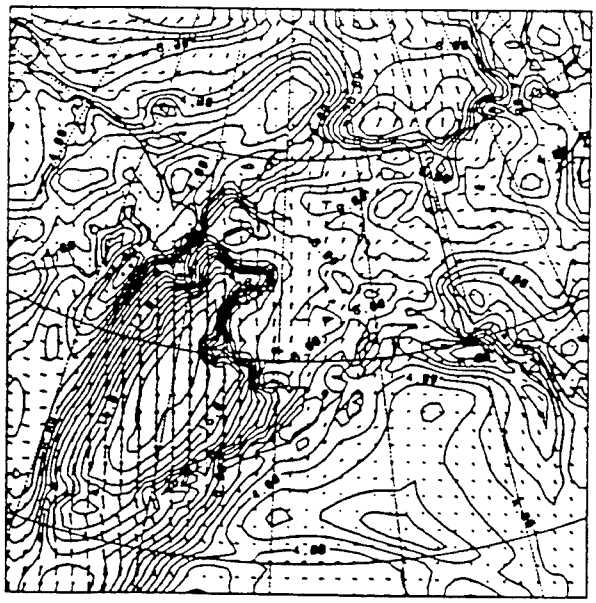

(d) RAMS - 17 Aug 94 - 0000 UTC forecast

Figure 4-6. Surface winds - Alaska. (Continued)

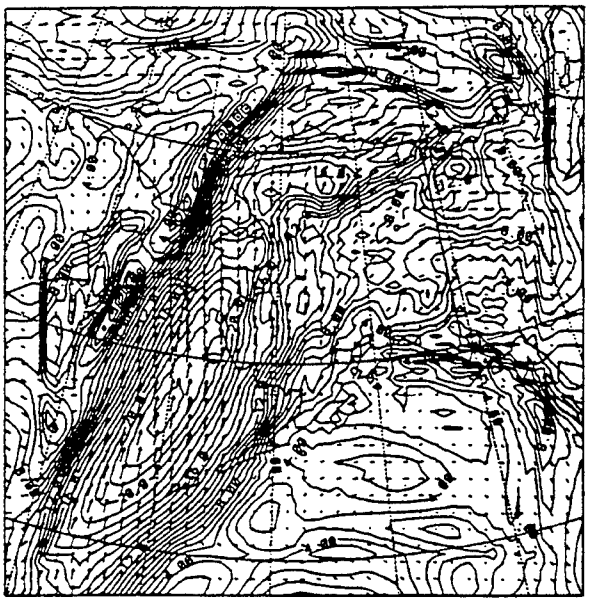

(e) RWM - 17 Aug 94 - 0000 UTC forecast

Figure 4-6. Surface winds - Alaska. (Continued)

Upper Air

At 500 mb, a jet streak dominated the domain with a core maximum speed of 38 m/s. All models had generally a good location and speed. The geopotential field had a trough west of Alaska and a ridge to the south. All did well, although RWM was again, numerically noisy.

Phenomenology results at 24 hours into the second forecast period (18 Aug 94 –1200 UTC).

Surface

The analysis showed that the low center had moved over the northern Alaska coast with a central pressure of 994 mb, although the circulation had weakened from the past 36 hours. All models under-predicted the intensity of the circulation with NORAPS6 at 999 mb, MM5 at 998 mb, RAMS at 1000 mb, and RWM too noisy to distinguish. Figure 4-7(a - e) show the predicted surface pressure fields.

MM5 and RAMS were still near saturated over water. NORAPS6 predicted many gradients that were not present in the data analysis. RWM, again, had problems because of the initial analysis.

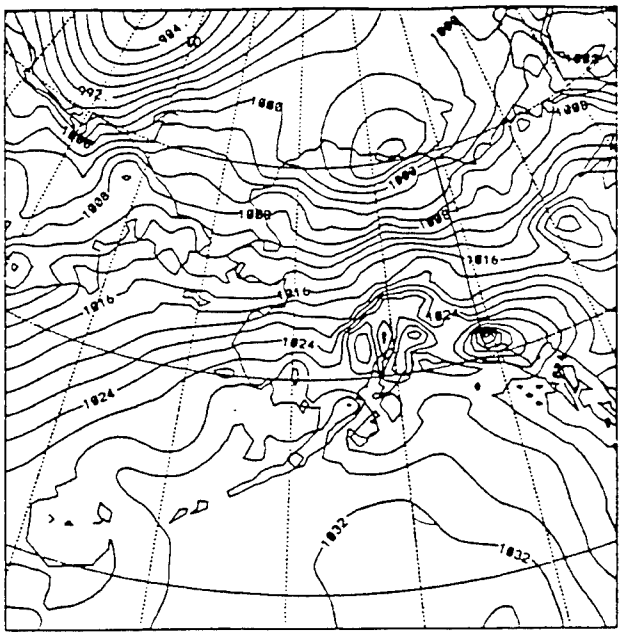

(a) Analysis at 18 Aug 94 - 1200 UTC

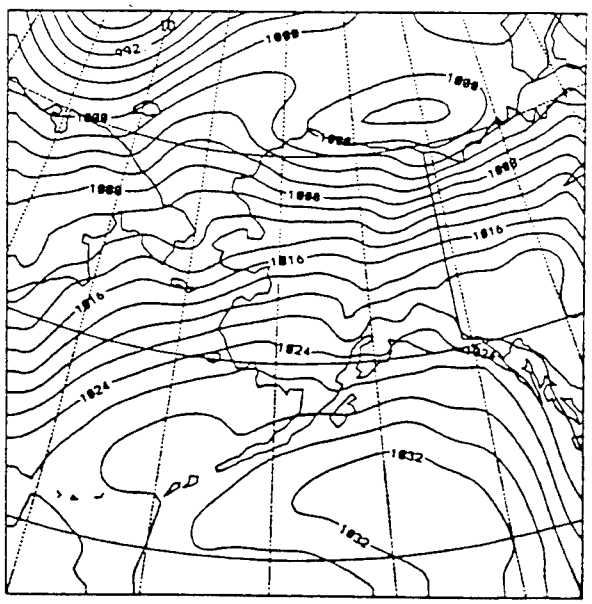

(b) MM5 - 18 Aug 94 - 1200 UTC forecast

Figure 4-7. Surface pressure.

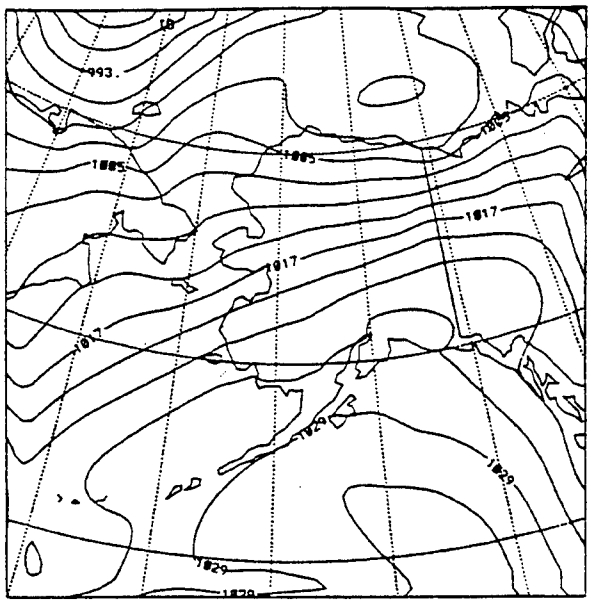

(c) NORAPS6 - 18 Aug 94 - 1200 UTC forecast

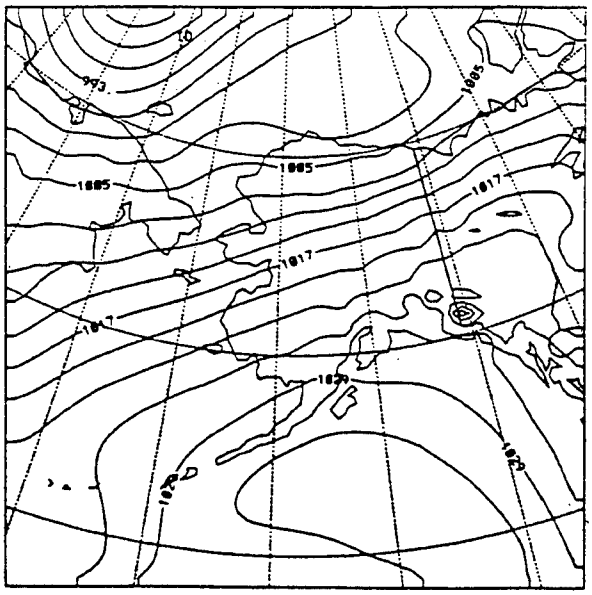

(d) RAMS - 18 Aug 94 - 1200 UTC forecast

Figure 4-7. Surface pressure. (Continued)

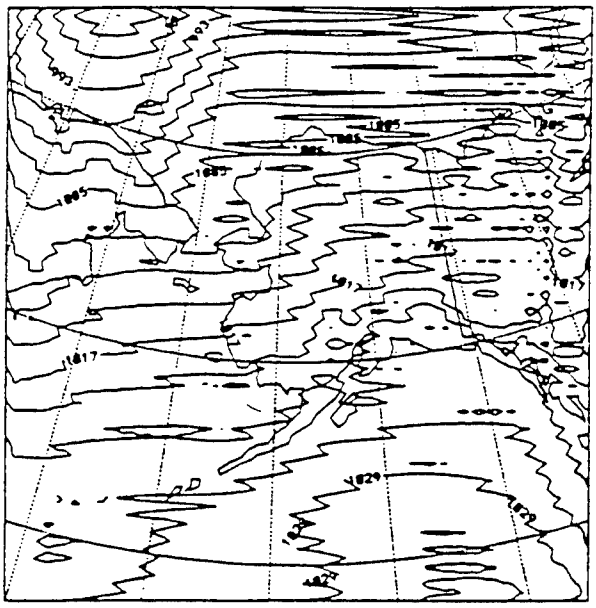

(e) RWM - 18 Aug 94 - 1200 UTC forecast

Figure 4-7. Surface pressure. (Continued)

Upper Air

As with surface low, all models under-predicted the intensity of the 500 mb trough over north Alaska.

An analyzed jet core of 40 m/s was associated with this trough. RWM produced a noisy, misplaced core with 36 m/s maximum speed. NORAPS6 over-predicted the speed at 48 m/s and placed the core too far to the northeast. RAMS and MM5 produced a good location, with RAMS slightly under at 38 and MM5 slightly over at 44 m/s.

4.1.2.5 Statistical Results - Alaska. Error frequency distributions were generated for temperature, surface pressure, dew point depression, wind speed below 20 knots, wind speed above 20 knots, and wind direction. Data from all forecast times, both August forecasts, and where appropriate, levels were merged. The central column corresponds to the desired error bounds. Two sets of figures were developed to describe the forecast results. One is a surface set that includes the large number of surface observations and the other is an upper air set that includes the more sparse upper air observations. Figures 4-8(a - f) are the surface results and Figures 4-9(a - e) are the upper air results.

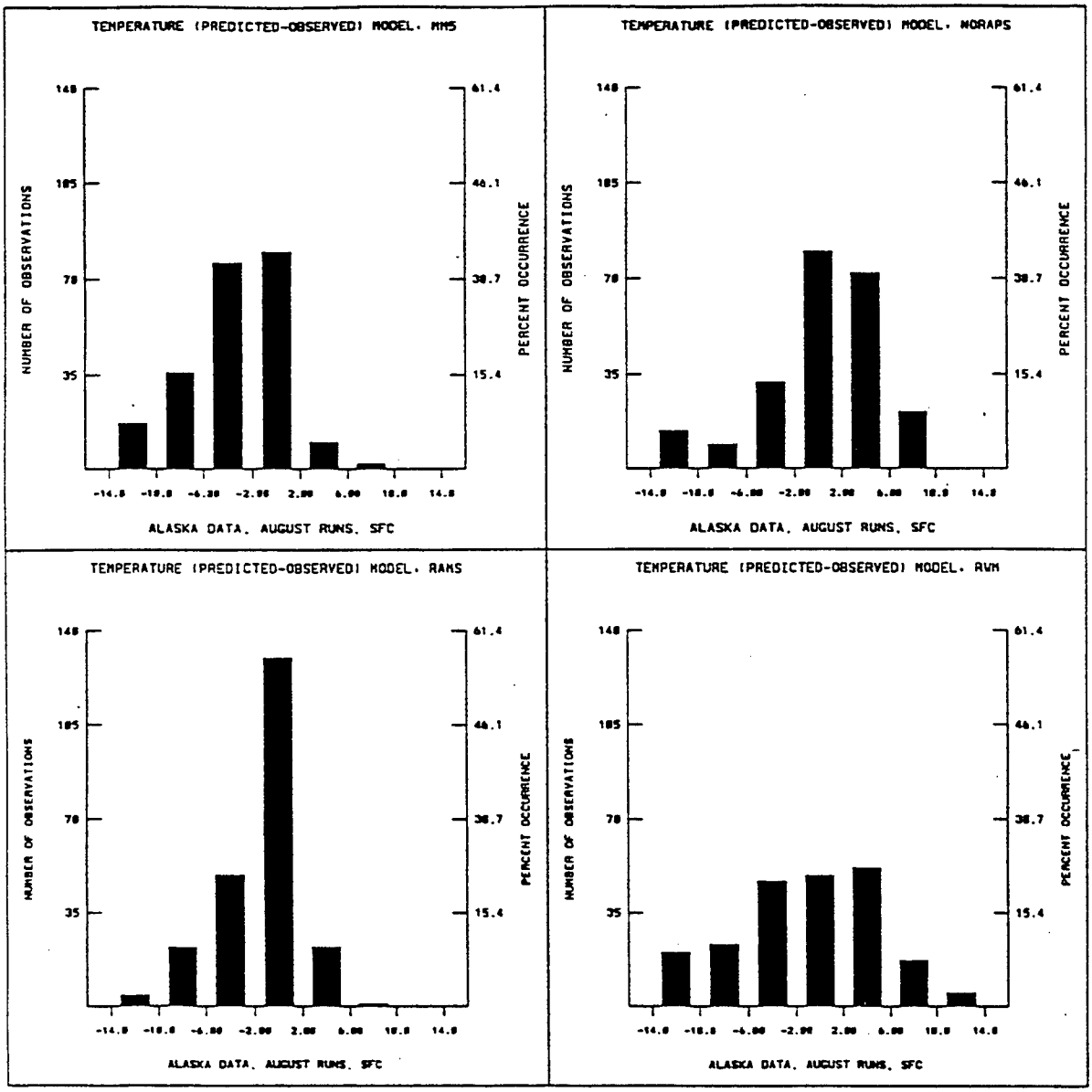

(a) August - Alaska temperature

Figure 4-8. Surface error statistics.

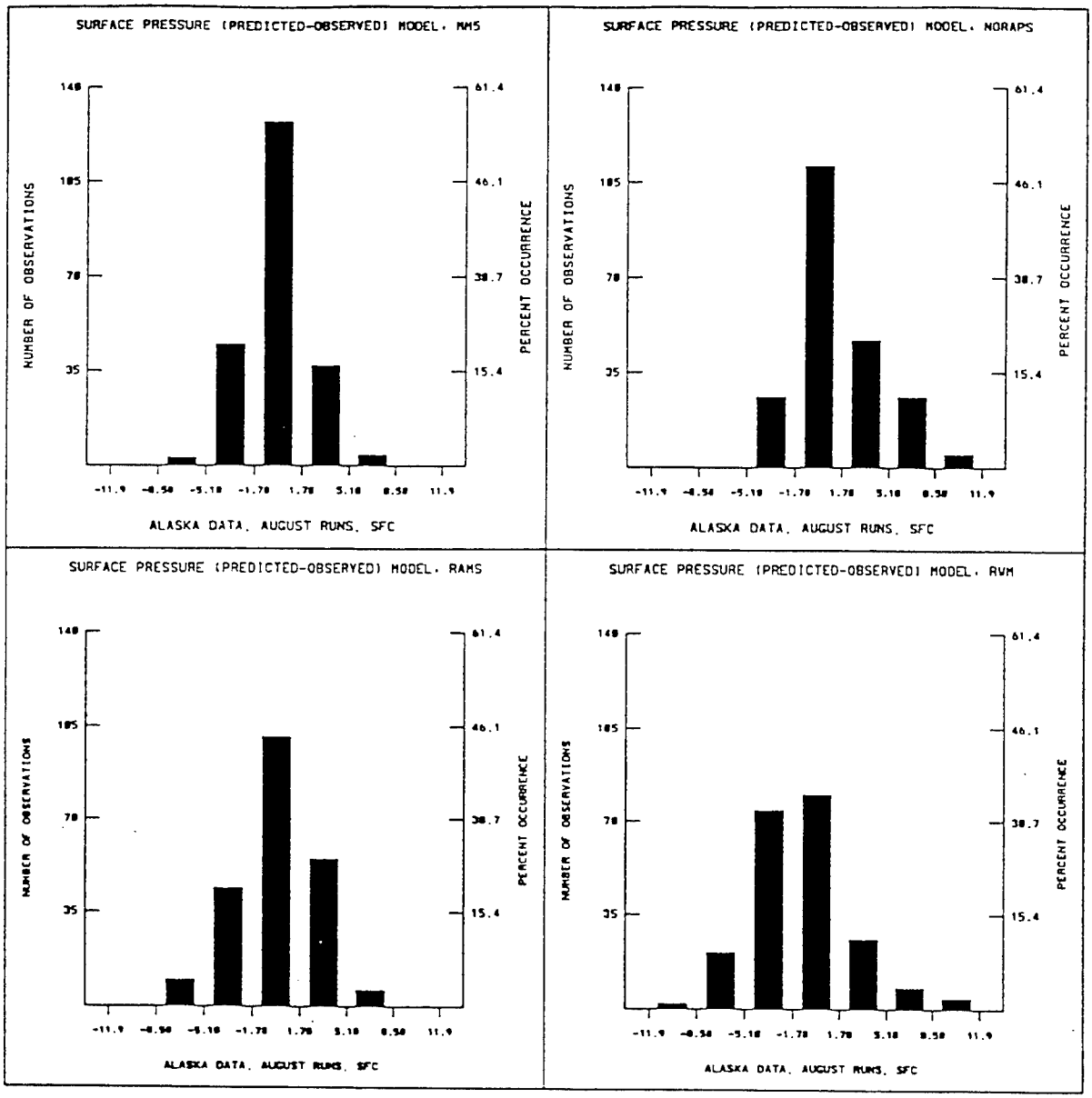

(b) August - Alaska pressure

Figure 4-8. Surface error statistics. (Continued)

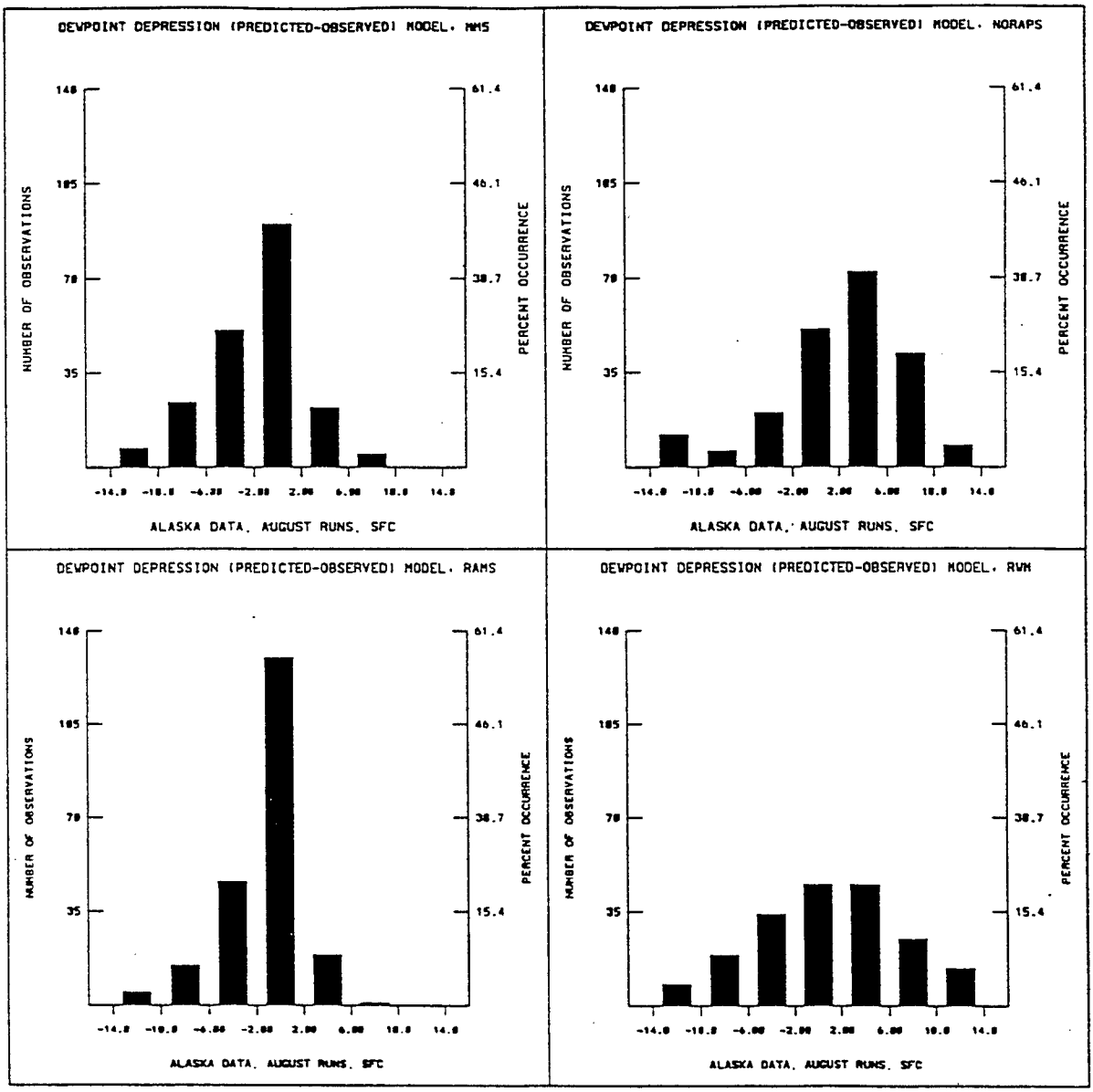

(c) August - Alaska dew point depression

Figure 4-8. Surface error statistics. (Continued)

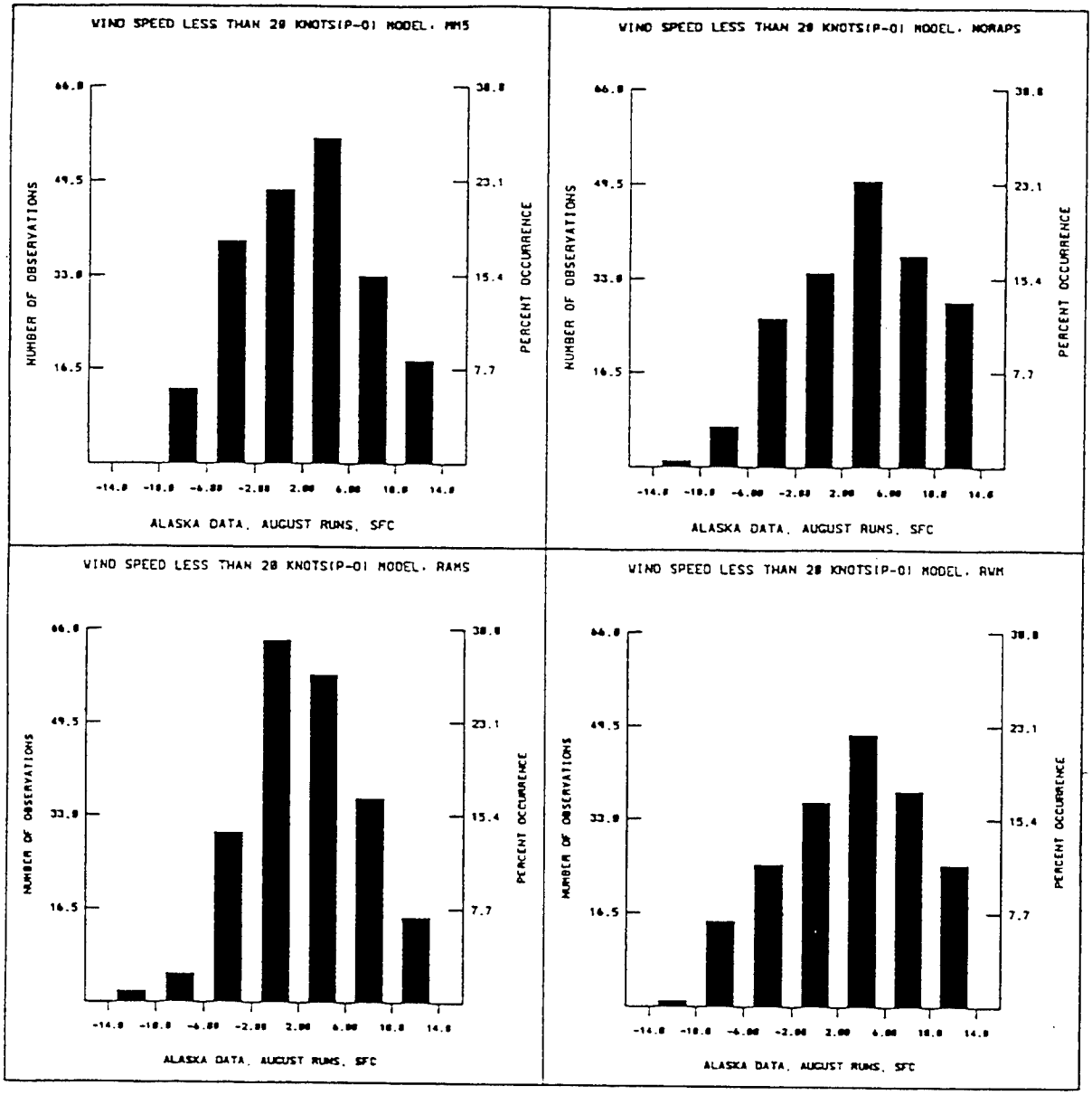

(d) August - Alaska wind speed < 20 Knots

Figure 4-8. Surface error statistics. (Continued)

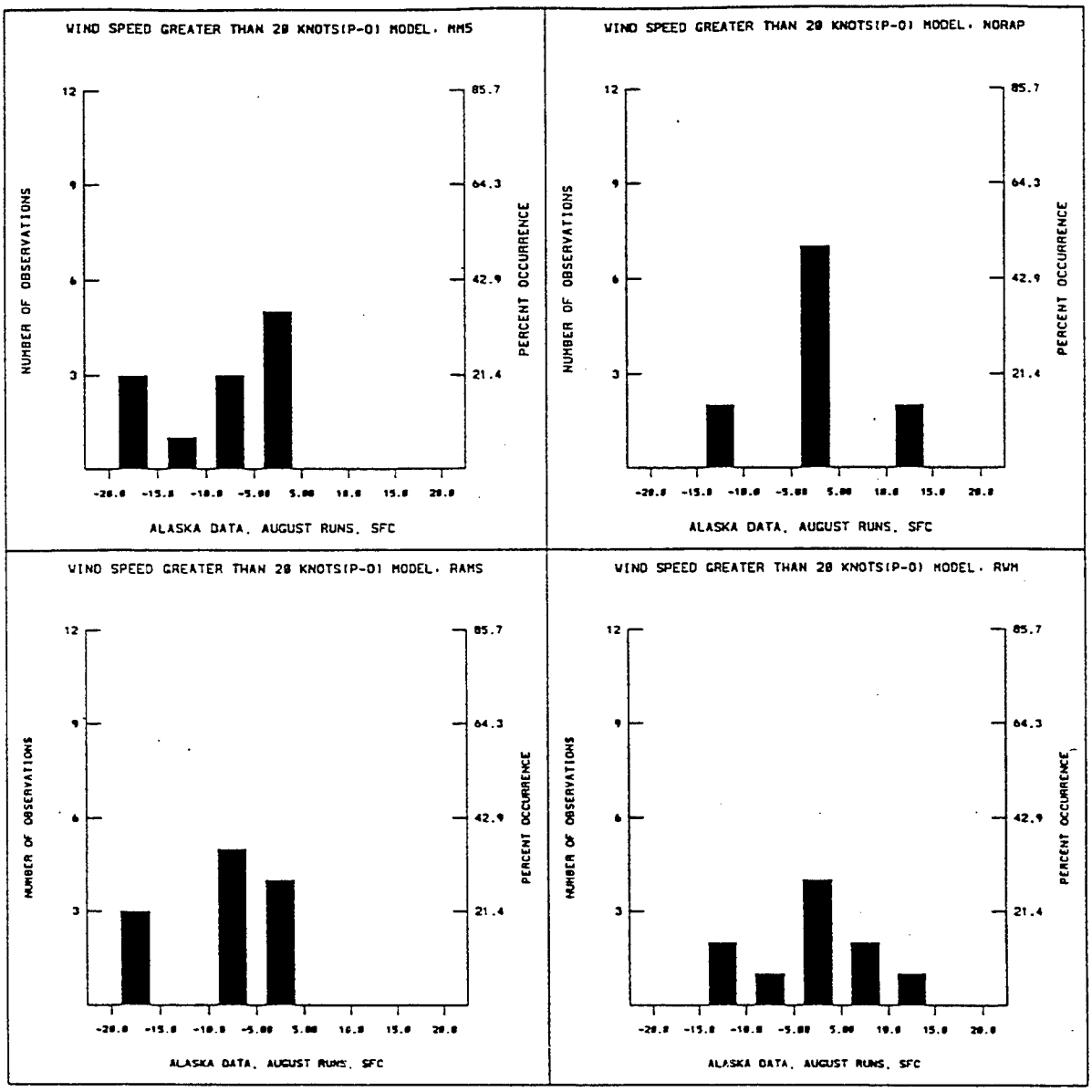

(e) August - Alaska wind speed > 20 Knots

Figure 4-8. Surface error statistics. (Continued)

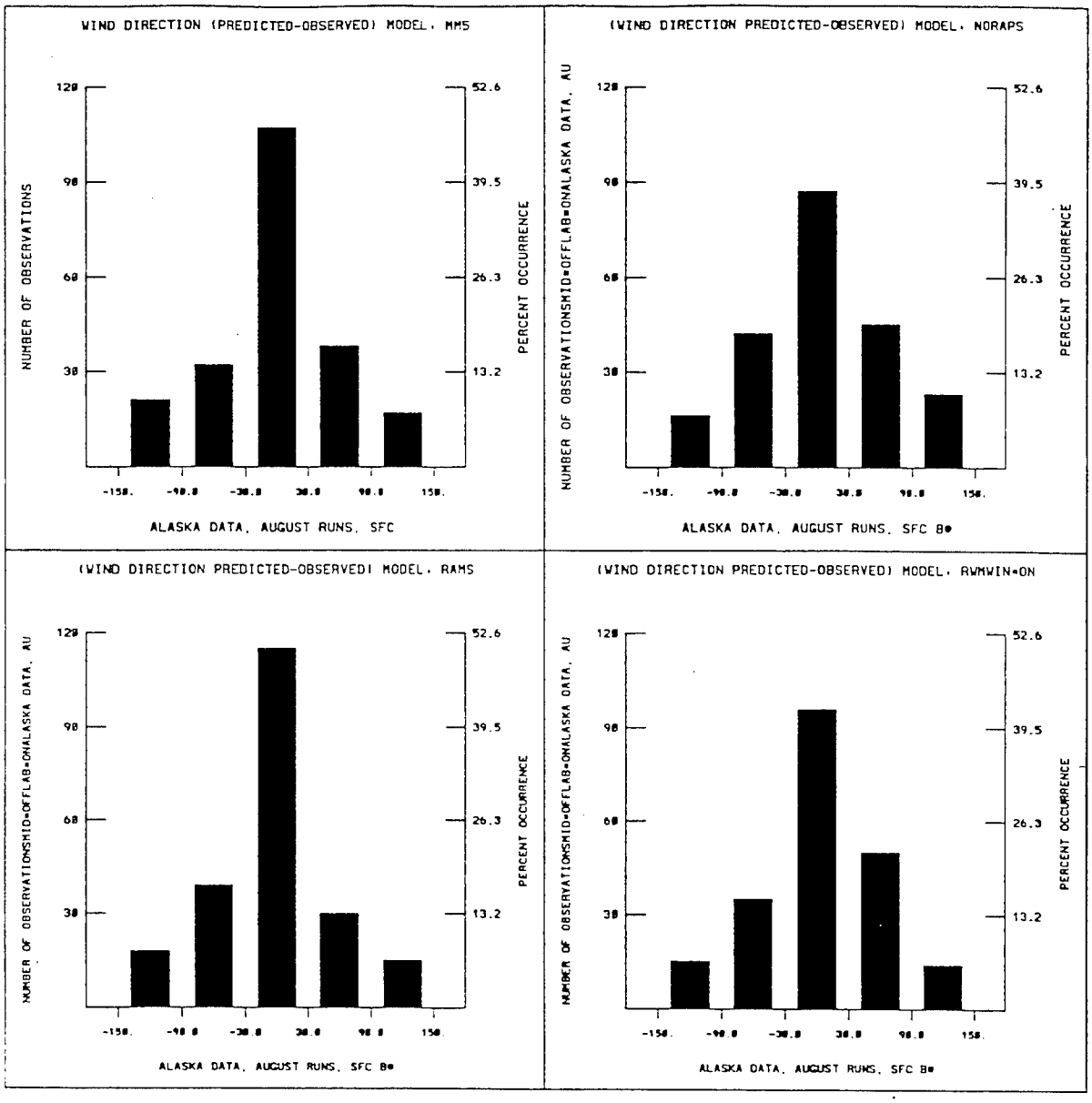

(f) August - Alaska wind direction

Figure 4-8. Surface error statistics. (Continued)

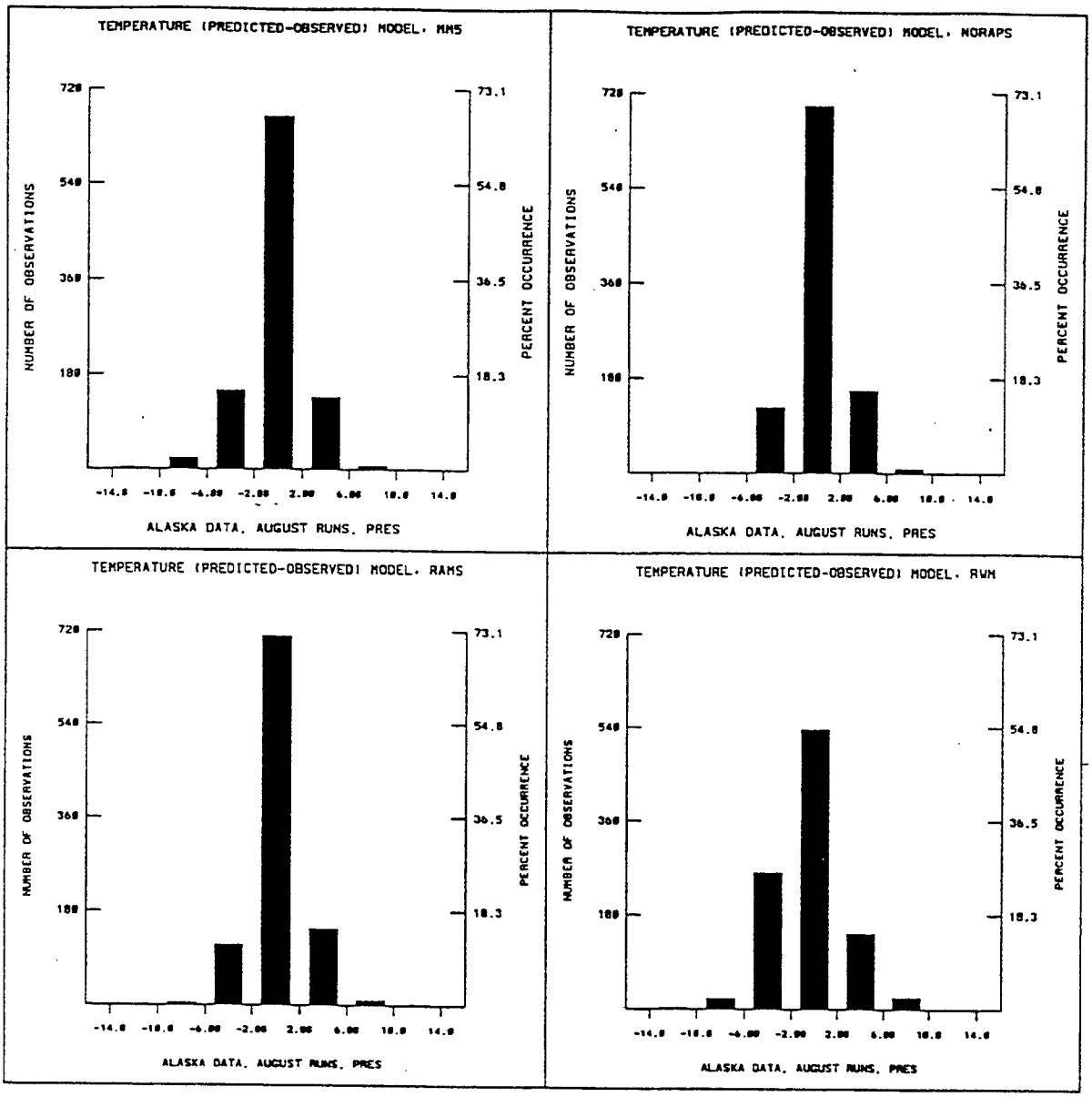

(a) August - Alaska temperature

Figure 4-9. Upper air error statistics.

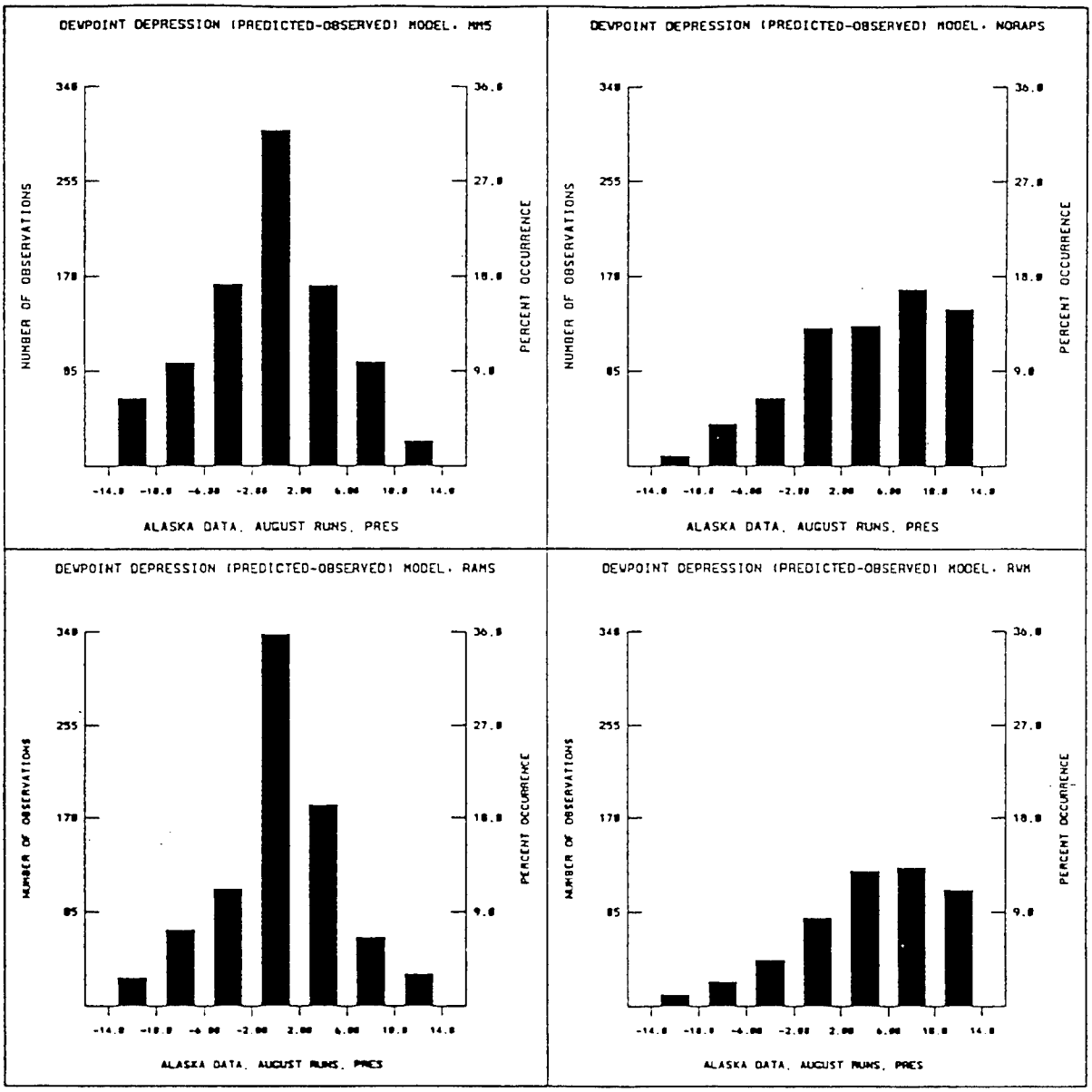

(b) August - Alaska dew point depression

Figure 4-9. Upper air error statistics. (Continued)

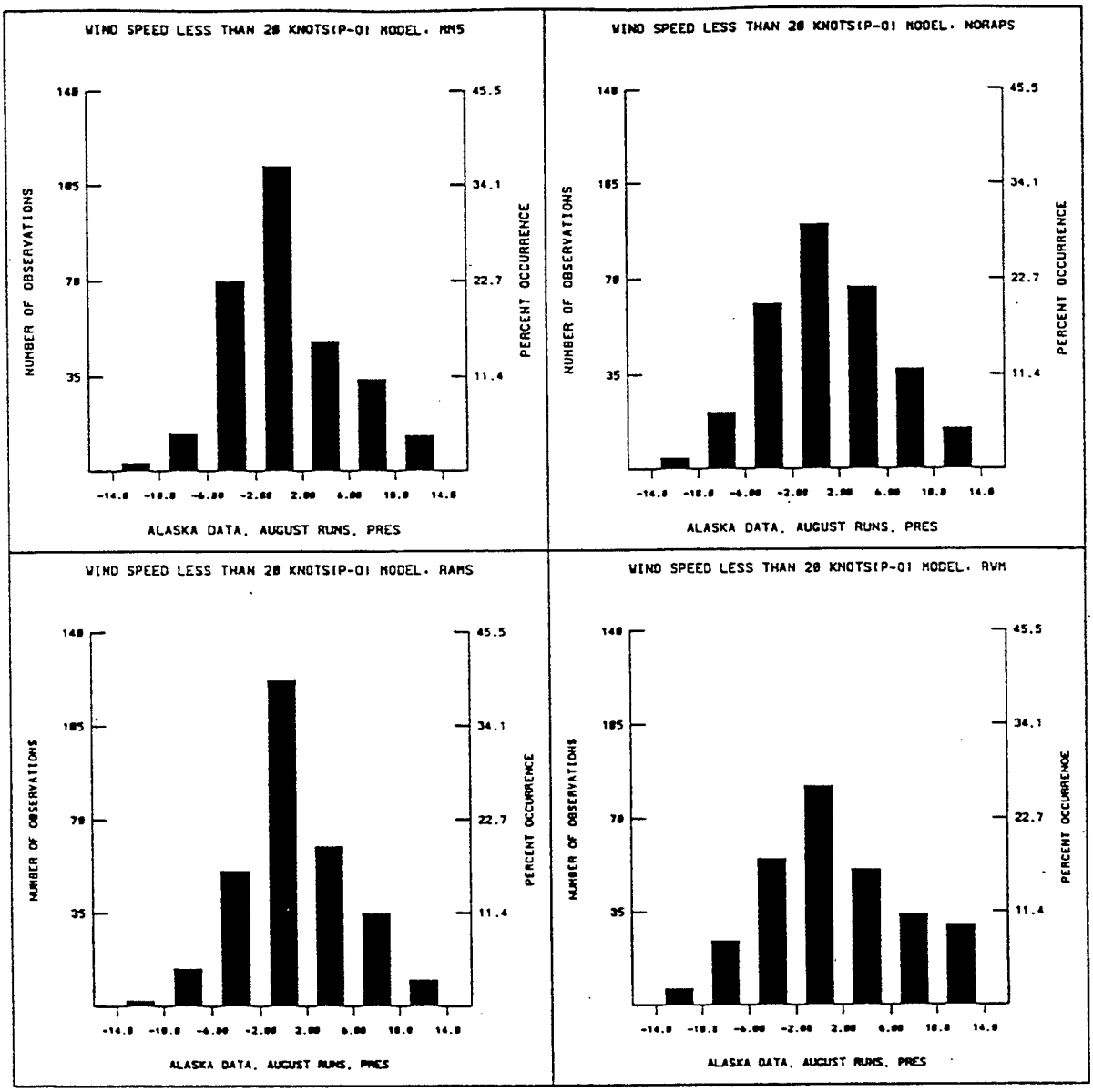

(c) August - Alaska wind speed < 20 Knots

Figure 4-9. Upper air error statistics. (Continued)

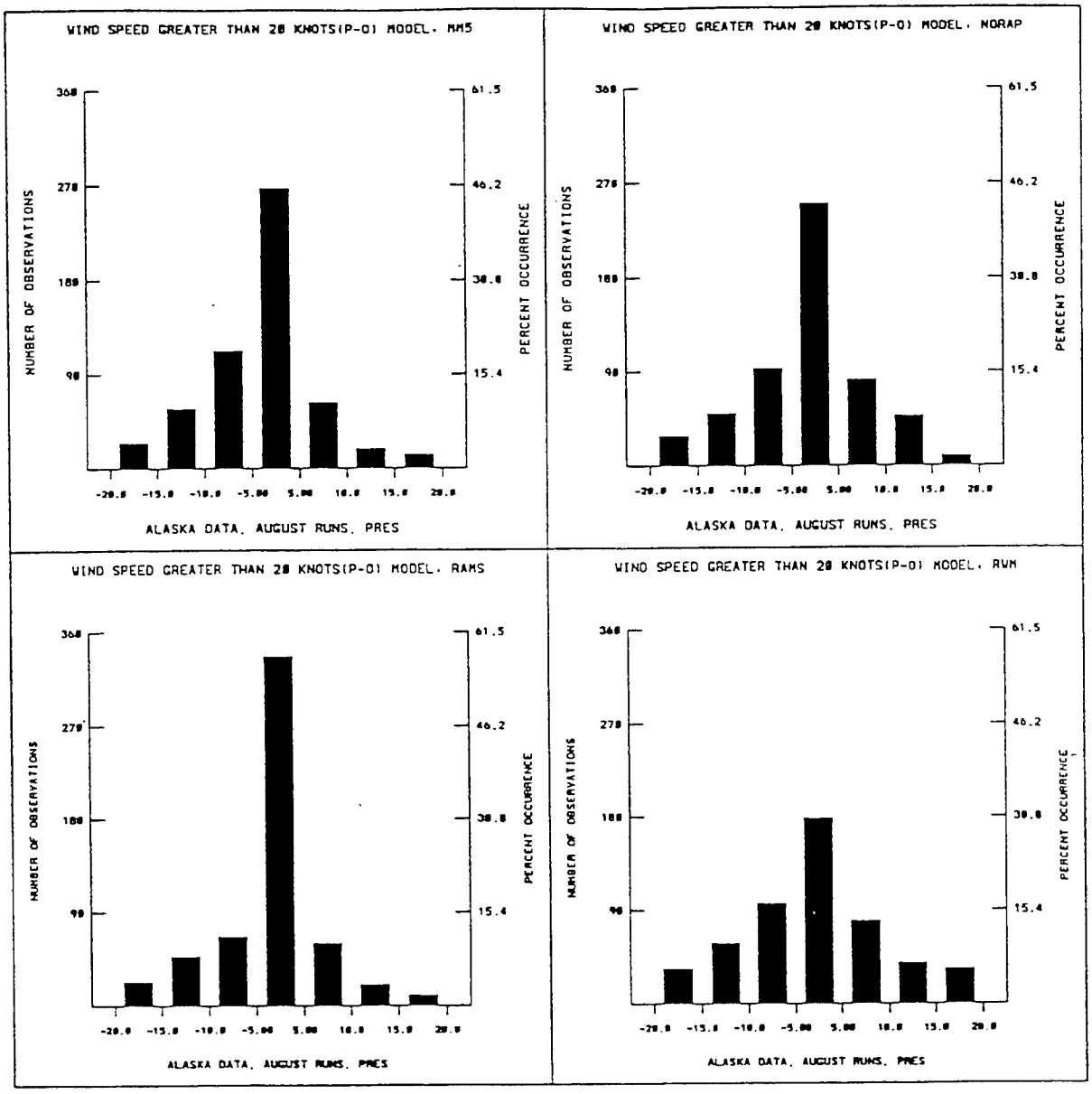

(d) August - Alaska wind speed > 20 Knots

Figure 4-9. Upper air error statistics. (Continued)

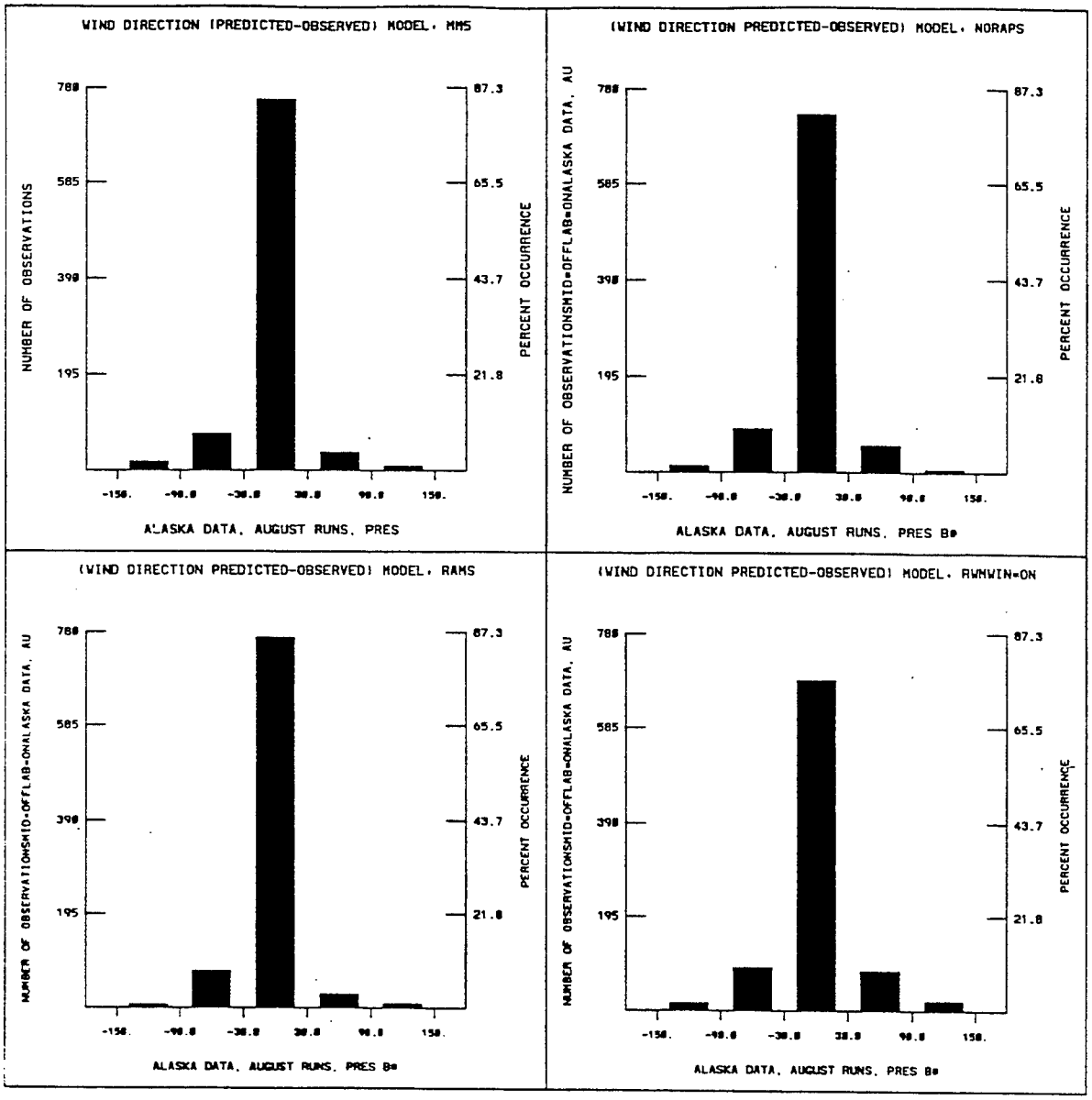

(e) August - Alaska wind direction

Figure 4-9. Upper air error statistics. (Continued)

4.1.2.6 Phenomenological Results – Korea. Phenomenology results at 24 hours into the first forecast period (17 Aug 94 – 0000 UTC).

Surface

The surface wind analysis was dominated by easterlies south of Japan, while a jet from the southwest was located over the Sea of Japan starting just northeast of the Korean peninsula extending along west coast of Japan. RAMS did very well with good speed and direction of both flow branches. NORAPS6 did very poorly. MM5 had good flow near Korea, but it cut off the jet with a southeasterly flow emanating from the boundary. RWM did fairly well with the direction, but over-predicted the maximum speed. Figures 4-10(a - e) show the surface wind. RAMS and MM5 produced near saturated over the water areas east and west of Korea. The analysis was also moist with the relative humidity analyzed at 90-95 percent. RAMS forecast an anomalous high region of relative humidity in the northwest corner of the domain. NORAPS6 and RWM produced large boundary gradients due to the initial analysis.

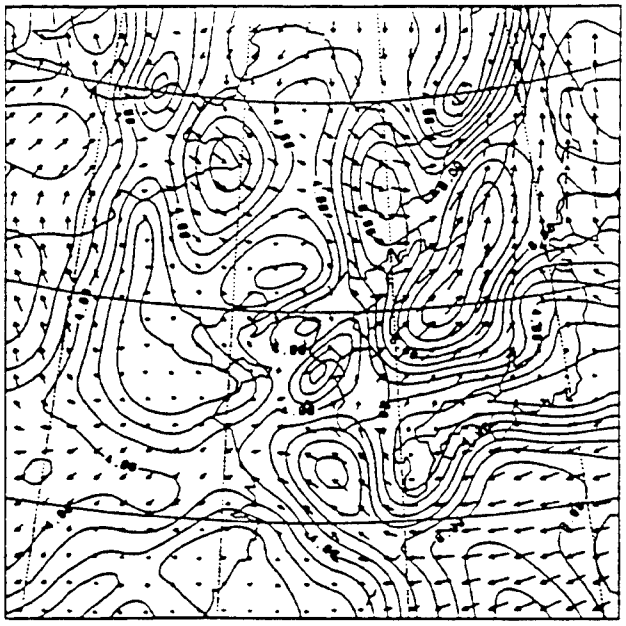

(a) Analysis at 17 Aug 94 - 0000 UTC

Figure 4-10. Surface wind - Korea.

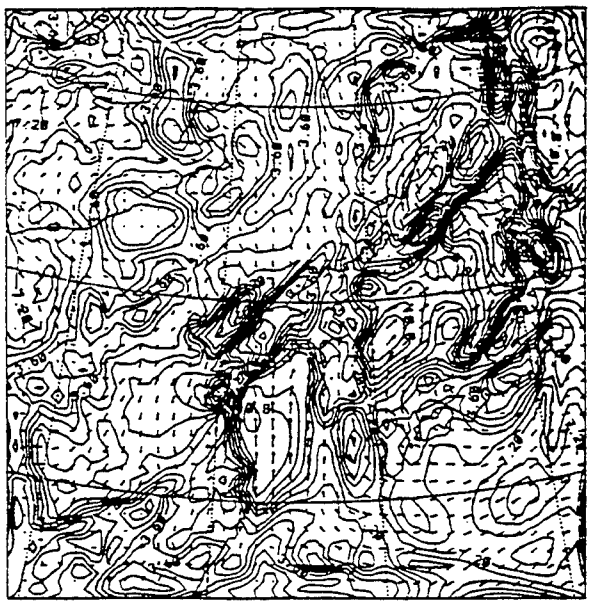

(b) MM5 - 17 Aug 94 - 0000 UTC forecast

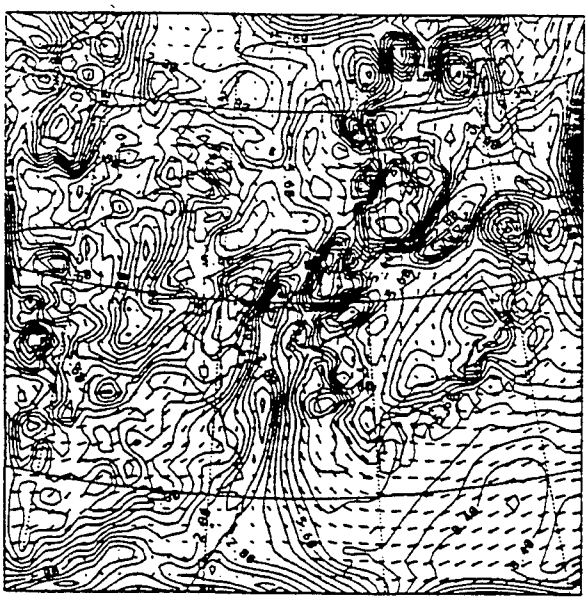

(c) NORAPS6 - 17 Aug 94 - 0000 UTC forecast

Figure 4-10. Surface wind - Korea. (Continued)

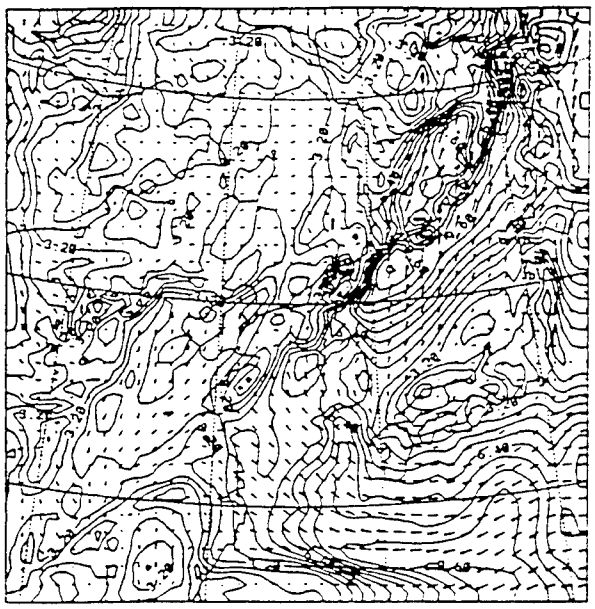

(d) RAMS - 17 Aug 94 - 0000 UTC forecast

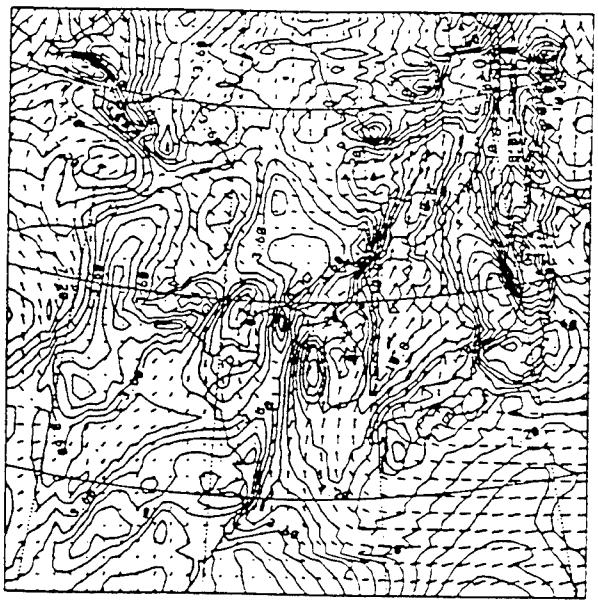

(e) RWM - 17 Aug 94 - 0000 UTC forecast

Figure 4-10. Surface wind - Korea. (Continued)

Upper Air

The analysis showed a weak surface front along the East Asian coast, extending from the low centered near the northern boundary. RAMS predicted a good location and strength for the front. MM5 over-developed the front and developed a new low center west-southwest of Korea that was not in the data analysis. NORAPS6 had a poor orientation of the northern portion of the front and had a high-pressure bias in the entire domain. RWM was again noisy and produced a too strong low. A jet streak, with a core speed of 30 m/s, extended from the southwest to the northeast of Korea in the data analysis. All models had a fair location and speed. RAMS and MM5 did a good job capturing the analyzed trough in the northern part of the domain and the ridge over Japan. NORAPS6 also did fairly well, while RWM continued to be noisy.

Phenomenology results at 24 hours into the second forecast period (18 Aug 94 - 1200 UTC).

Surface

At this time, high pressure dominated the Korean region, with a northeasterly flow in the Sea of Japan, east of Korea, while the winds turned anticyclonicly south and west of Korea. NORAPS6 and RWM forecast a fairly good direction, while MM5 produced easterly winds over the Asian continent instead of southerly. RAMS produced a southwesterly rather than northeasterly flow in the Sea of Japan. This is seen in Figures 4-11(a - e).

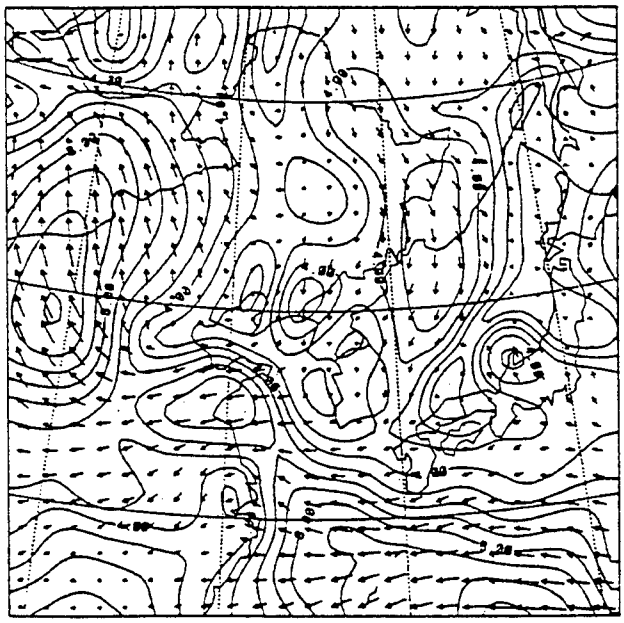

(a) Analysis at 18 Aug 94 - 1200 UTC

Figure 4-11. Surface wind - Korea.

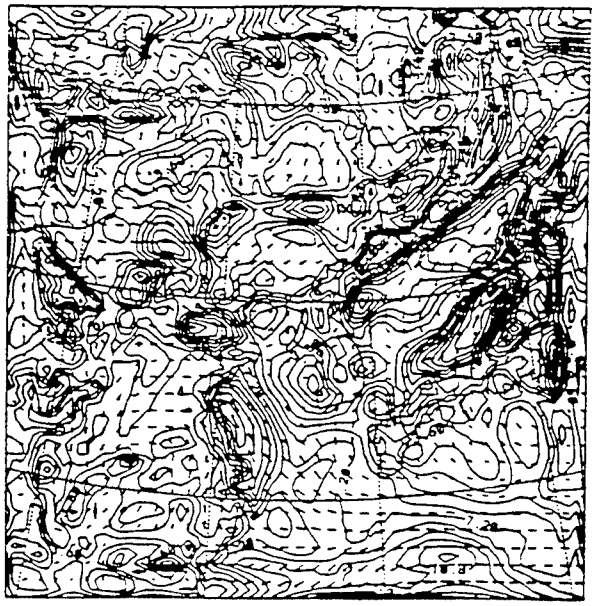

(b) MM5 - 18 Aug 94 - 1200 UTC forecast

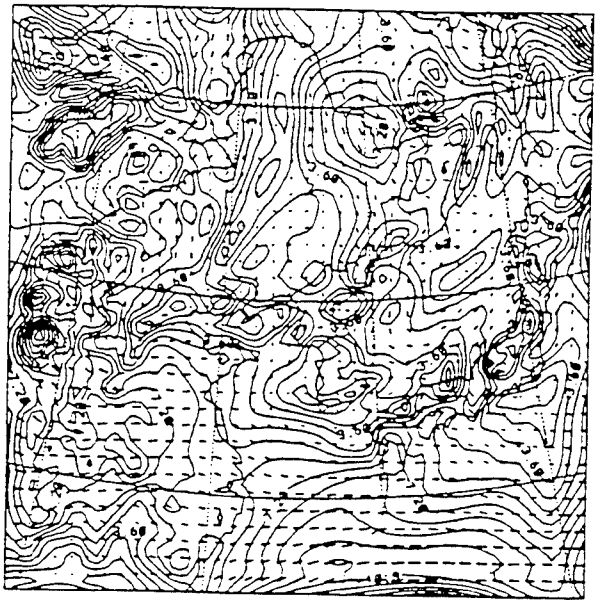

(c) NORAPS6 - 18 Aug 94 - 1200 UTC forecast

Figure 4-11. Surface wind - Korea. (Continued)

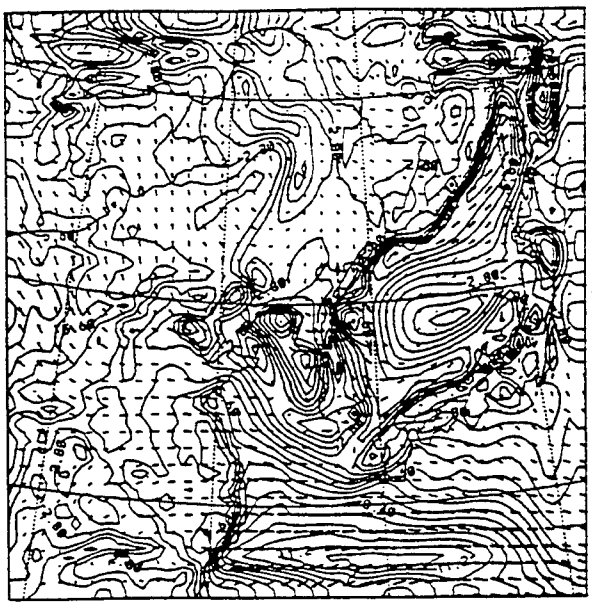

(d) RAMS - 18 Aug 94 - 1200 UTC forecast

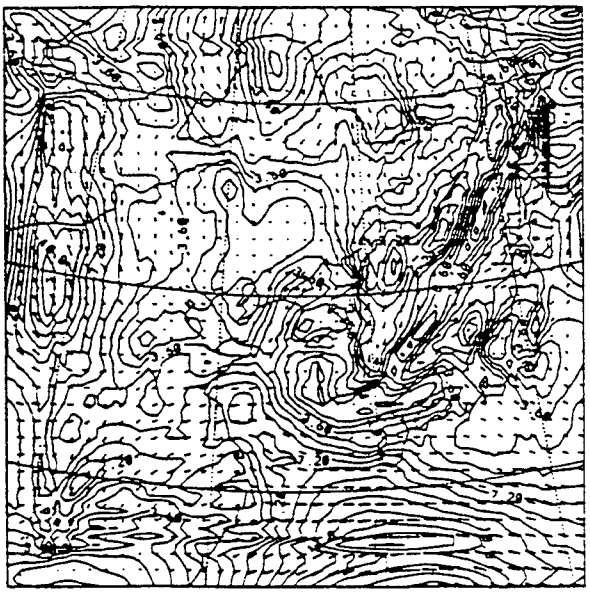

(e) RWM - 18 Aug 94 - 1200 UTC forecast

Figure 4-11. Surface wind - Korea. (Continued)

The data analysis showed a large low-pressure system moving in from the west boundary. All models captured the entry of this system, but RAMS and NORAPS6 over-predicted a low development near the northeastern corner of the domain. MM5 produced a fictitious low in the southwestern part of the domain.

Upper Air

The 500 mb analysis showed an upper level ridge over the western part of the domain and a trough over the eastern part. All models did a fairly good job, but under-predicted the ridge intensity over the China mainland.

4.1.2.7 Statistical Results – Korea. Error frequency distributions were generated for temperature, surface pressure, dew point depression, wind speed below 20 knots, wind speed above 20 knots, and wind direction. Data from all forecast times, both August forecasts, and where appropriate, levels were merged. The central column corresponds to the desired error bounds. Two sets of figures were developed to describe the forecast results. One is a surface set that includes the large number of surface observations and the other is an upper air set that includes the more sparse upper air observations. Figures 4-12(a - f) are the surface results and Figures 4-13(a - e) are the upper air results.

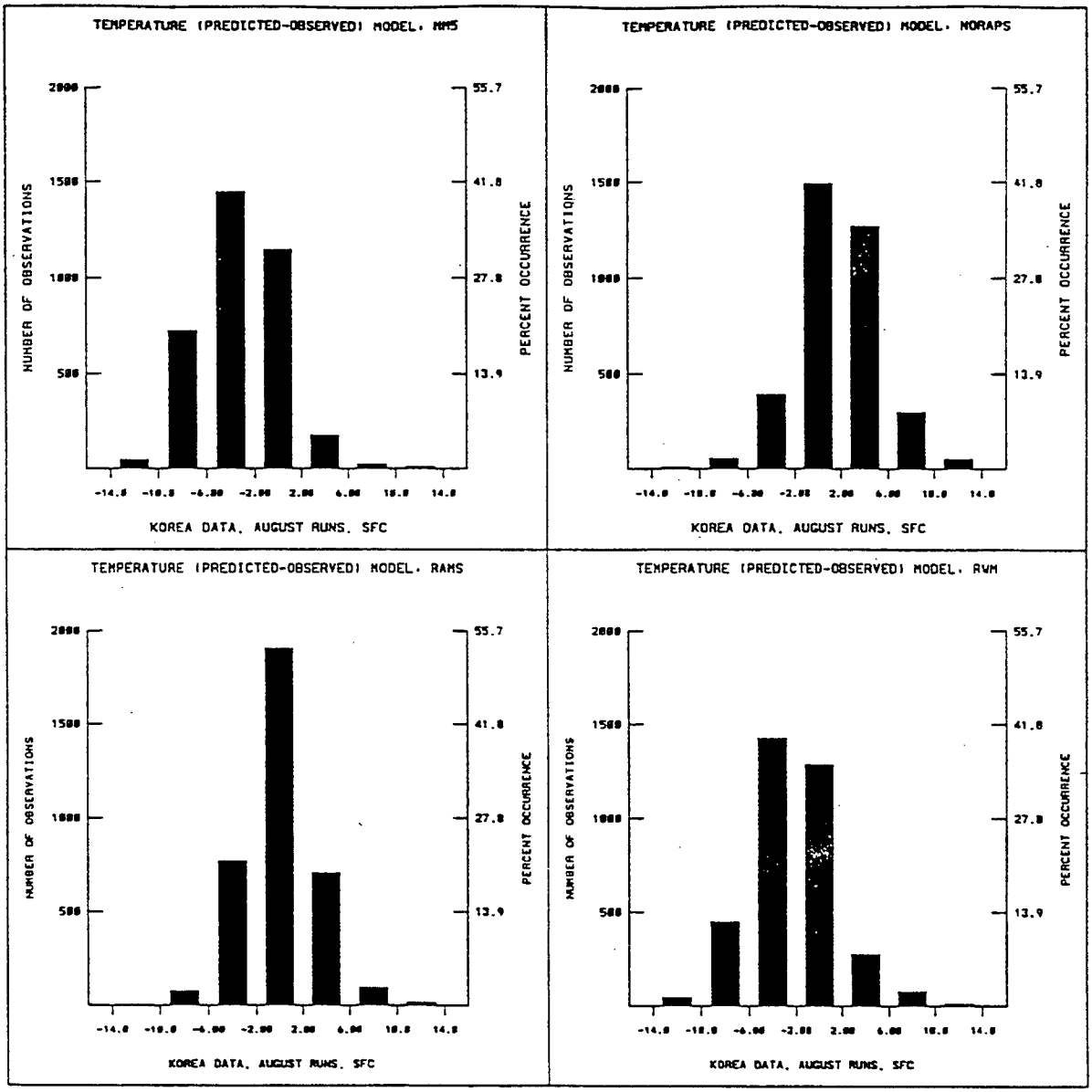

(a) Temperature

Figure 4-12. Surface error statistics, August - Korea.

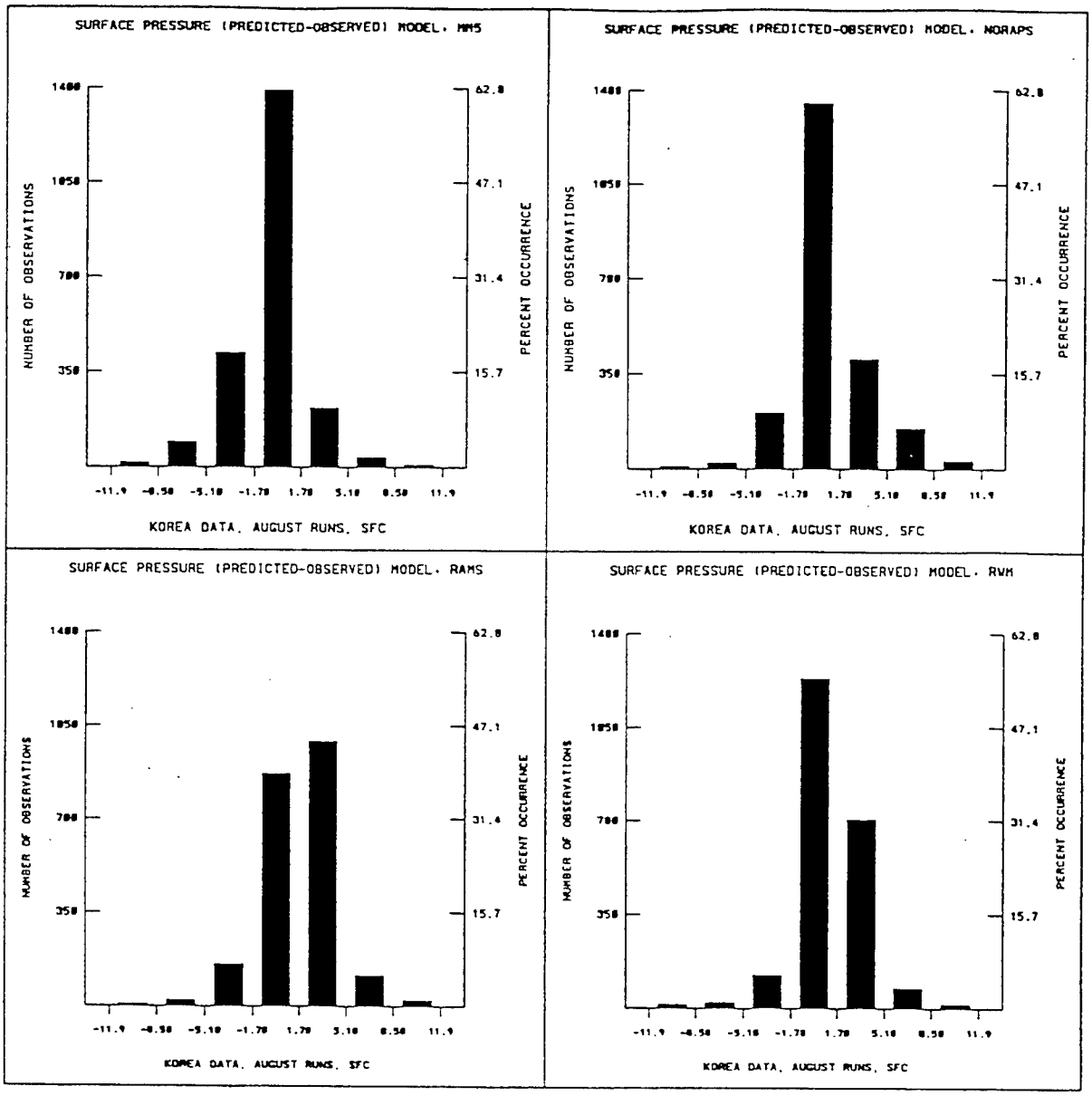

(b) Pressure

Figure 4-12. Surface error statistics, August - Korea. (Continued)

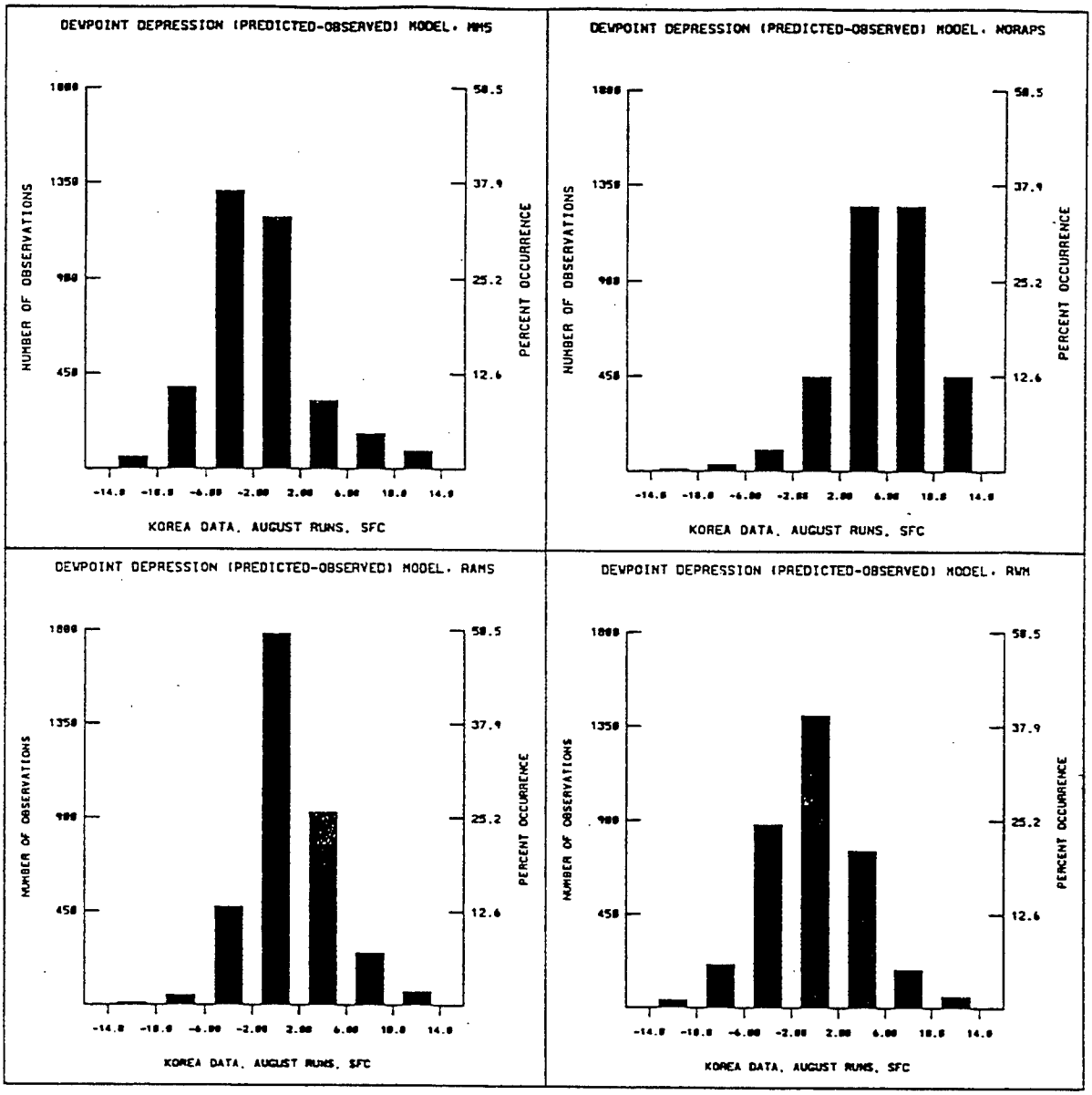

(c) Dew point depression

Figure 4-12. Surface error statistics, August - Korea. (Continued)

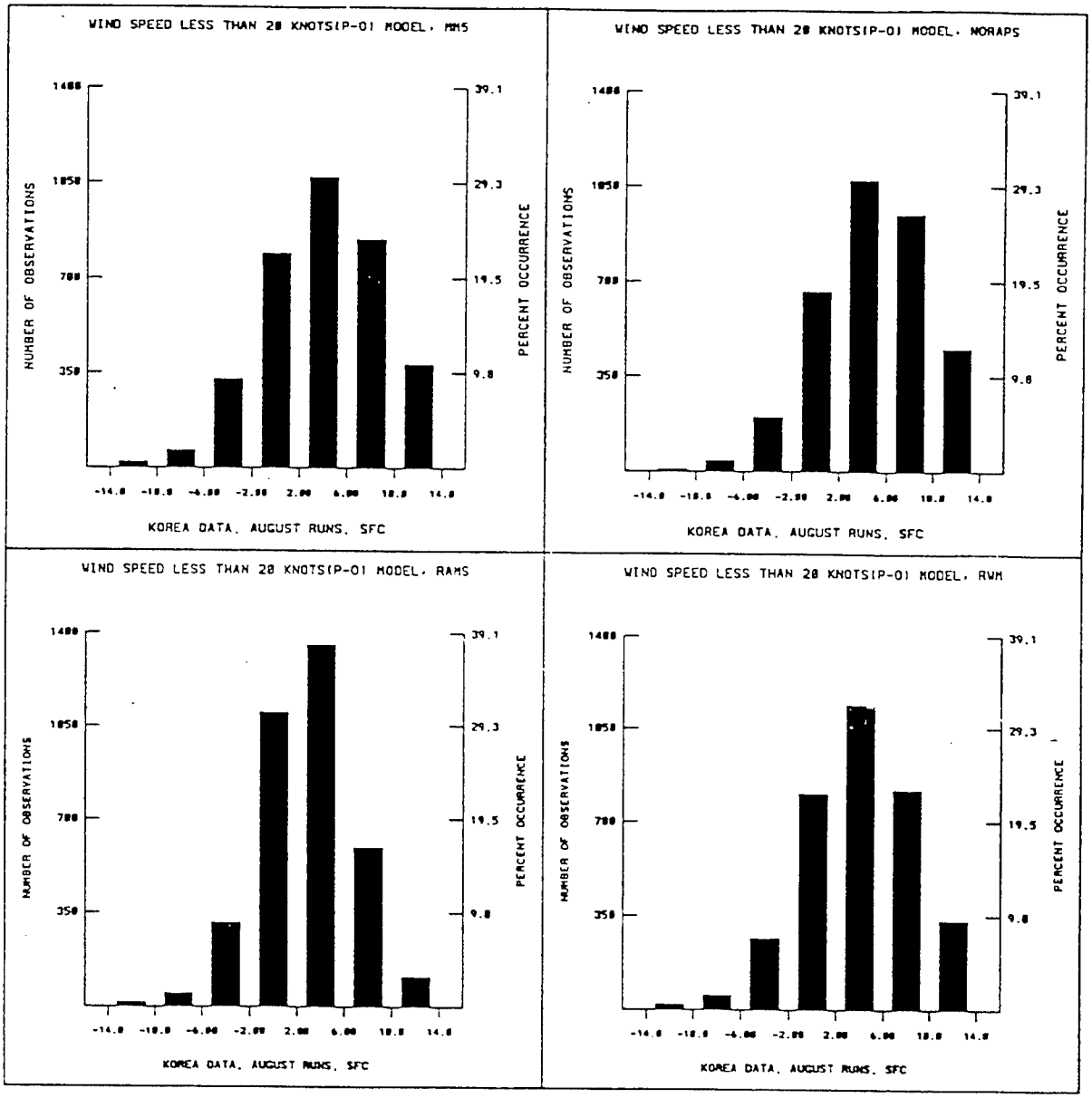

(d) Wind speed < 20 Knots

Figure 4-12. Surface error statistics, August - Korea. (Continued)

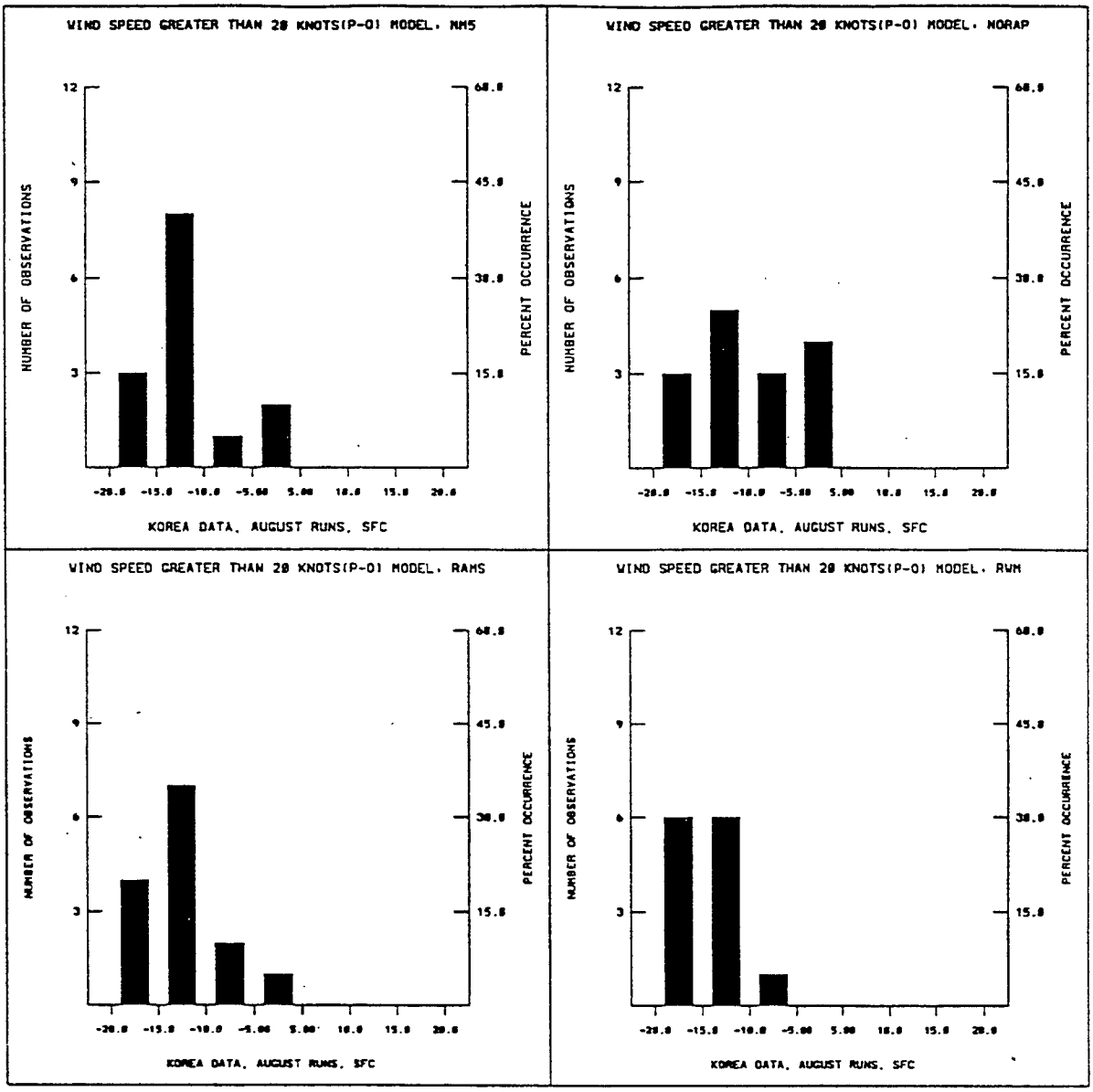

(e) Wind speed > 20 Knots

Figure 4-12. Surface error statistics, August - Korea. (Continued)

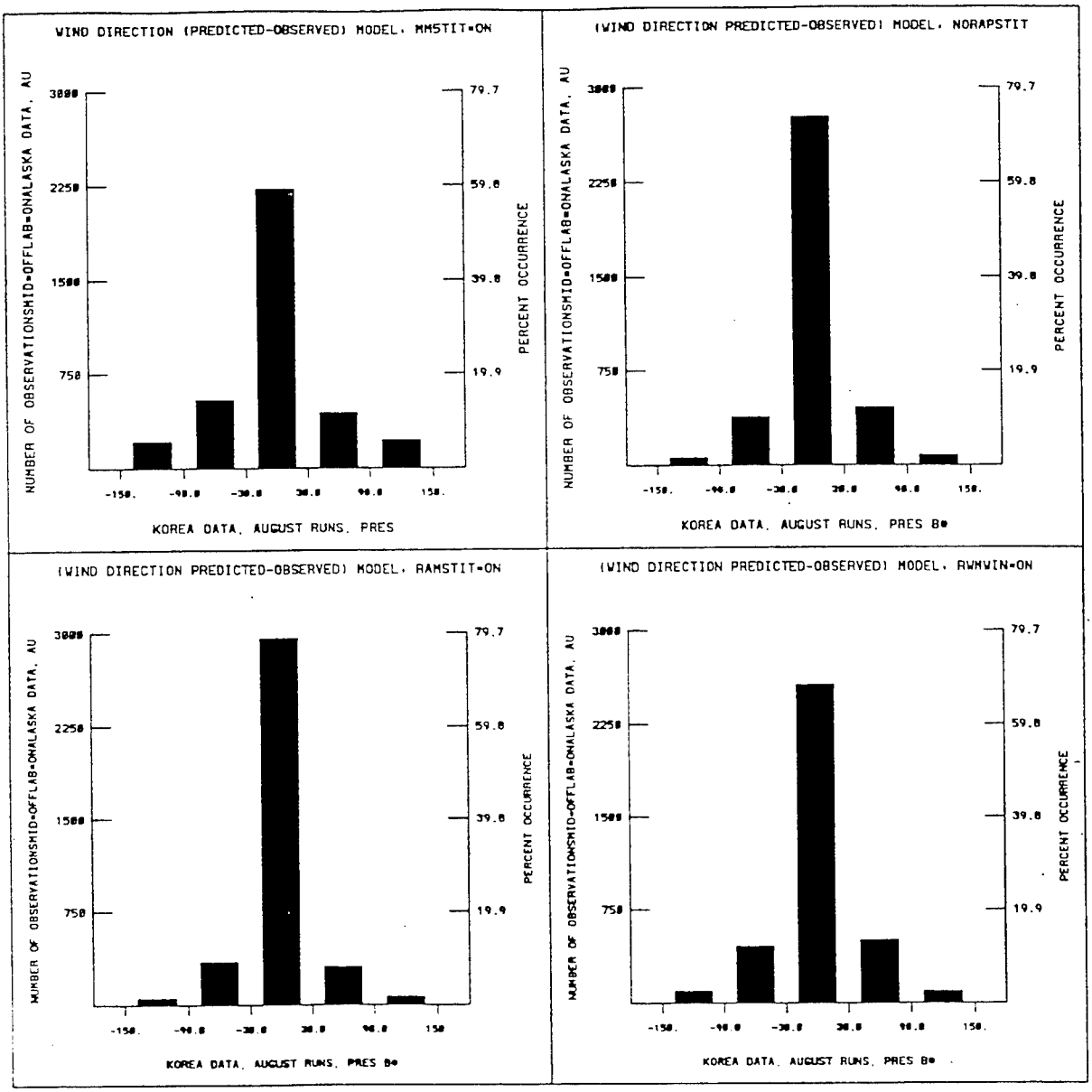

(f) Wind direction

Figure 4-12. Surface error statistics, August - Korea. (Continued)

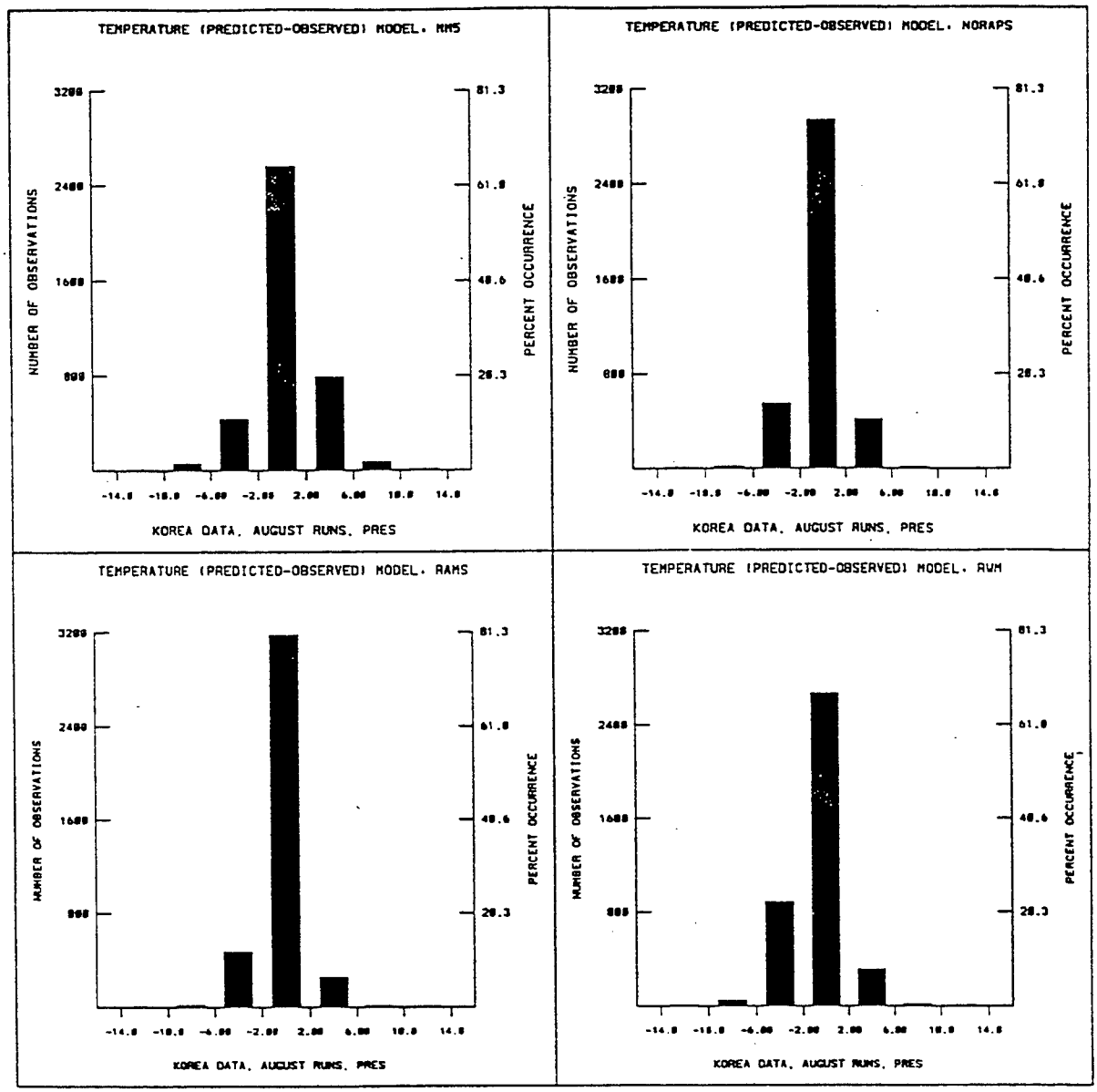

(a) Temperature

Figure 4-13. Upper air error statistics, August - Korea.

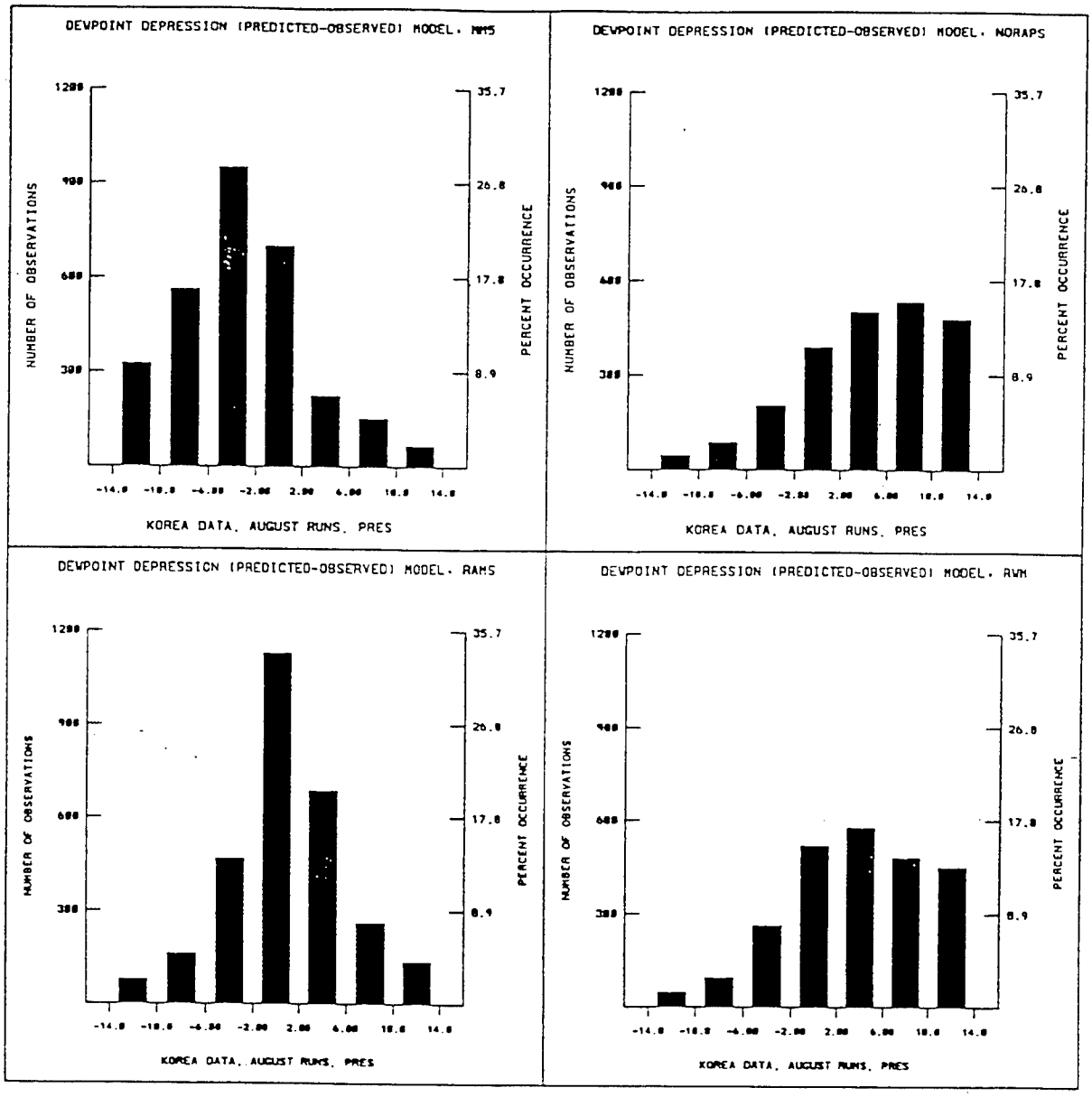

(b) Dew point depression

Figure 4-13. Upper air error statistics, August - Korea. (Continued)

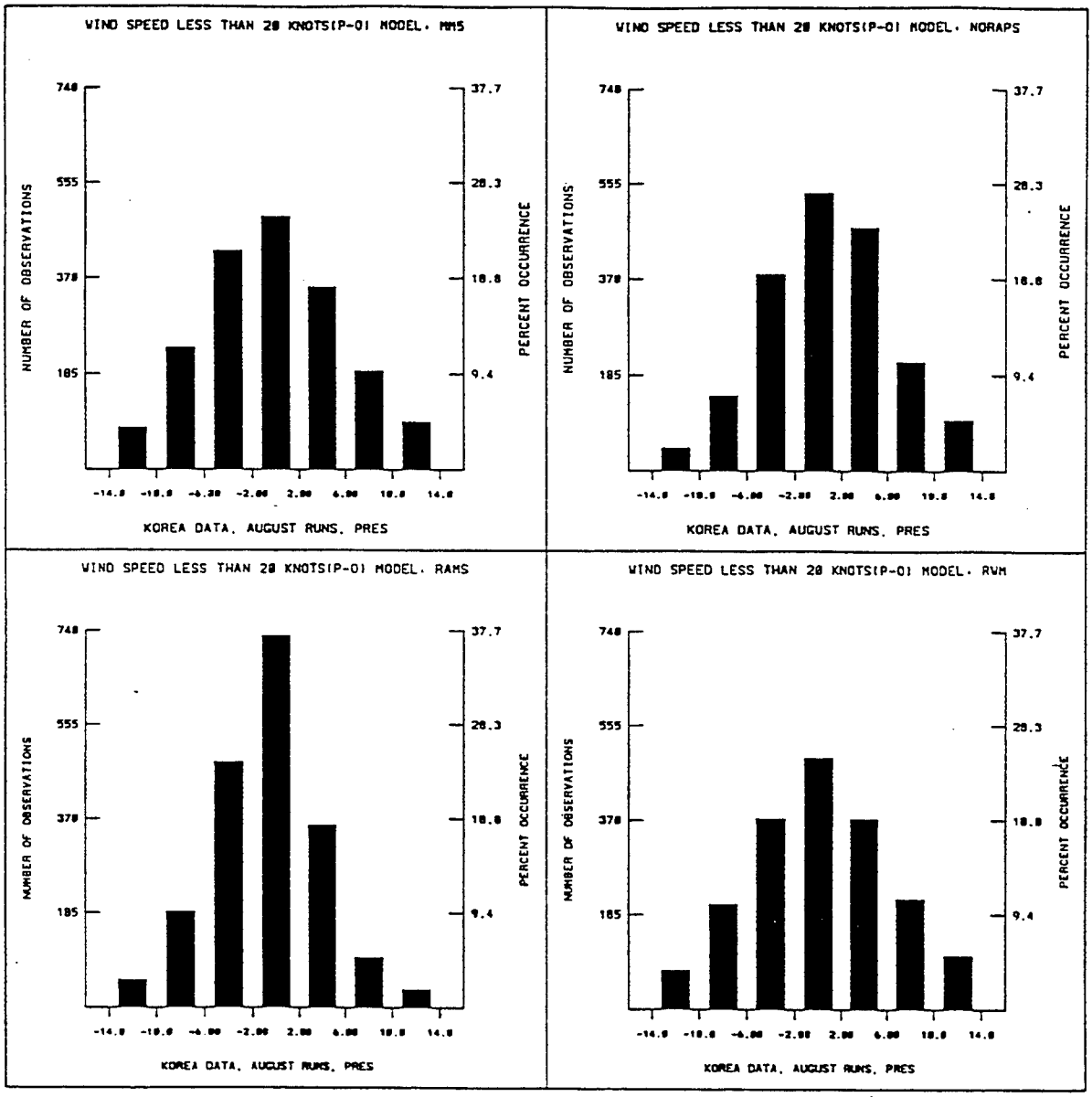

(c) Wind speed < 20 Knots

Figure 4-13. Upper air error statistics, August - Korea. (Continued)

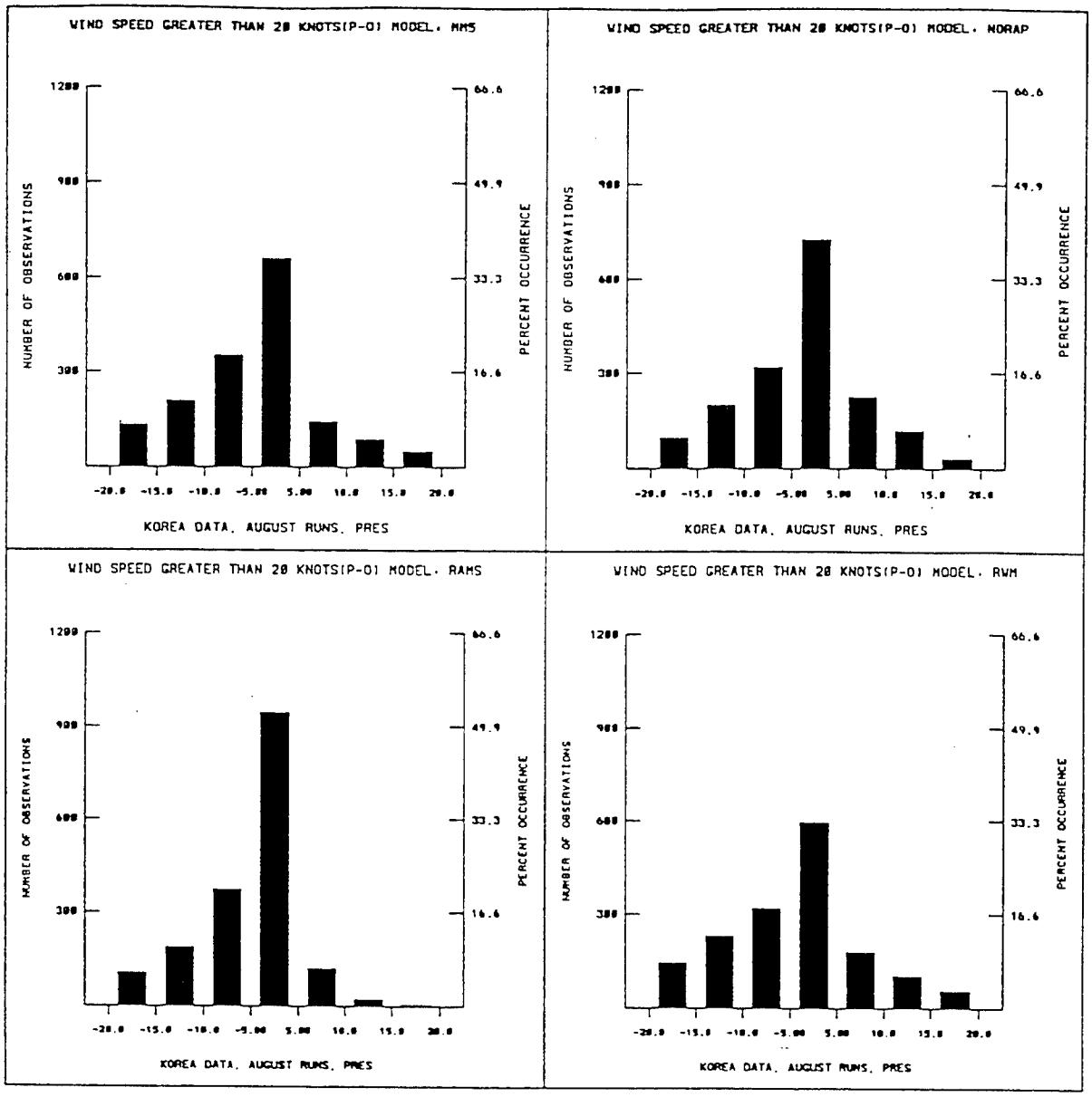

(d) Wind speed > 20 Knots

Figure 4-13. Upper air error statistics, August - Korea. (Continued)

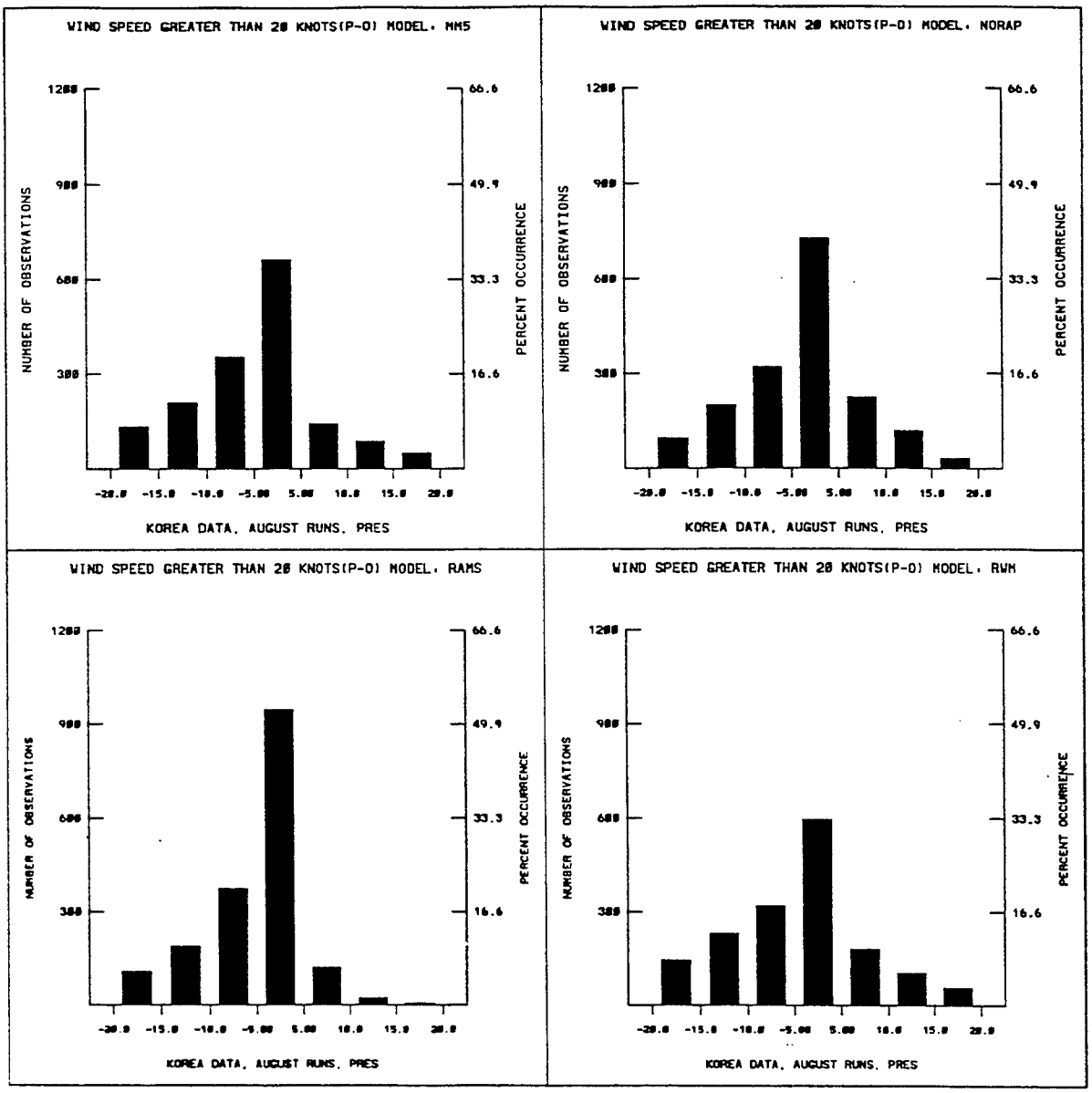

(e) Wind direction

Figure 4-13. Upper air error statistics, August - Korea. (Continued)

4.1.2.8 Phenomenological Results - Middle East. Phenomenology results at 24 hours into the first forecast period (17 Aug 94 – 0000 UTC).

Surface

The surface sea level pressure analysis showed a "heat low" with a broad center over much of the Persian Gulf/Saudi Arabian region with localized areas of 992 mb pressure. All models captured the general pattern and all also had the general pattern of cooling over Turkey and Iran, with higher temperatures over Saudi Arabia. All models were moister than the data analysis, although RAMS was driest.

Upper Air

The 500 mb data analysis showed an anticyclone over Saudi Arabia and the Red Sea. MM5 predicted a trough, while all others had an anticyclone that was slightly weaker than the analysis.

Phenomenology results at 24 hours into the second forecast period (17 Aug 94 – 0000 UTC).

Surface

The most significant feature in the surface analysis was a "heat low" elongated from the northwest to the southeast over Iran of 986 mb central pressure. RAMS captured this feature very well, forecasting a good orientation and central pressure of 986 mb. MM5 forecast a weak center of 996 mb and shifted south over Saudi Arabia. It forecast a 1010 mb localized high over Iran. NORAPS6 and RWM also show a ridge over Iran. RAMS also did very well with the relative humidity forecast; all other models were too high over the desert region for the August period. In conjunction with this, RAMS did very well with the temperature forecasts while the others did not heat enough during the day. Figures 4-14(a - e) show the surface pressure.

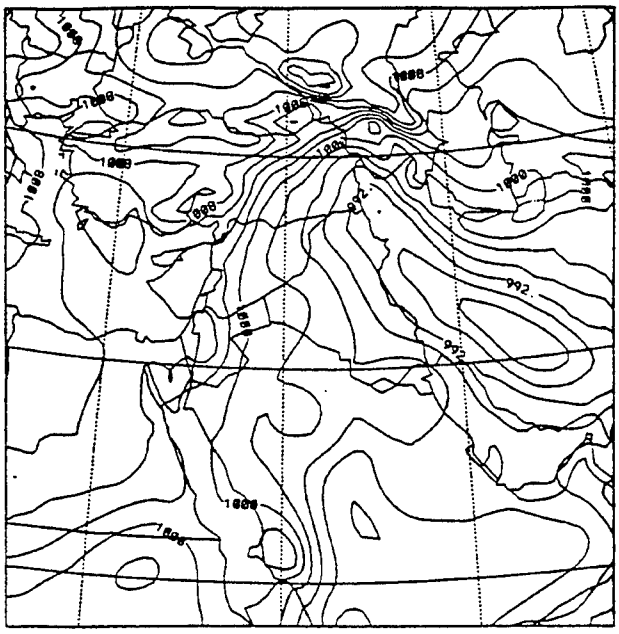

sea level pressure (mb)

(a) Analysis at 18 Aug 94 - 1200 UTC

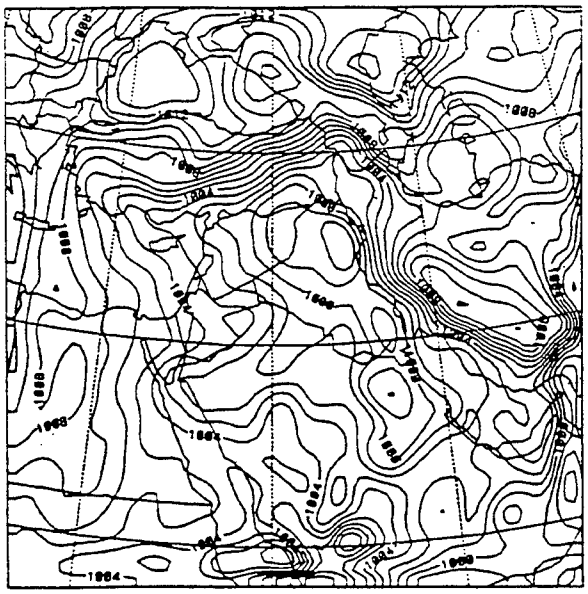

(b) MM5 - 18 Aug 94 - 1200 UTC forecast

Figure 4-14. Surface pressure - Middle East.

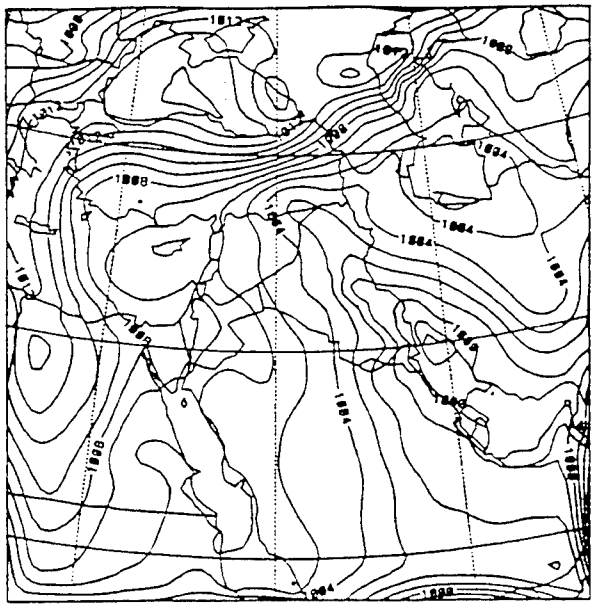

(c) NORAPS6 - 18 Aug 94 - 1200 UTC forecast

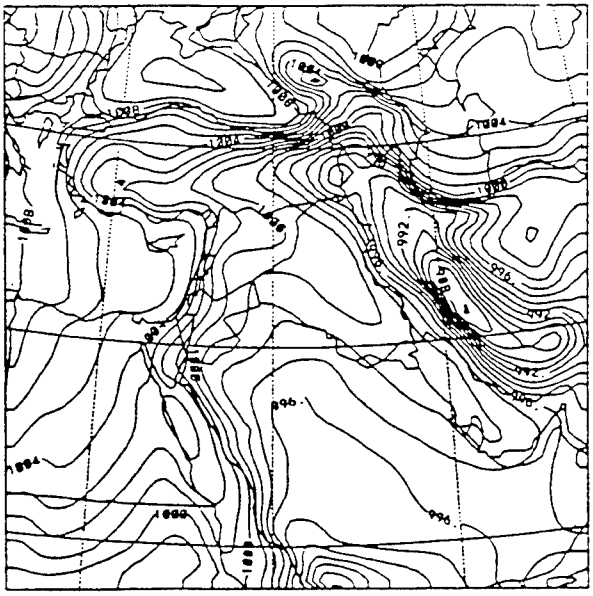

(d) RAMS - 18 Aug 94 - 1200 UTC forecast

Figure 4-14. Surface pressure - Middle East. (Continued)

(e) RWM - 18 Aug 94 - 1200 UTC forecast

Figure 4-14. Surface pressure - Middle East. (Continued)

Upper Air

The 500 mb analysis showed an anticyclone in southern part of the domain with weak trough in the north. MM5 did not forecast the anticyclone, while all other models did. All models forecast the trough to one extent or another, although the data analysis was difficult to interpret.

4.1.2.9 Statistical Results Middle East. Error frequency distributions were generated for temperature, surface pressure, dew point depression, wind speed below 20 knots, wind speed above 20 knots, and wind direction. Data from all forecast times, both August forecasts, and where appropriate, levels were merged. The central column corresponds to the desired error bounds. Two sets of figures were developed to describe the forecast results. One is a surface set that includes the large number of surface observations and the other is an upper air set that includes the more sparse upper air observations. Figures 4-15(a - f) are the surface results and Figures 4-16(a - e) are the upper air results.

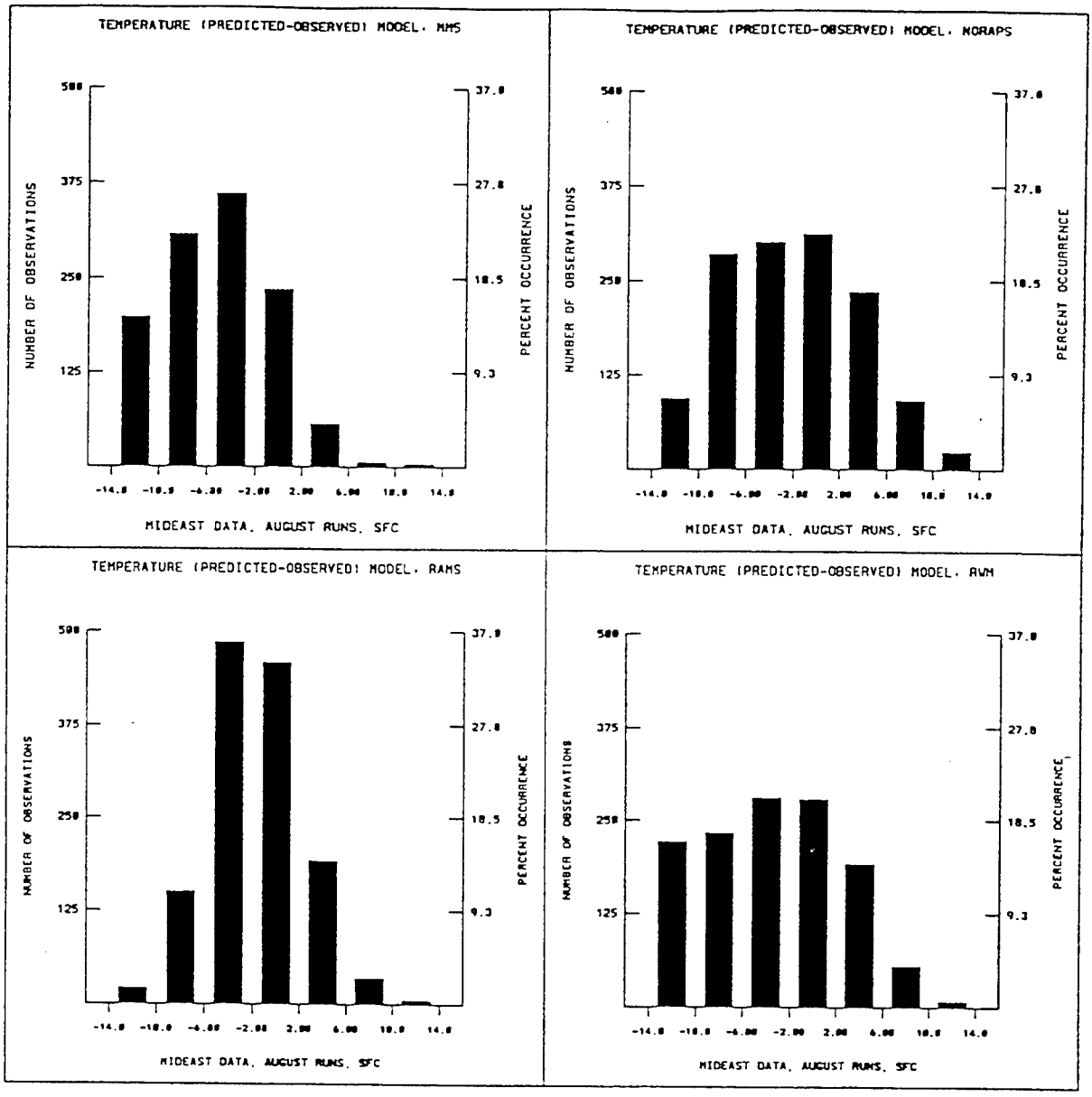

(a) Temperature

Figure 4-15. Surface error statistics, August - Middle East.

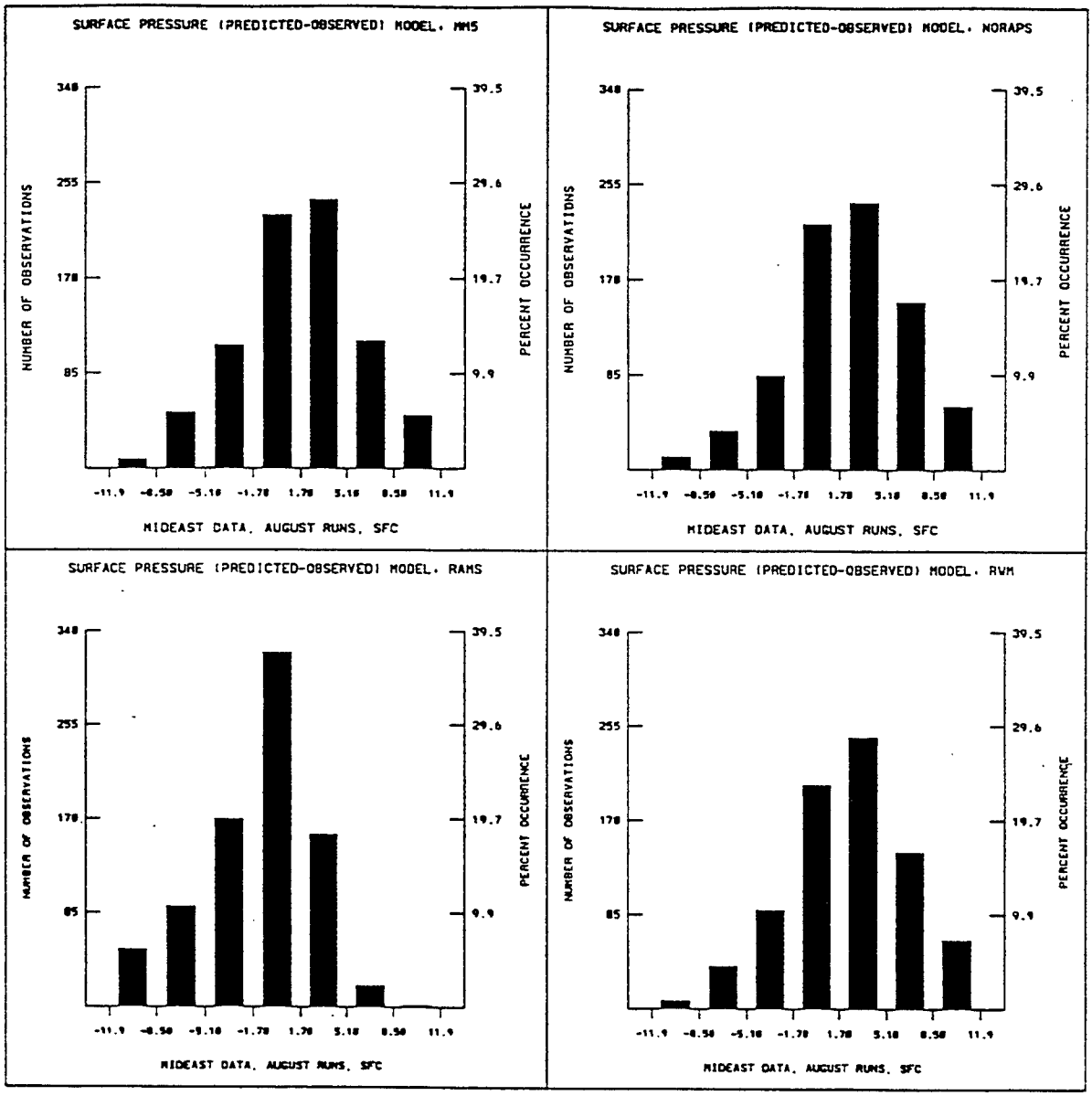

(b) Pressure

Figure 4-15. Surface error statistics, August - Middle East. (Continued)

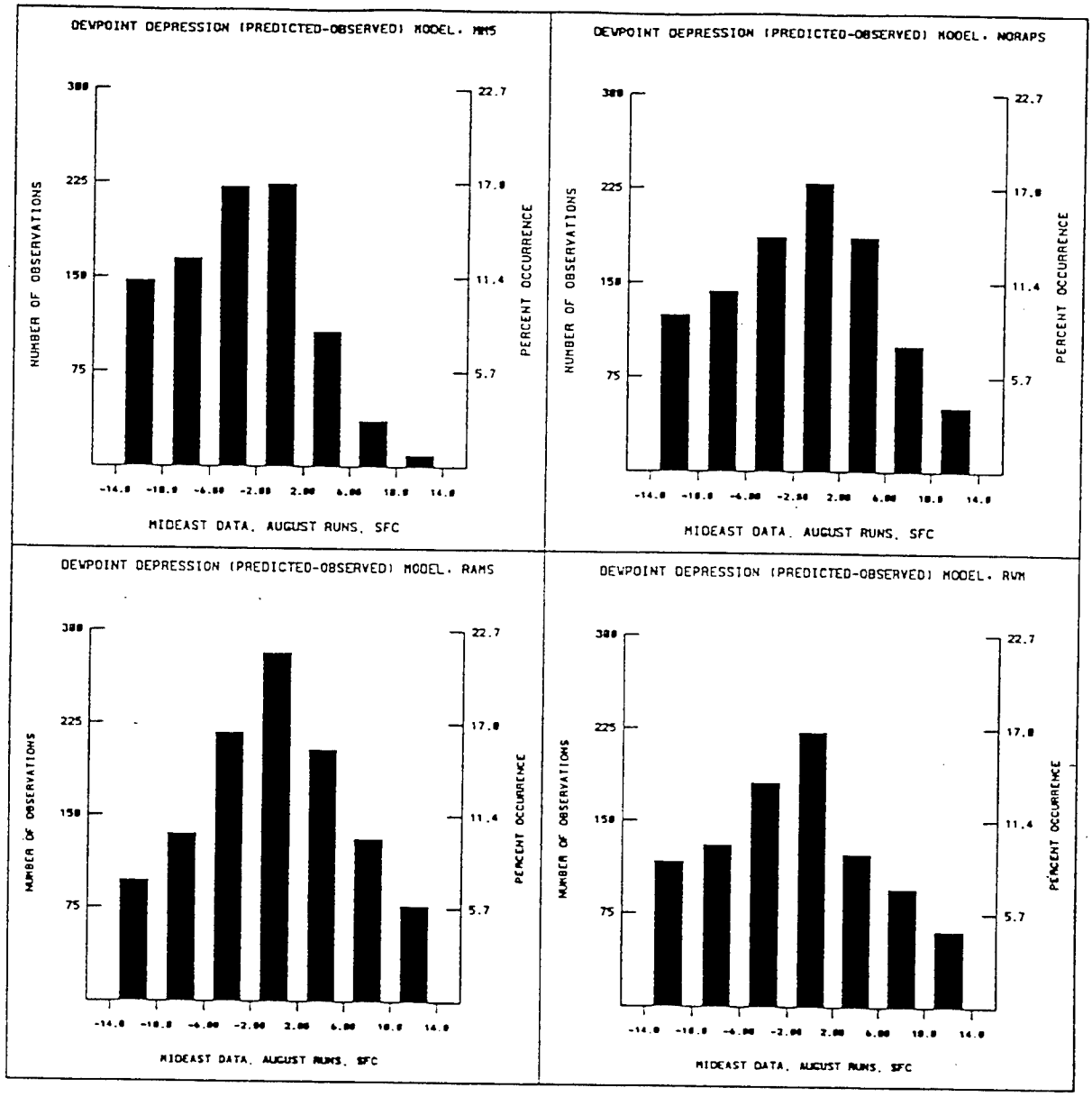

(c) Dew point depression

Figure 4-15. Surface error statistics, August - Middle East. (Continued)

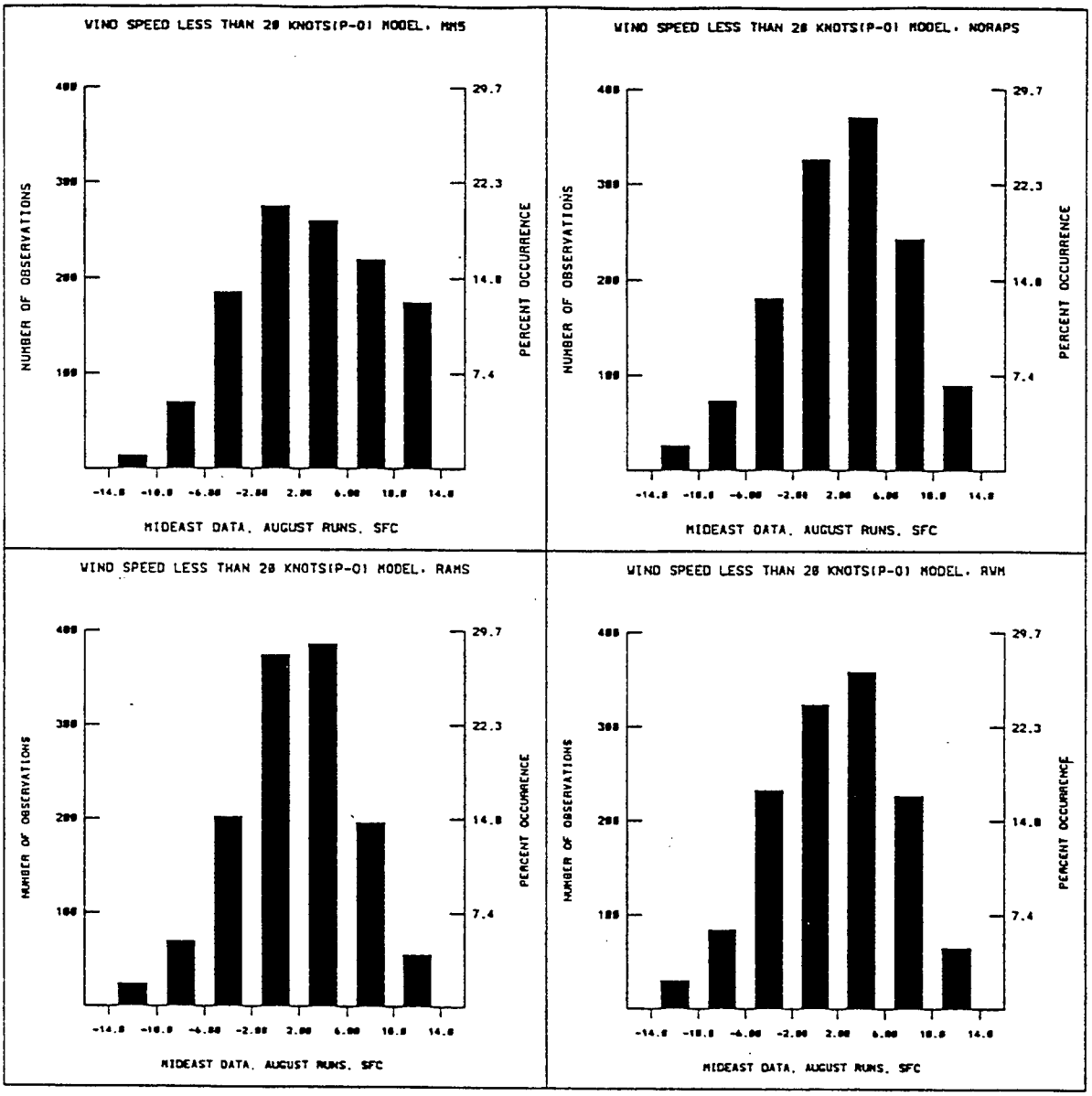

(d) Wind speed < 20 Knots

Figure 4-15. Surface error statistics, August - Middle East. (Continued)

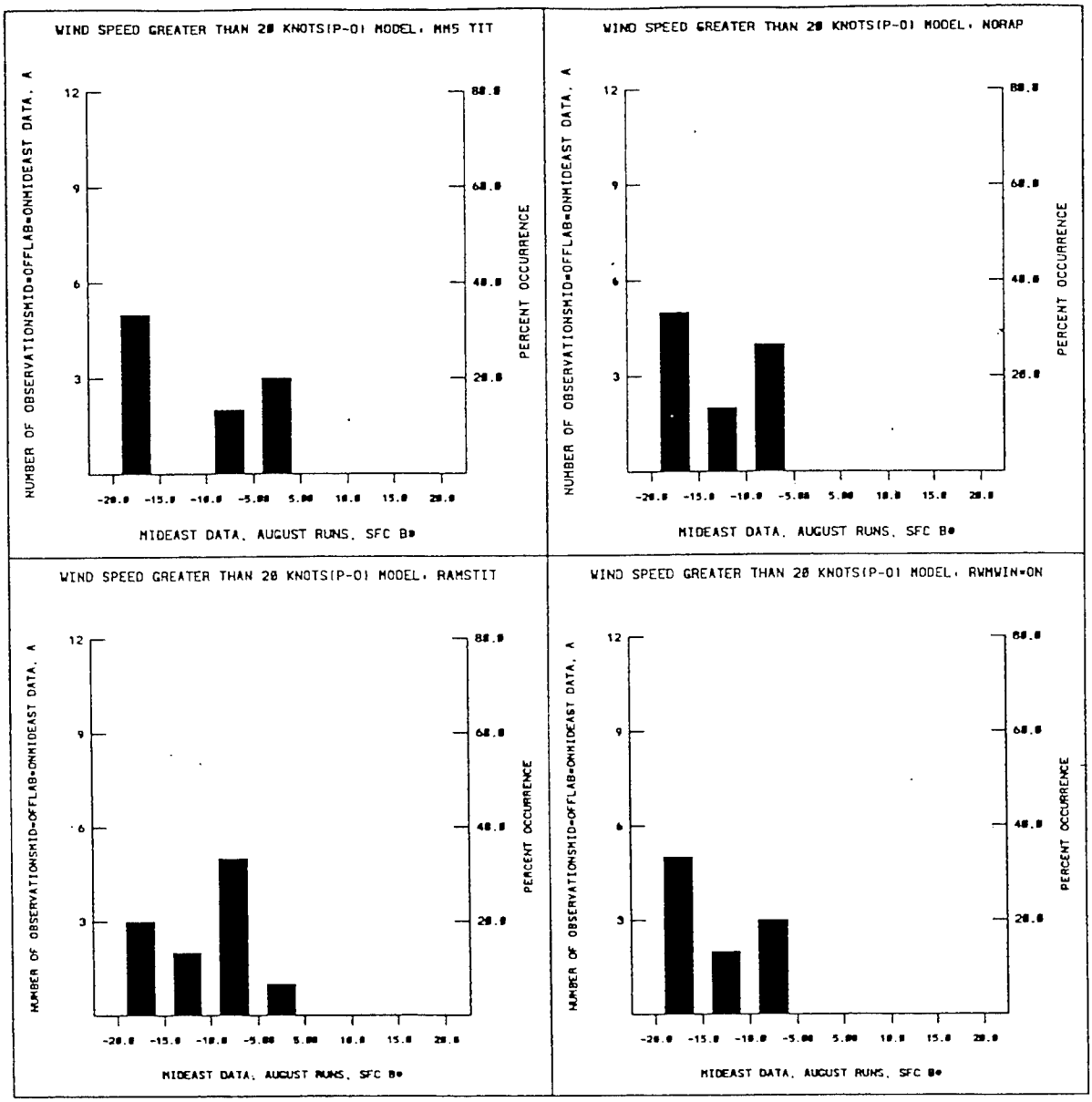

(e) Wind speed > 20 Knots

Figure 4-15. Surface error statistics, August - Middle East. (Continued)

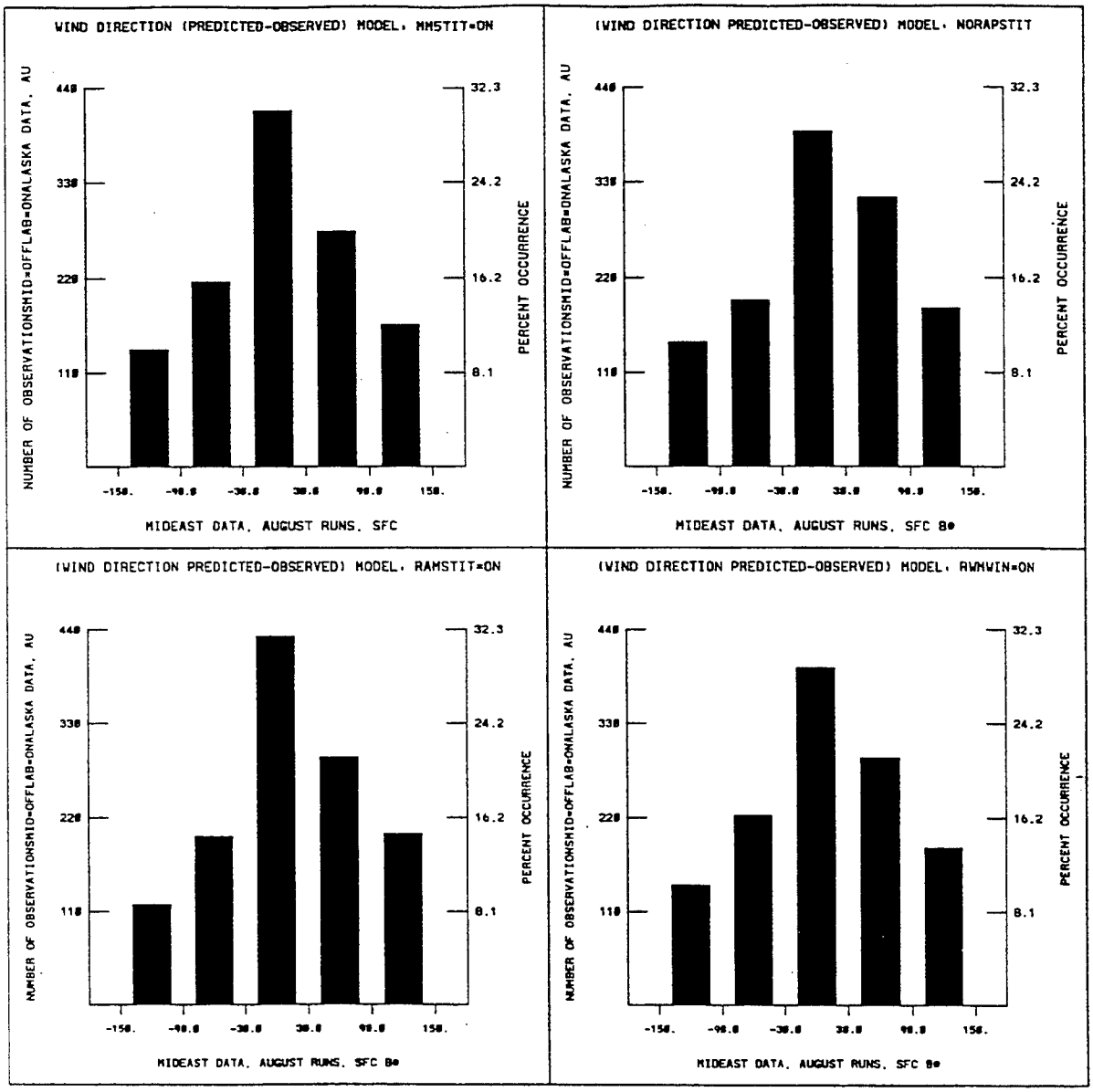

(f) Wind direction

Figure 4-15. Surface error statistics, August - Middle East. (Continued)

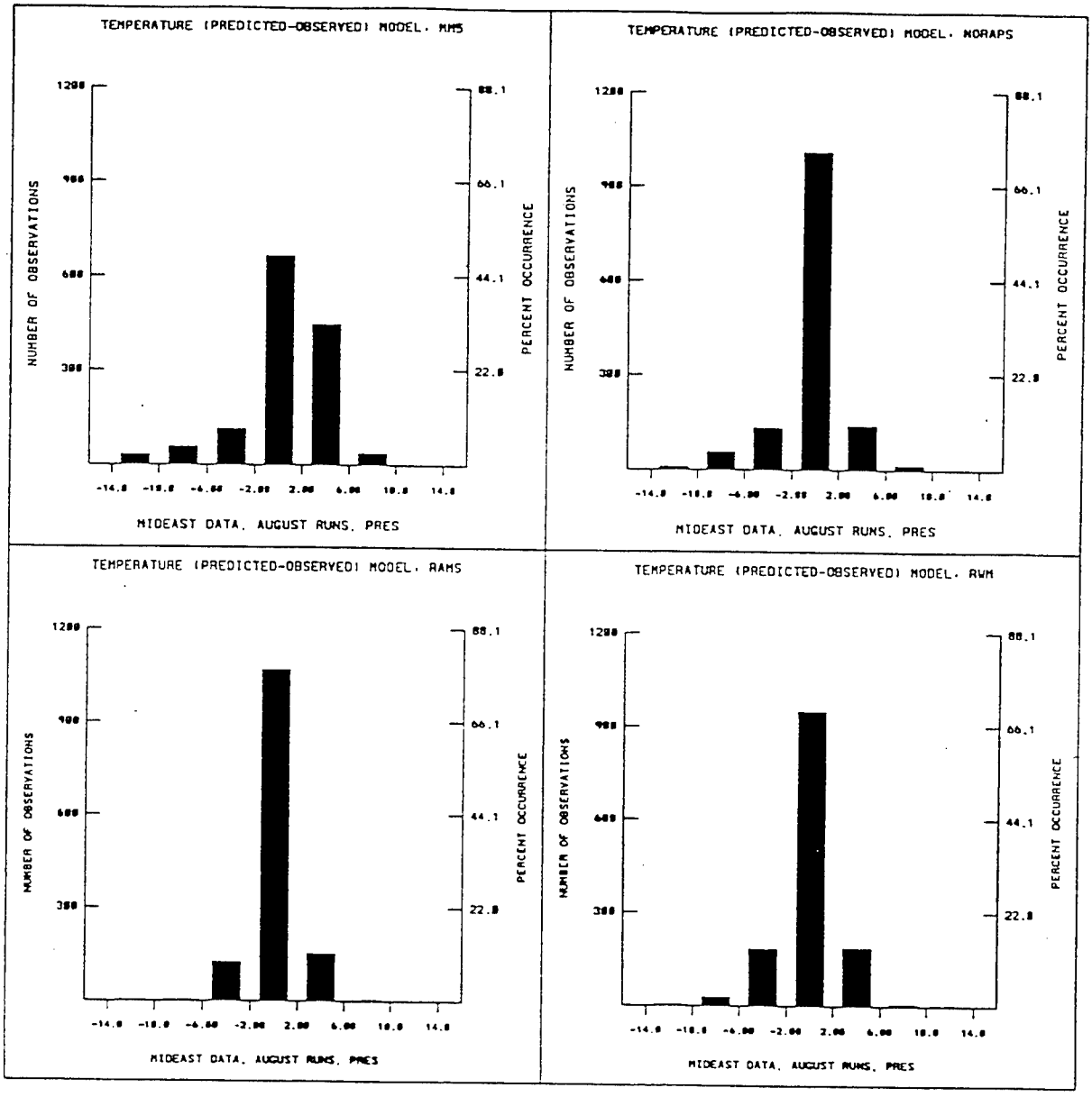

(a) Temperature

Figure 4-16. Upper air error statistics, August - Middle East.

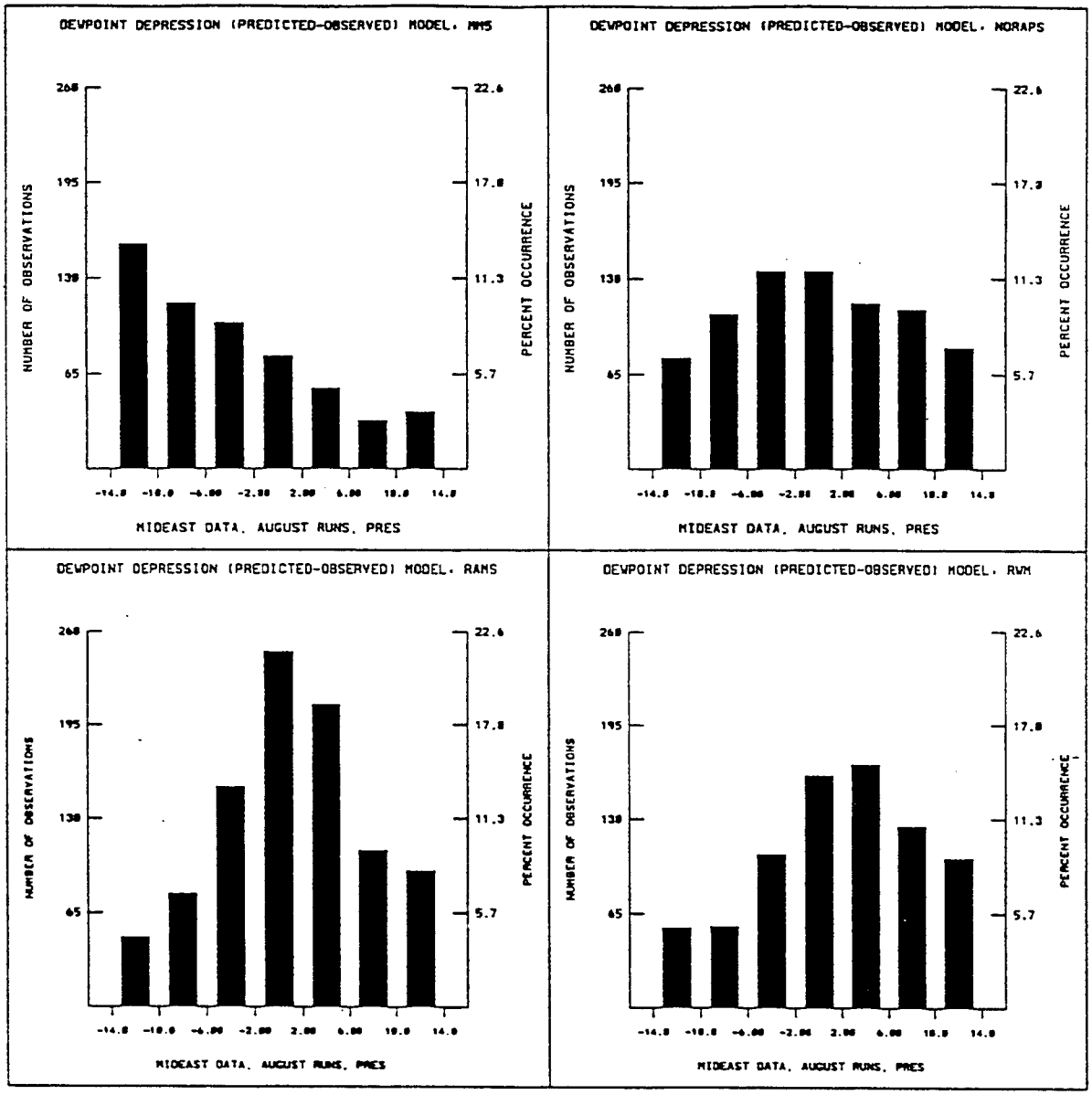

(b) Dew point depression

Figure 4-16. Upper air error statistics, August - Middle East. (Continued)

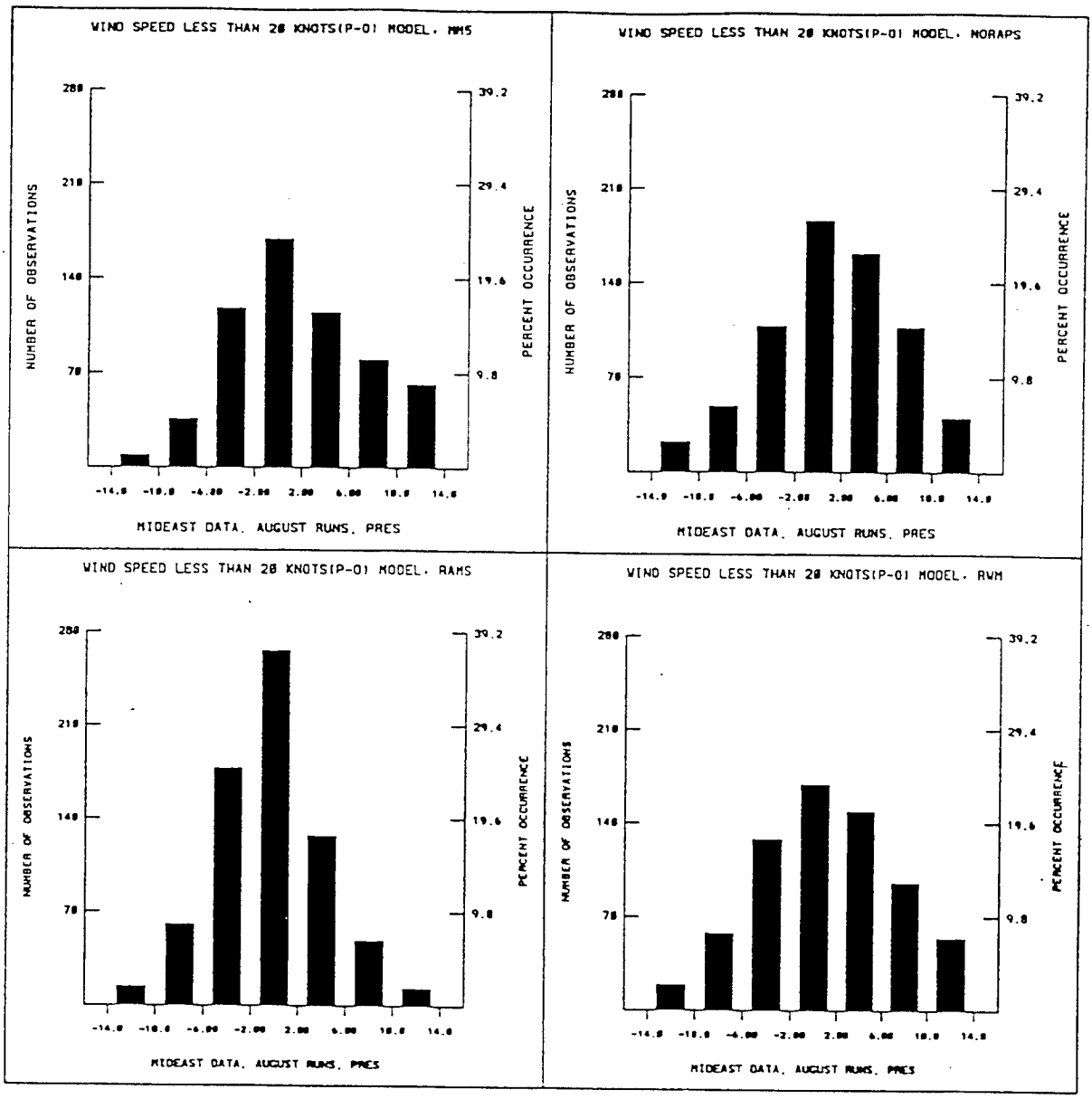

(c) Wind speed < 20 Knots

Figure 4-16. Upper air error statistics, August - Middle East. (Continued)

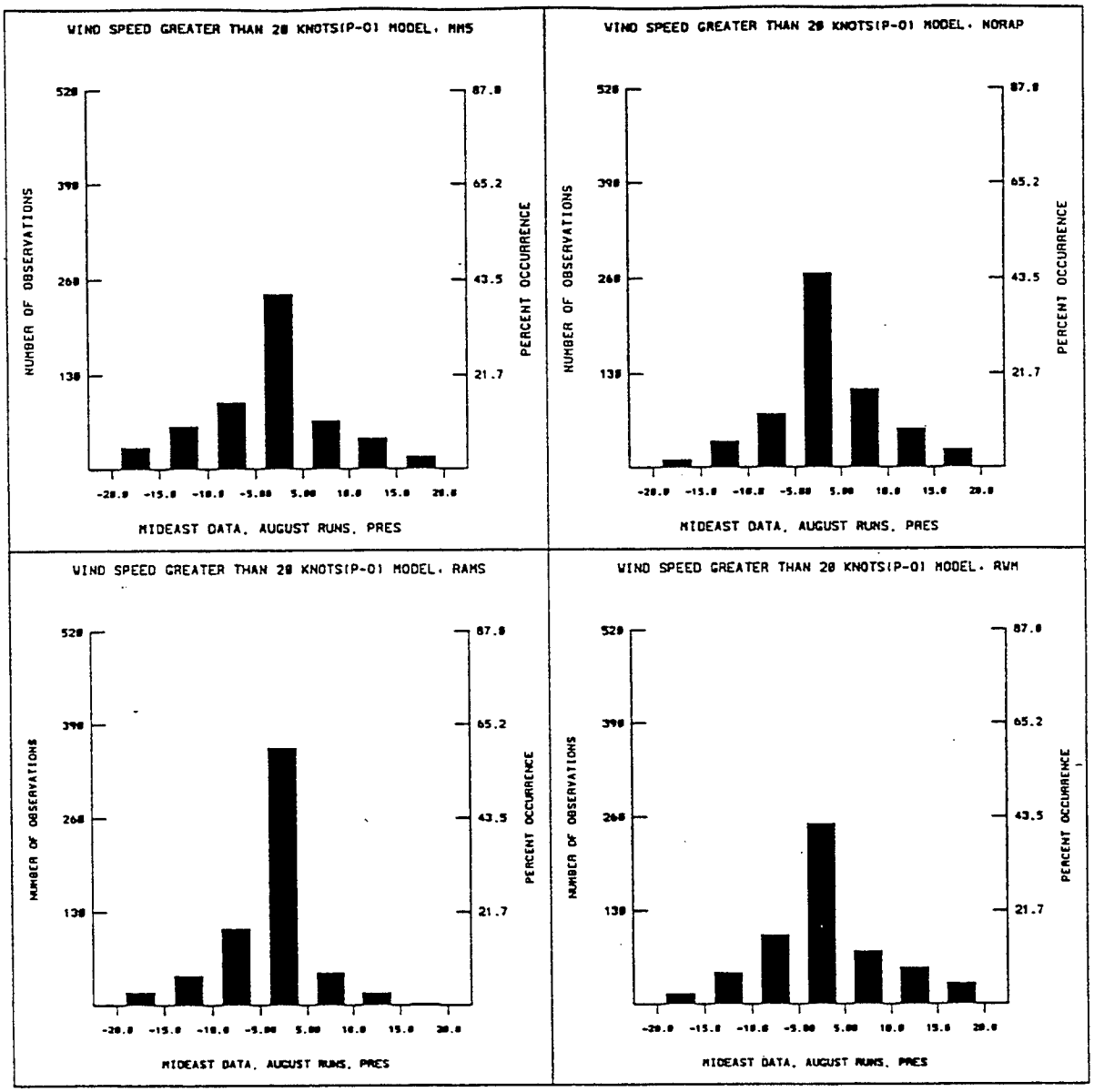

(d) Wind speed > 20 Knots

Figure 4-16. Upper air error statistics, August - Middle East. (Continued)

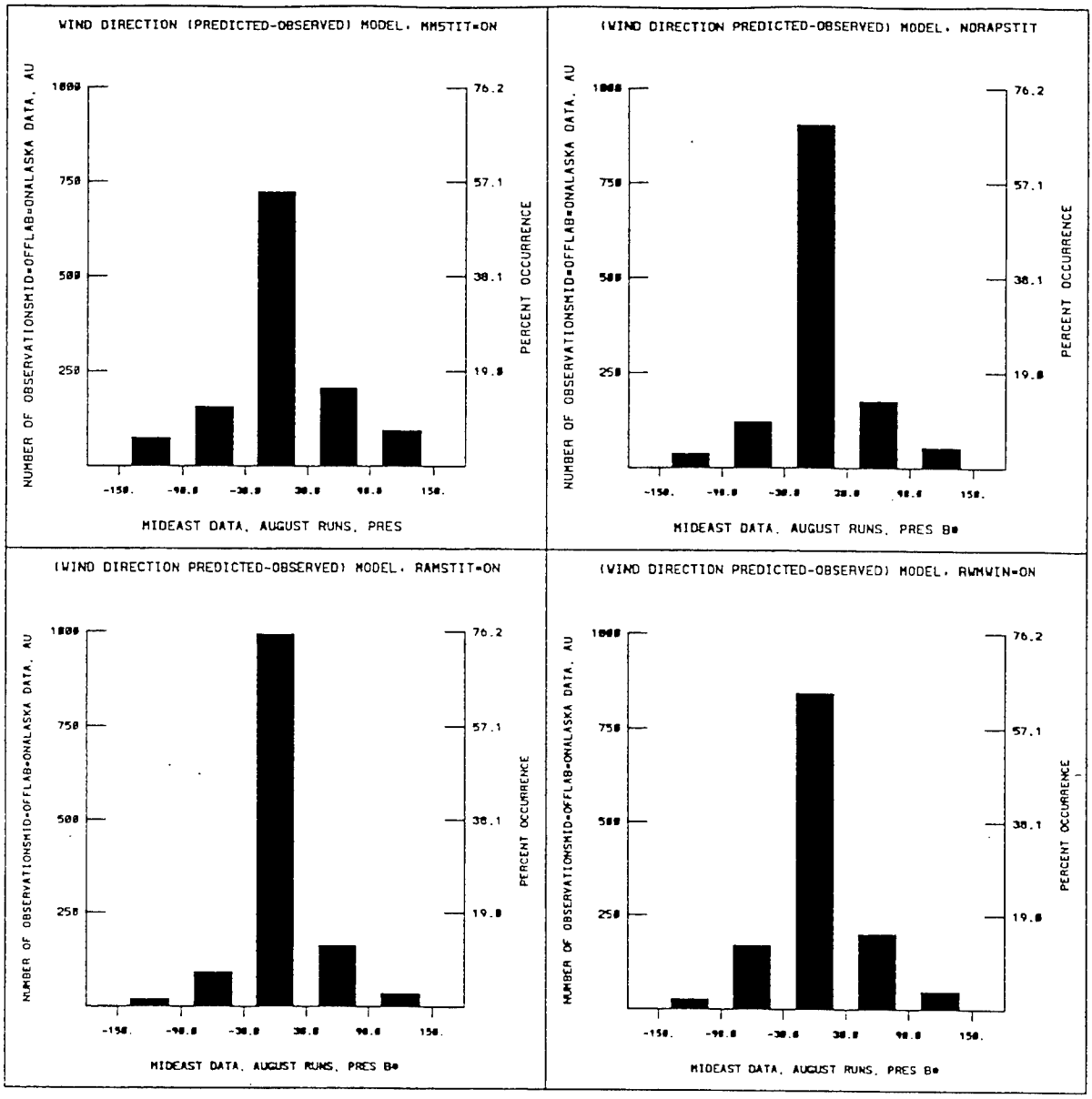

(e) Wind direction

Figure 4-16. Upper air error statistics, August - Middle East. (Continued)

4.1.2.10 Phenomenological Results - Central America. Phenomenology results at 24 hours into the first forecast period (17 Aug 94 – 0000 UTC).

Surface

This domain had the least amount of observation than any of the regions. RAMS, MM5, and RWM showed evidence of a sea breeze convergence zone on the southern coast of Central America. NORAPS6 did not, probably due to the lack of a land-use parameterization. Temperatures generally looked reasonable in RAMS, MM5, and RWM. MM5 looked too moist over the water areas, while NORAPS6 and RWM seemed too dry.

Upper Air

All models had the 500 mb flow reasonably correct. MM5 had strong perturbation due to convective scheme over Haiti. The RAMS 500 mb height field looked good along with MM5, although MM5 demonstrated a few boundary perturbations. NORAPS6 seemed to have incorrect gradients near the northern boundary, while RWM was noisy but seemed to have reasonable values.

Phenomenology results at 24 hours into the second forecast period (17 Aug 94 – 0000 UTC).

Surface

NORAPS6 cooled more than the others did over the land areas. RAMS was still reasonable on the relative humidity forecast, while MM5 continued too wet and NORAPS6 and RWM too dry. MM5 and RWM forecast a low development north of Panama, which was not in the data analysis. RAMS and NORAPS6 did not reproduce the low. RAMS had a high sea level pressure bias in this run.

Upper Air

The 500 mb wind analysis showed an easterly jet core centered about 300 km north of Panama with a maximum speed of 16 m/s. RAMS forecast the core slightly weaker at 13 m/s and too far east. MM5 produced a more diffuse core with localized areas up to 20 m/s. NORAPS6 placed the core too far to the northwest with a maximum speed of 14 m/s. RWM had a good location with a maximum speed of 15 m/s. All models produced reasonably similar 500 mb height patterns, with RAMS having a high bias and RWM continuing to be noisy. The 500 mb winds are shown in Figures 4-17(a - e).

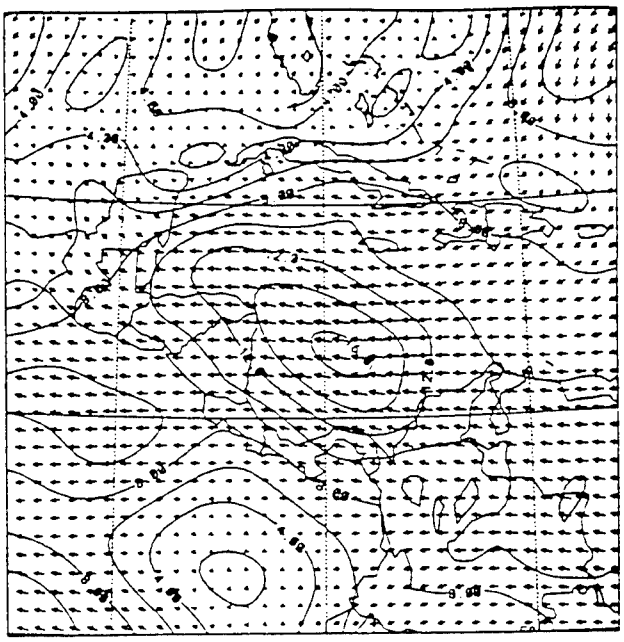

(a) Analysis at 18 Aug 94 - 1200 UTC

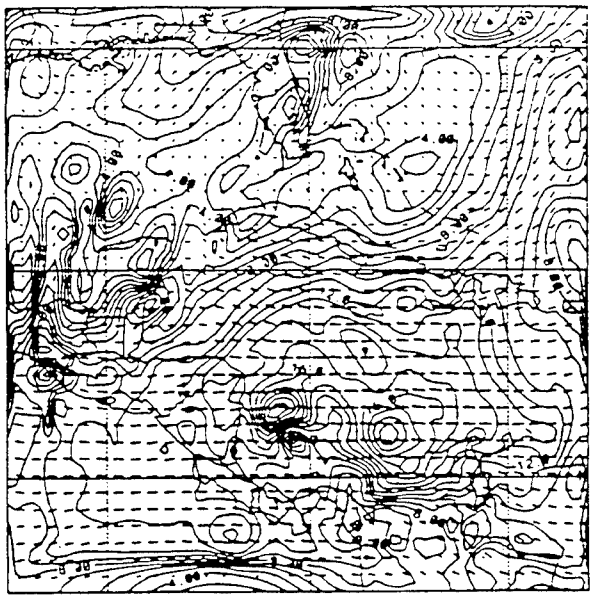

(b) MM5 - 18 Aug 94 - 1200 UTC forecast

Figure 4-17. 500mb winds - Central America.

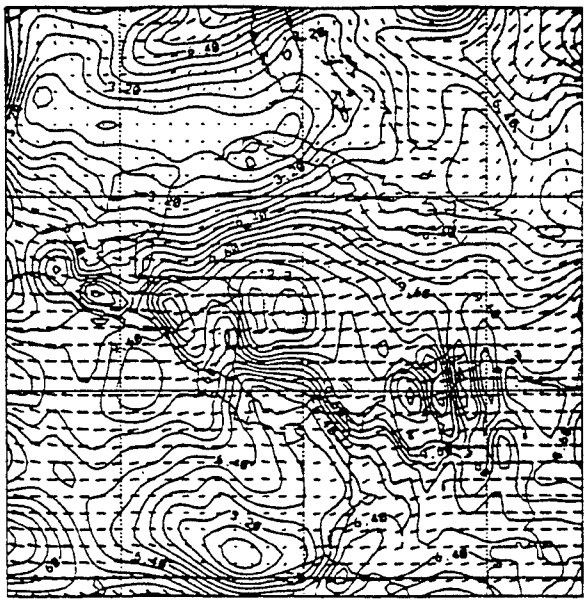

(c) NORAPS6 - 18 Aug 94 - 1200 UTC forecast

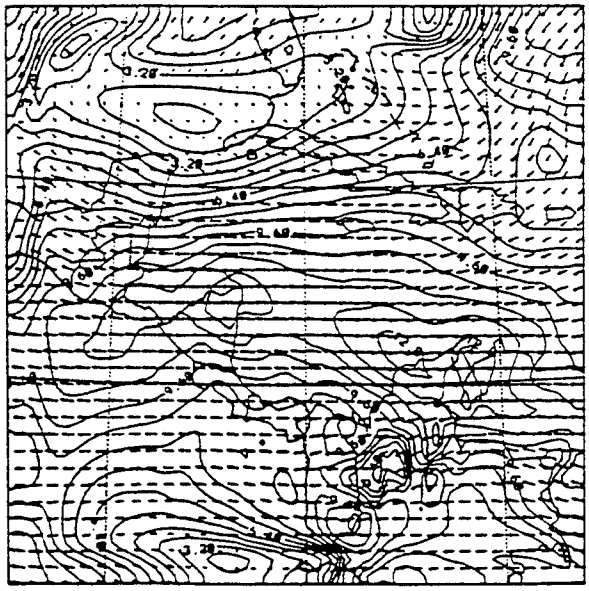

(d) RAMS - 18 Aug 94 - 1200 UTC forecast

Figure 4-17. 500mb winds - Central America. (Continued)

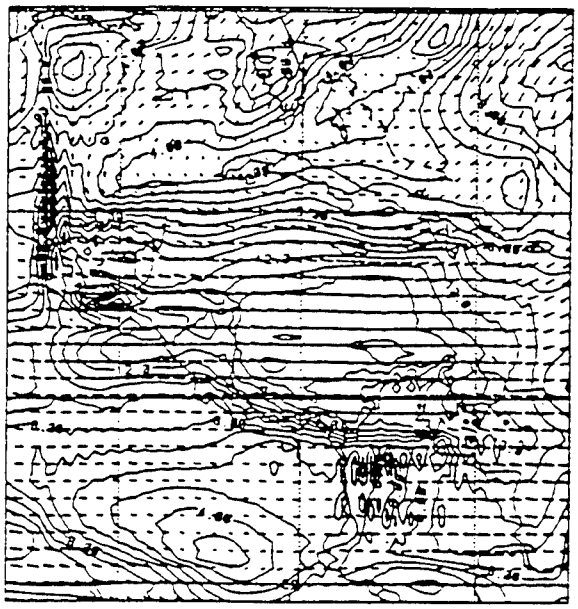

(e) RWM - 18 Aug 94 - 1200 UTC forecast

Figure 4-17. 500mb winds - Central America. (Continued)

4.1.2.11 Statistical Results Central America. Error frequency distributions were generated for temperature, surface pressure, dew point depression, wind speed below 20 knots, wind speed above 20 knots, and wind direction. Data from all forecast times, both August forecasts, and where appropriate, levels were merged. The central column corresponds to the desired error bounds. Two sets of figures were developed to describe the forecast results. One is a surface set that includes the large number of surface observations and the other is an upper air set that includes the more sparse upper air observations. Figures 4-18(a - f) are the surface results and Figures 4-19(a - e) are the upper air results.

4.1.3 November 1994 - Alaska, Korea, Middle East, Central America Theaters.

4.1.3.1 Objective. To compare 36 hour forecasts from the candidate models in a four representative regions or theaters. This information will supplement that developed during the previous forecasts using data obtained from the AF. These runs were to emulate an operational setting. The data was obtained from the AFGWC in a fashion analogous to the way it would be obtained in an operational situation. A specific cut off time was established and only data and corrections received before this time were included.

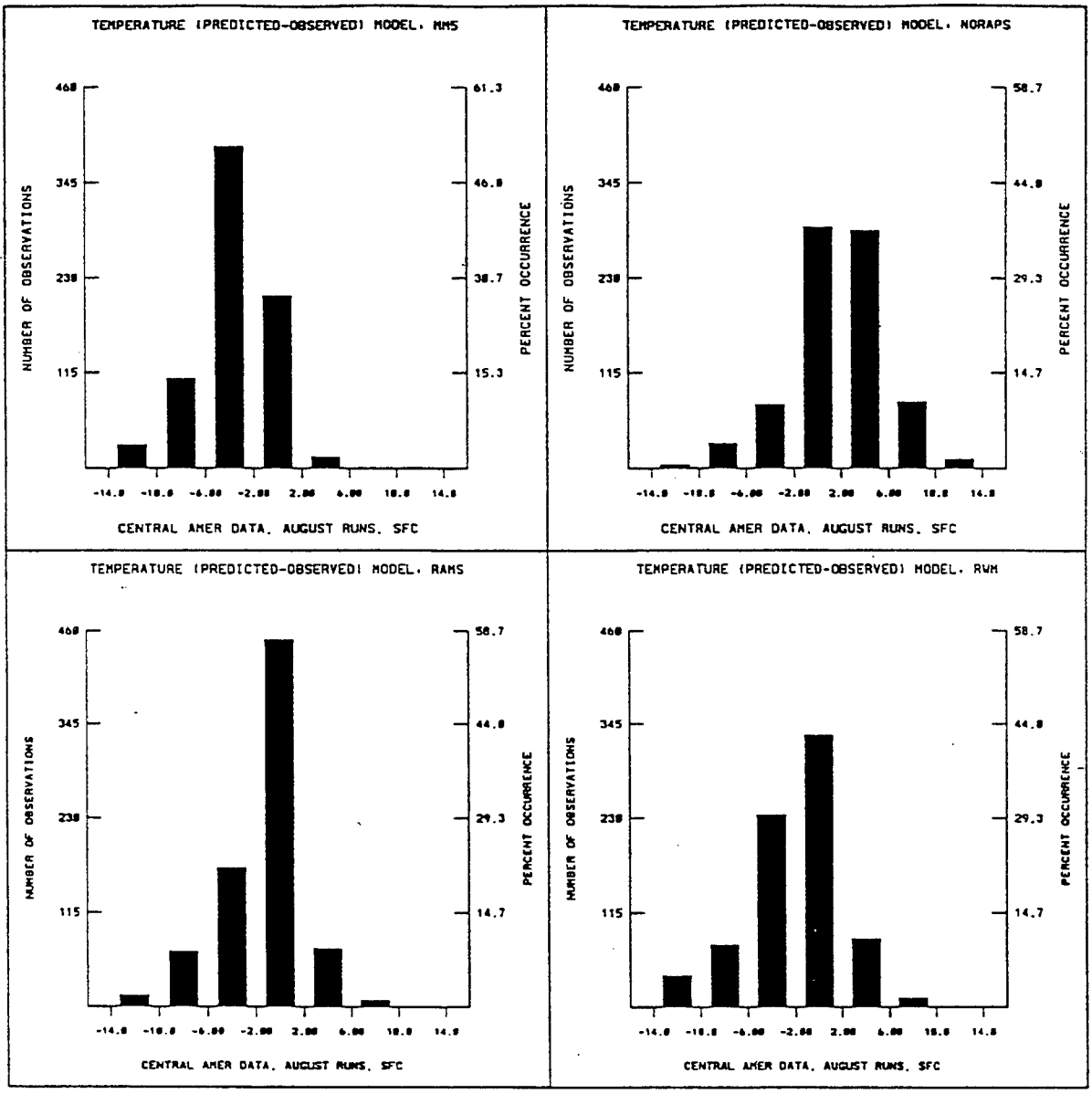

(a) Temperature

Figure 4-18. Surface error statistics, August - Central America.

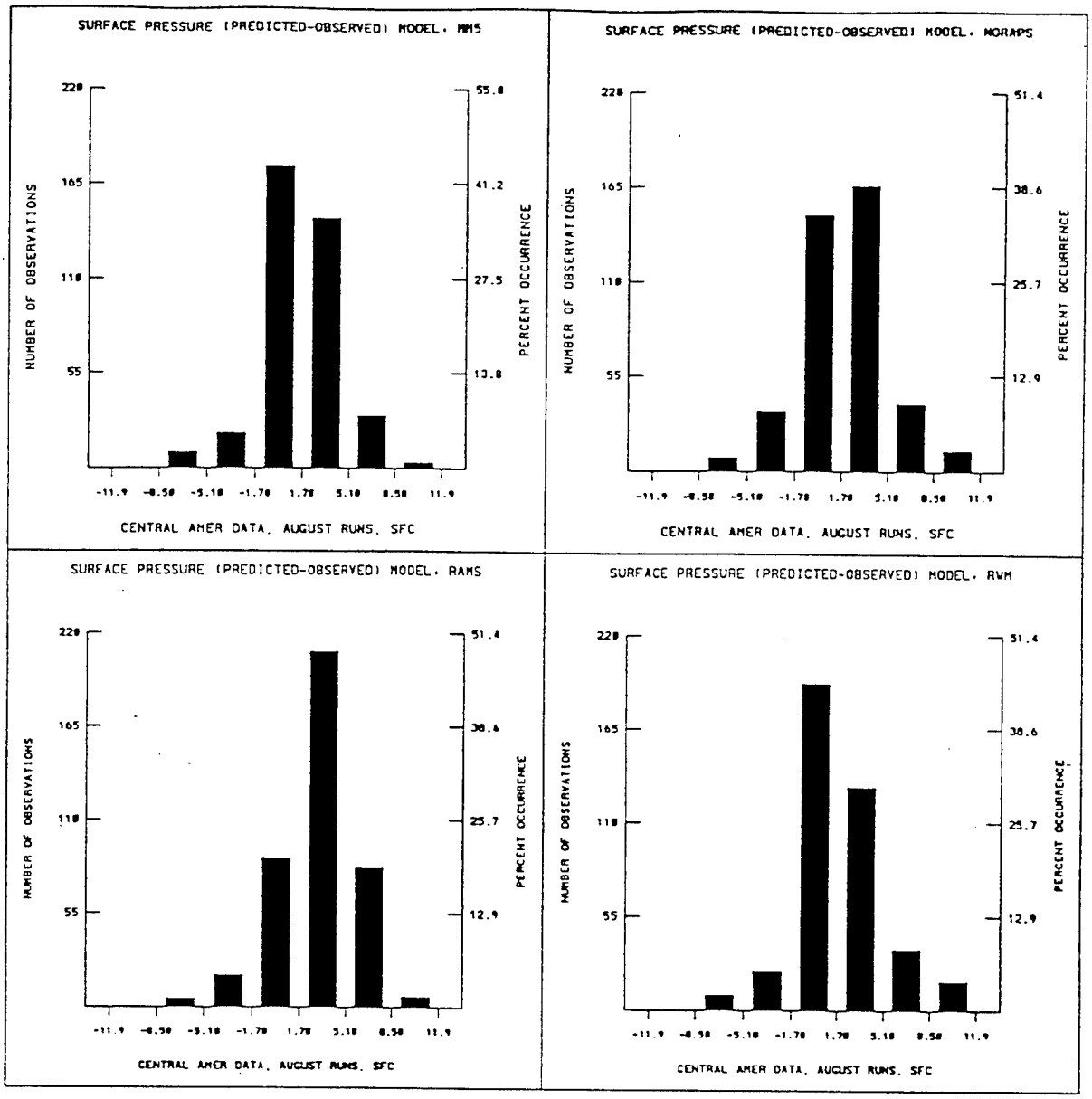

(b) Pressure

Figure 4-18. Surface error statistics, August - Central America. (Continued)

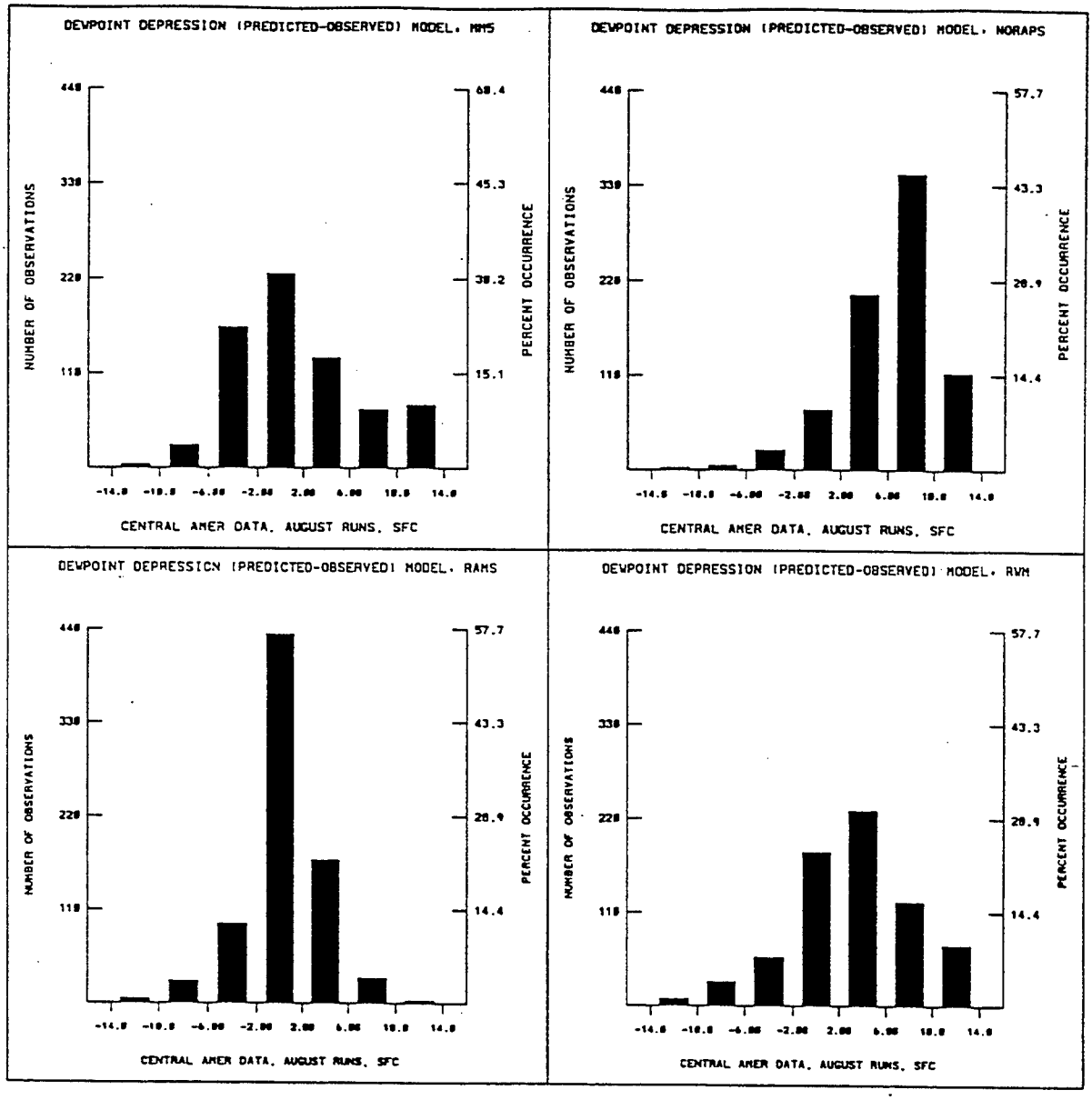

(c) Dew point depression

Figure 4-18. Surface error statistics, August - Central America. (Continued)

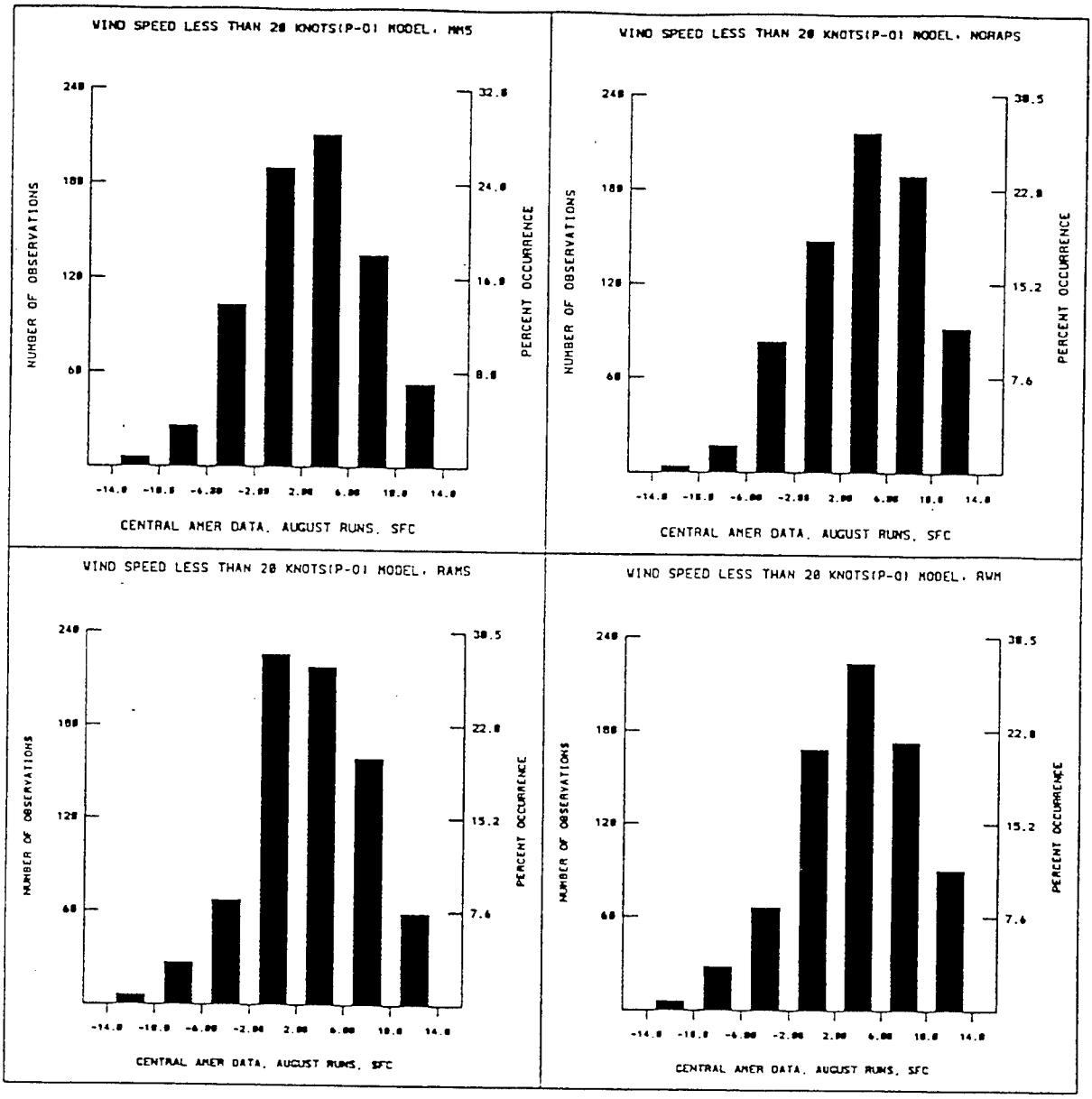

(d) Wind speed < 20 Knots

Figure 4-18. Surface error statistics, August - Central America. (Continued)

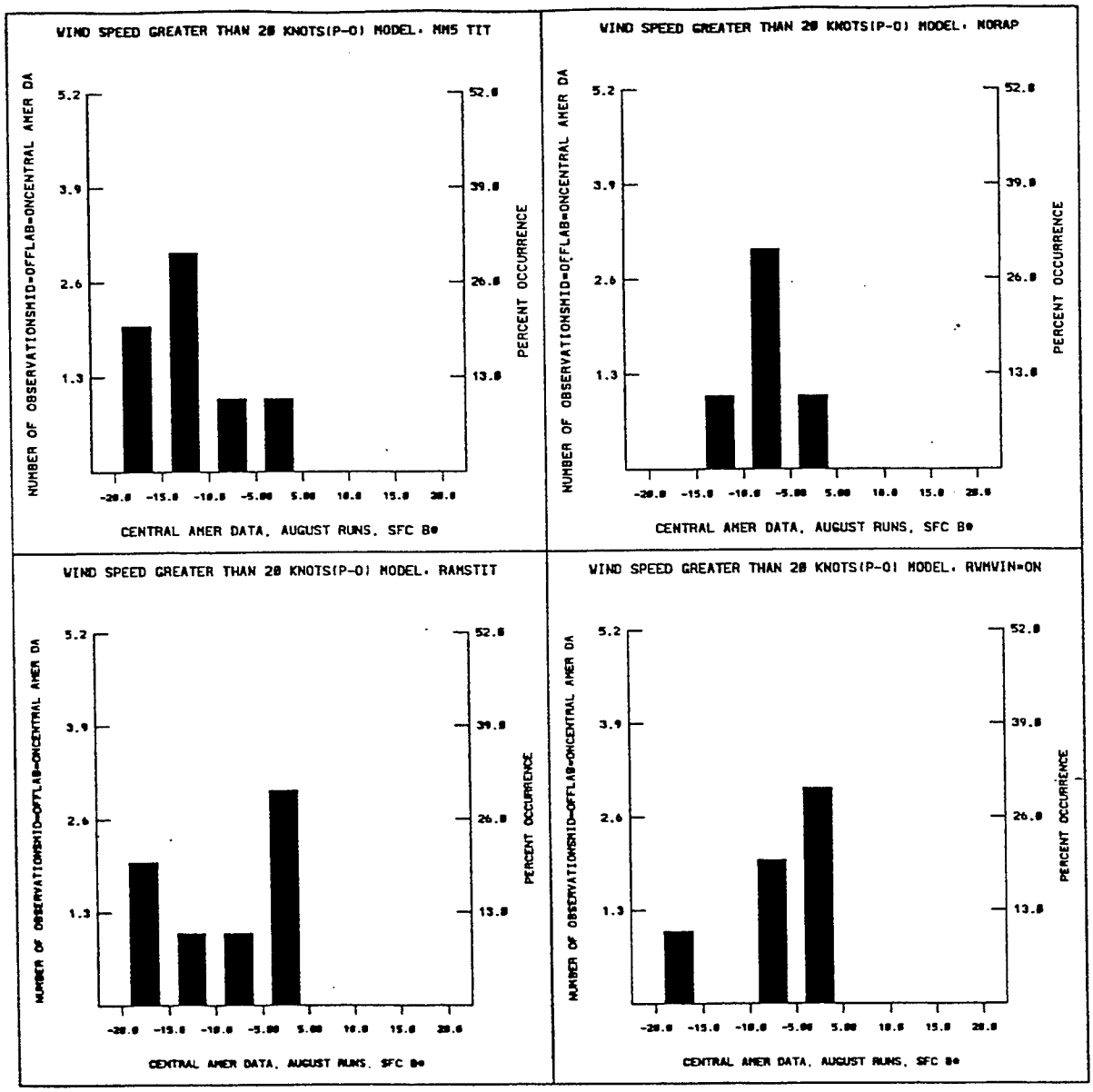

(e) Wind speed > 20 Knots

Figure 4-18. Surface error statistics, August - Central America. (Continued)

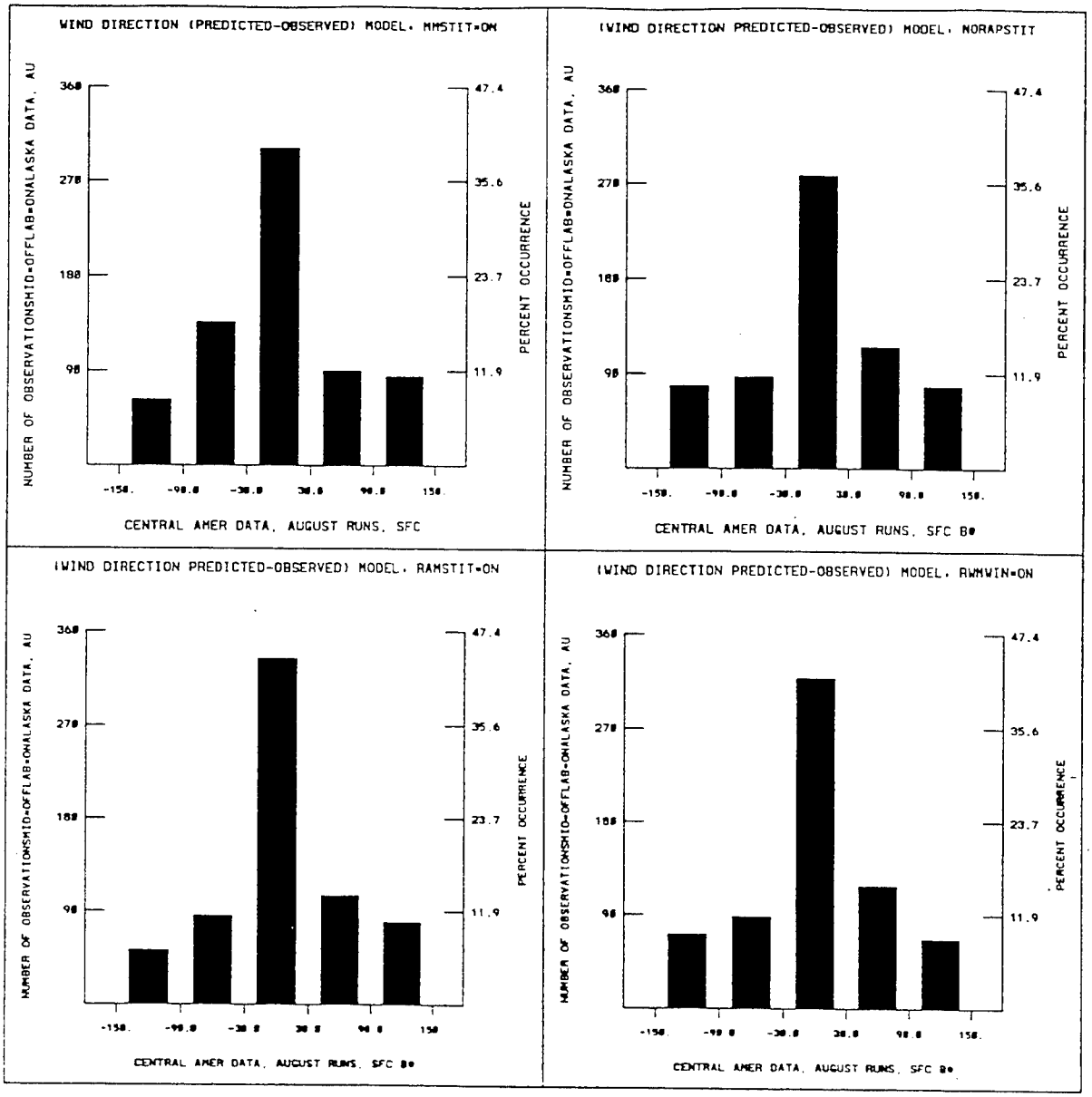

(f) Wind direction

Figure 4-18. Surface error statistics, August - Central America. (Continued)

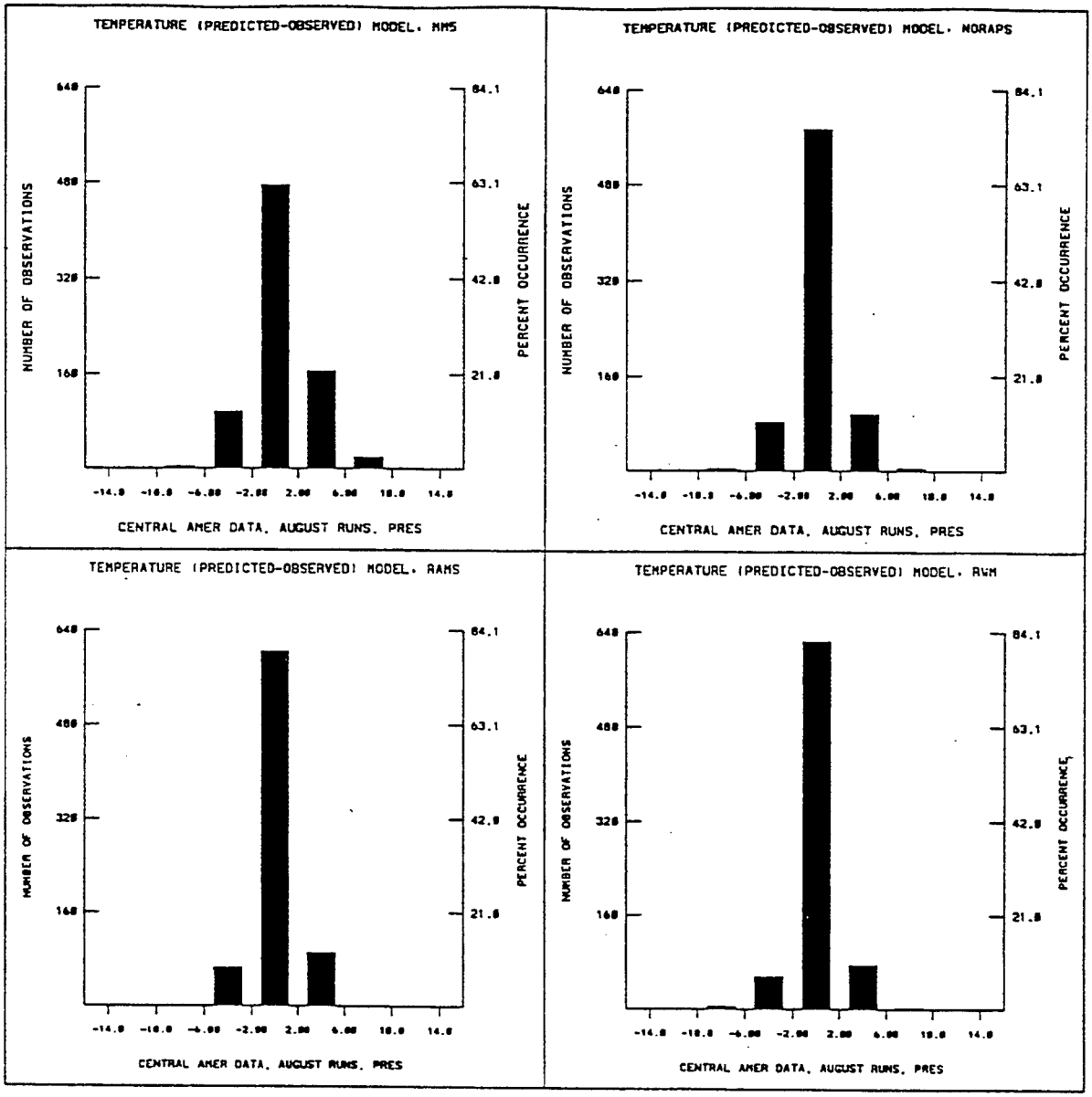

(a) Temperature

Figure 4-19. Upper air error statistics, August - Central America.

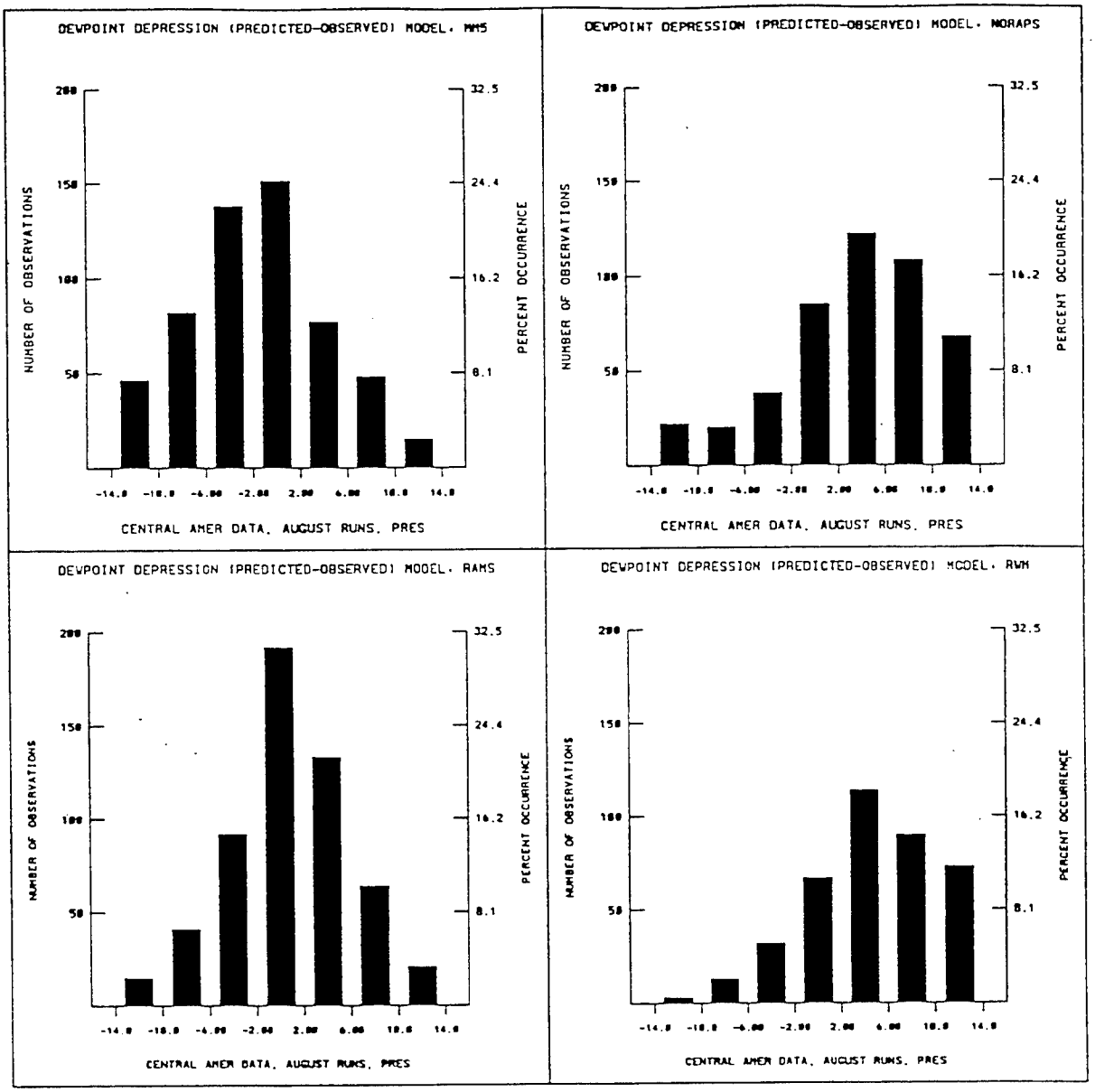

(b) Dew point depression

Figure 4-19. Upper air error statistics, August - Central America. (Continued)

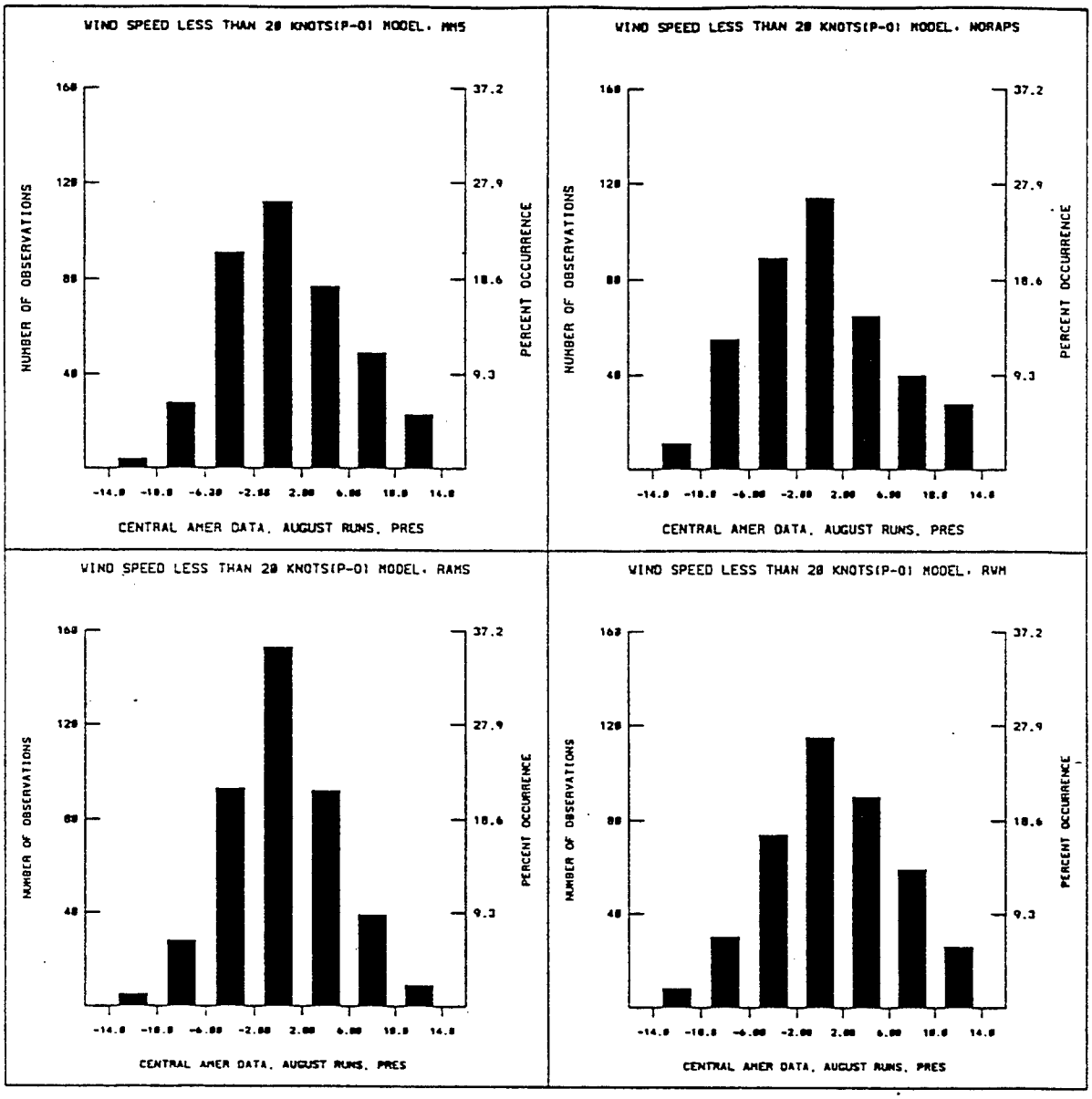

(c) Wind speed < 20 Knots

Figure 4-19. Upper air error statistics, August - Central America. (Continued)

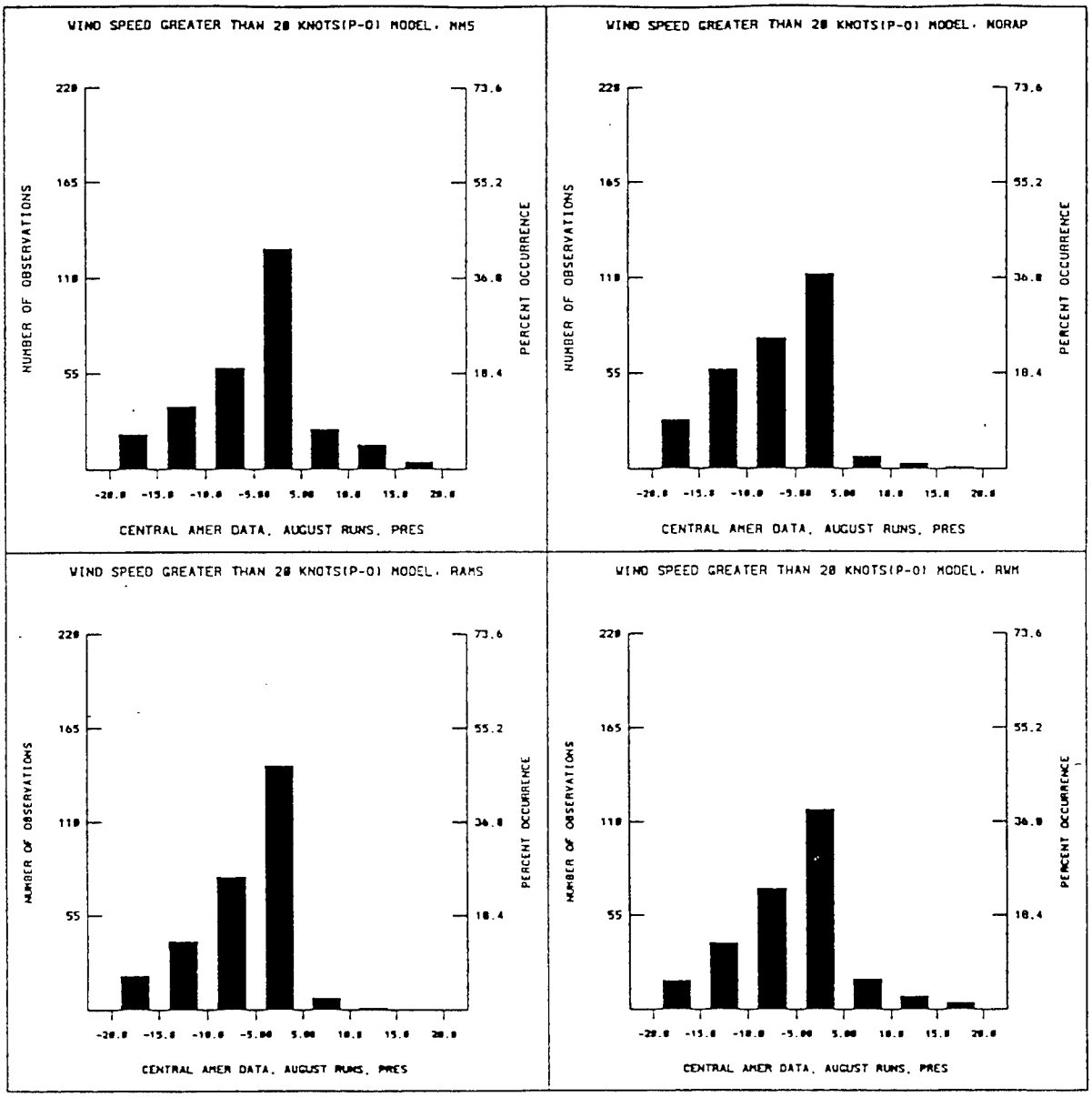

(d) Wind speed > 20 Knots

Figure 4-19. Upper air error statistics, August - Central America. (Continued)

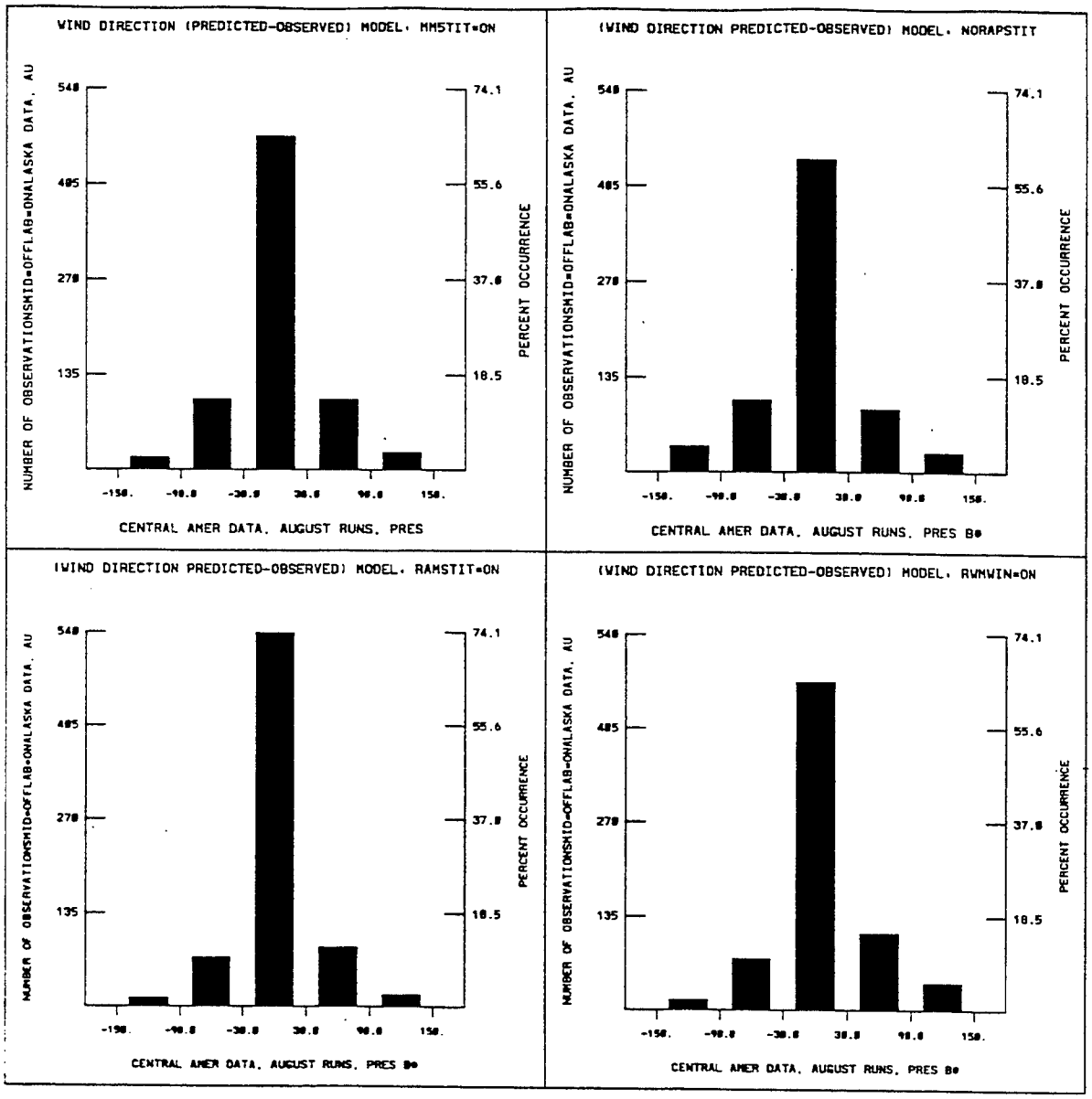

(e) Wind direction

Figure 4-19. Upper air error statistics, August - Central America. (Continued)

4.1.3.2 Description. Surface and 500 mb maps were produced from the GSM gridded data files for 1200Z 14 Nov 1994. These maps indicated that a strong trough had passed over Korea, leaving a prominent high-pressure system with considerable thermal contrast across the peninsula. An impressive surface low was present just off the Alaska coast, and a strong temperature gradient existed across the state. A surface front extended from Nebraska northeastward into the upper Midwest, with an approaching trough from the intermountain region. Relatively benign conditions existed over the Middle East with the closest weather feature being a broad trough in the proximity of Turkey. The weather highlight for these five geographic areas is a strong cyclone off the north coast of Cuba, which produces mainly northeast flow aloft over the Central American theater.

The desire to emulate an operational forecast resulted in some minor changes in the way the codes were operated. The August runs mirrored the typical procedures used to compare historical forecasts. An analysis of the observations and global model output were used each twelve hour period to provide the outer edge boundary conditions. However, the November runs were accomplished using only the global model output to provide the boundary conditions. Code initialization in both August and November were identical. The analysis charts that are provided in this section for comparison to the candidate model's output only contain GSM data. The phenomenology comparisons are therefore against the GSM output, which is always smoother because of its coarser output.

The fact that any of the TFM-candidate models would differ from the GSM forecasts should not necessarily be taken as poor performance; in fact, such differences should be expected because of the much higher resolution used for the candidate models. A side effect is increased boundary "noise" since the candidate model boundaries are forced to match the smoother GSM fields at the boundary. The statistical data was generated using the actual observations at the forecast times.

4.1.3.3 Data Source. All data was supplied by AFGWC and consisted of GSM analysis at the initial time for each 36 hour run (14 Nov. 1200 UTC and 16 Nov. 0000 UTC), rawinsonde and surface observations from those times, and forecast data at 12 hour intervals from the GSM forecast runs. Surface observation and rawinsonde data at the forecast times was also obtained from the same source and used for statistical data preparation.

Note: The observational data received from AFGWC had far fewer stations reporting in the vast majority of data times as compared to the data archived at NCAR. This is probably a reflection of the data cut off time used.

4.1.3.4 Phenomenological Results – Alaska. Phenomenology results at 24 hours into the first forecast period (15 Nov 94 – 1200 UTC).

Surface

GSM forecast a 972 mb surface low over west central Alaska at this time. RAMS, MM5, and NORAPS6 predicted the center farther to the northwest with a central pressure of 975 mb for RAMS, 981 for MM5 and 981 for NORAPS6. RWM's prediction was very different from the rest, with a very elongated center extending up to the northeast Alaska coast. Its field lacked the distinct closed center present in the other 4 models.

Upper Air

The 500 mb fields were dominated by an intense short-wave supporting the surface low. All models produced similar fields, except for RWM, which moved the wave faster than the others.

Phenomenology results at 24 hours into the second forecast period (17 Nov 94 – 0000 UTC).

Surface

Thirty-six hours later, GSM predicted the surface low to move over the northern Yukon/Northwest territories and weakening with a 990 mb central pressure. It also developed a frontal wave over the ocean to the southwest of Alaska with a 1000 mb pressure. RAMS, MM5, and NORAPS6 all favored the development of the southern system, further to the east than GSM, with NORAPS6 producing a 1000 mb central pressure, 999 for MM5, and 994 for RAMS. RWM produced a much weaker system, somewhat similar to GSM. The northern low was weakened much more by the regional models with central pressures between 998 mb and 1001 mb. RWM was weakest of all at 1006 mb. (Figures 4-20(a - e).

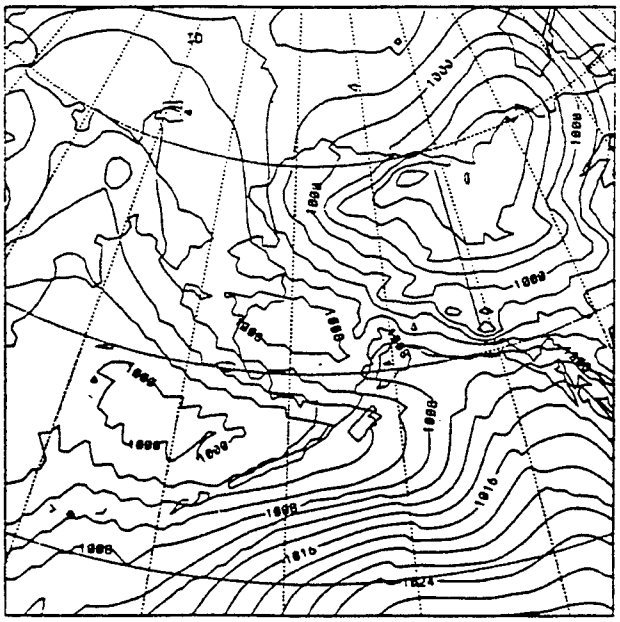

(a) GSM Analysis at 17 Nov 94 - 0000 UTC

Figure 4-20. Surface pressure - Alaska.

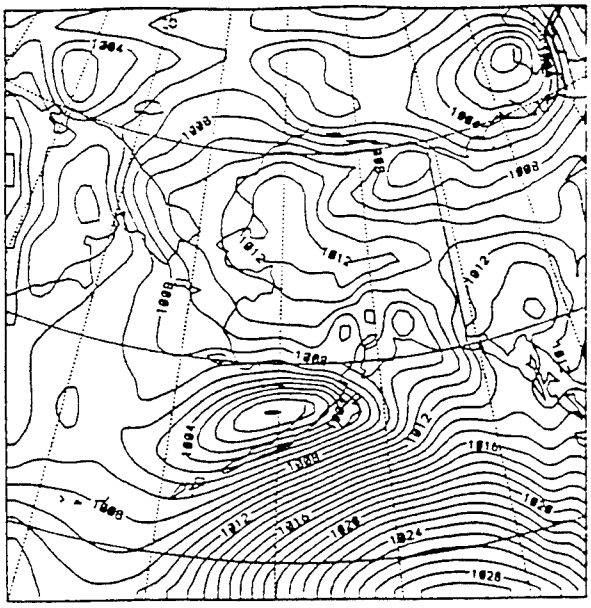

(b) MM5 - 17 Nov 94 - 0000 UTC forecast

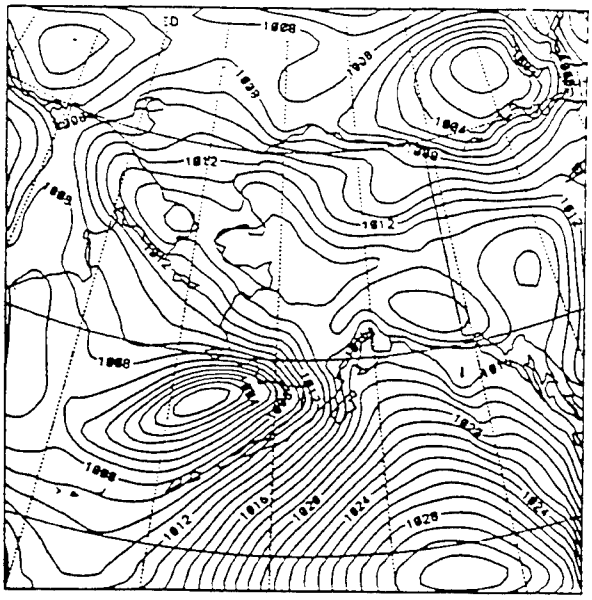

(c) NORAPS6 - 17 Nov 94 - 0000 UTC forecast

Figure 4-20. Surface pressure - Alaska. (Continued)

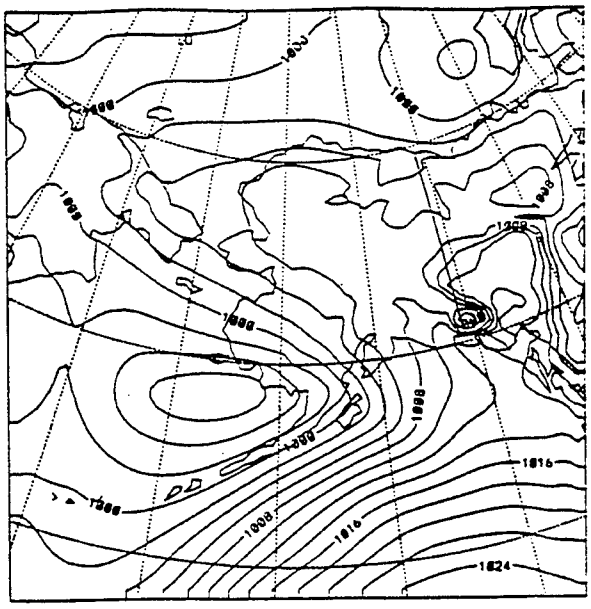

(d) RAMS - 17 Nov 94 - 0000 UTC forecast

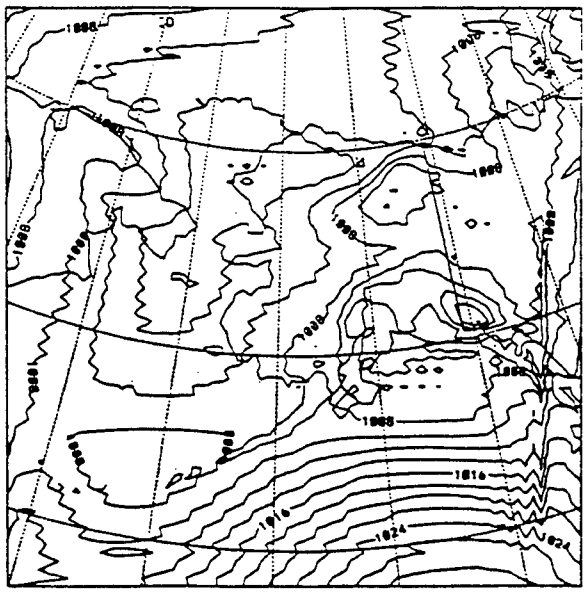

(e) RWM - 17 Nov 94 - 0000 UTC forecast

Figure 4-20. Surface pressure - Alaska. (Continued)

Upper Air

The 500 mb wind field displayed a general ridging in the southern part of the domain. The forecasts were similar for all models, except for RWM, which moved the jet core much further east than the others were.

4.1.3.5 Statistical Results - Alaska. Error frequency distributions were generated for temperature, surface pressure, dew point depression, wind speed below 20 knots, wind speed above 20 knots, and wind direction. Data from all forecast times, both November forecasts, and where appropriate, levels were merged. The central column corresponds to the desired error bounds. Two sets of figures were developed to describe the forecast results. One is a surface set that includes the large number of surface observations and the other is an upper air set that includes the more sparse upper air observations. Figures 4-21(a - f) are the surface results and Figures 4-22(a - e) are the upper air results.

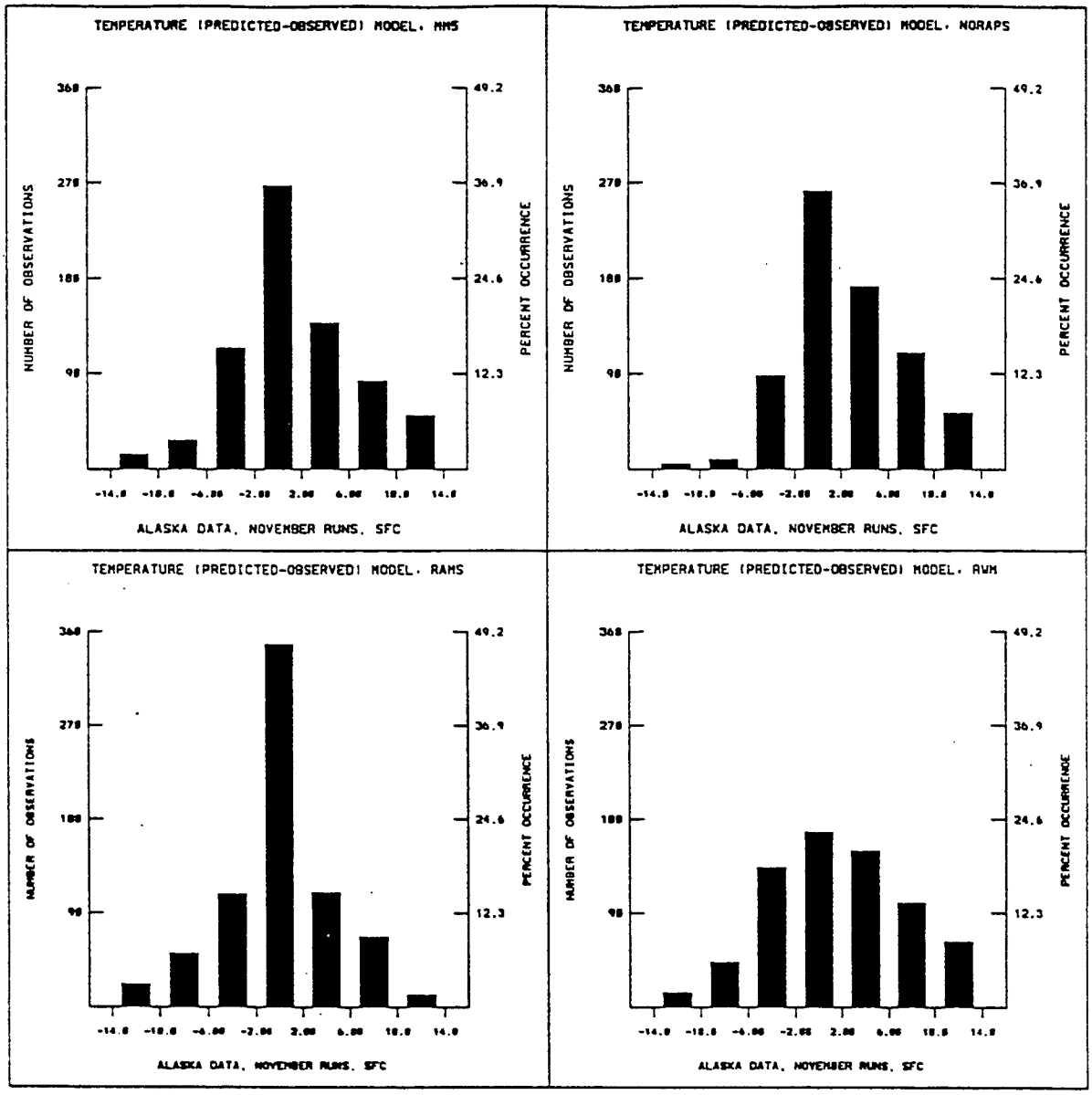

(a) Temperature

Figure 4-21. Surface error statistics, November - Alaska.

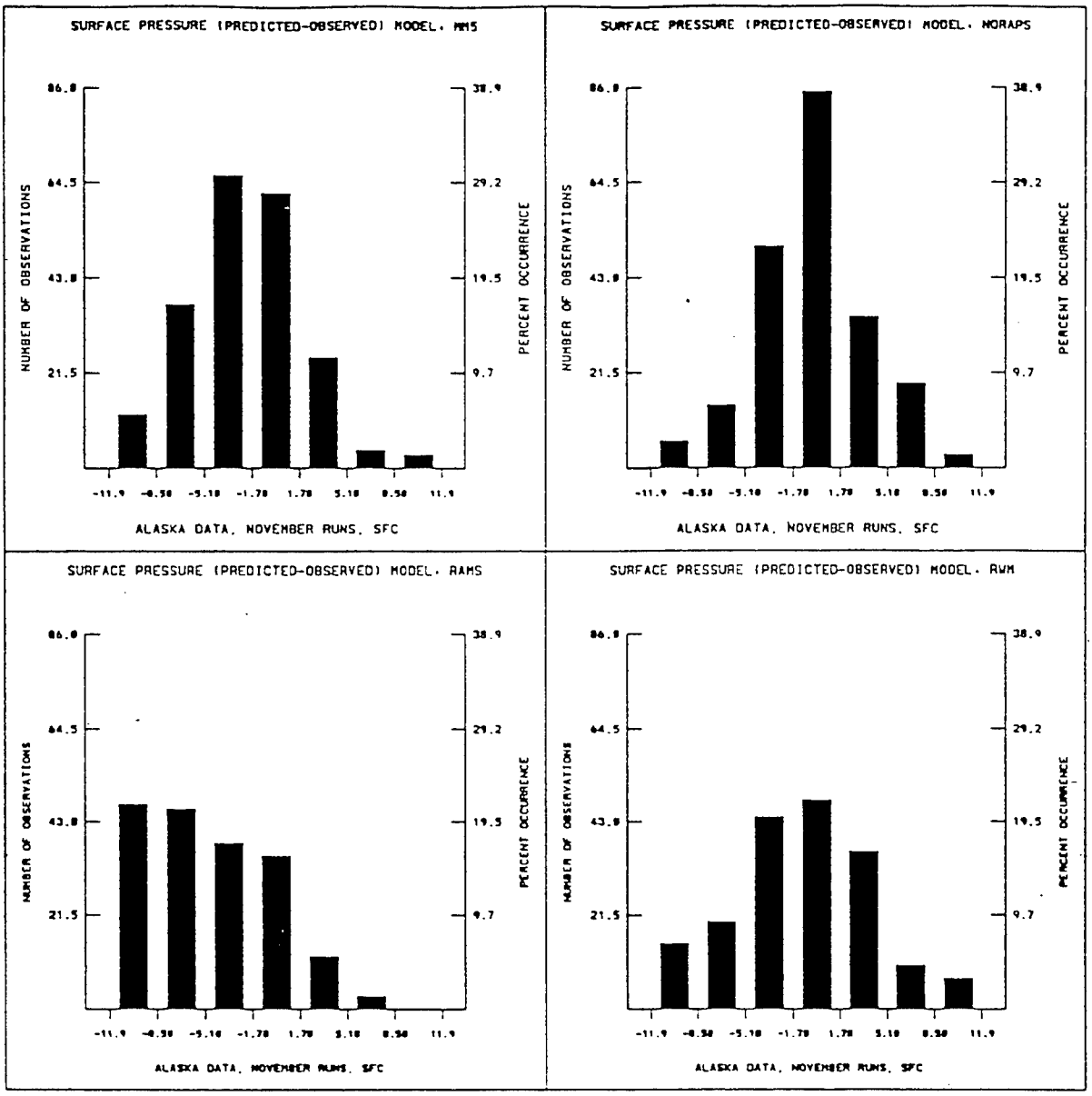

(b) Pressure

Figure 4-21. Surface error statistics, November - Alaska. (Continued)

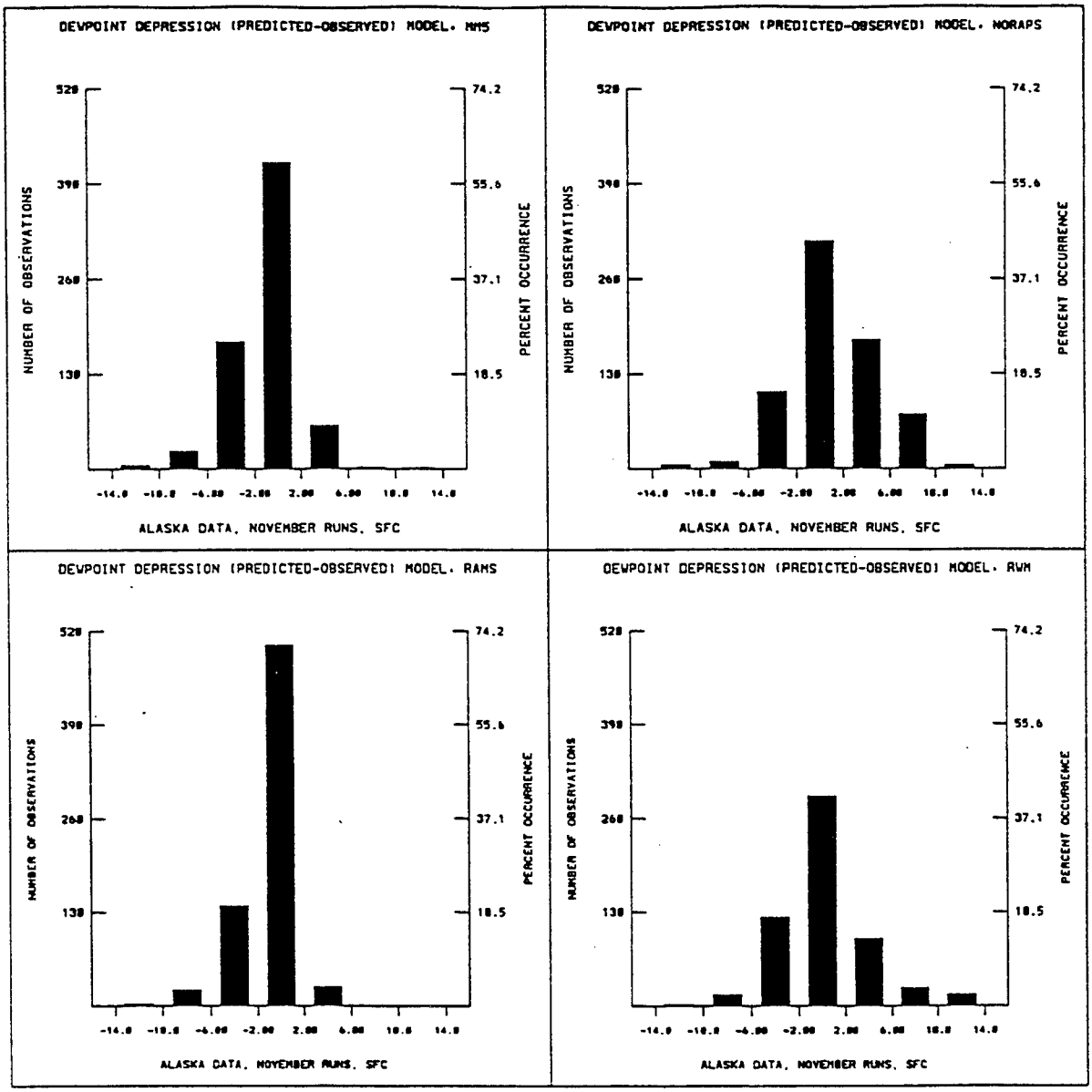

(c) Dew point depression

Figure 4-21. Surface error statistics, November - Alaska. (Continued)

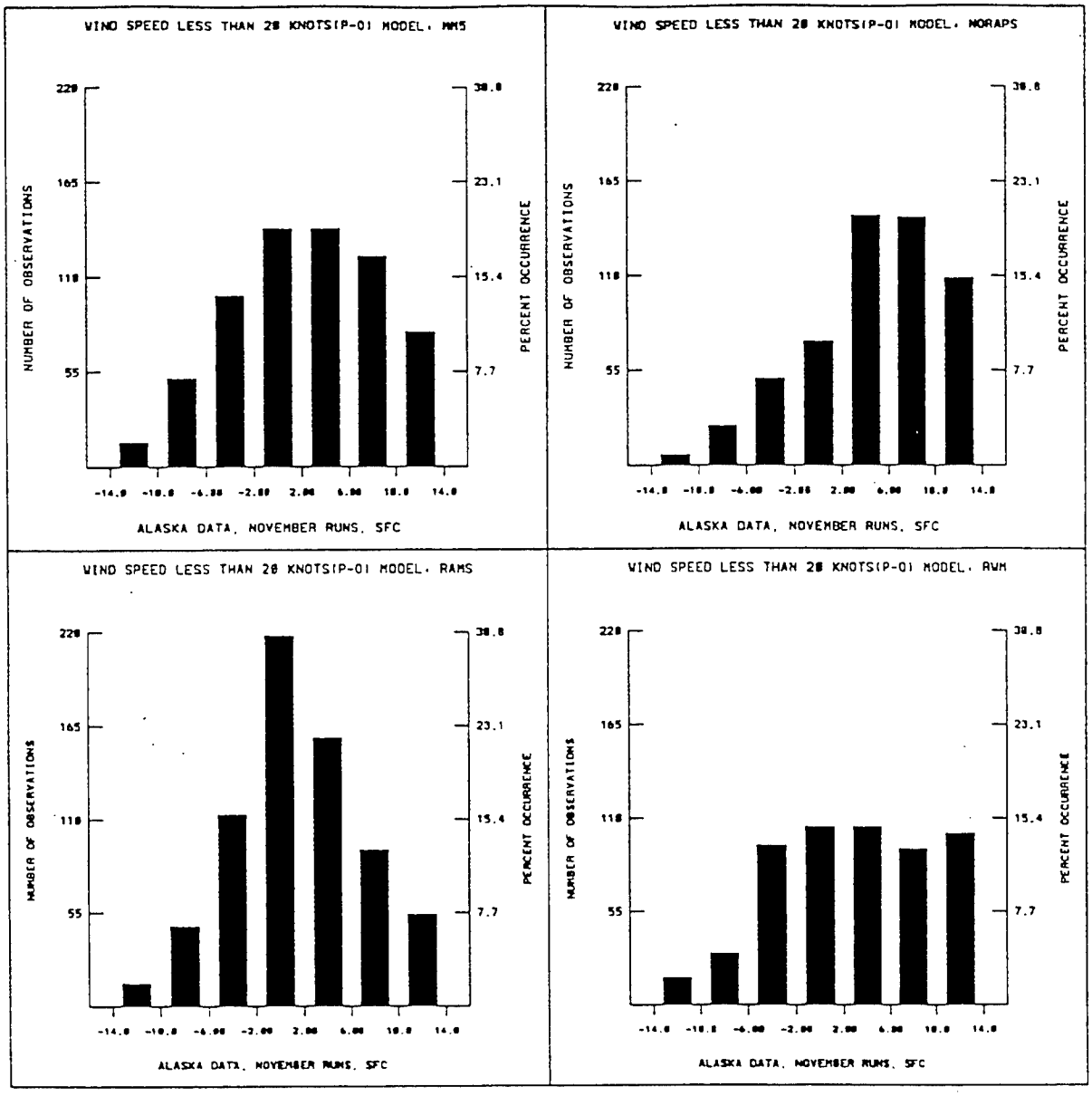

(d) Wind speed < 20 Knots

Figure 4-21. Surface error statistics, November - Alaska. (Continued)

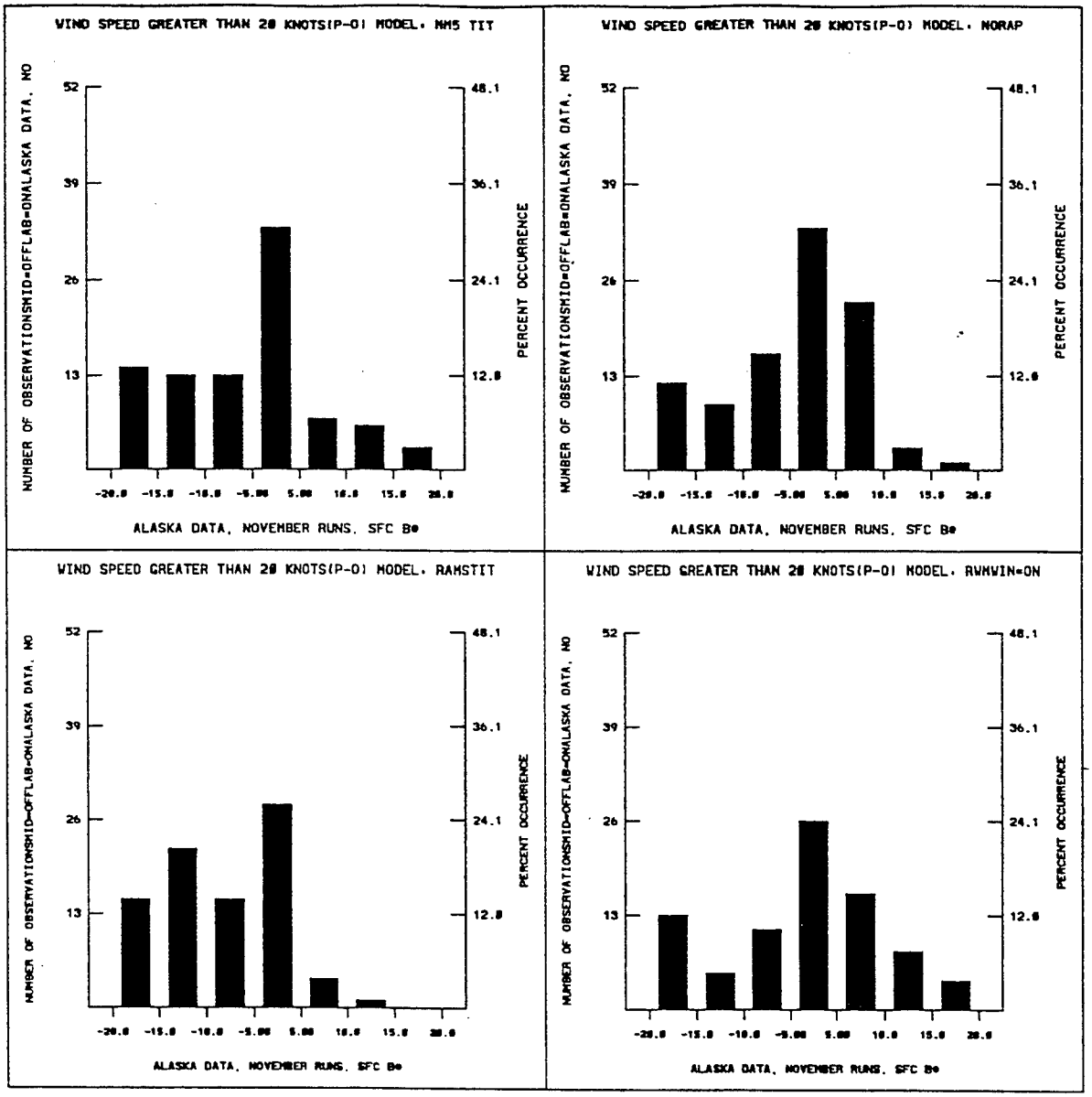

(e) Wind speed > 20 Knots

Figure 4-21. Surface error statistics, November - Alaska. (Continued)

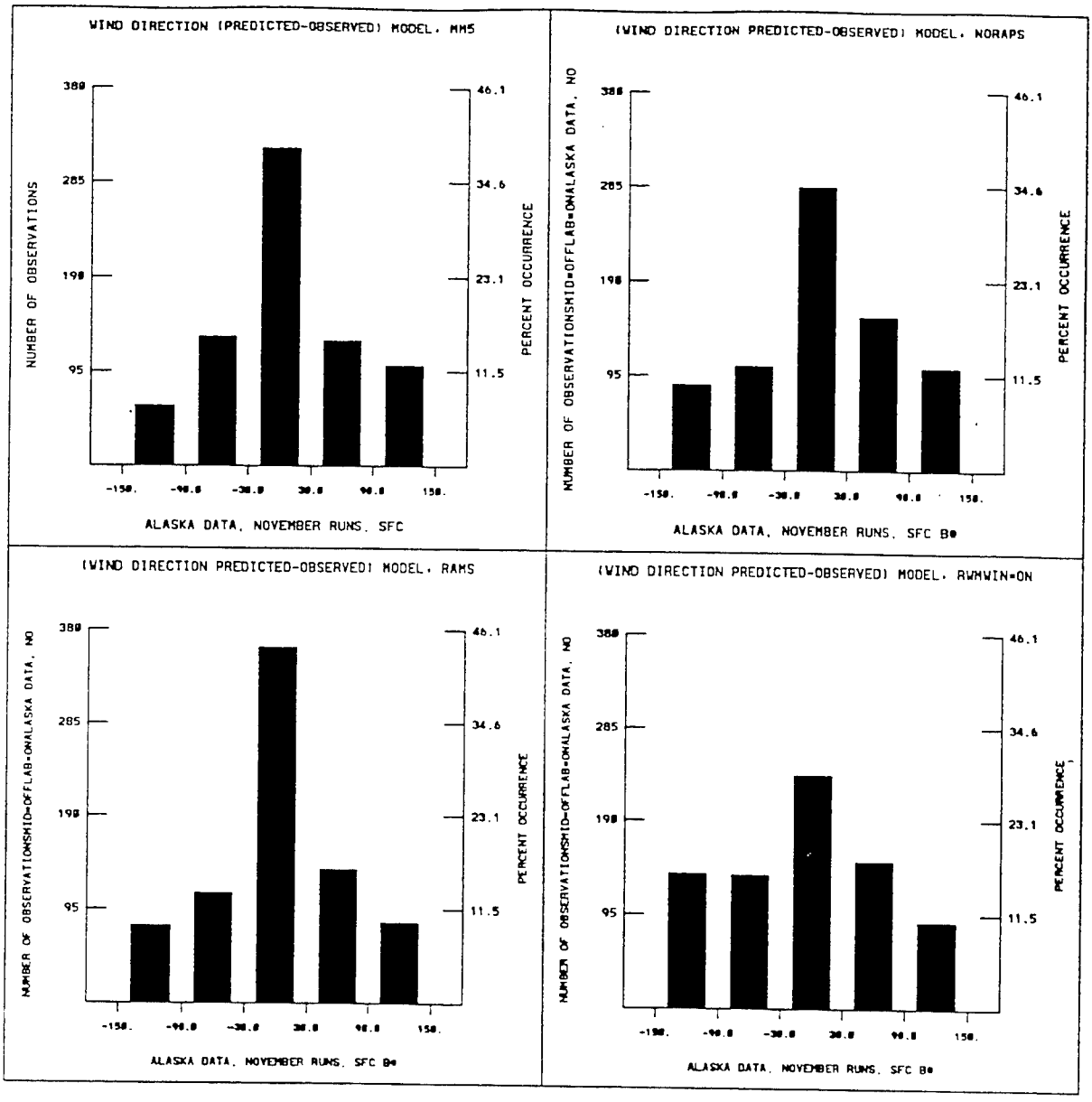

(f) Wind direction

Figure 4-21. Surface error statistics, November - Alaska. (Continued)

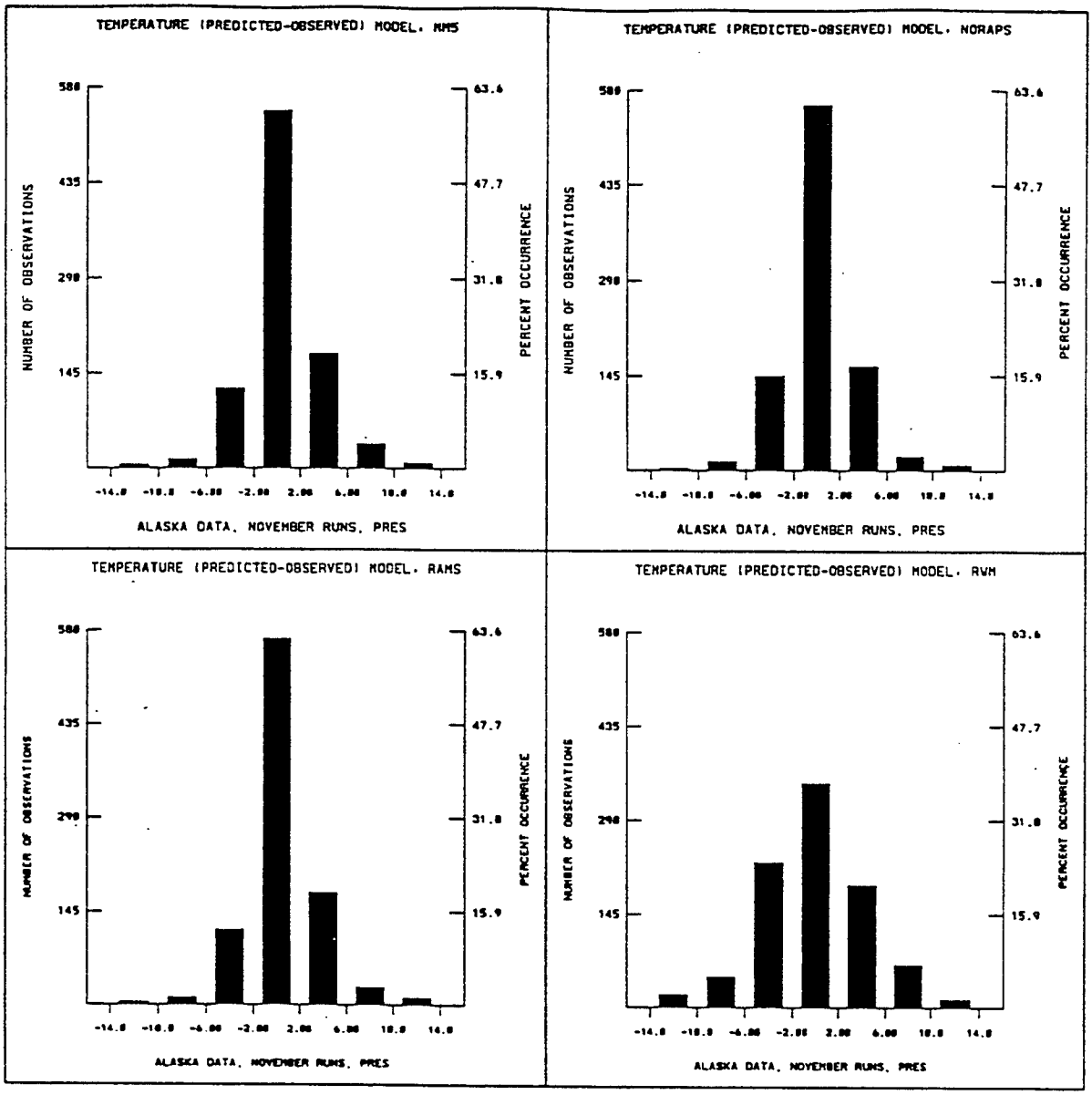

(a) Temperature

Figure 4-22. Upper air error statistics, November - Alaska.

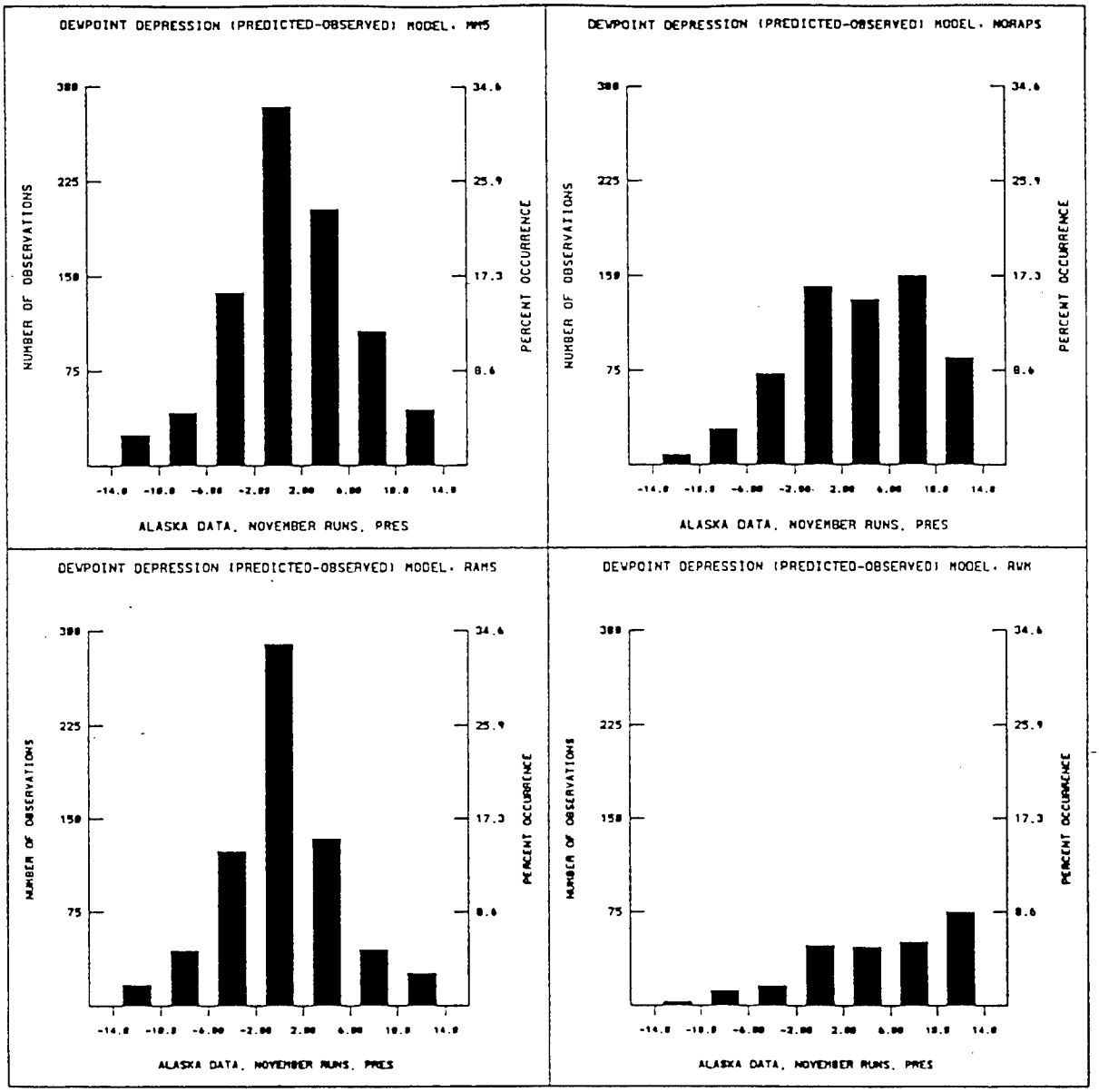

(b) Dew point depression

Figure 4-22. Upper air error statistics, November - Alaska. (Continued)

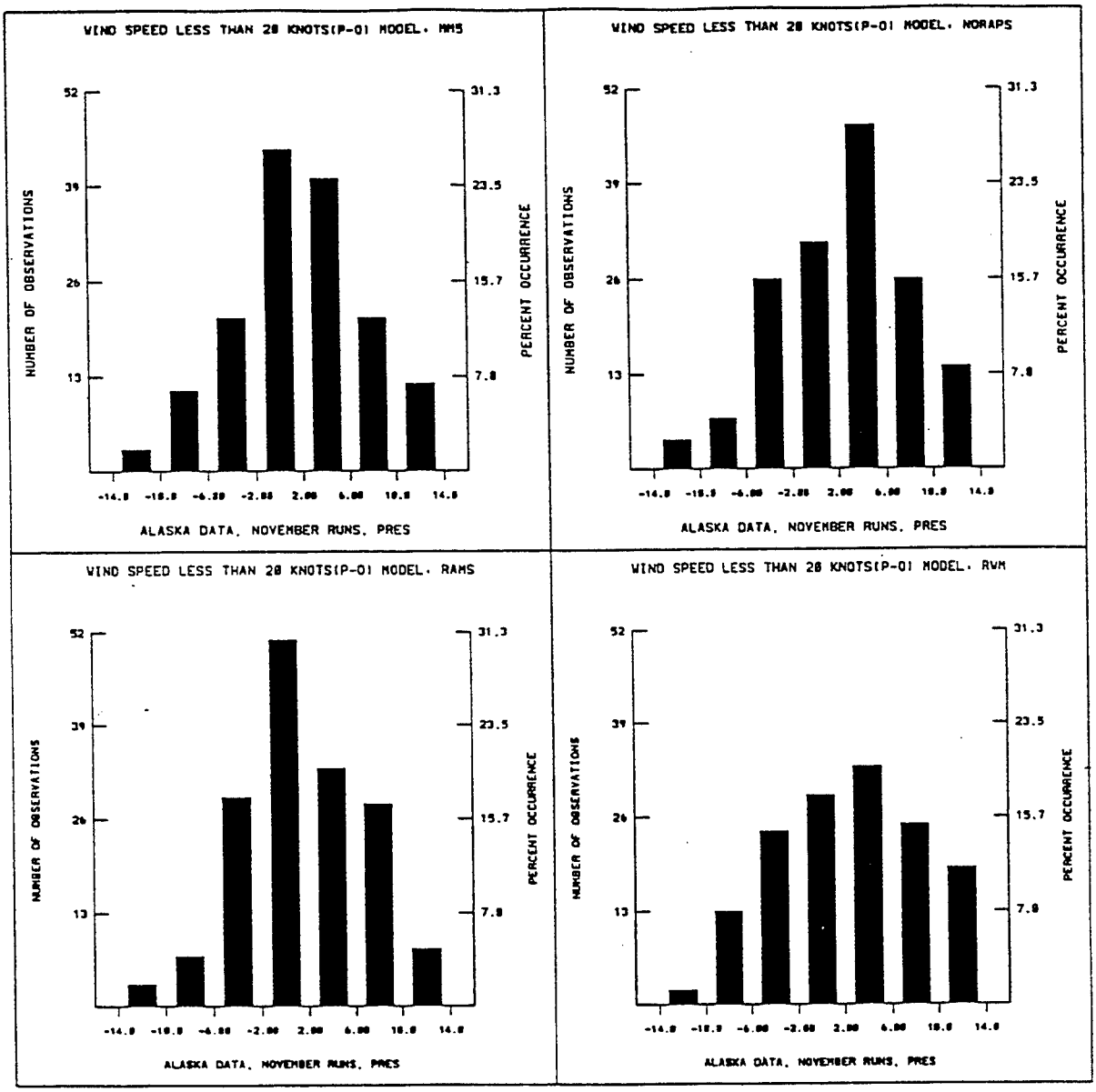

(c) Wind speed < 20 Knots

Figure 4-22. Upper air error statistics, November - Alaska. (Continued)

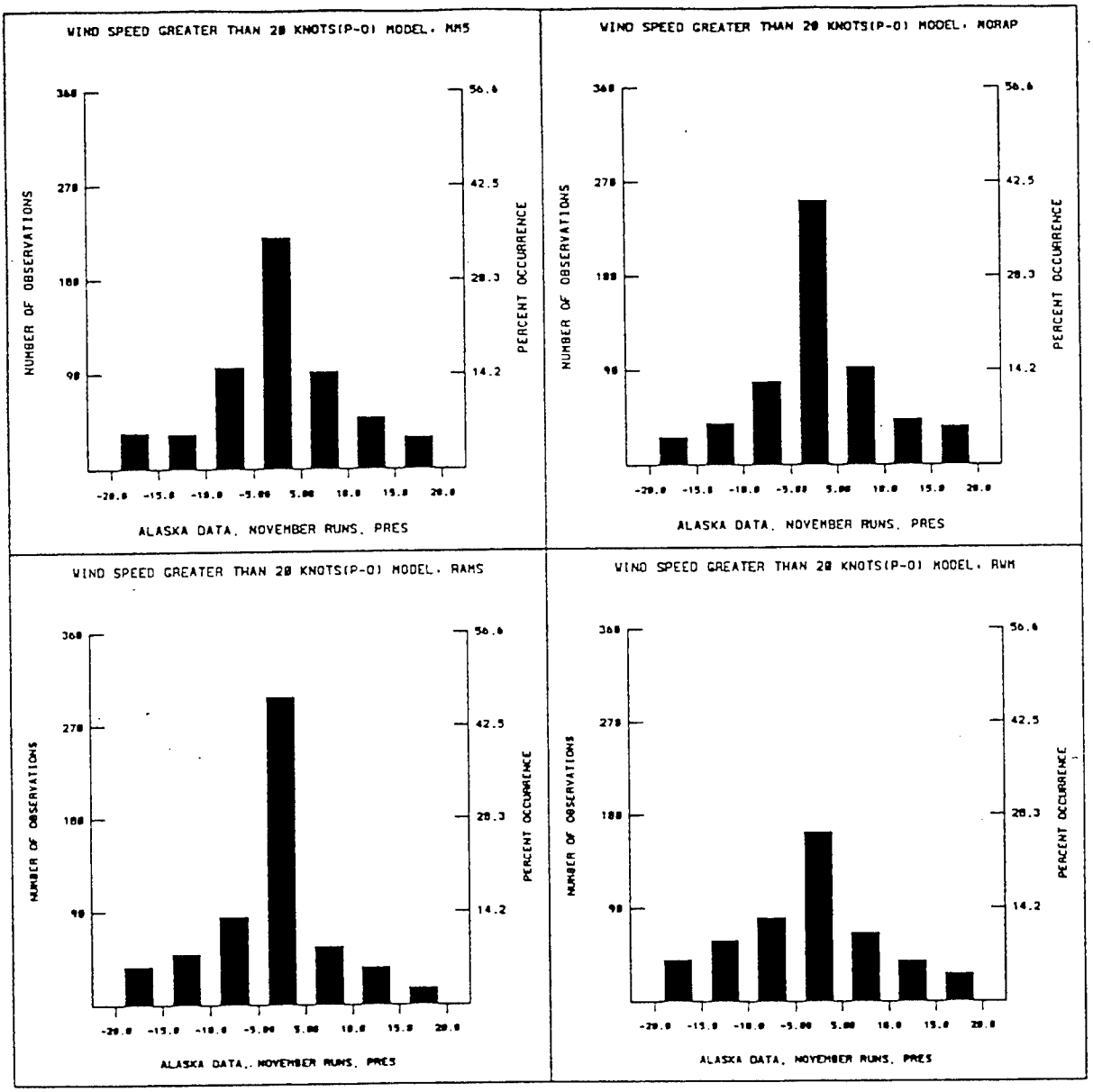

(d) Wind speed > 20 Knots

Figure 4-22. Upper air error statistics, November - Alaska. (Continued)

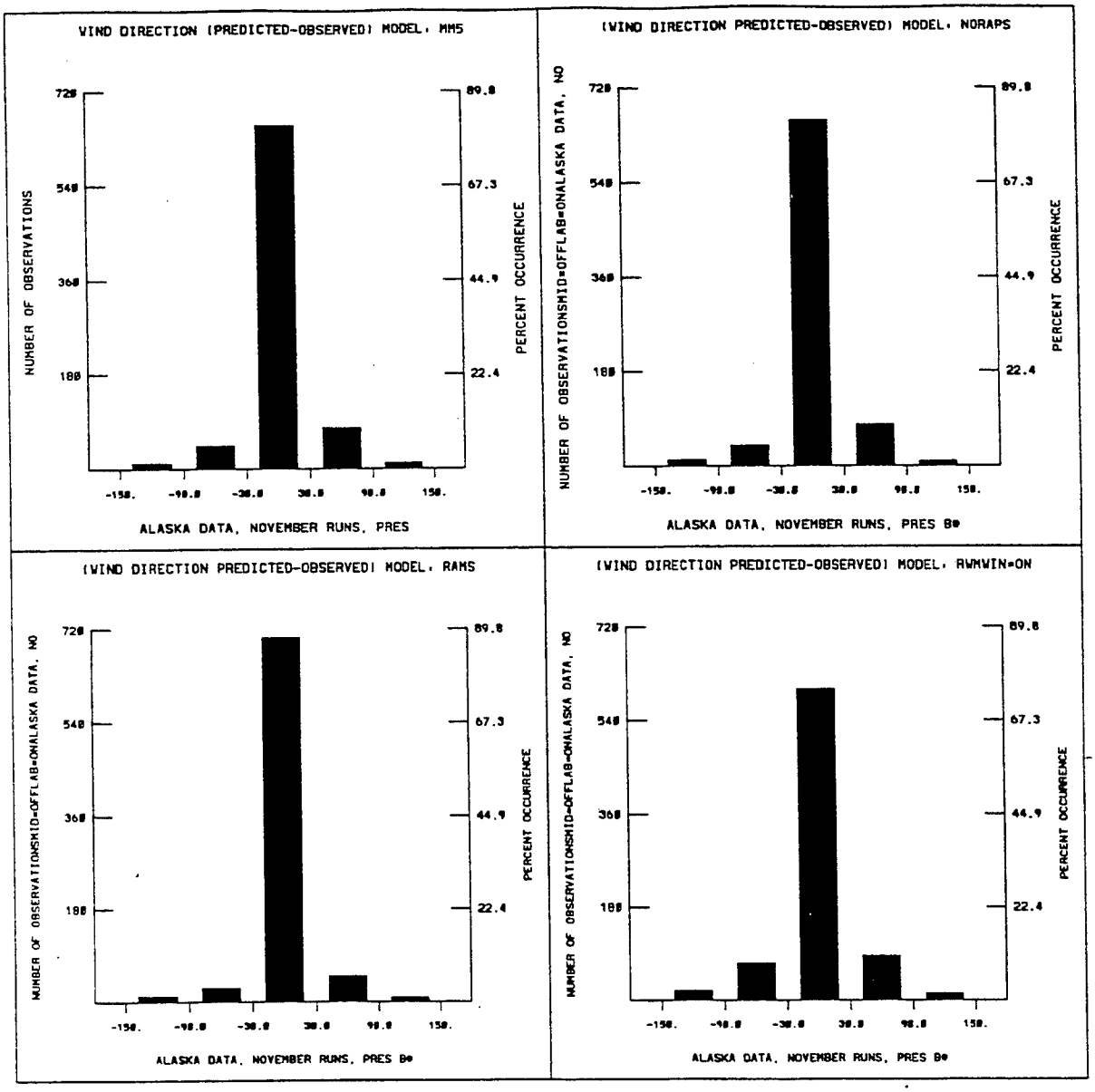

(e) Wind direction

Figure 4-22. Upper air error statistics, November - Alaska. (Continued)

4.1.3.6 Phenomenological Results - Korea. Phenomenology results at 24 hours into the first forecast period (15 Nov. 94 – 1200 UTC).

Surface

The GSM forecast at this time was dominated by a surface high of 1052 mb central pressure centered to the northeast of Korea. All models showed a similar forecast. The main surface thermal gradient in the regional models was located roughly coincident with the coastlines (due to the warmer waters of the Sea of Japan), while GSM showed very little effect of the coast (because of its coarser resolution) and had the front well south of Japan.

Upper Air

At 500 mb, all 5 models showed the same general ridging pattern over the region.

Phenomenology results at 24 hours into the first forecast period (17 Nov 94 – 0000 UTC).

Surface

At this time, the models moved the main high-pressure center to the east of Japan and left behind a secondary high over China. The main differences among the models concerned this secondary high. GSM and RAMS located the high to the west-southwest of Korea with about a 1034 mb center. NORAPS6 had the high in approximately the same place but with a 1039 mb center, while MM5 located the high well to the south with a 1037 mb center. RWM, although generally controlling its numerical noise better with the GSM boundary conditions, was too noisy to interpret in this case. The surface thermal gradients showed similar characteristics to the previous 36 hours. The nighttime cooling was different among the models with RAMS, MM5, and NORAPS6 cooling down to about -14 C while GSM and RWM cooled to only about -4 C. Figures 4-23(a - e) show the predicted surface pressure.

Upper Air

The maximum winds over the Korean region at 500 mb were predicted by MM5, NORAPS6, and RWM to be about 22 m/s and located directly over the Korean peninsula. GSM and RAMS had the maximum winds located to the north of the peninsula at 20 m/s. A 500 mb trough was moving in from the western boundary over the Chinese mainland. All models handled this similarly.

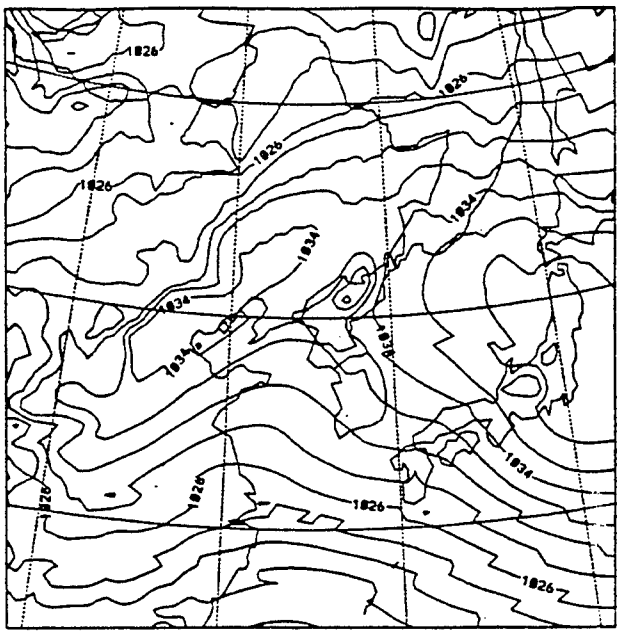

sea level pressure (mb)

(a) GSM Analysis at 17 Nov 94 - 0000 UTC

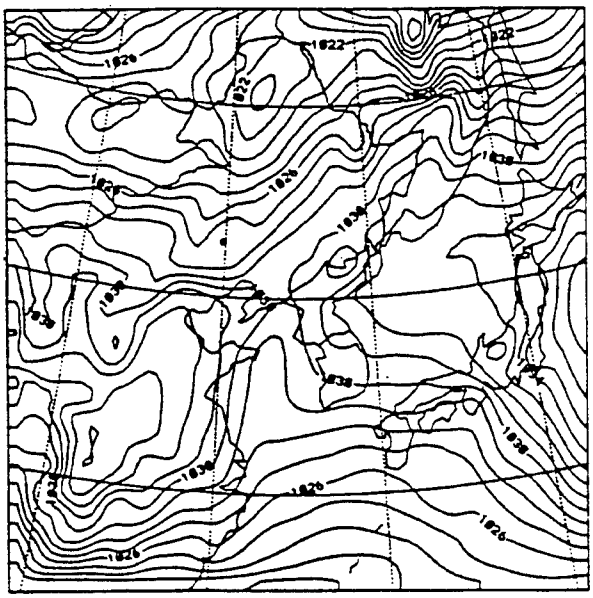

(b) MM5 - 17 Nov 94 - 0000 UTC forecast

Figure 4-23. Surface pressure - Korea.

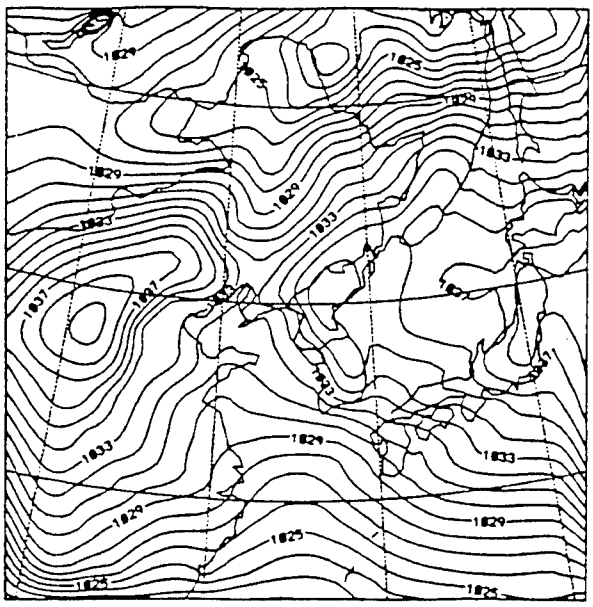

(c) NORAPS6 - 17 Nov 94 - 0000 UTC forecast

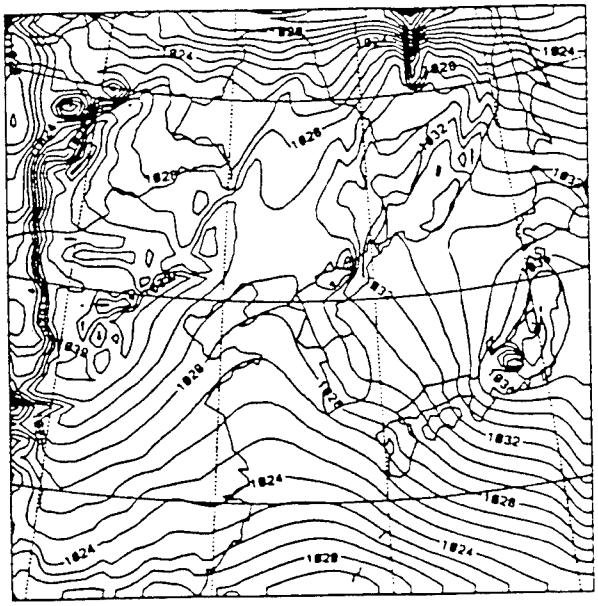

(d) RAMS - 17 Nov 94 - 0000 UTC forecast

Figure 4-23. Surface pressure - Korea. (Continued)

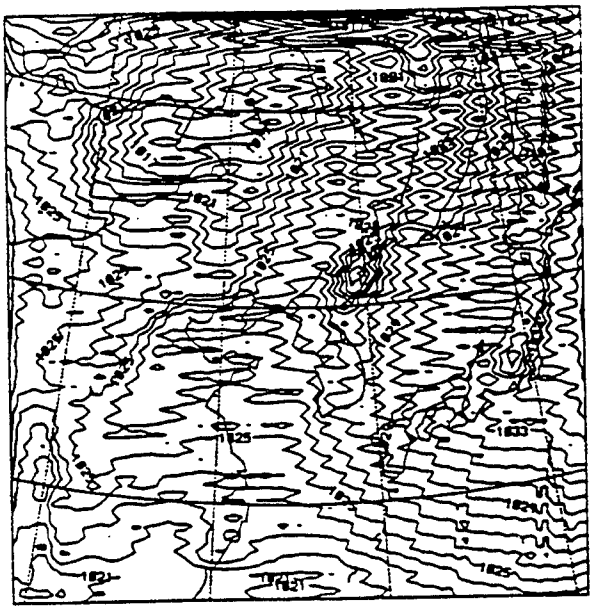

(e) RWM - 17 Nov 94 - 0000 UTC forecast

Figure 4-23. Surface pressure - Korea. (Continued)

4.1.3.7 Statistical Results – Korea. Error frequency distributions were generated for temperature, surface pressure, dew point depression, wind speed below 20 knots, wind speed above 20 knots, and wind direction. Data from all forecast times, both November forecasts, and where appropriate, levels were merged. The central column corresponds to the desired error bounds. Two sets of figures were developed to describe the forecast results. One is a surface set that includes the large number of surface observations and the other is an upper air set that includes the more sparse upper air observations. Figures 4-24(a - f) are the surface results and Figures 4-25(a - e) are the upper air results.

4.1.3.8 Phenomenological Results - Middle East. Phenomenology results at 24 hours into the first forecast period (15 Nov. 94 – 1200 UTC).

Surface

The surface pressure field at this time was a rather confused field with several small-scale features handled differently by all models. The consistent features included a weak surface low over the eastern Mediterranean Sea and a very small scale low to the east of the Black Sea. RAMS produced a heat low over Saudi Arabia and a localized region of high pressure (due to precipitation) over Iran.

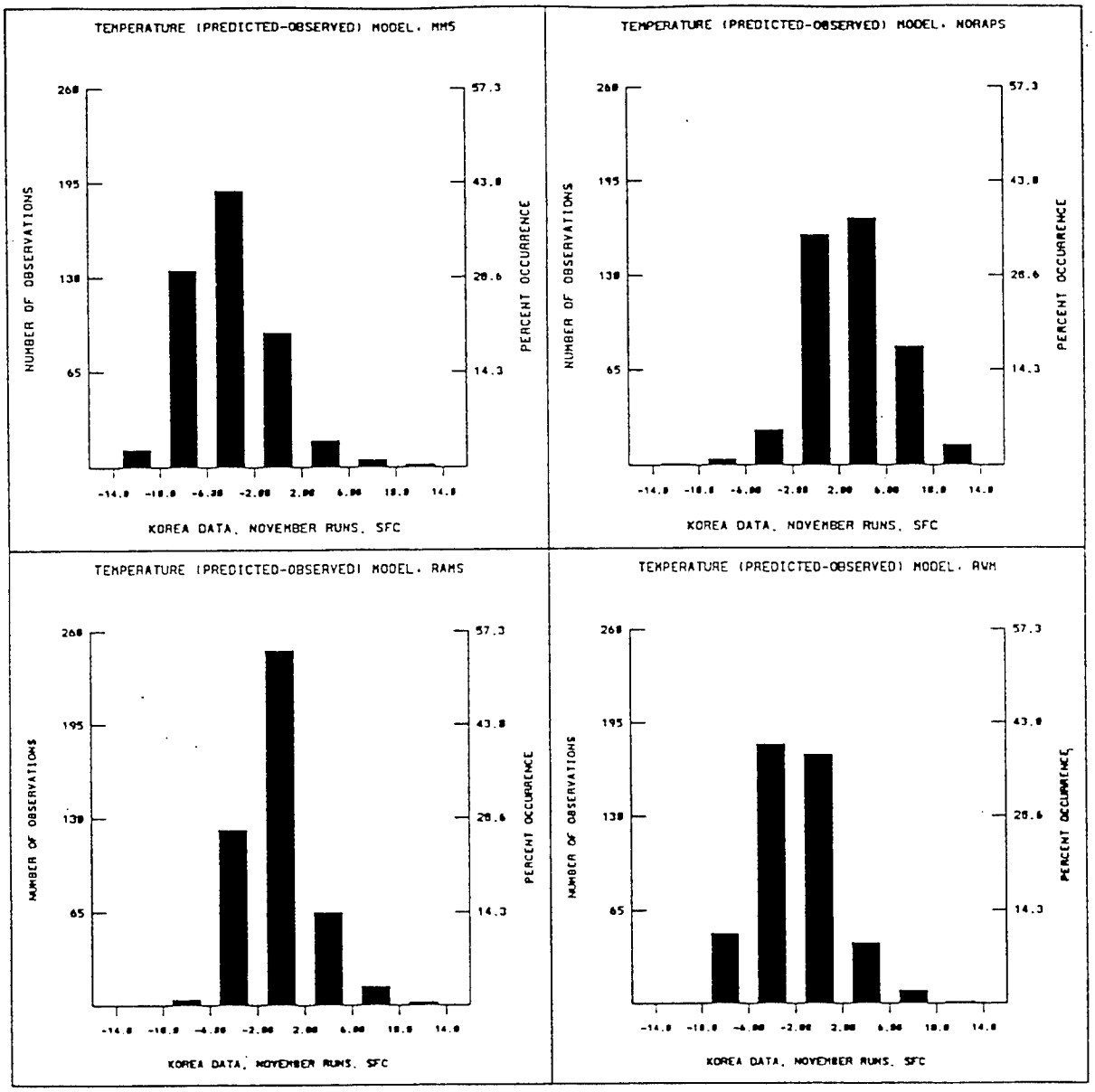

(a) Temperature

Figure 4-24. Surface error statistics, November - Korea.

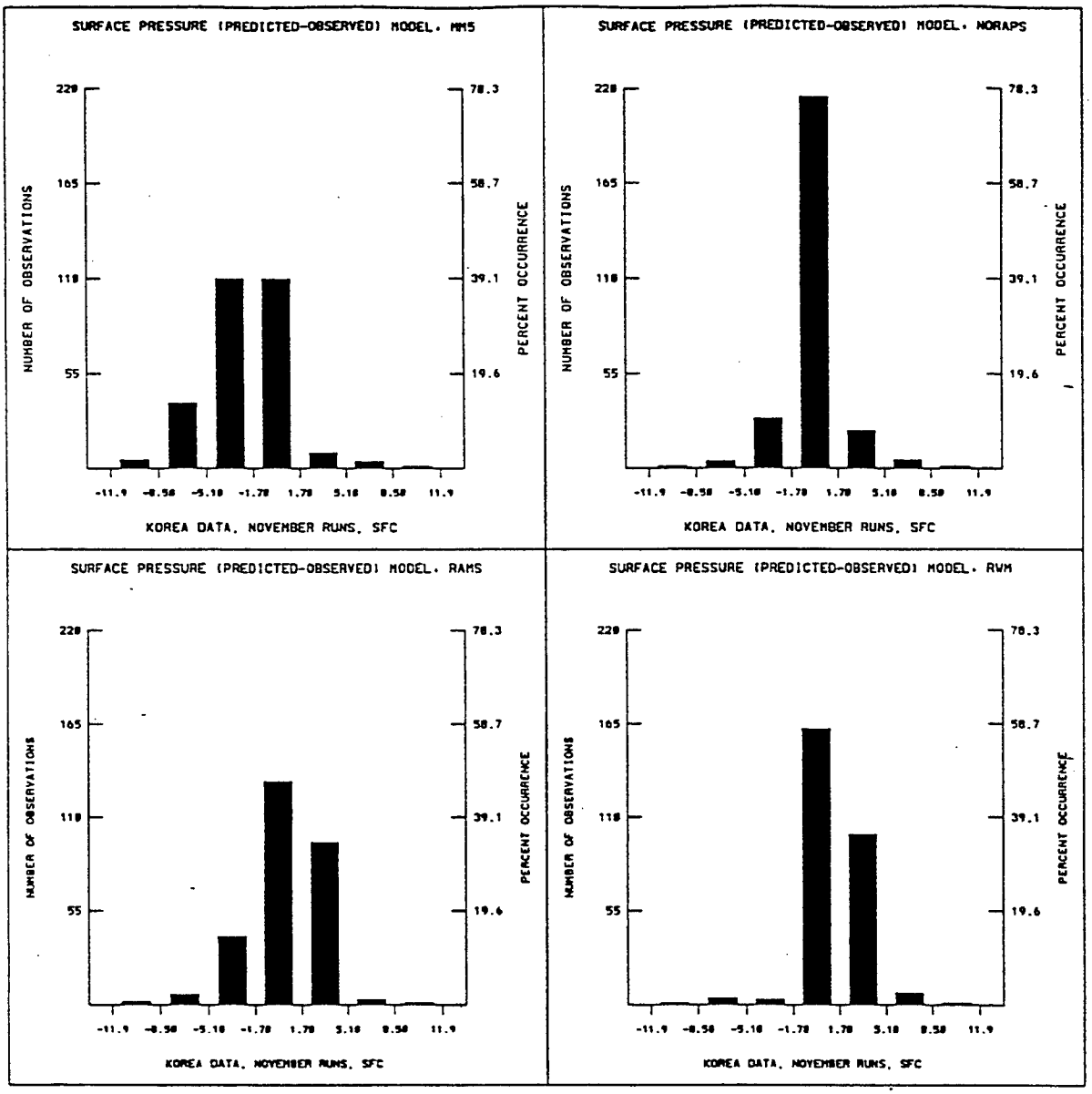

(b) Pressure

Figure 4-24. Surface error statistics, November - Korea. (Continued)

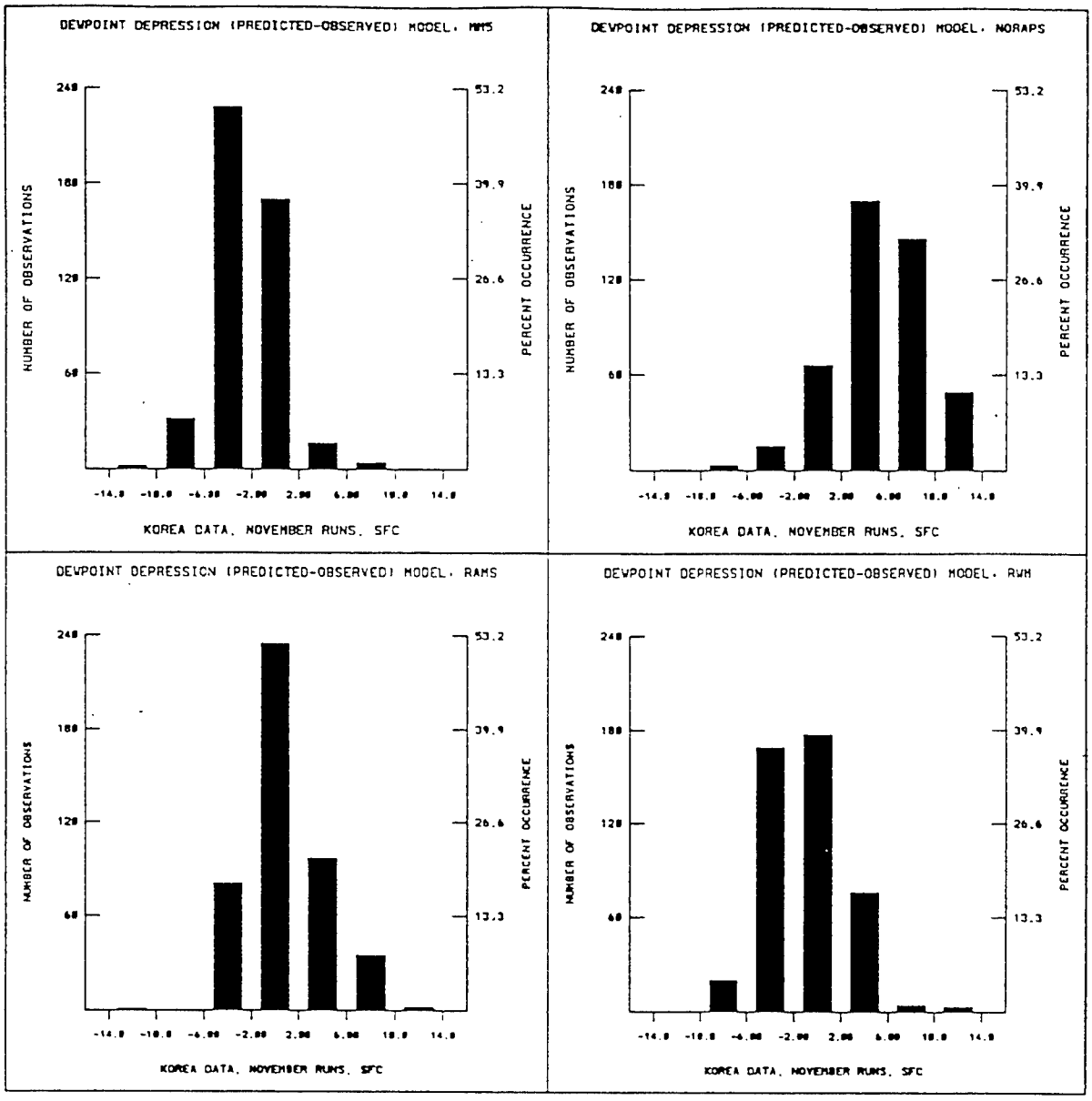

(c) Dew point depression

Figure 4-24. Surface error statistics, November - Korea. (Continued)

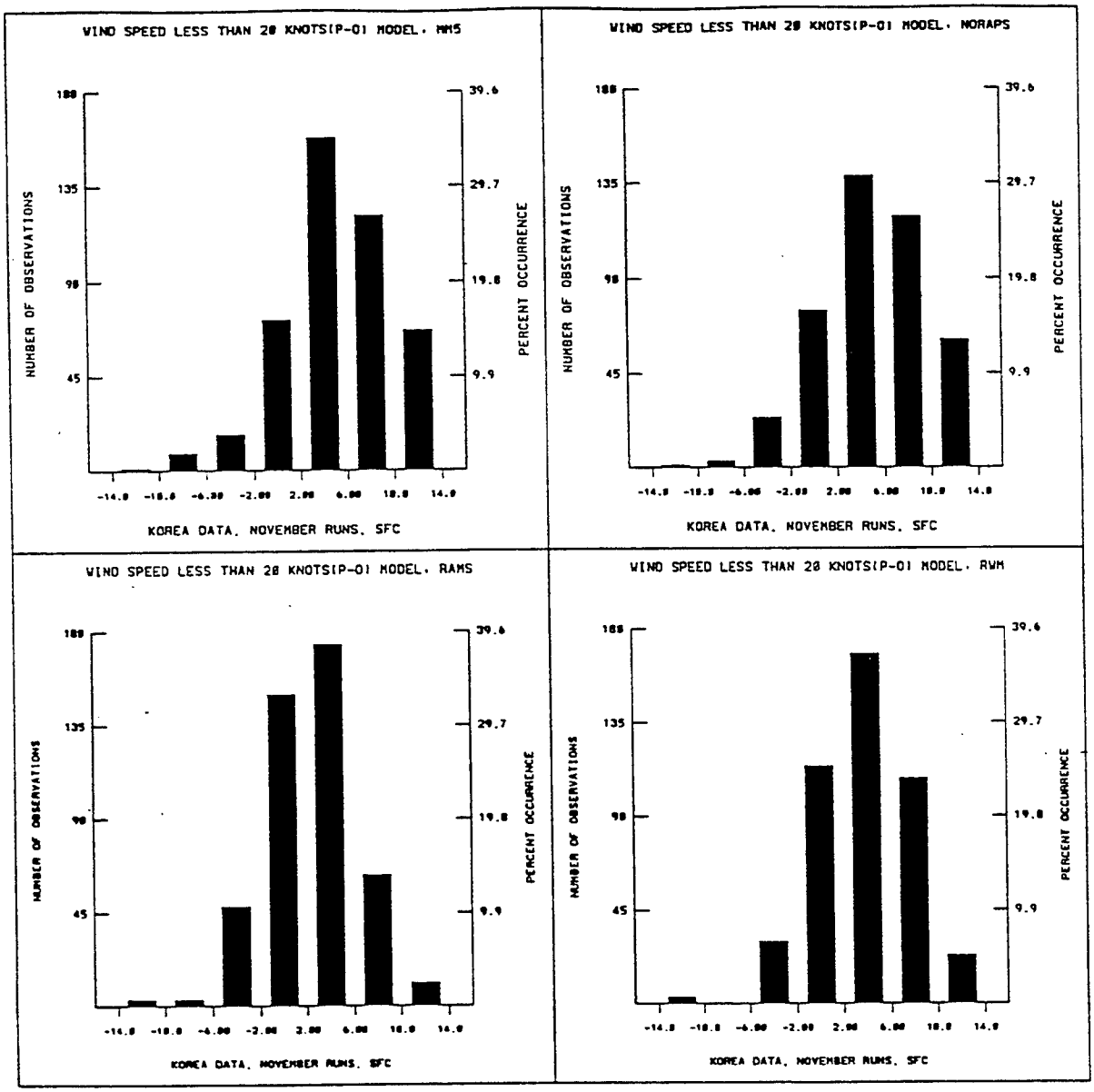

(d) Wind speed < 20 Knots

Figure 4-24. Surface error statistics, November - Korea. (Continued)

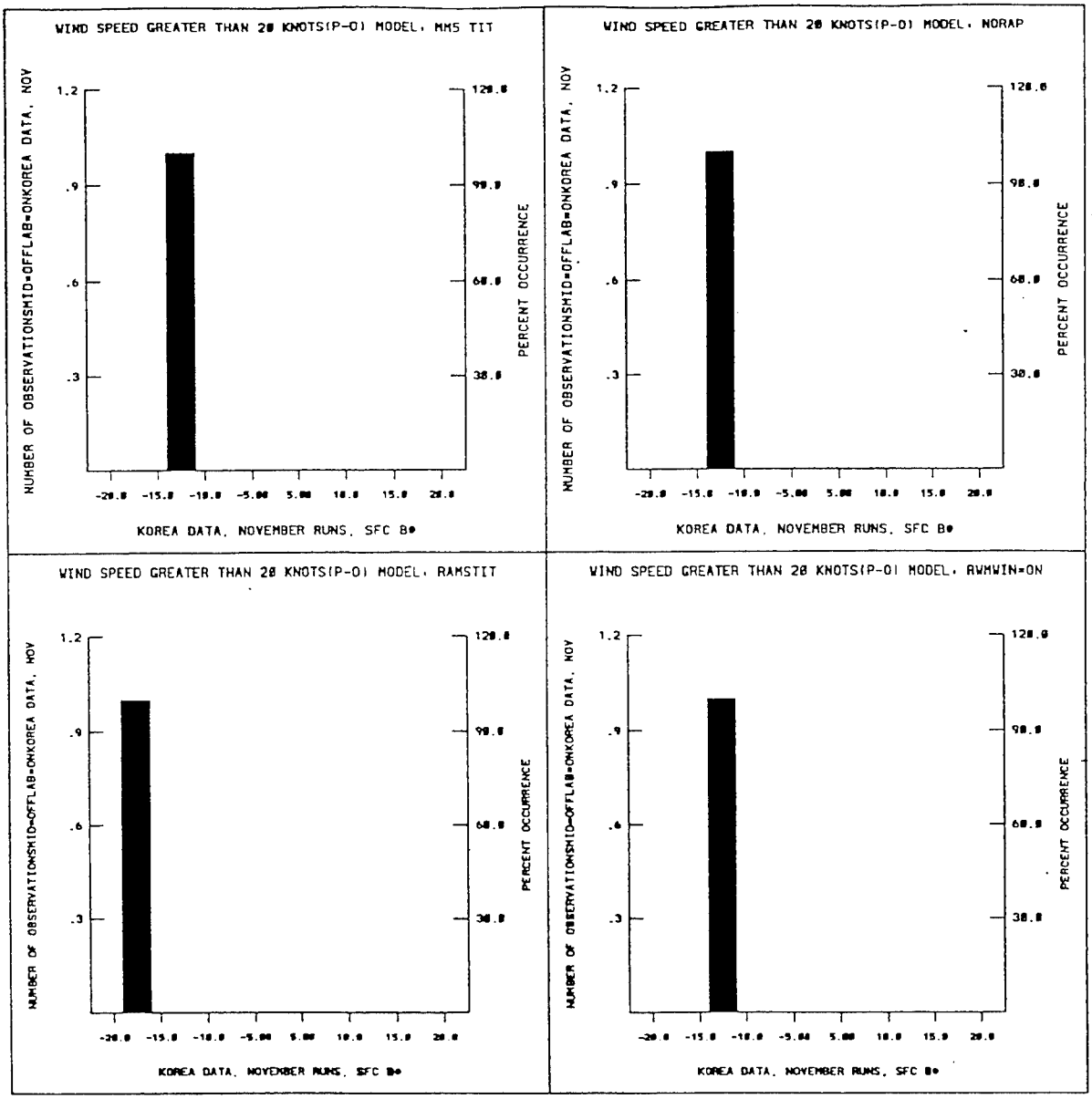

(e) Wind speed > 20 Knots

Figure 4-24. Surface error statistics, November - Korea. (Continued)

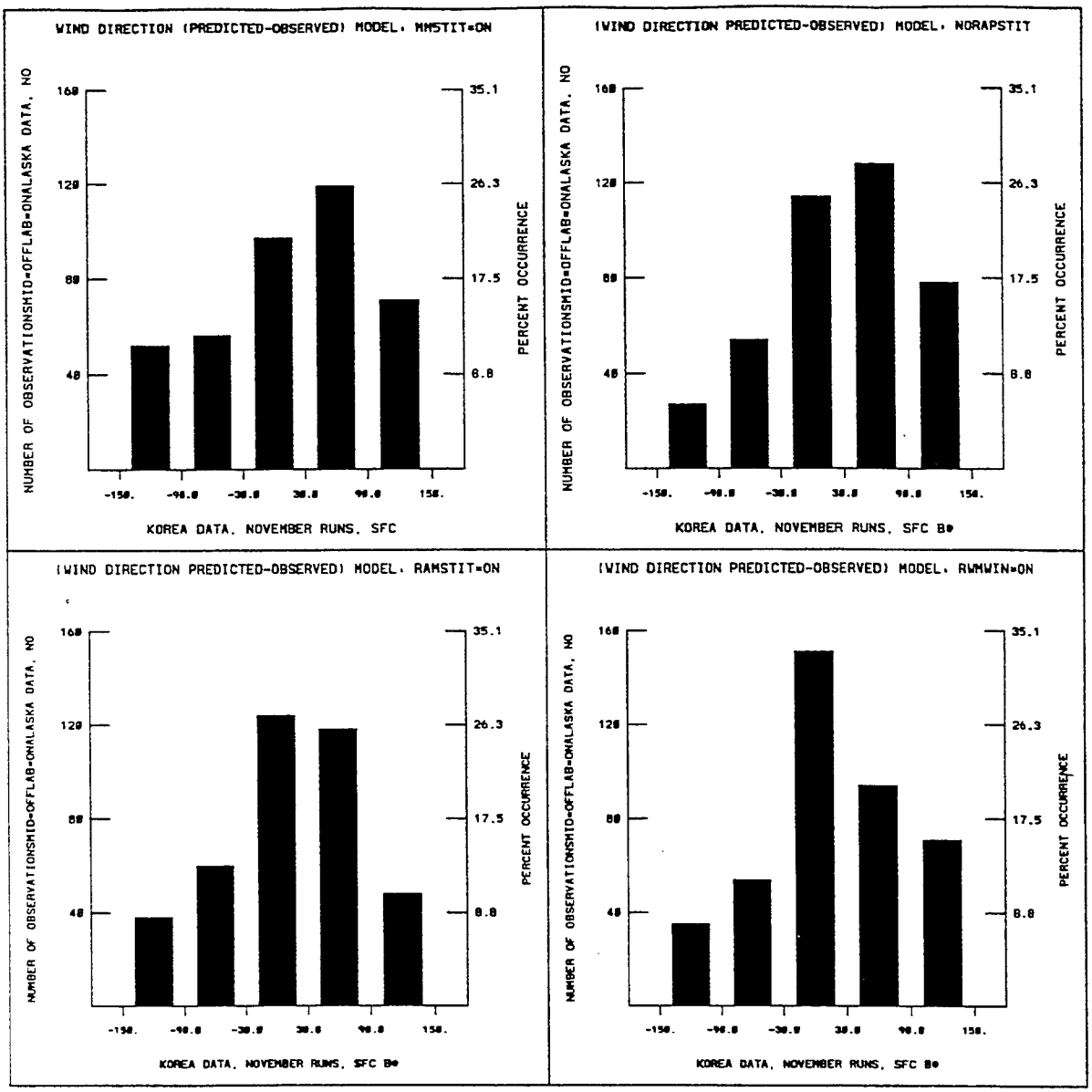

(f) Wind Direction

Figure 4-24. Surface error statistics, November - Korea. (Continued)

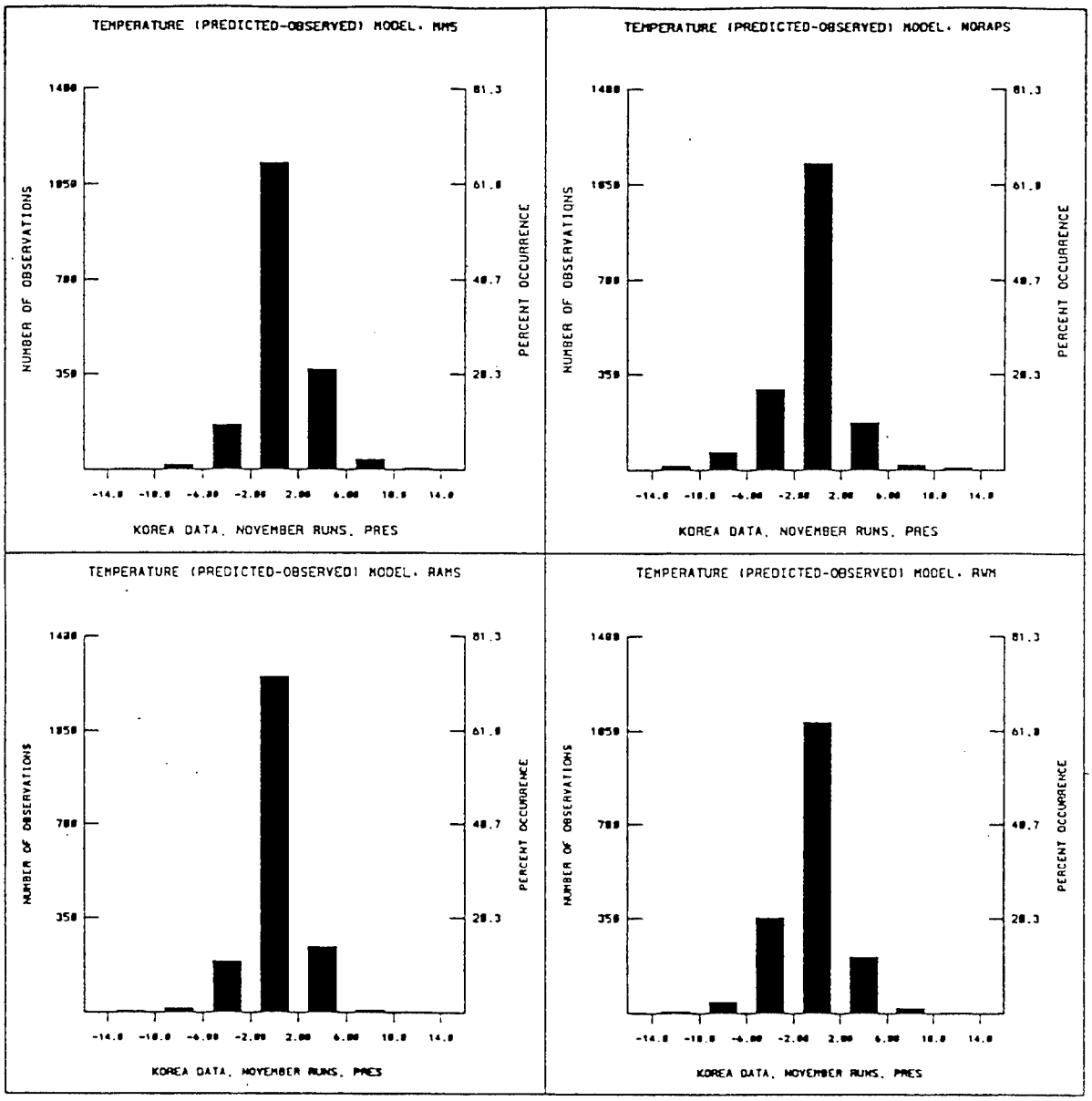

(a) Temperature

Figure 4-25. Upper air error statistics, November - Korea.

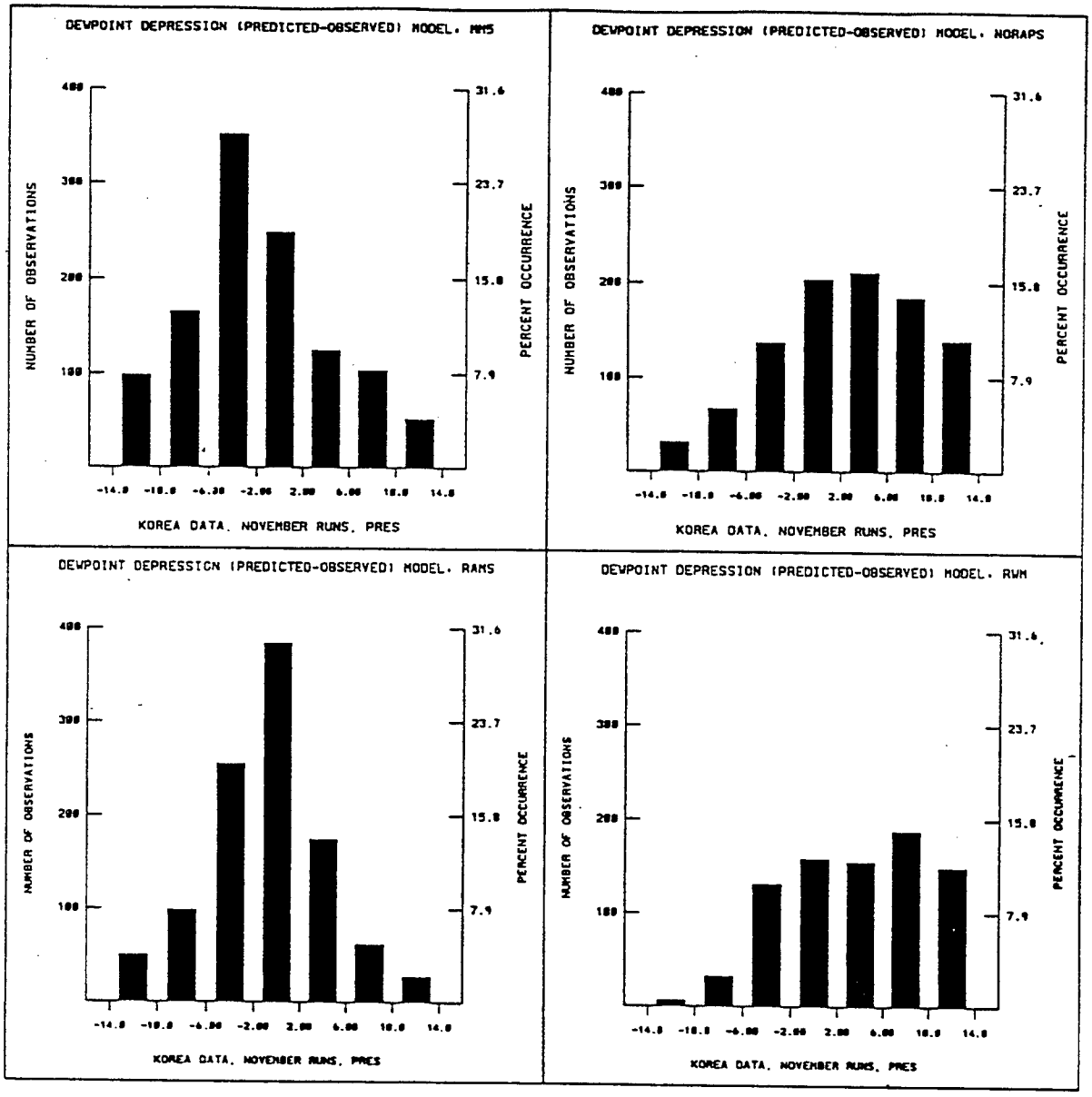

(b) Dew point depression

Figure 4-25. Upper air error statistics, November - Korea. (Continued)

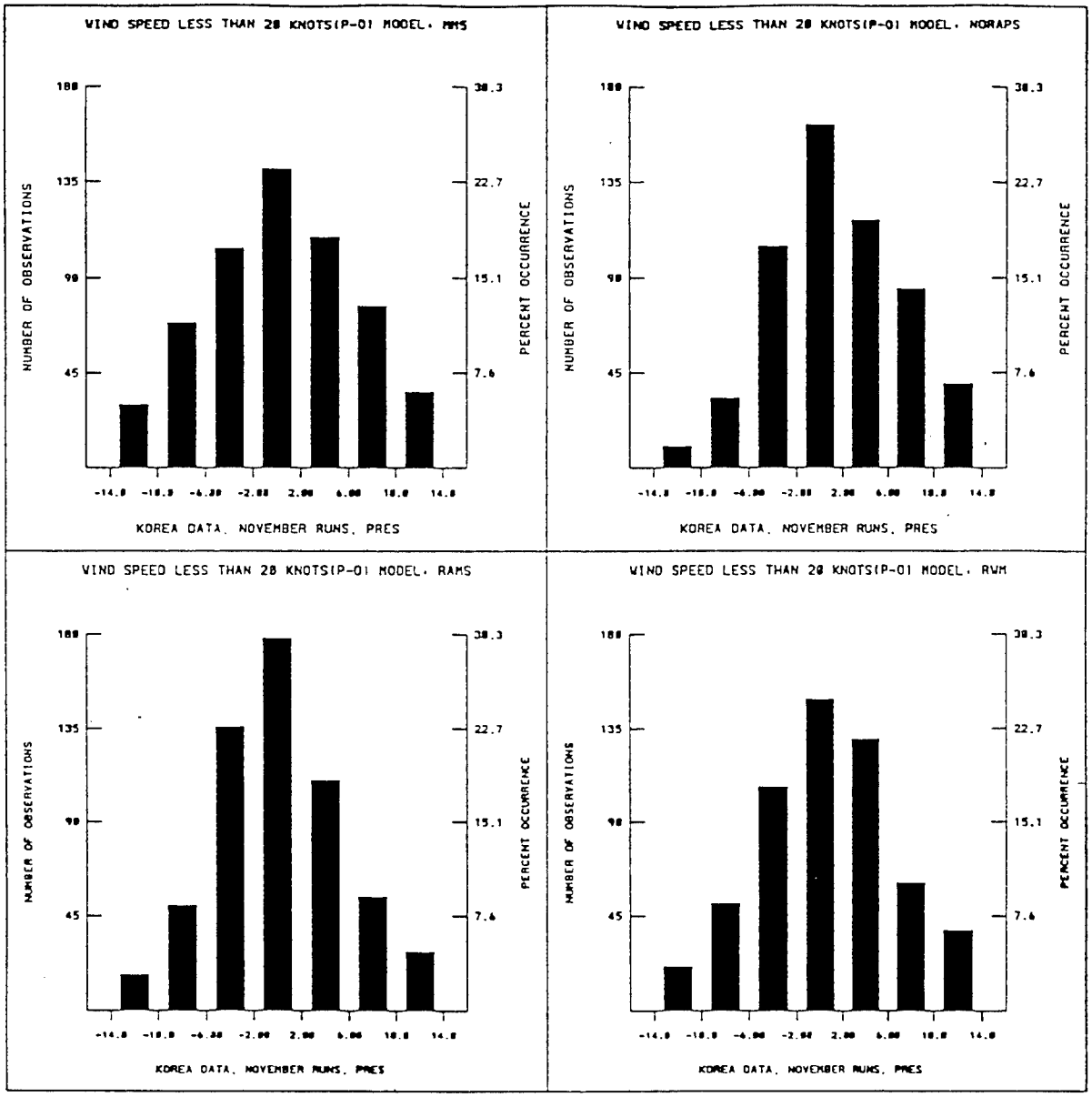

(c) Wind speed < 20 Knots

Figure 4-25. Upper air error statistics, November - Korea. (Continued)

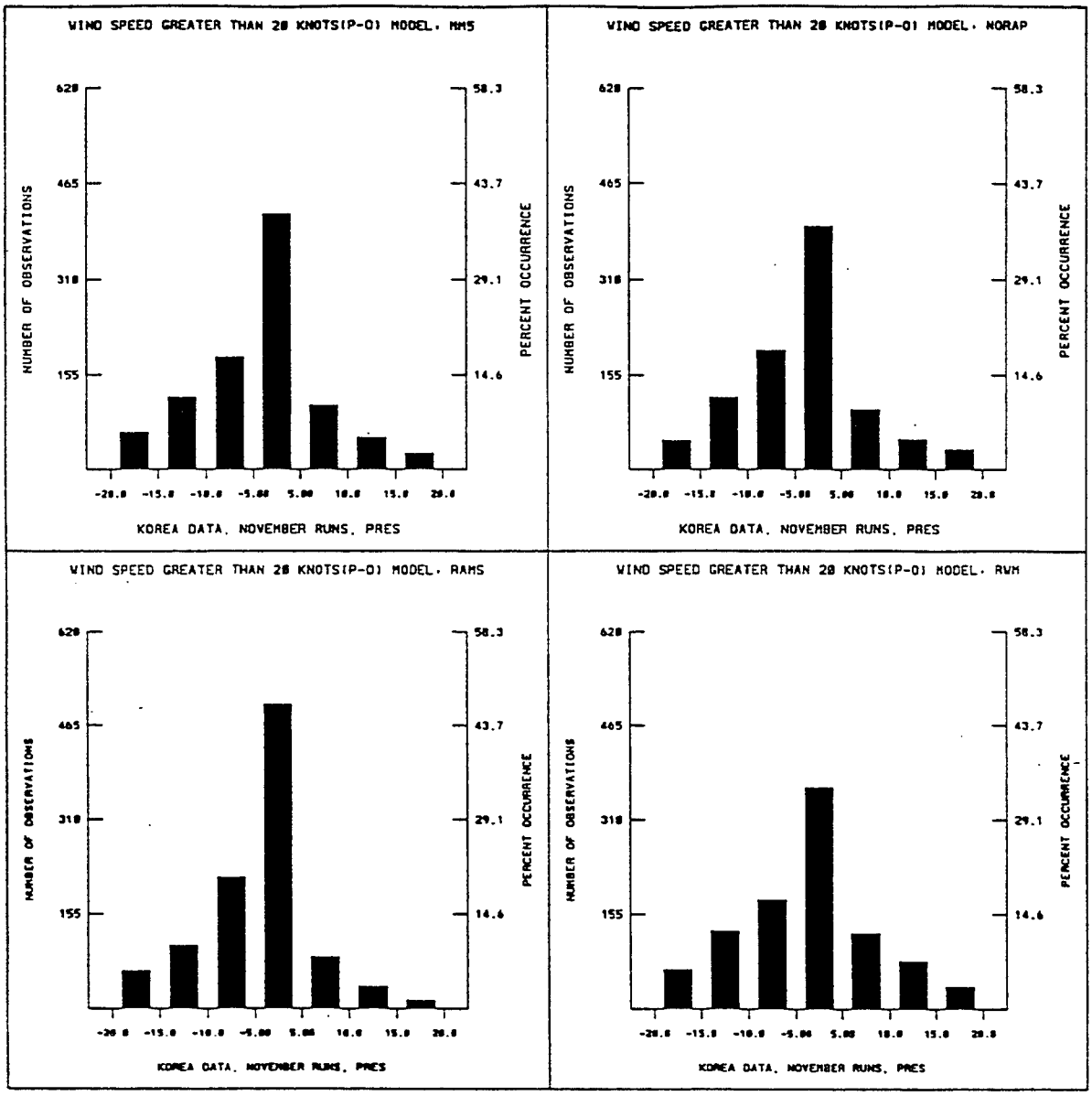

(d) Wind speed > 20 Knots

Figure 4-25. Upper air error statistics, November - Korea. (Continued)

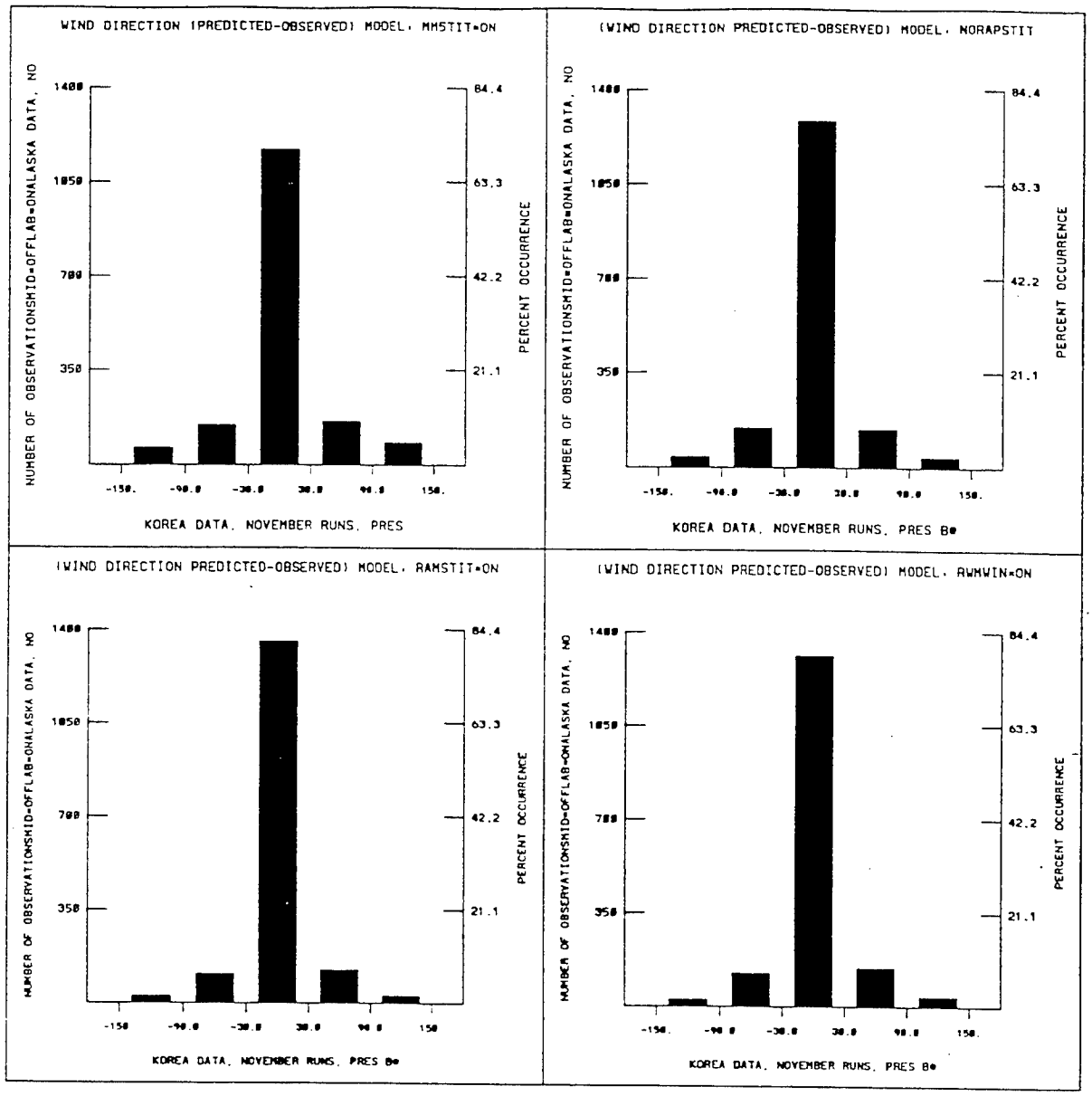

(e) Wind direction

Figure 4-25. Upper air error statistics, November - Korea. (Continued)

Upper Air

The main feature in the 500 mb geopotential field was a closed trough over the southern Turkey coast. All models handled this similarly although with slightly different central heights. RWM had the most diffuse centered and located further east than the others did. GSM had the lowest central height of 5520 meters, RAMS the highest at 5580 meters. All models placed the 500 mb jet maximum over the northern tip of the Red Sea, except for RWM which moved it eastward over northwest Saudi Arabia. Figures 4-26(a - e) depict the geopotential height.

Phenomenology results at 24 hours into the second forecast period (17 Nov. 94 – 0000 UTC).

Surface

Thirty-six hours later, the low from the eastern Mediterranean was moved by the models eastward. RAMS, MM5, and GSM had the center located over northwest Iran, while NORAPS6 lagged the center farther behind in northeastern Iraq. RWM again had an extremely noisy sea level pressure field. RAMS, MM5, and NORAPS6 developed a stronger ridging over Egypt and Saudi Arabia than GSM.

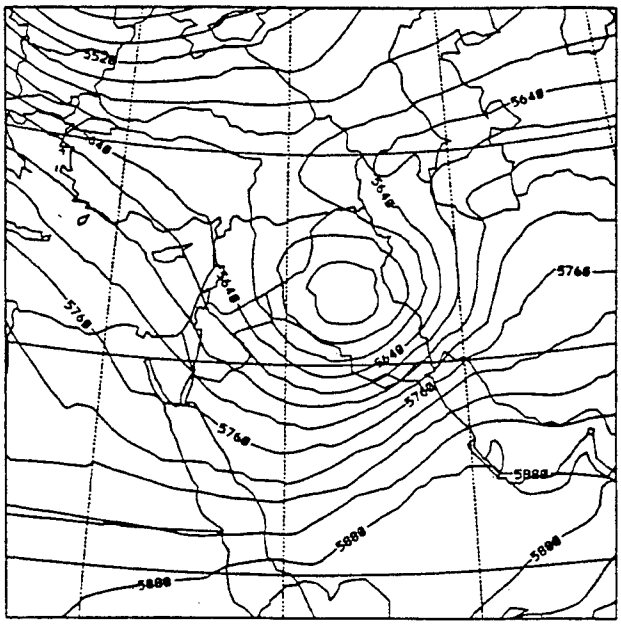

(a) GSM Analysis at 15 Nov 94 - 1200 UTC

Figure 4-26. Geopotential height - Middle East.

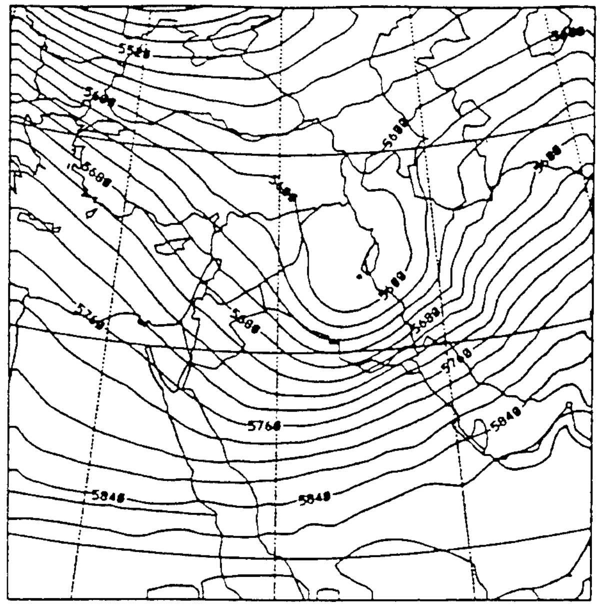

(b) MM5 - 15 Nov 94 - 1200 UTC forecast

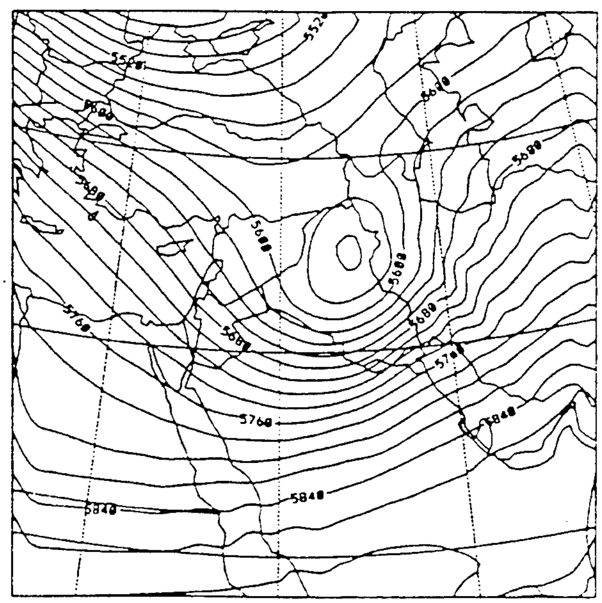

(c) NORAPS6 - 15 Nov 94 - 1200 UTC

Figure 4-26. Geopotential height - Middle East. (Continued)

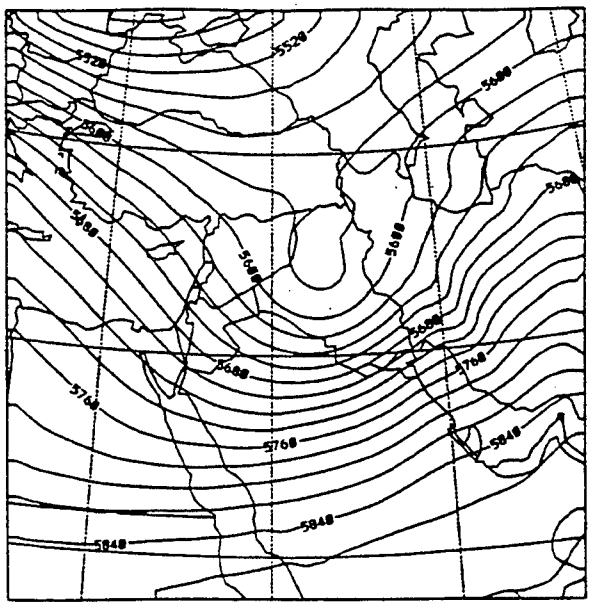

(d) RAMS - 15 Nov 94 - 1200 UTC forecast

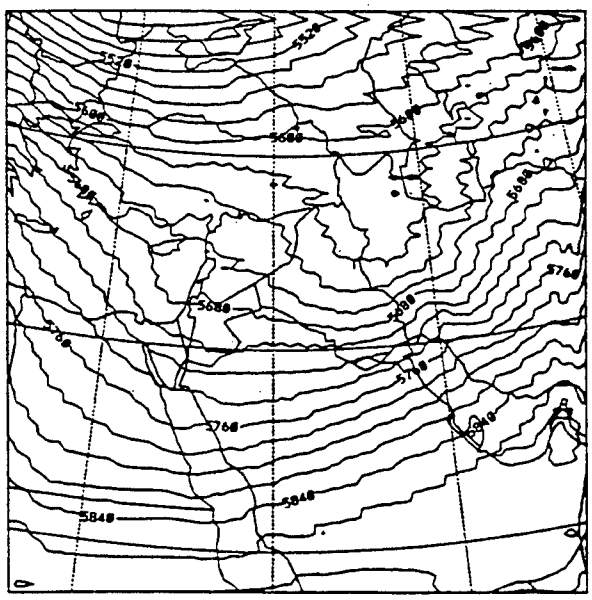

(e) RWM - 15 Nov 94 - 1200 UTC forecast

Figure 4-26. Geopotential height - Middle East. (Continued)

At 500 mb, all regional models developed a double-core structure to the mid-level jet stream while GSM maintained a single core over Kuwait. RWM had the weakest core maximum of 31 m/s, NORAPS6 38 m/s, RAMS 37 m/s, and MM5 40 m/s.

4.1.3.9 Statistical Results - Middle East. Error frequency distributions were generated for temperature, surface pressure, dew point depression, wind speed below 20 knots, wind speed above 20 knots, and wind direction. Data from all forecast times, both November forecasts, and where appropriate, levels were merged. The central column corresponds to the desired error bounds. Two sets of figures were developed to describe the forecast results. One is a surface set that includes the large number of surface observations and the other is an upper air set that includes the more sparse upper air observations. Figures 4-27(a - f) are the surface results and Figures 4-28(a - e) are the upper air results.

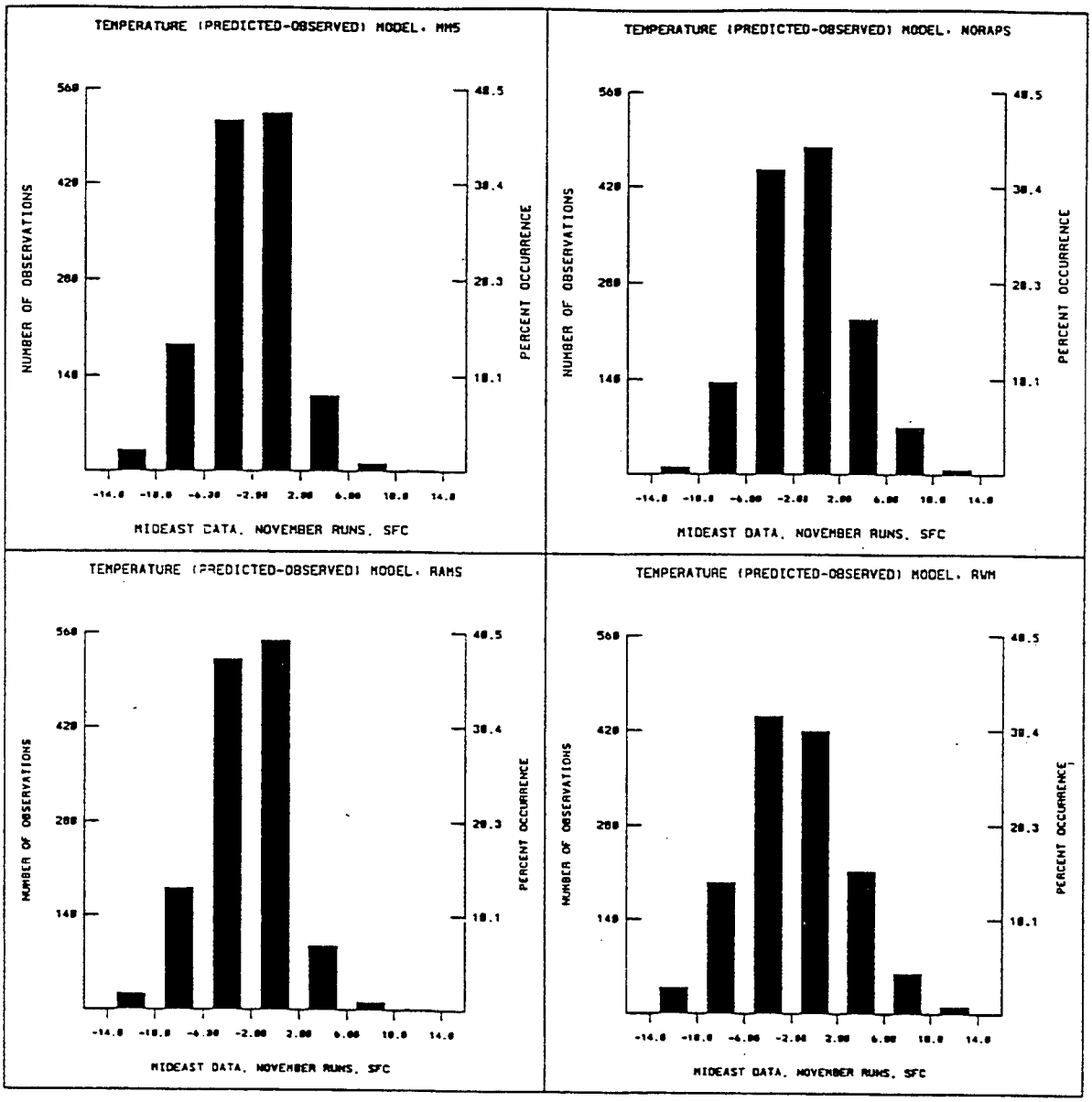

(a) Temperature

Figure 4-27. Surface error statistics, November - Middle East.

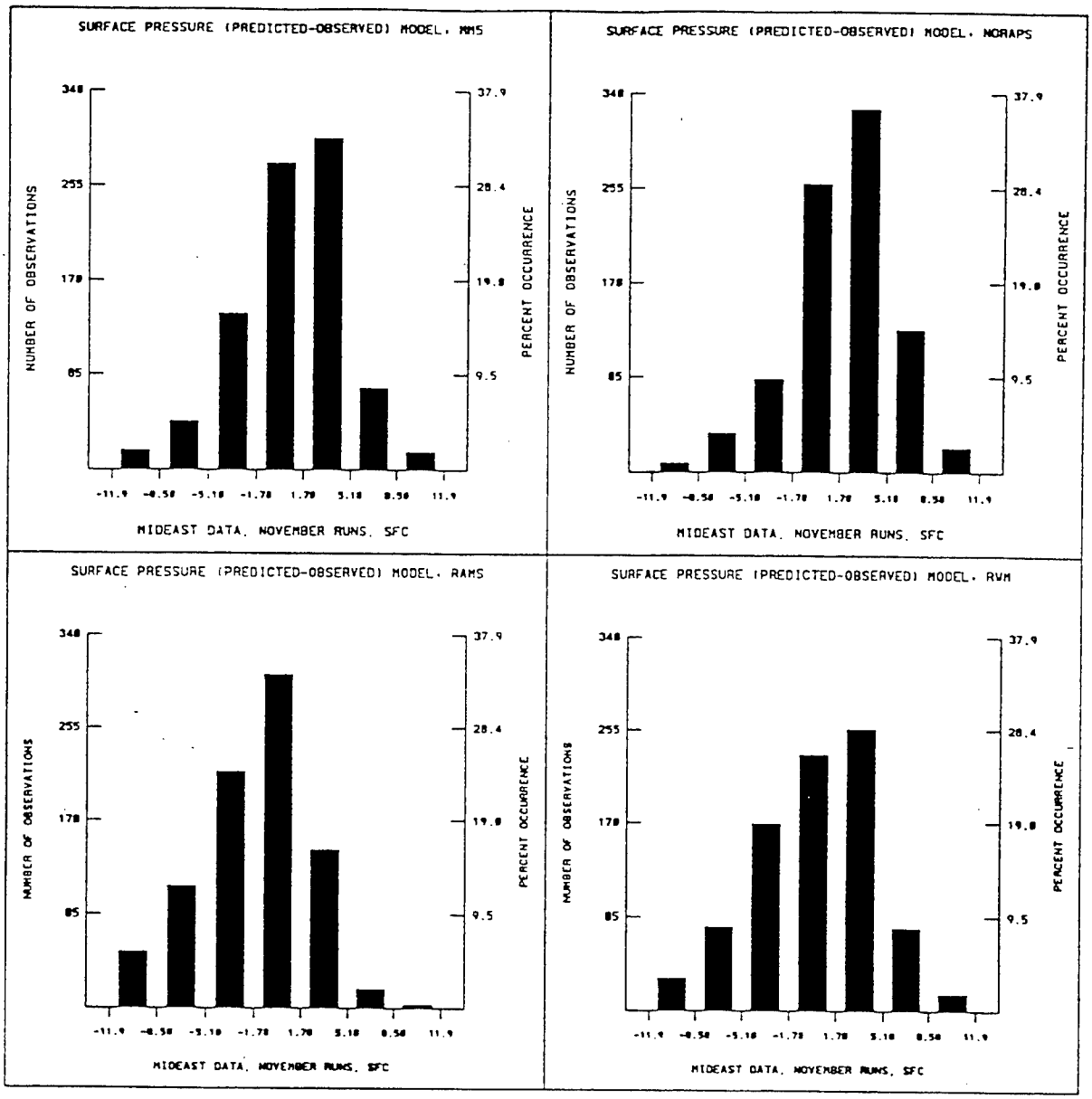

(b) Pressure

Figure 4-27. Surface error statistics, November - Middle East. (Continued)

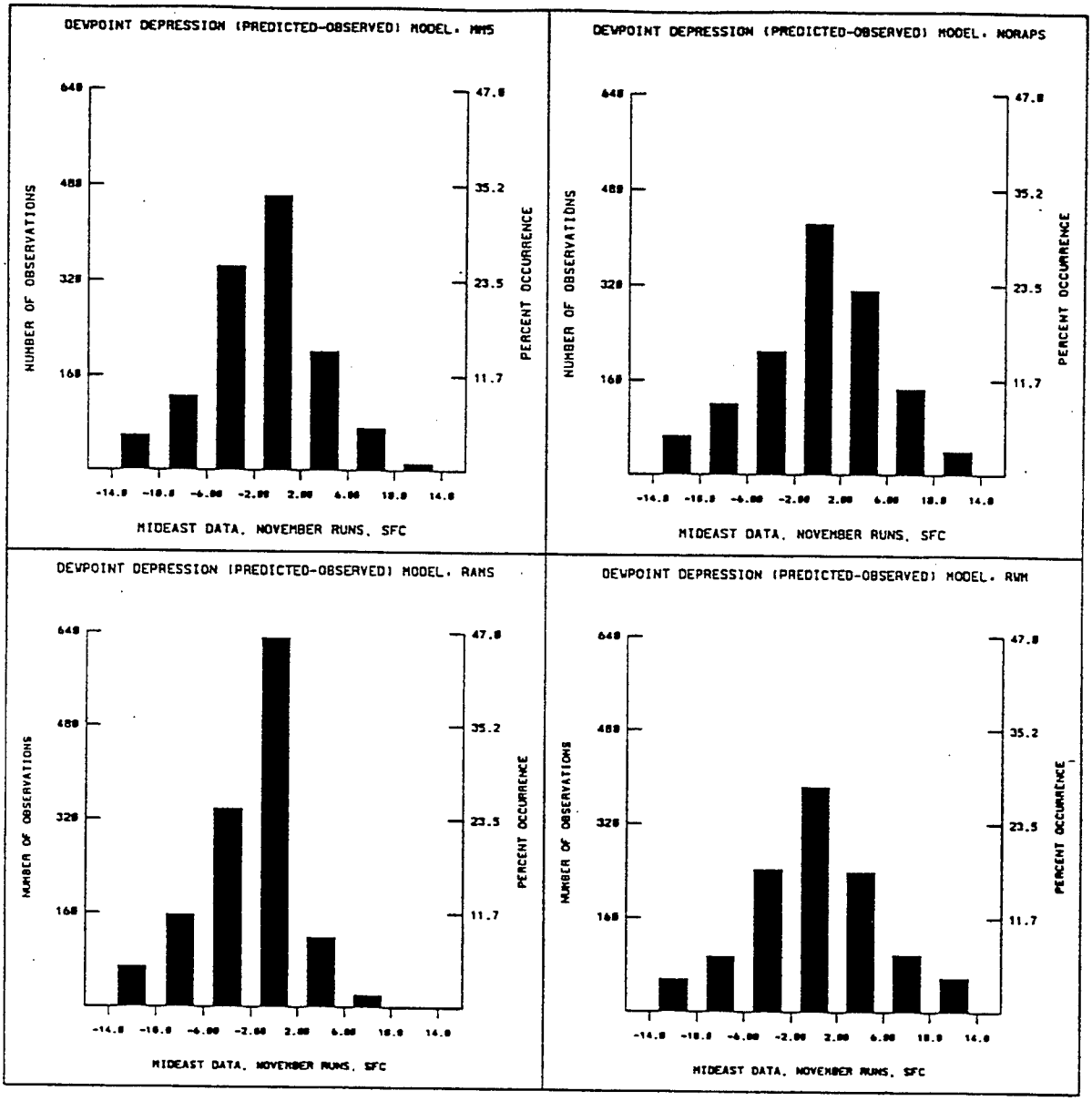

(c) Dew point depression

Figure 4-27. Surface error statistics, November - Middle East. (Continued)

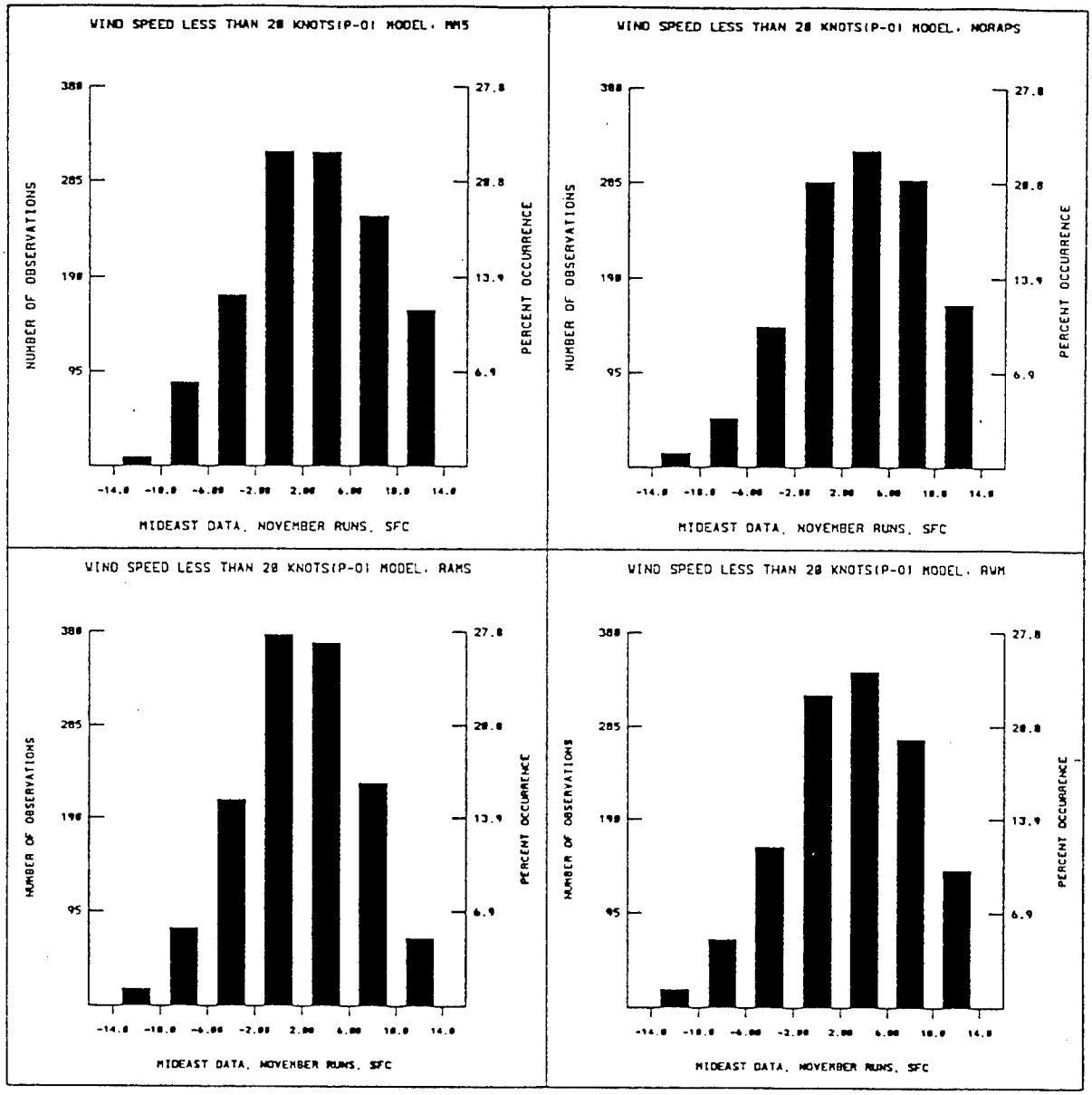

(d) Wind speed < 20 Knots

Figure 4-27. Surface error statistics, November - Middle East. (Continued)

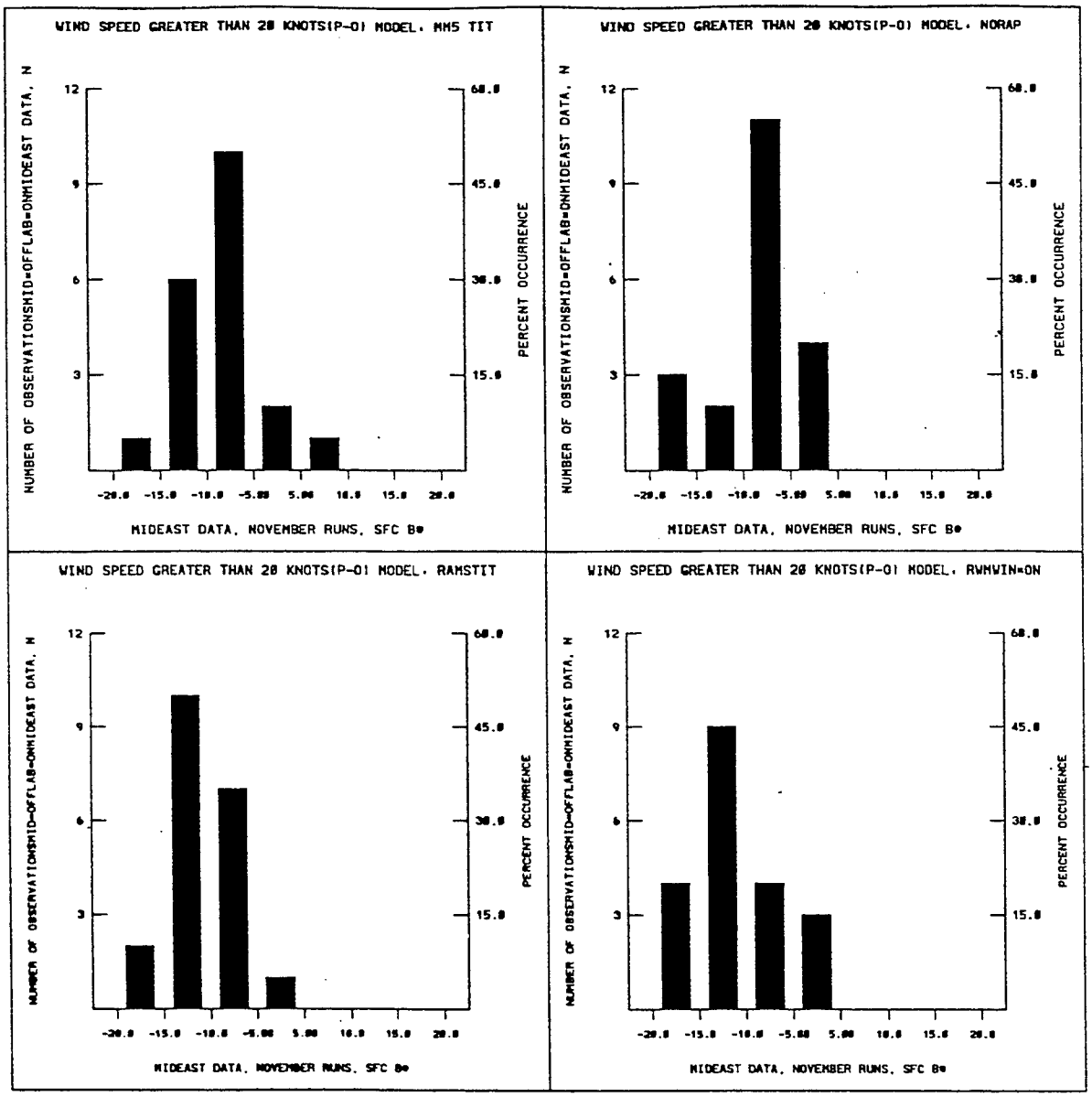

(e) Wind speed > 20 Knots

Figure 4-27. Surface error statistics, November - Middle East. (Continued)

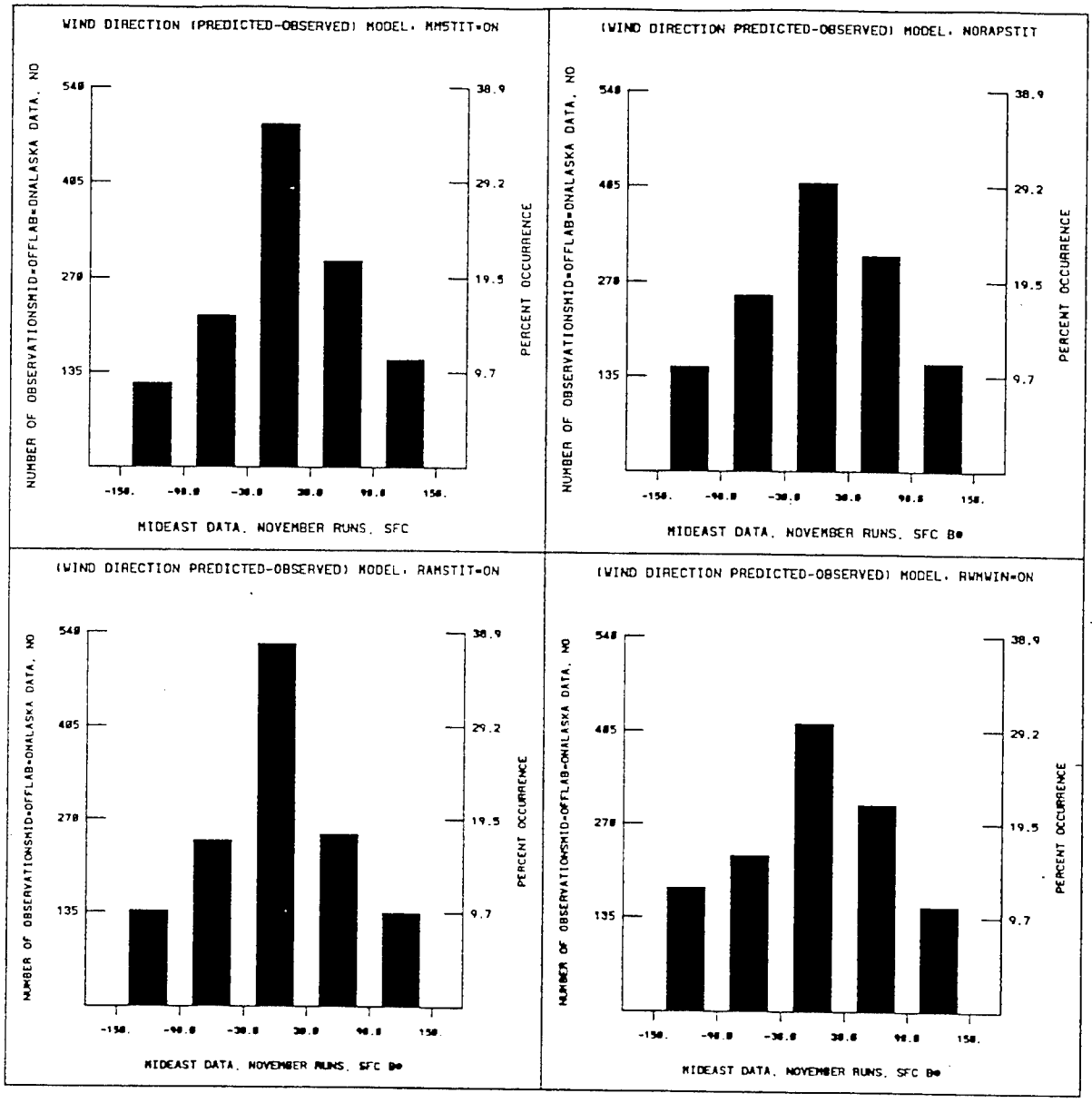

(f) Wind direction

Figure 4-27. Surface error statistics, November - Middle East. (Continued)

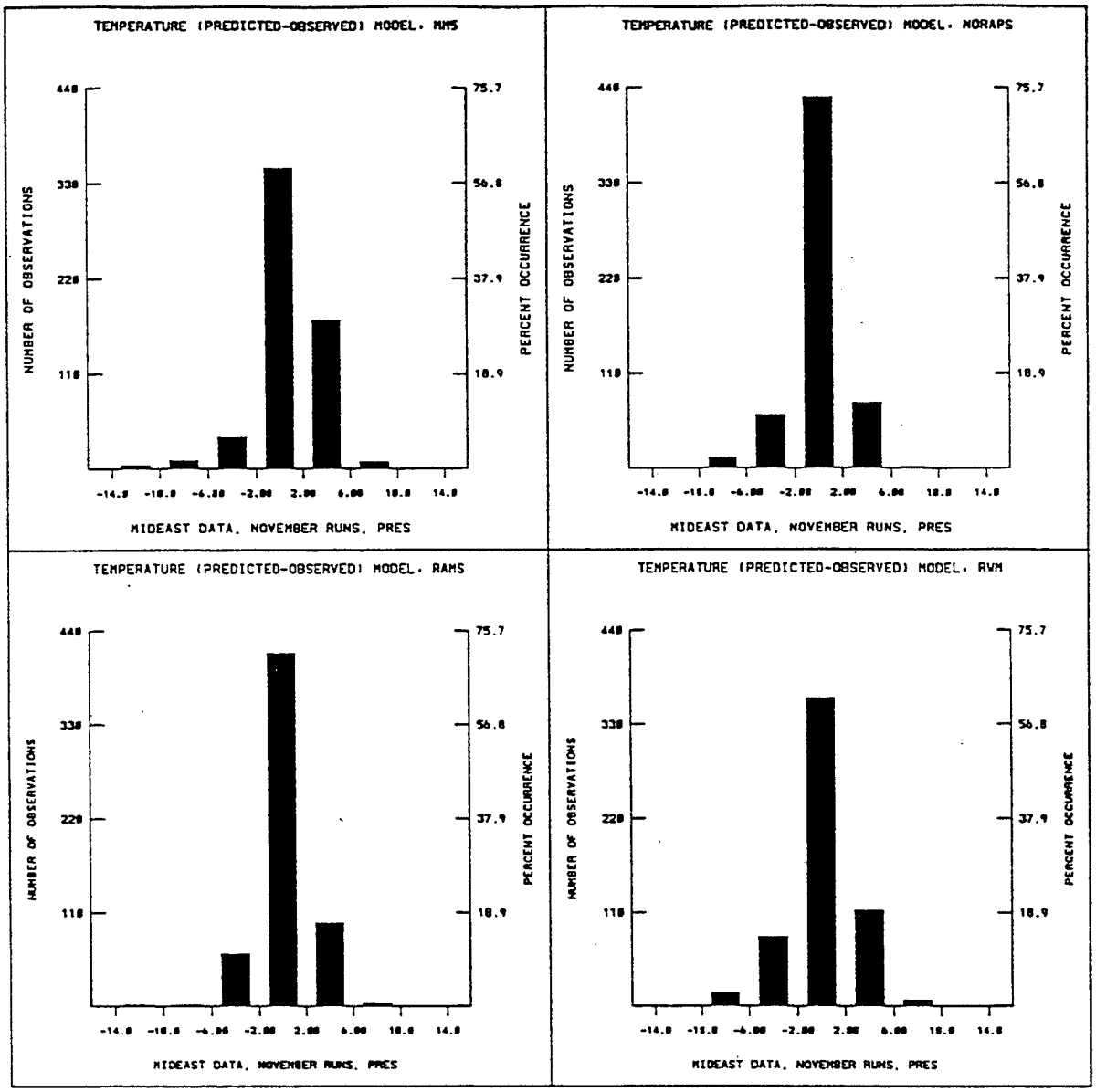

(a) Temperature

Figure 4-28. Upper air error statistics, November - Middle East.

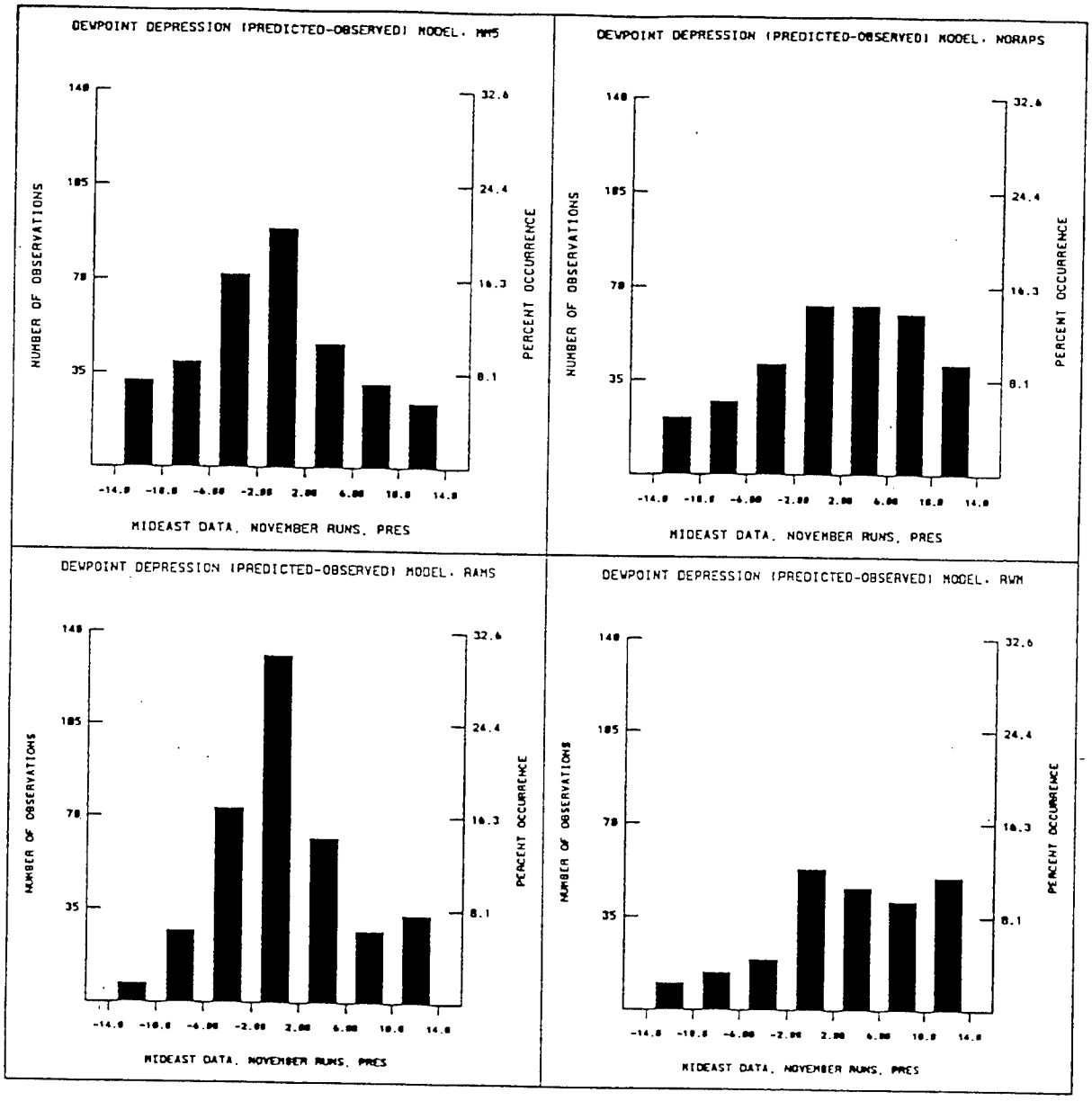

(b) Dew point depression

Figure 4-28. Upper air error statistics, November - Middle East. (Continued)

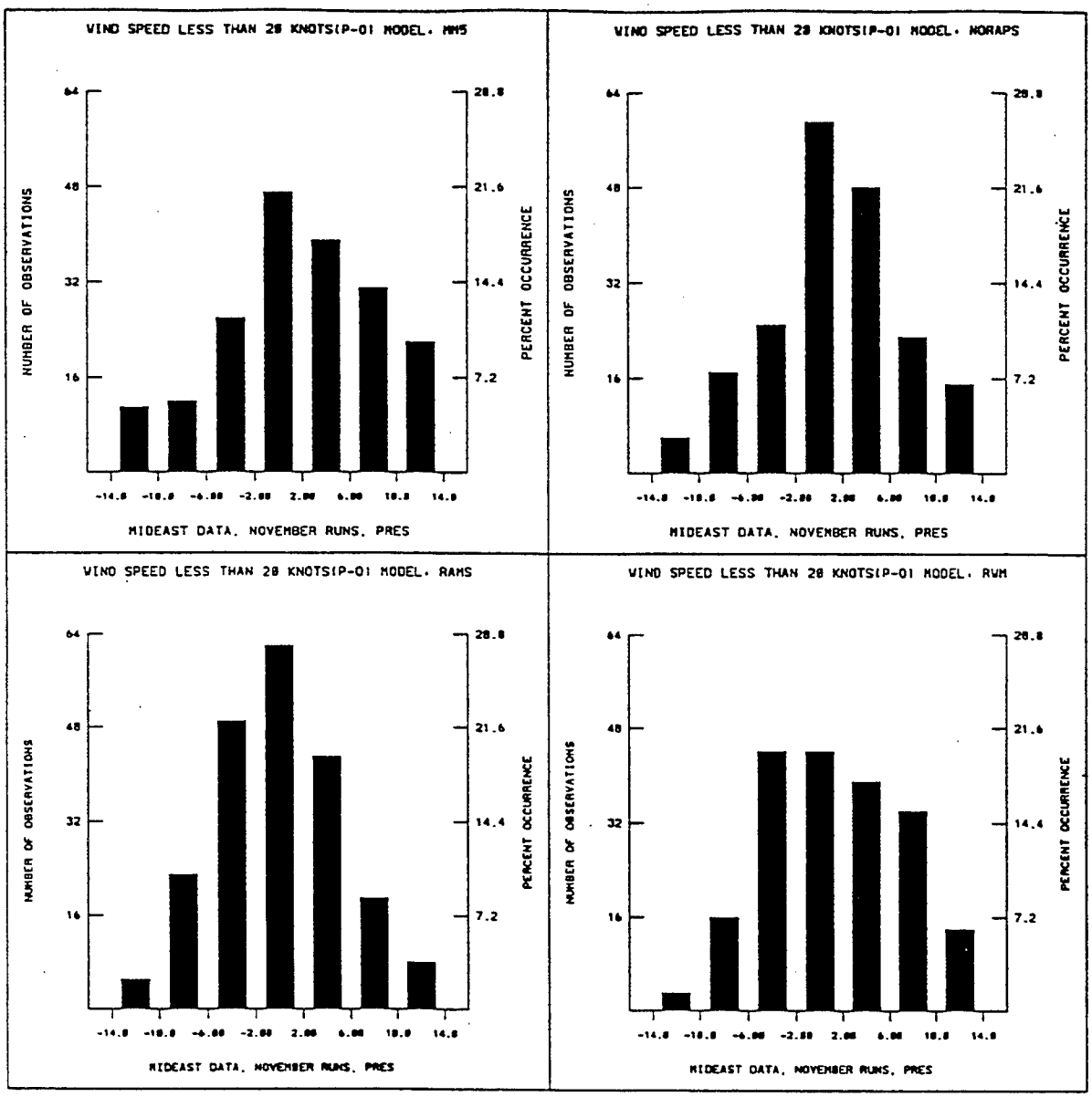

(c) Wind speed < 20 Knots

Figure 4-28. Upper air error statistics, November - Middle East. (Continued)

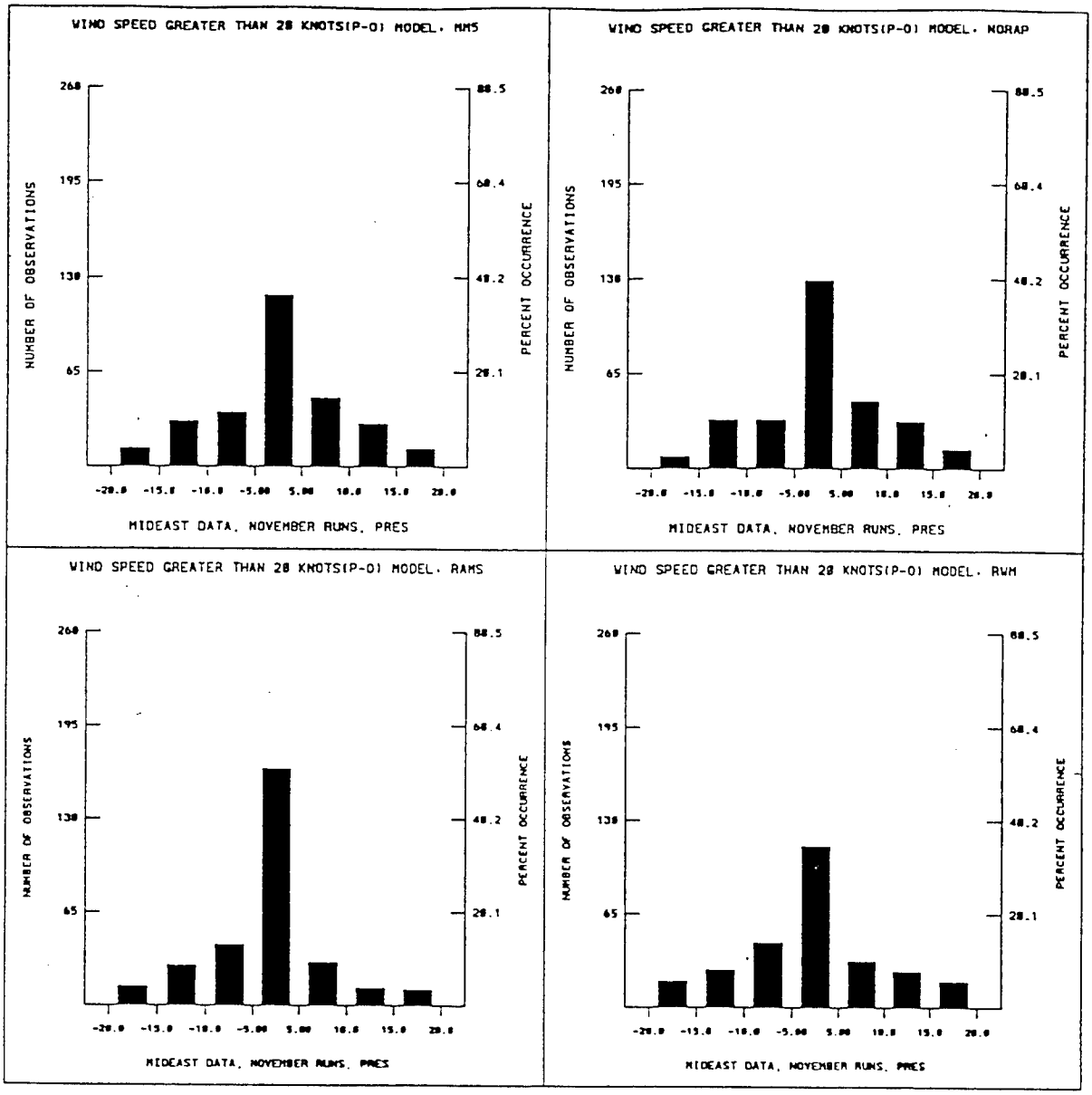

(d) Wind speed > 20 Knots

Figure 4-28. Upper air error statistics, November - Middle East. (Continued)

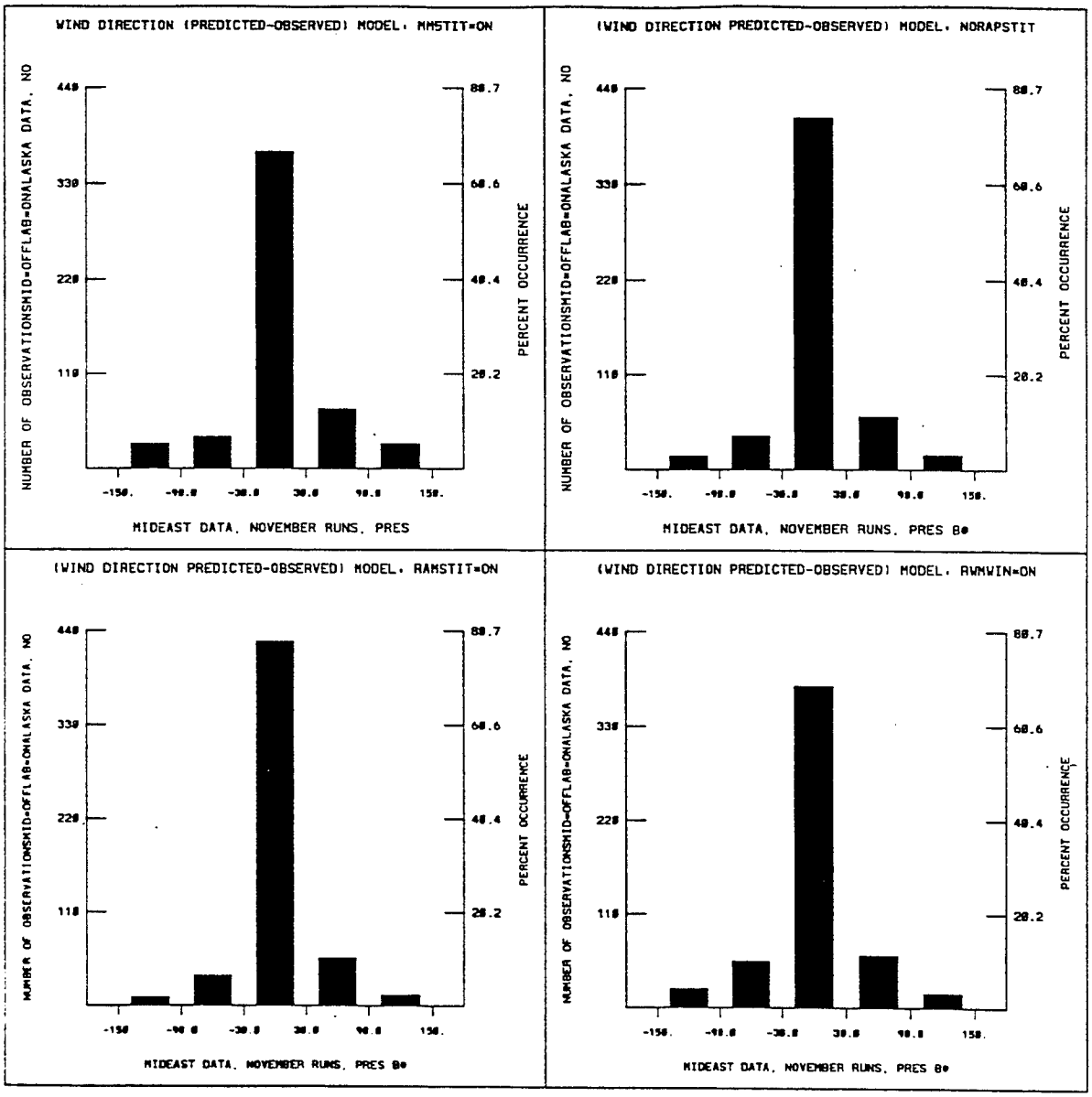

(e) Wind direction

Figure 4-28. Upper air error statistics, November - Middle East. (Continued)

4.1.3.10 Phenomenological Results - Central America. Phenomenology results at 24 hours into the first forecast period (15 Nov. 94 – 1200 UTC).

Surface

The most significant surface feature in the region at this time was a surface cyclone located near the southern tip of Florida. All models had the center located in a similar position with GSM having a 1006 mb center, MM5 1004 mb, RAMS 1009 mb, NORAPS6 1008 mb, and RWM 1009 mb and again extremely noisy. RWM did not have a well-defined circulation around the center, while all other models showed a closed circulation of up to 12 m/s maximum winds. Both the pressure and wind fields are presented in Figures 4-29(a - e) and Figures 4-30(a - e).

Upper Air

The cyclonic circulation continued up into the upper atmosphere. The maximum 500 mb winds were 20 m/s for GSM, RWM, and RAMS and 19 m/s for NORAPS6. MM5 generated localized regions of 27 m/s due to momentum transfer in its convective parameterization.

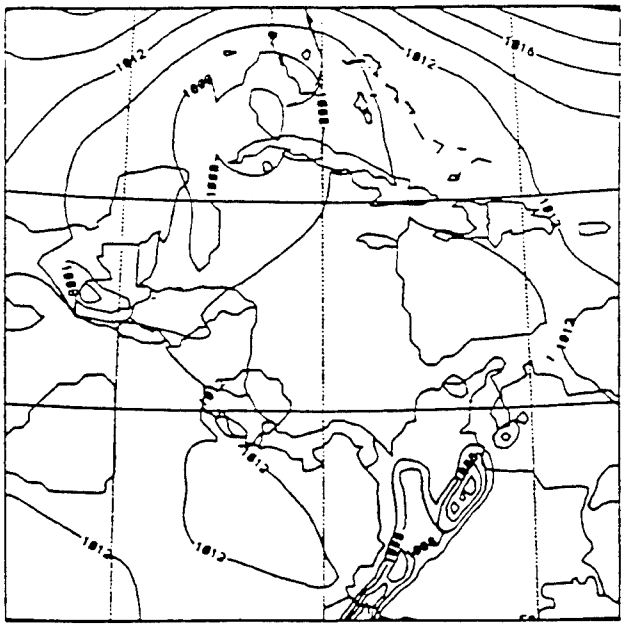

(a) GSM Analysis at 15 Nov 94 - 1200 UTC

Figure 4-29. Surface pressure - Central America.

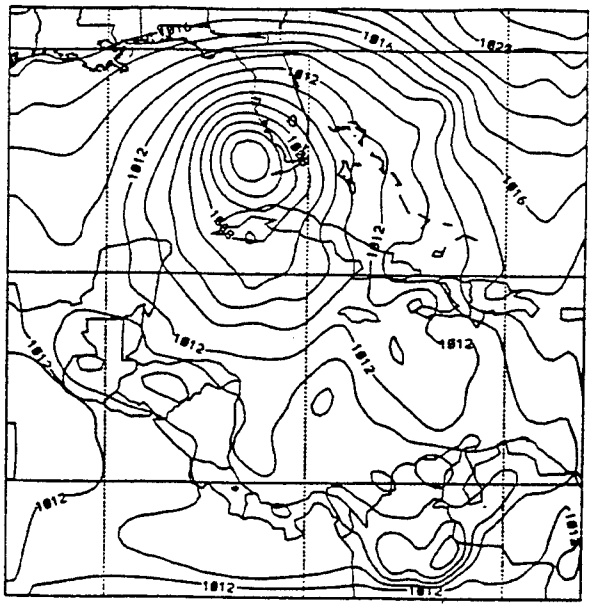

(b) MM5 - 15 Nov 94 - 1200 UTC forecast

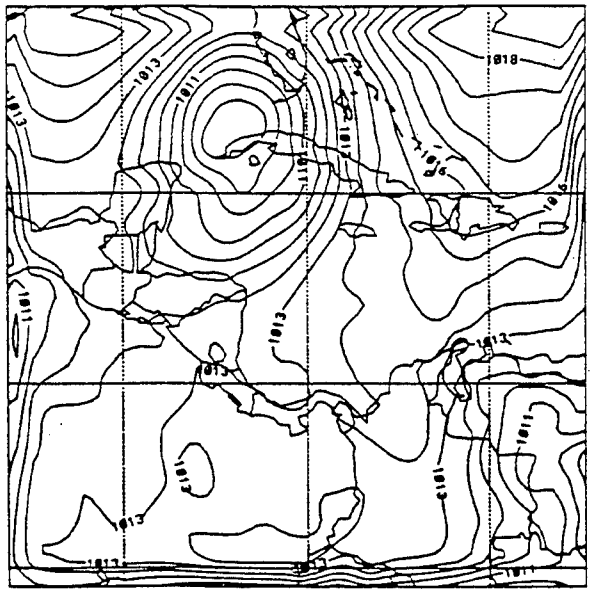

(c) NORAPS6 - 15 Nov 94 - 1200 UTC forecast

Figure 4-29. Surface pressure - Central America. (Continued)

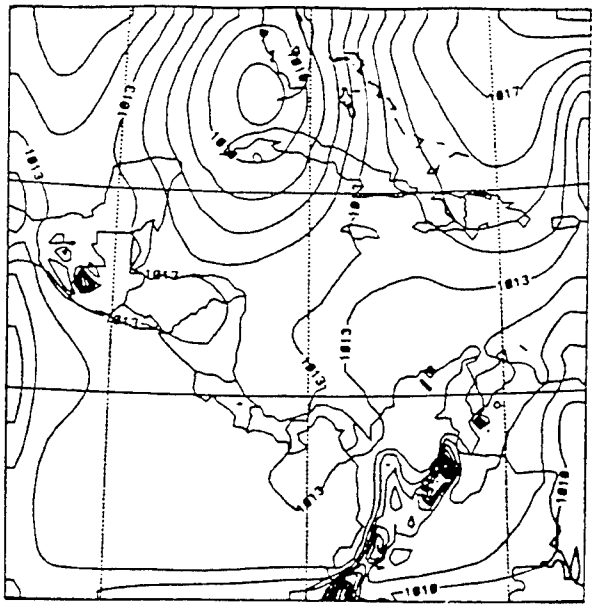

(d) RAMS - 15 Nov 94 - 1200 UTC forecast

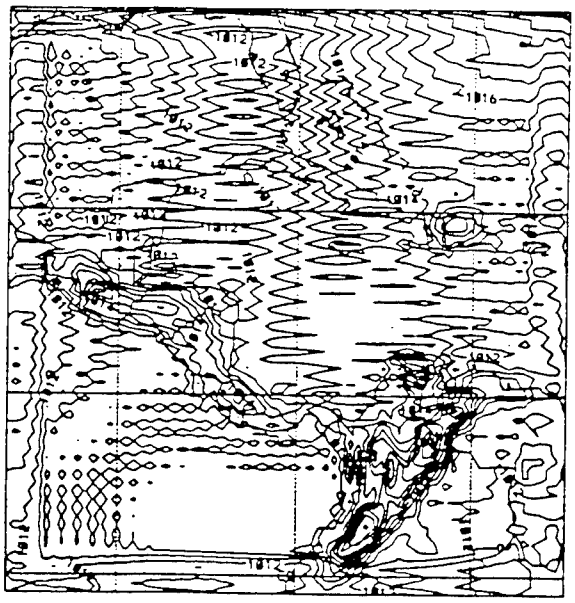

(e) RWM - 15 Nov 94 - 1200 UTC forecast

Figure 4-29. Surface pressure - Central America. (Continued)

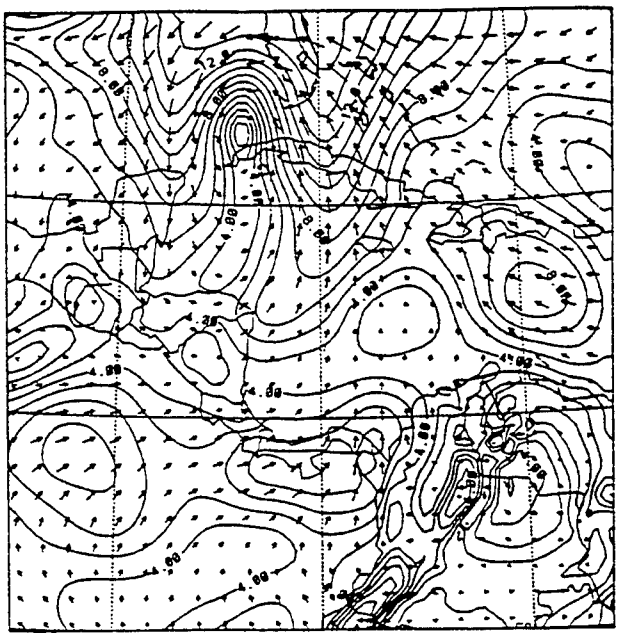

(a) GSM Analysis at 15 Nov 94 - 1200 UTC

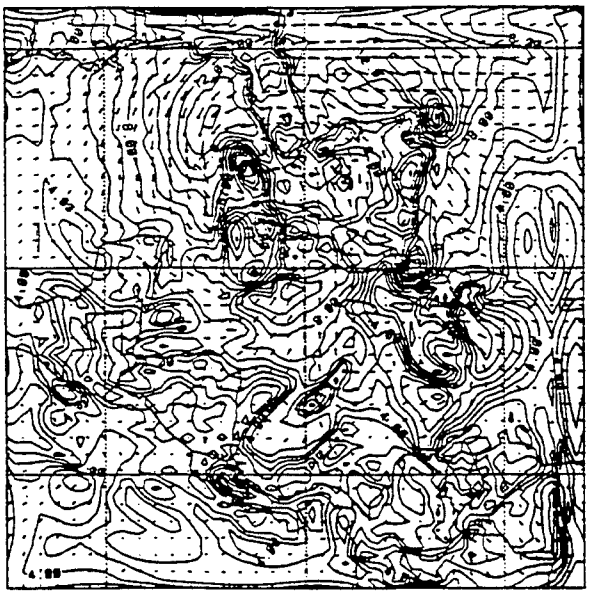

(b) MM5 - 15 Nov 94 - 1200 UTC forecast

Figure 4-30. Surface winds - Central America. (Continued)

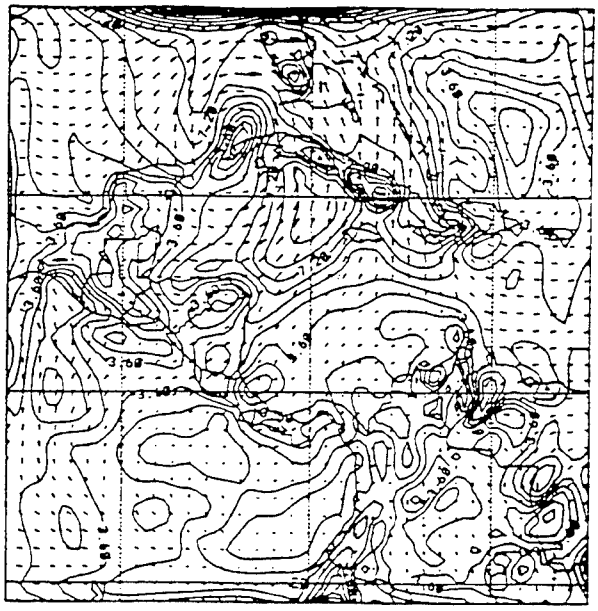

(c) NORAPS6 - 15 Nov 94 - 1200 UTC forecast

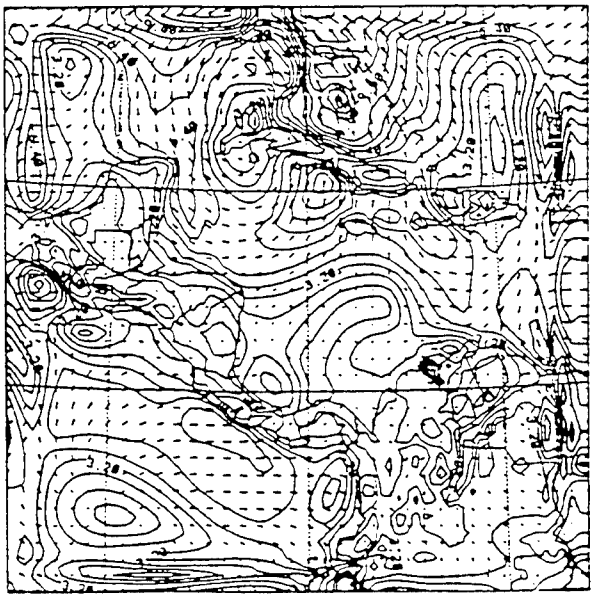

(d) RAMS - 15 Nov 94 - 1200 UTC forecast

Figure 4-30. Surface winds - Central America. (Continued)

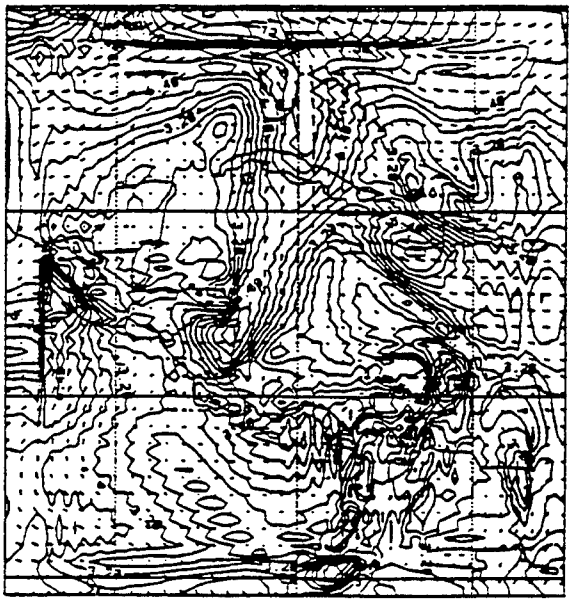

(e) RWM - 15 Nov 94 - 1200 UTC forecast

Figure 4-30. Surface winds - Central America. (Continued)

Phenomenology results at 24 hours into the second forecast period (17 Nov. 94 – 0000 UTC).

Surface

Thirty-six hours later, the cyclone had moved to the north boundary of the domain where the models could not handle it properly. RAMS, MM5, and GSM started to develop another cyclonic circulation, just off the southern coast of El Salvador. RWM and NORAPS6 did not form this low-pressure circulation.

Upper Air

This developing cyclone was also reflected in the 500 mb flow field. RAMS had up to a 12 m/s maximum speed around the 500 mb center, MM5 about 11 m/s, and GSM about 10 m/s. NORAPS6 and RWM had winds from the east to southeast at 5-8 m/s.

4.1.3.11 Statistical Results - Central America. Error frequency distributions were generated for temperature, surface pressure, dew point depression, wind speed below 20 knots, wind speed above 20 knots, and wind direction. Data from all forecast times, both November forecasts, and where appropriate, levels were merged. The central column corresponds to the desired error bounds. Two sets of figures were developed to describe the forecast results. One is a surface set that includes the large number of surface observations and the other is an upper air set that includes the more sparse upper air observations. Figures 4-31(a - f) are the surface results and Figures 4-32(a - e) are the upper air results.

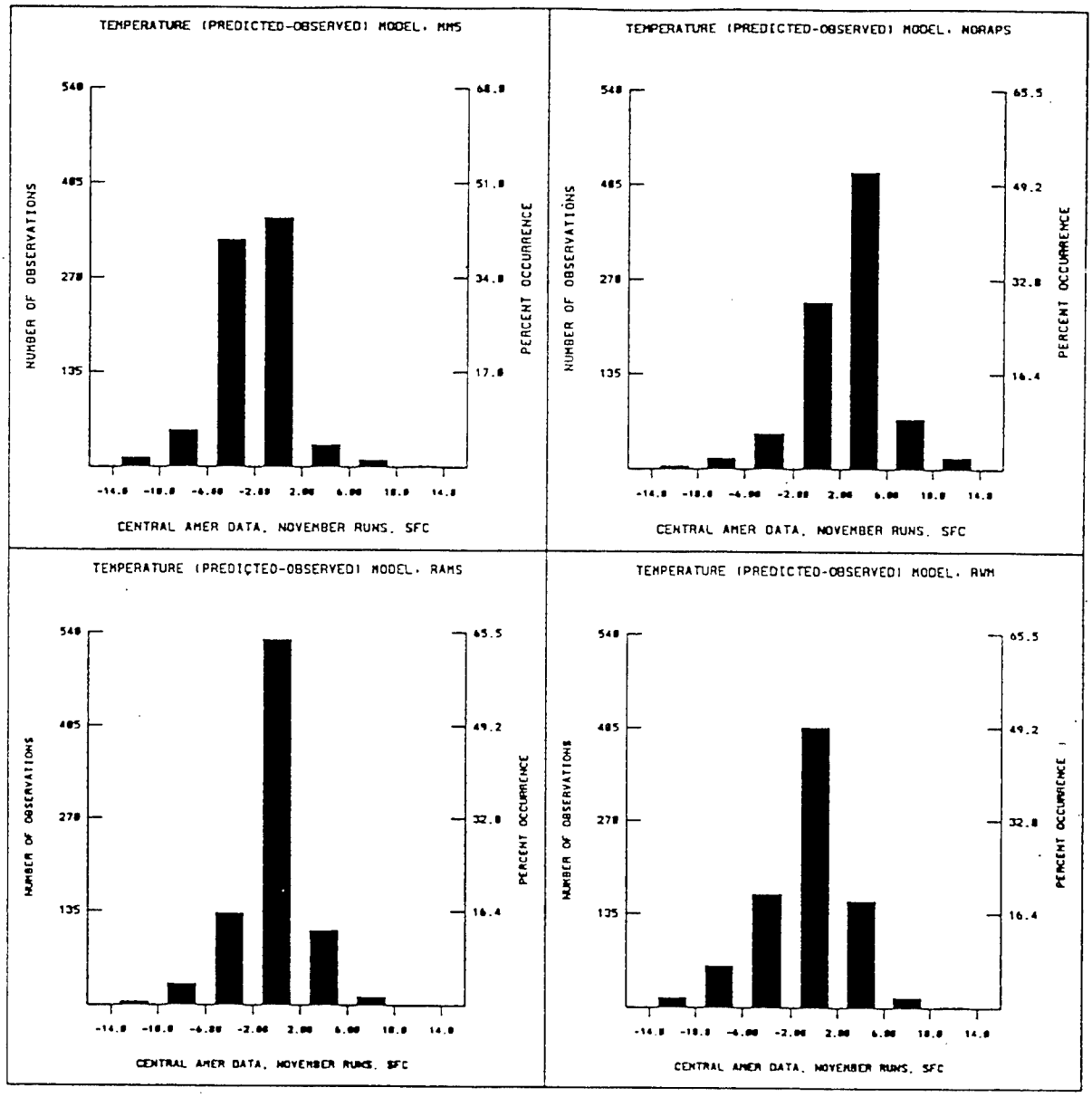

(a) Temperature

Figure 4-31. Surface error statistics, November -Central America.

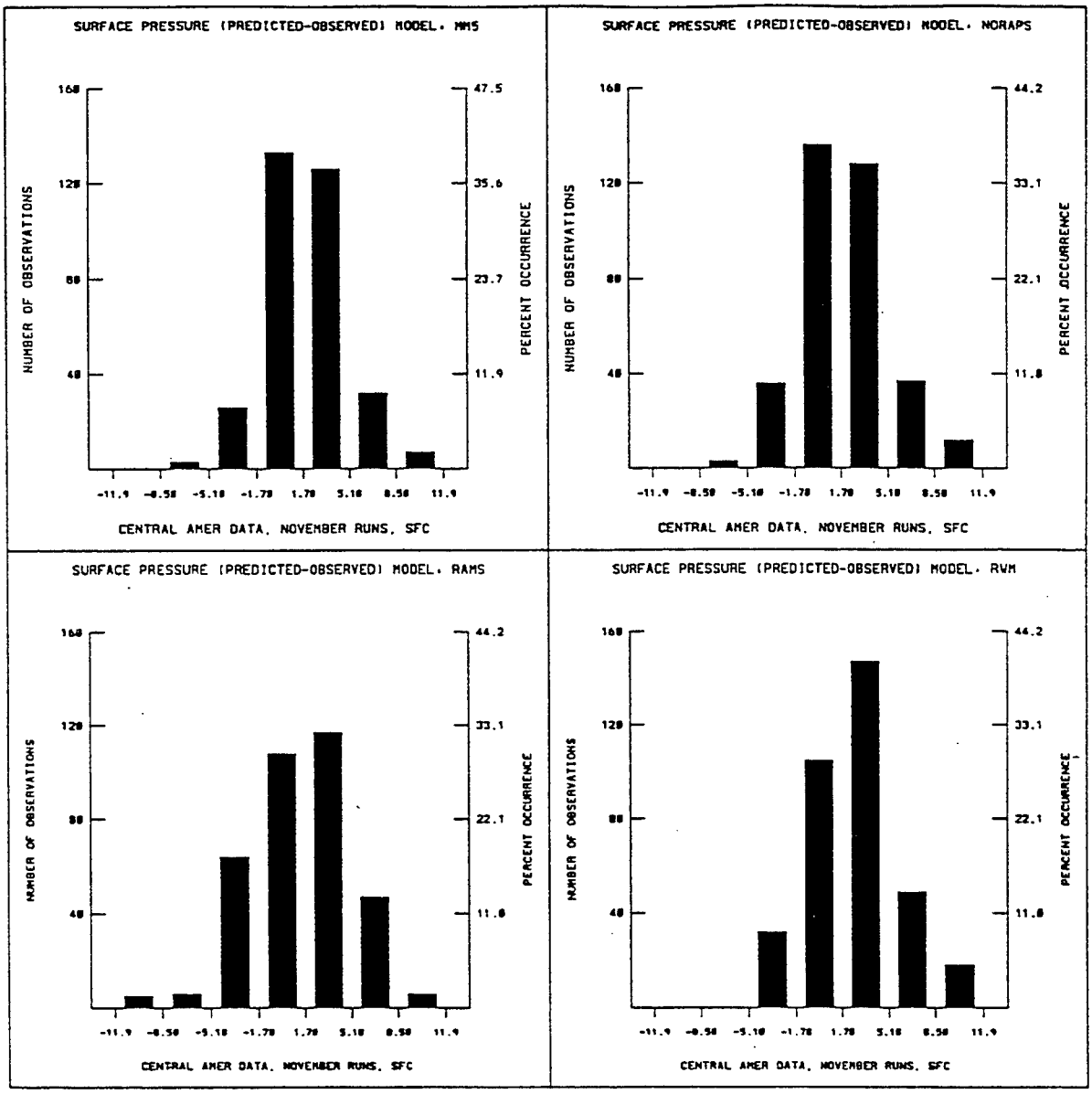

(b) Pressure

Figure 4-31. Surface error statistics, November -Central America. (Continued)

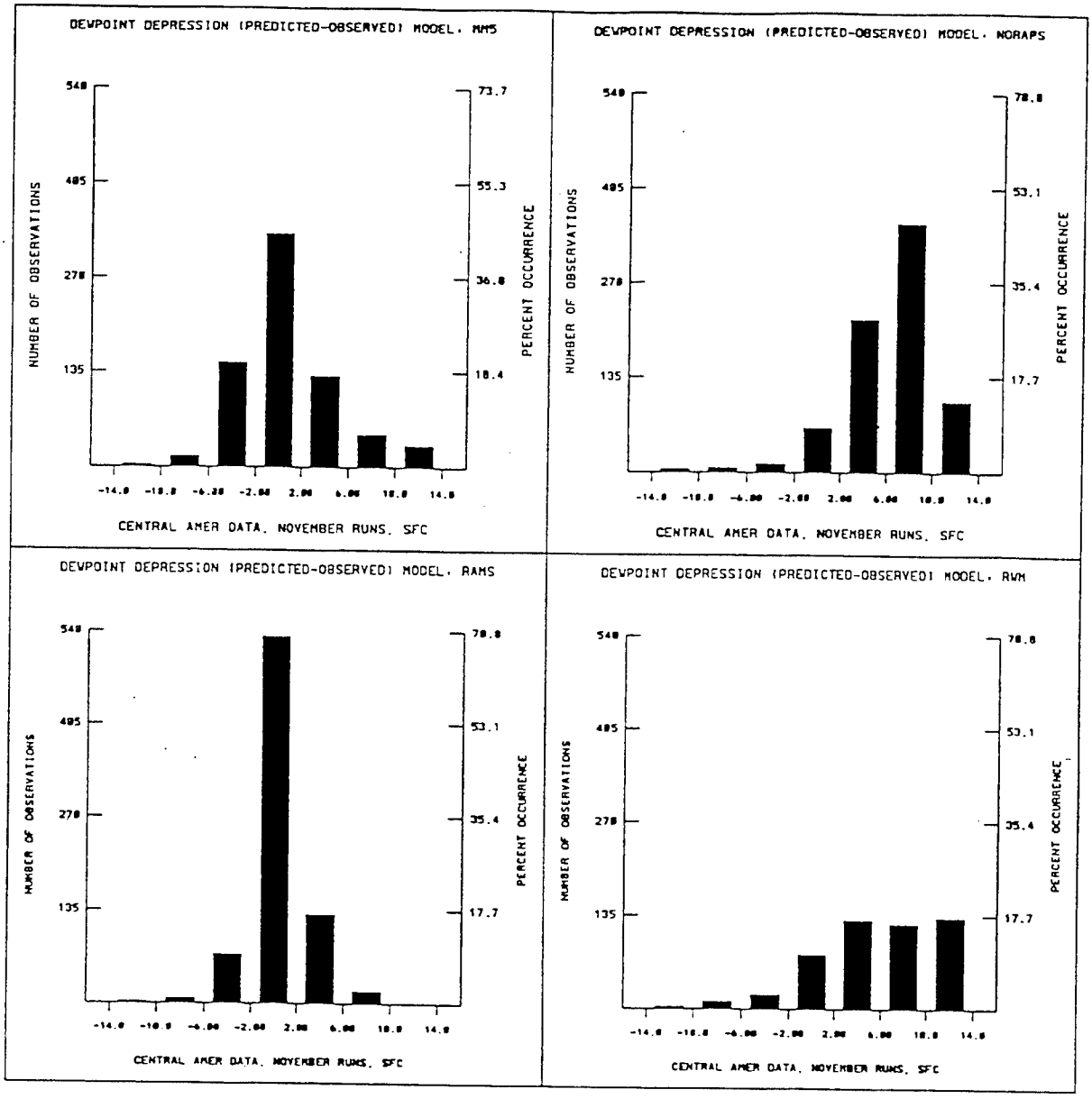

(c) Dew point depression

Figure 4-31. Surface error statistics, November -Central America. (Continued)

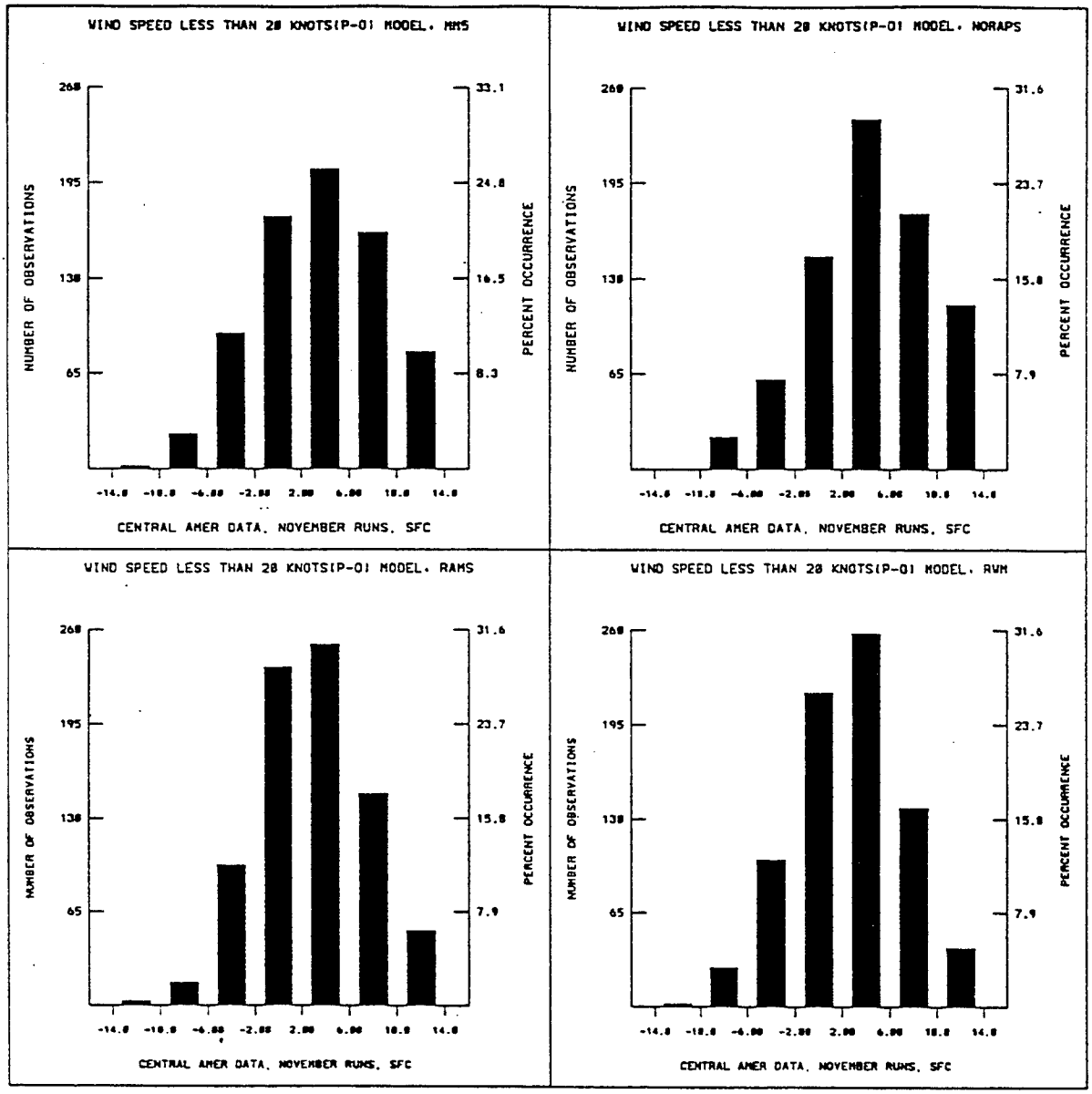

(d) Wind speed < 20 Knots

Figure 4-31. Surface error statistics, November -Central America. (Continued)

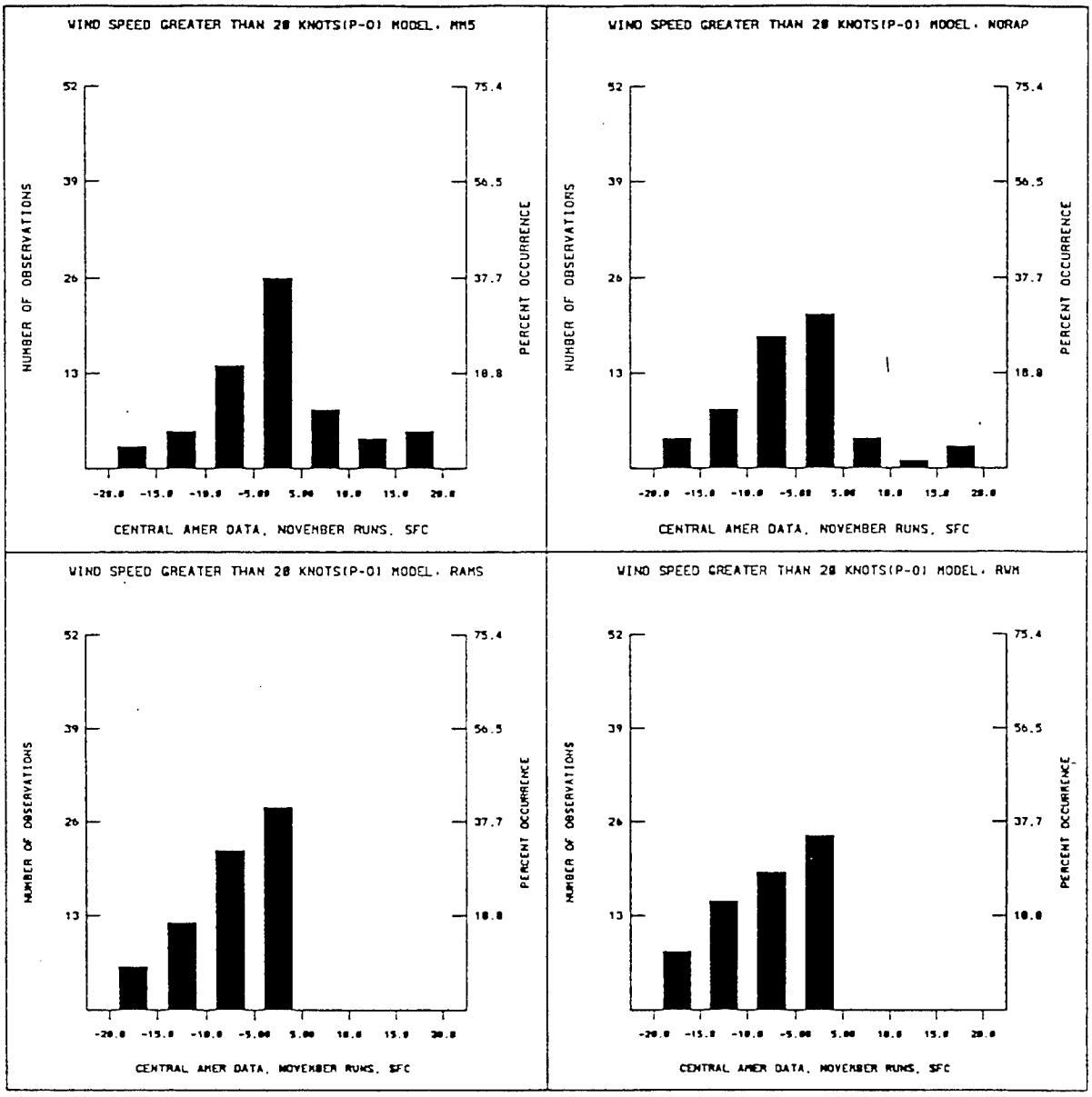

(e) Wind speed > 20 Knots

Figure 4-31. Surface error statistics, November -Central America. (Continued)

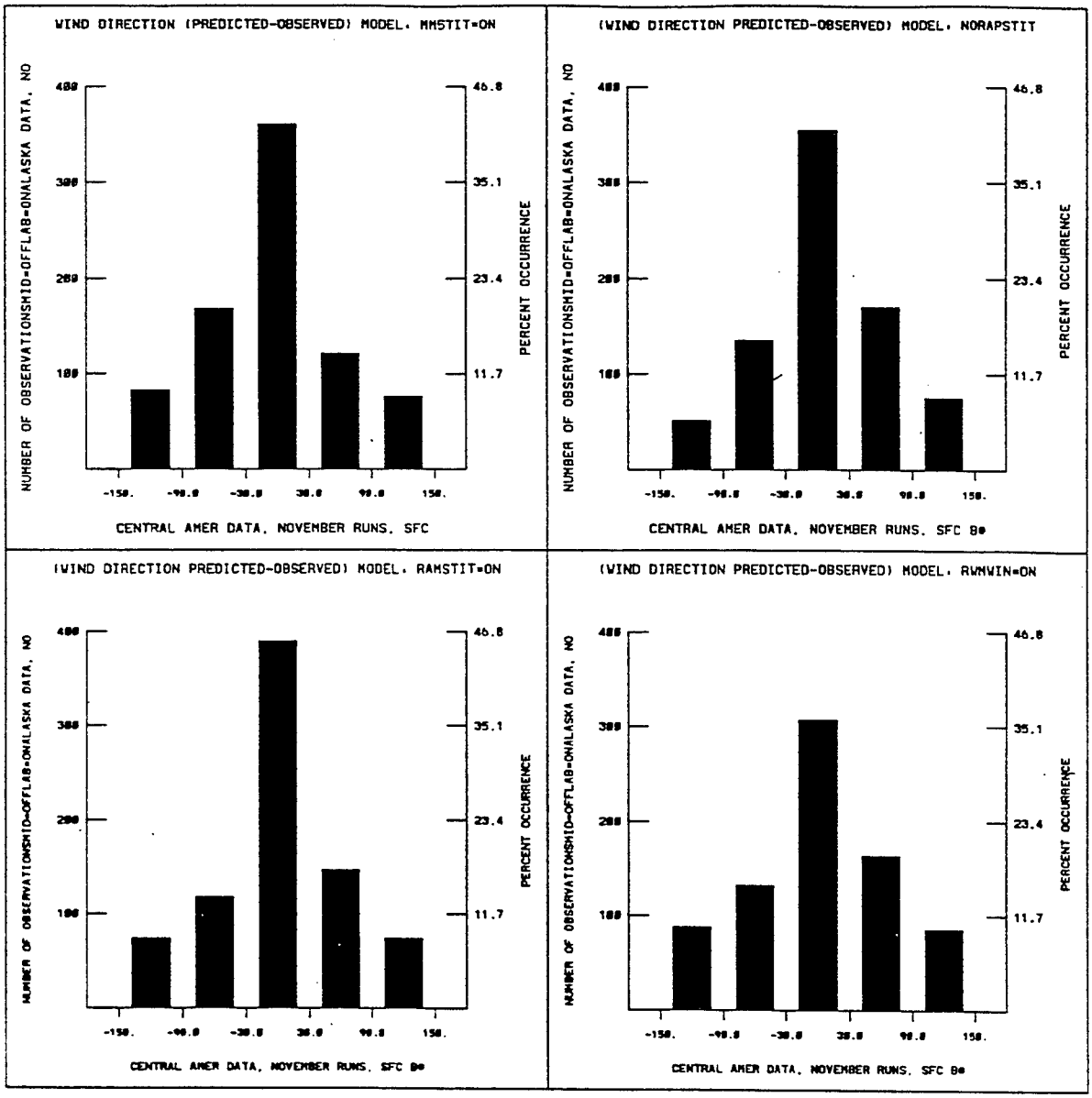

(f) Wind direction

Figure 4-31. Surface error statistics, November -Central America. (Continued)

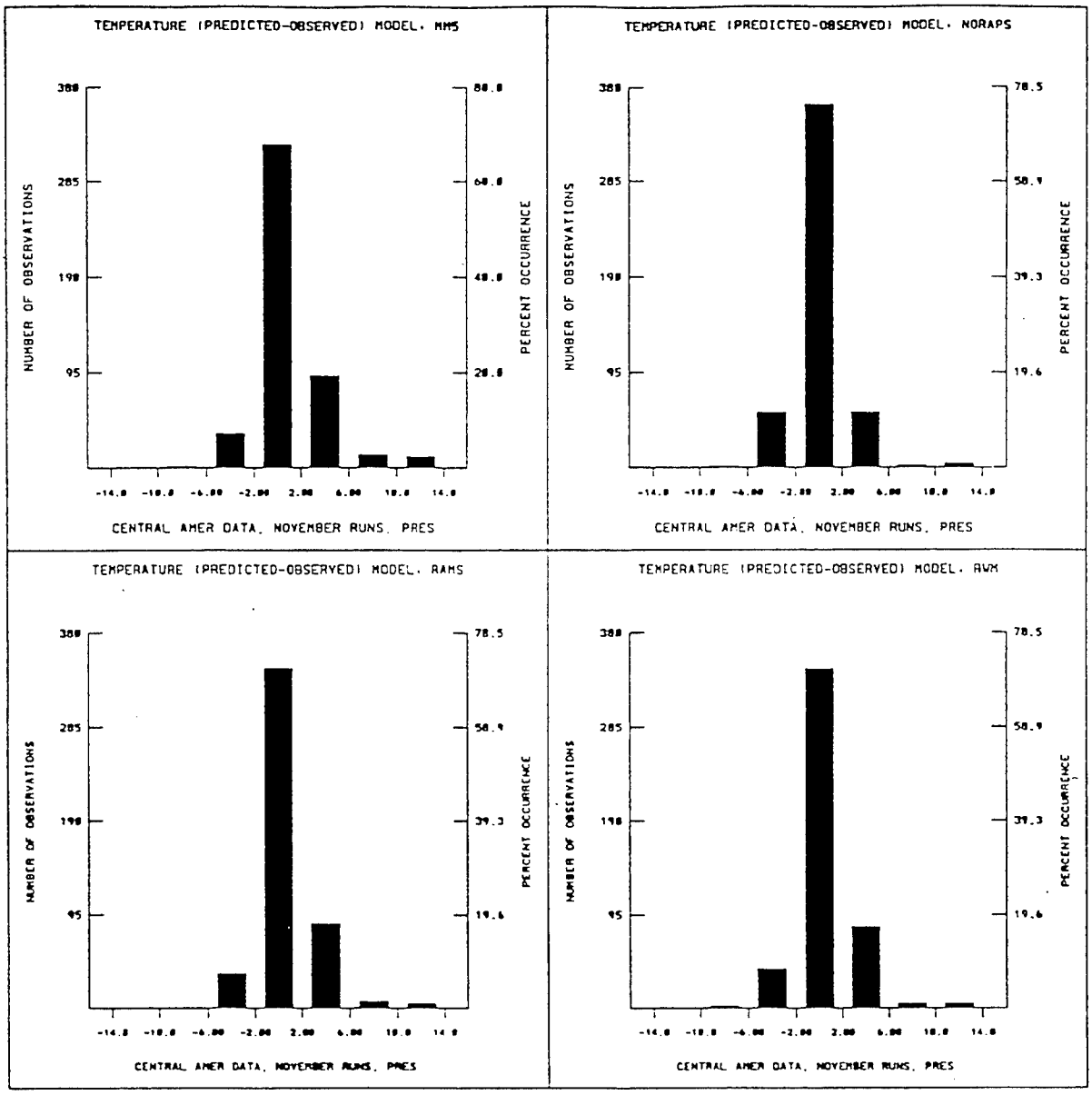

(a) Temperature

Figure 4-32. Upper air error statistics, November - Central America.

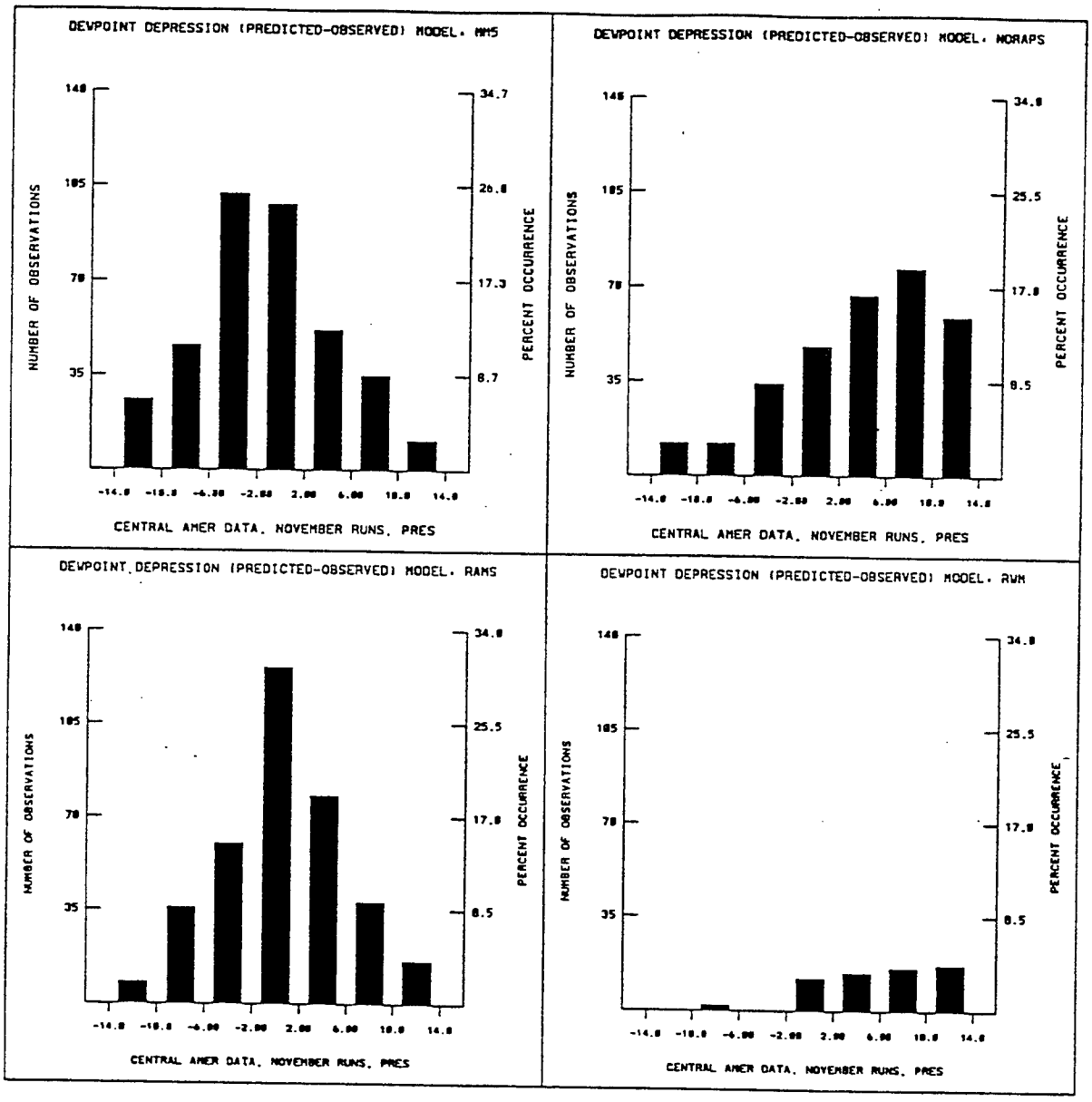

(b) Dew point depression

Figure 4-32. Upper air error statistics, November - Central America. (Continued)

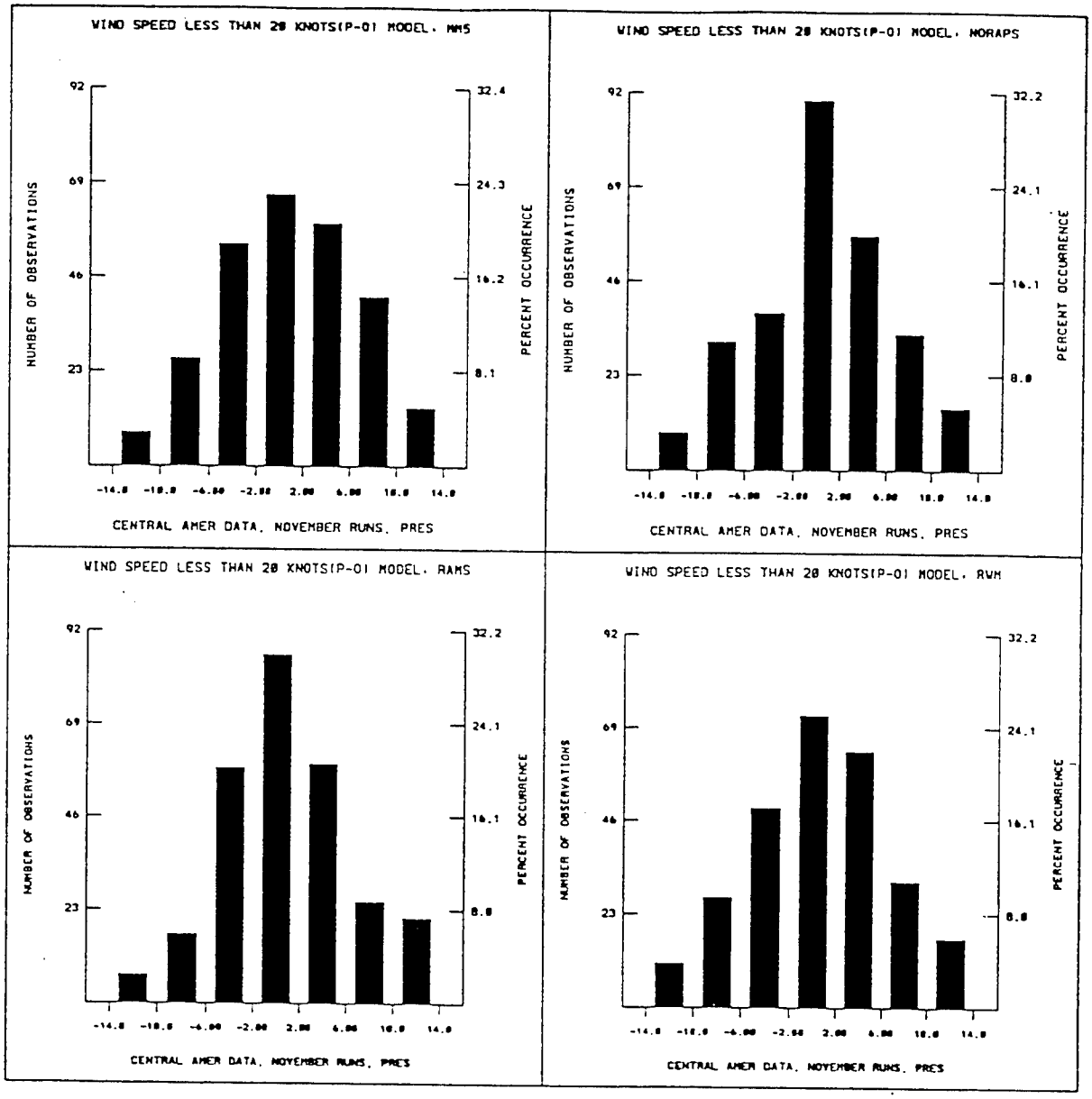

(c) Wind speed < 20 Knots

Figure 4-32. Upper air error statistics, November - Central America. (Continued)

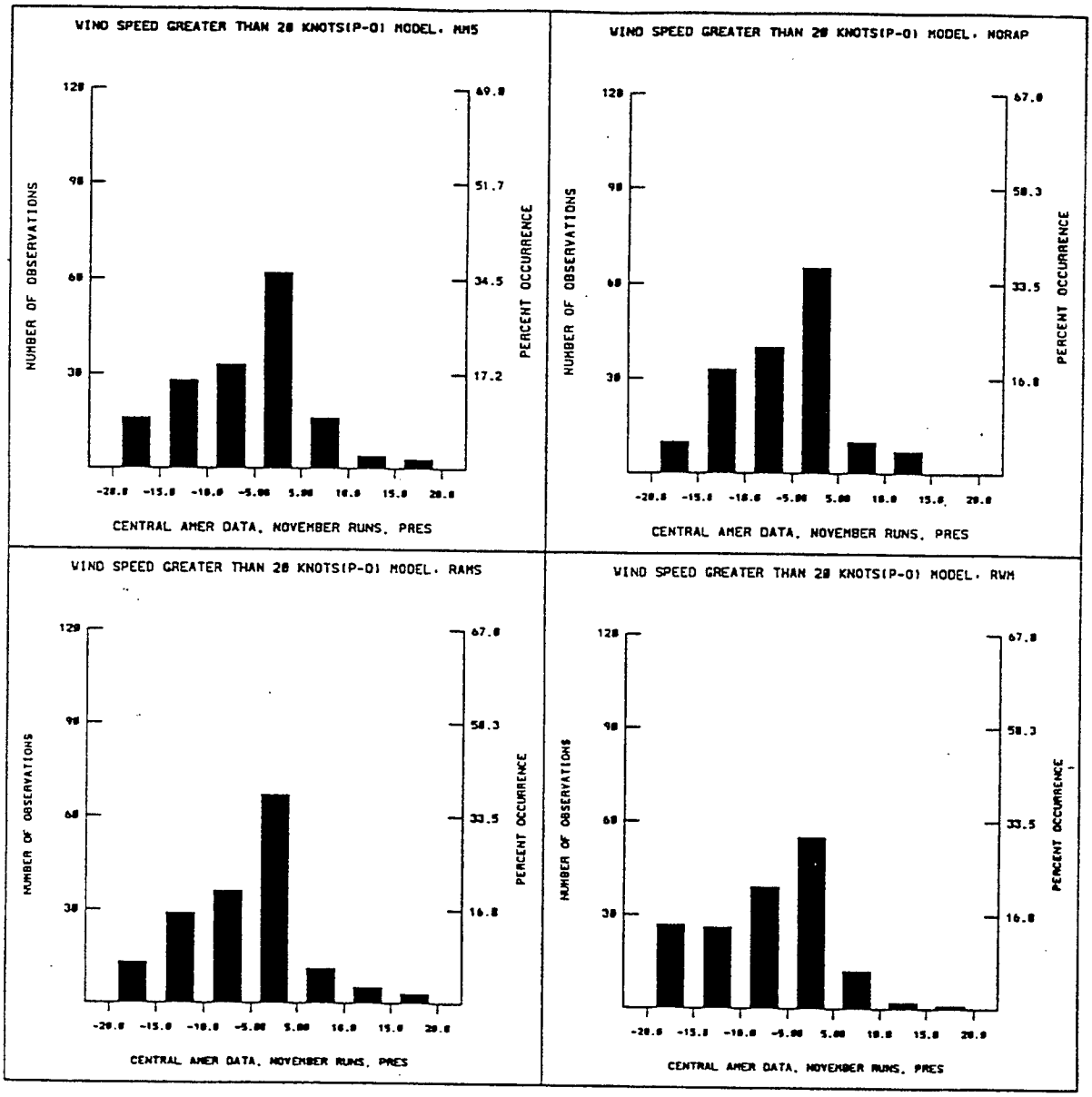

(d) Wind speed > 20 Knots

Figure 4-32. Upper air error statistics, November - Central America. (Continued)

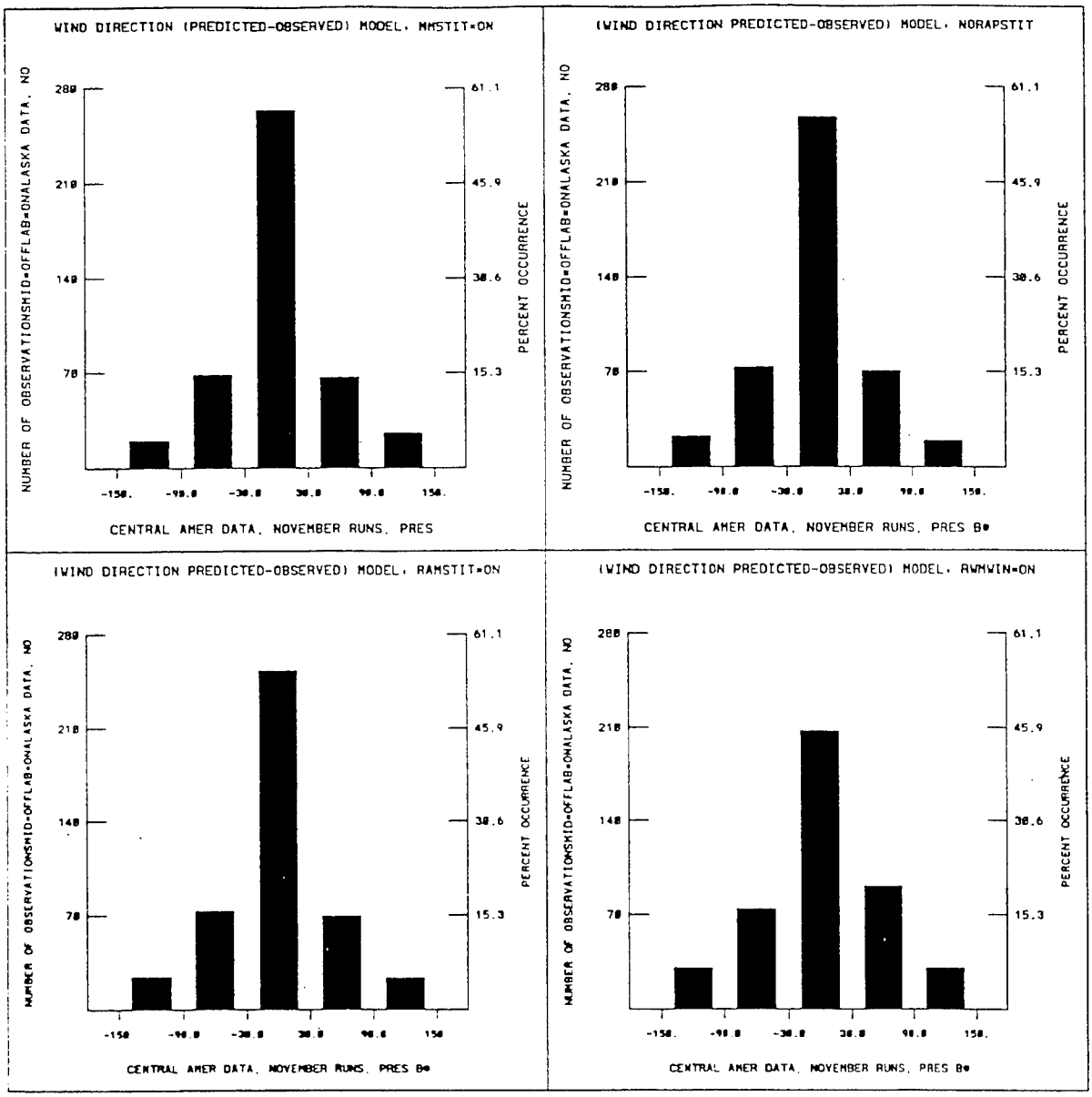

(e) Wind direction

Figure 4-32. Upper air error statistics, November - Central America. (Continued)

4.2 DATA DENIED IN KOREAN THEATER.

4.2.1 Objective.

This test explored each model's ability to provide a valid forecast when normally available observations cannot be obtained. Two possibilities will be considered. For data denied by enemy action, we will eliminate all surface and upper air data from North Korea and China. The second case will consider a communications failure and a single observation point. Upper air observation in Seoul will be used to initialize the forecast. These will be compared for all models with forecasts made with all the observation data and NMC data.

4.2.2 Description.

The 72 hour period from 1200Z, 27 Sep 93 to 1200Z, 30 Sep 93 was chosen due to the presence of an impressive cutoff low at 500 mb to the north of the Korean peninsula. This cutoff low traversed almost due east across northeast China from the eastern border of China and Mongolia to the coast, and was reinforced by another shortwave moving in the jet to the north at the end of the period. The upper level feature forced at least two cold fronts through the Korean peninsula; the first around 0000Z, 29 September and a second stronger front around 0000Z, 30 September.

4.2.3 Data Source.

NMC gridded data are contained within the NCAR data archives in ds082.0, tape Y17440. The rawinsonde data are in ds353.1, tape Y17946 while the surface observations at 0 UTC and 12 UTC are in ds464.0, tape Y17936.

4.2.4 Phenomenology Results - All Data.

In this calculation, all available surface and upper air data in the theater was used. It provides a comparison for the remainder of the denied cases.

Surface

The surface meteorology was dominated by a low-pressure system with a double center analyzed at 1004 mb to NNW of Korea and 1008 mb NE of Korea. RAMS predicted a single center of 1006 mb although it produced a lobe toward the region of the second center. MM5 also produced a single elongated center more closely coinciding with the analyzed center to the NE of Korea. NORAPS6 and MM5 did produce a dual center structure although RWM probably under-predicted the secondary center.

Upper Air

The 500 mb level geopotential field was dominated by the upper air support for the surface low. A strong closed-core circulation with an analyzed central height of 5310 m was located to the NNW of Korea. All models had a good location, with RAMS having a central height of 5400 m, MM5 5340 m, NORAPS6 5340 m, and RWM 5370 m.

4.2.5 Phenomenology Results - No data from China and North Korea.

For the data-denied run, the models' results were not very different from the full data run. All models showed similar behavior; the surface low was just slightly weaker as was the upper air circulation. This is an understandable behavior since there is more of a reliance on the smoother gridded pressure data in generating the initial and boundary conditions rather than using the additional observational data. Also,

because of the relatively coarse grid resolution used in these runs and the omission of even a large number of observations, as long as the gridded data is available, it is not as detrimental to the forecast results as compared to a run with higher grid resolutions. Figures 4-33(a - h) shows the surface pressure maps with all data and the same maps for the no data from North Korea and China. Corresponding maps of the geopotential height are shown on Figures 4-34(a - h). All data are for the forecast fields at 1200 UTC on 28 September 1993.

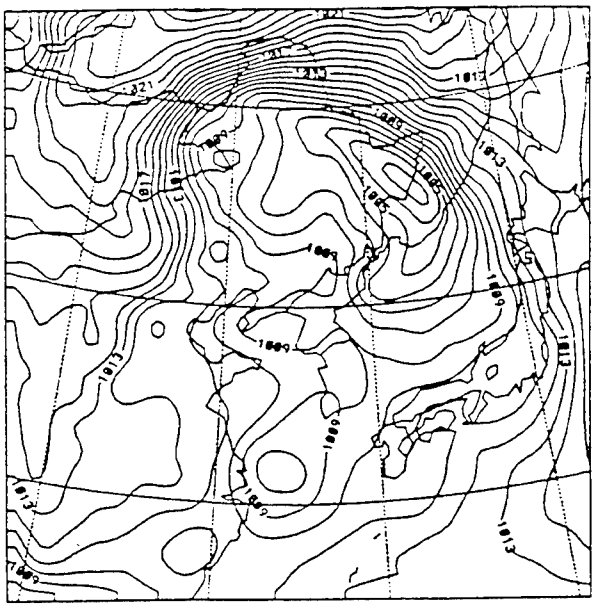

(a) MM5 - all data

Figure 4-33. Surface pressure - Korea.

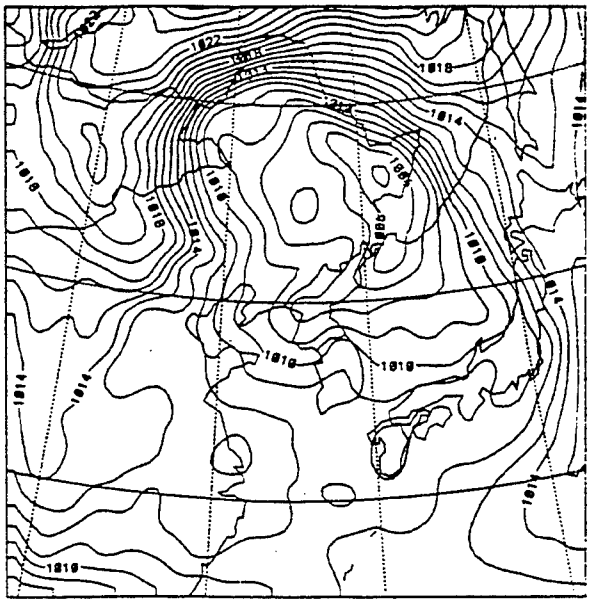

(b) MM5 - no data from North Korea and China.

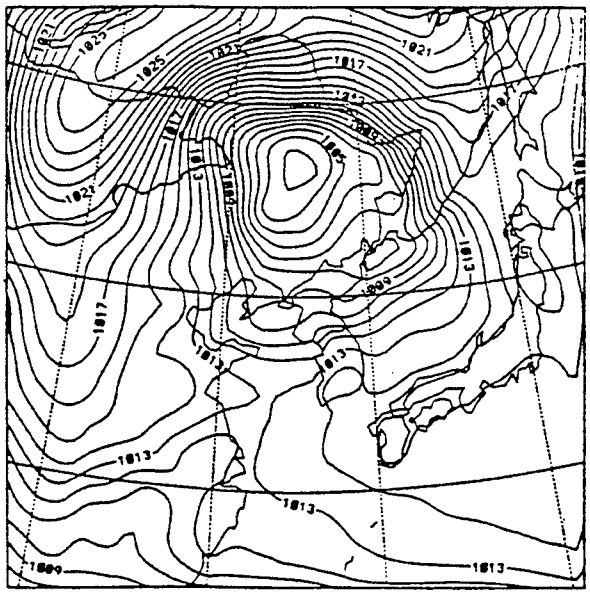

(c) NORAPS6 - all data

Figure 4-33. Surface pressure - Korea. (Continued)

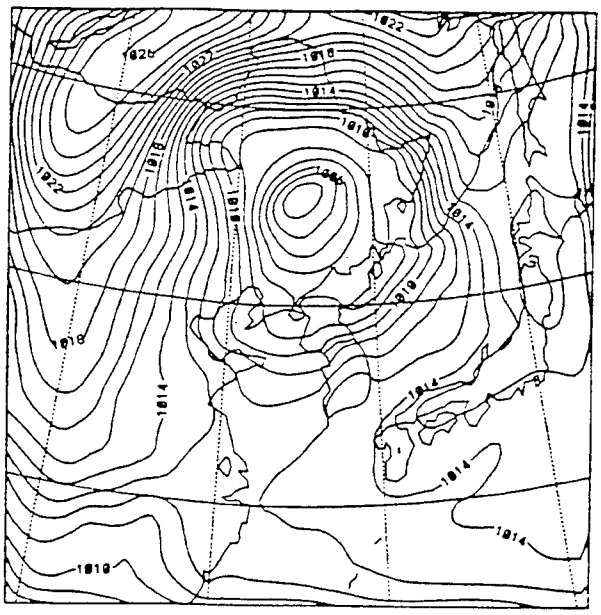

(d) NORAPS6 - no data from North Korea and China.

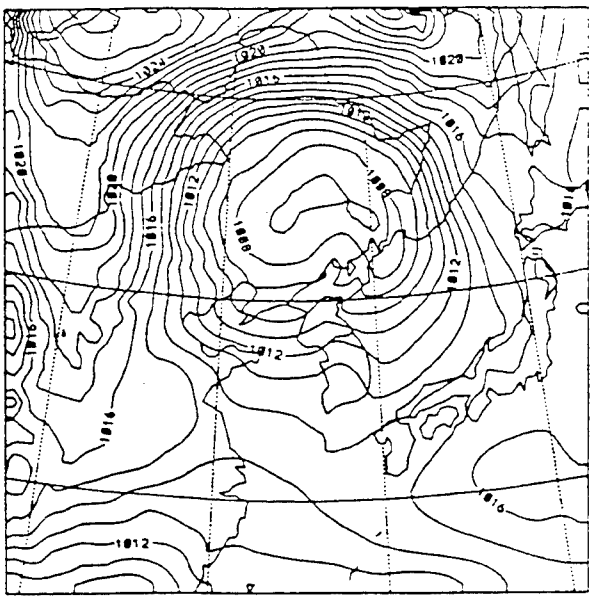

(e) RAMS - all data

Figure 4-33. Surface pressure - Korea. (Continued)

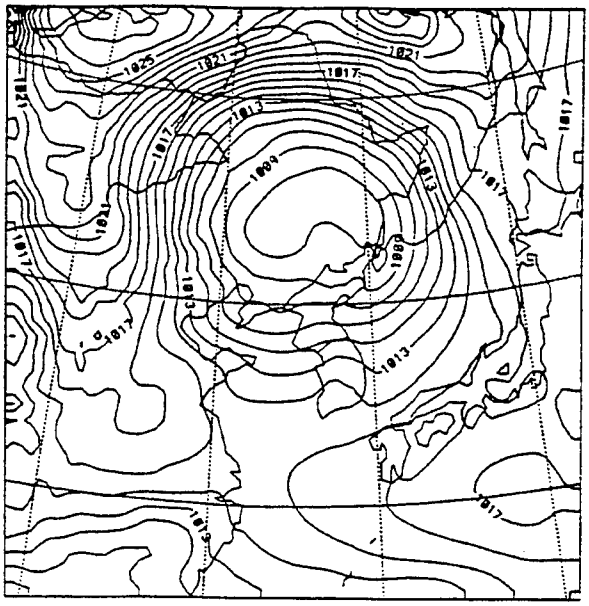

(f) RAMS - no data from North Korea and China.

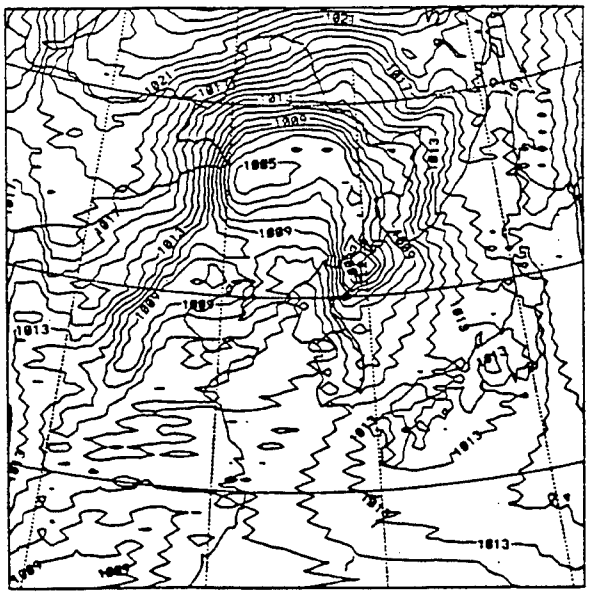

(g) RWM - all data

Figure 4-33. Surface pressure - Korea. (Continued)

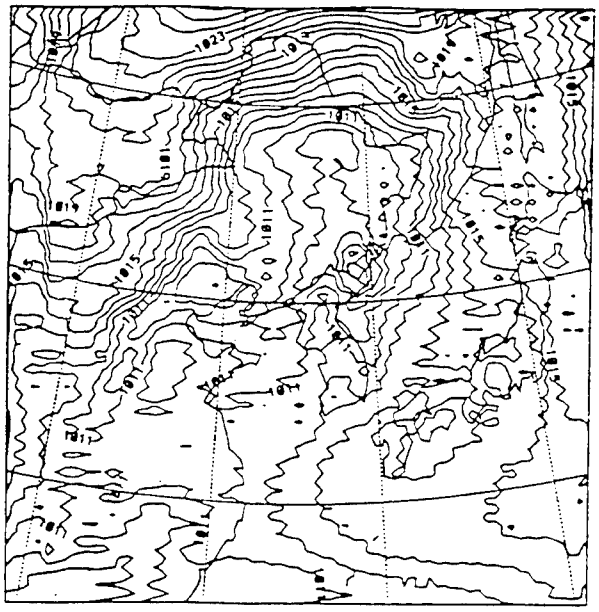

(h) RWM - no data from North Korea and China.

Figure 4-33. Surface pressure - Korea. (Continued)

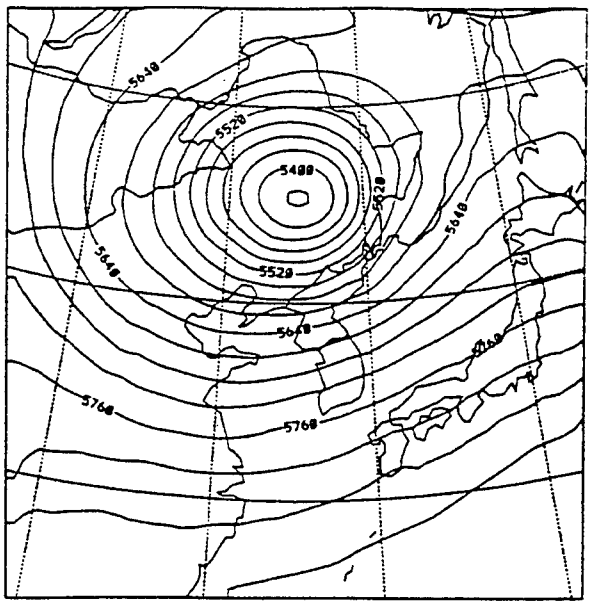

(a) MM5 - all data

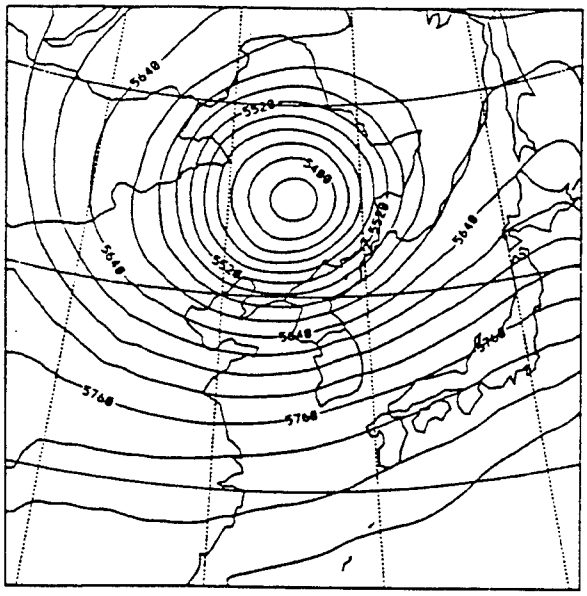

(b) MM5 - no data from North Korea and China.

Figure 4-34. Geopotential height - Korea.

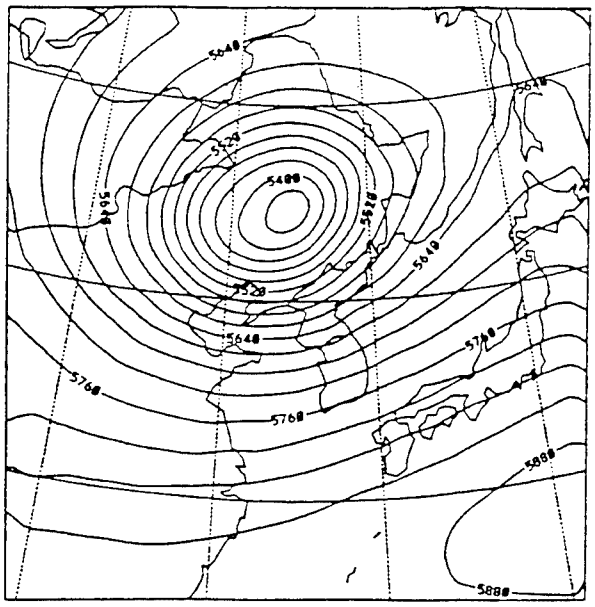

(c) NORAPS6 - all data

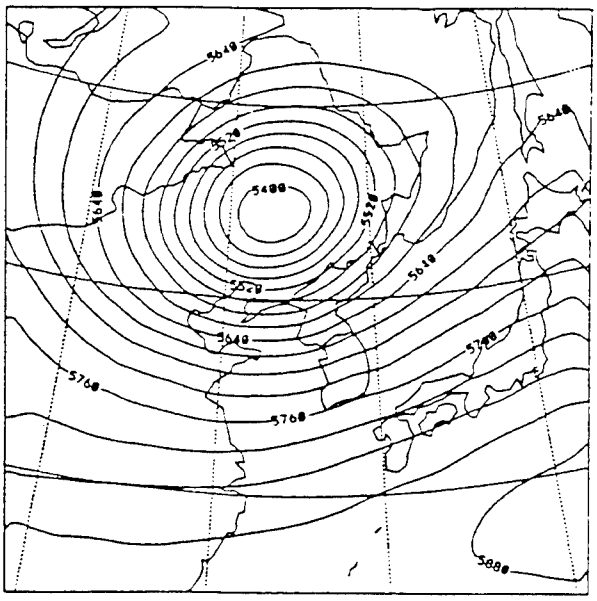

(d) NORAPS6 - no data from North Korea and China.

Figure 4-34. Geopotential height - Korea. (Continued)

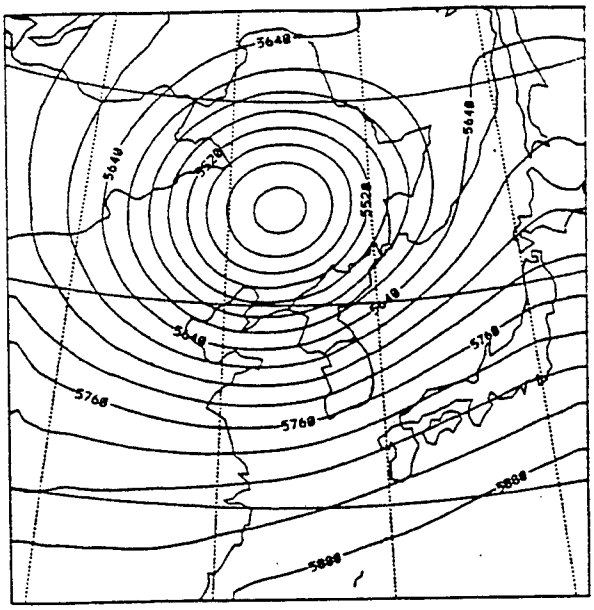

(e) RAMS - all data

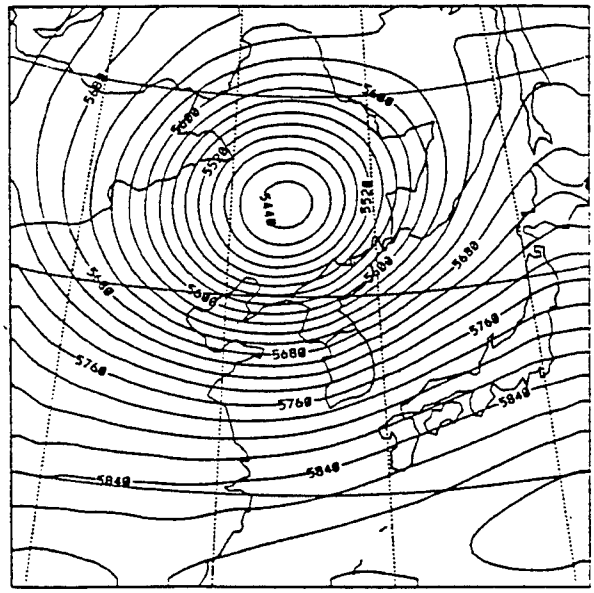

(f) RAMS - no data from North Korea and China

Figure 4-34. Geopotential height - Korea. (Continued)

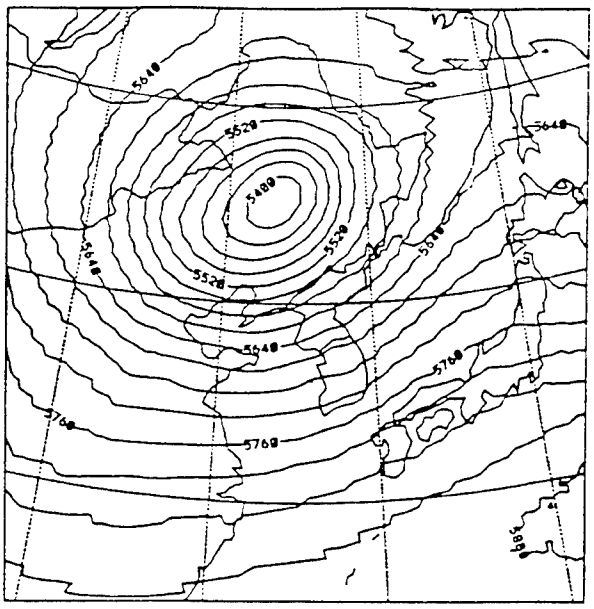

(g) RWM - all data

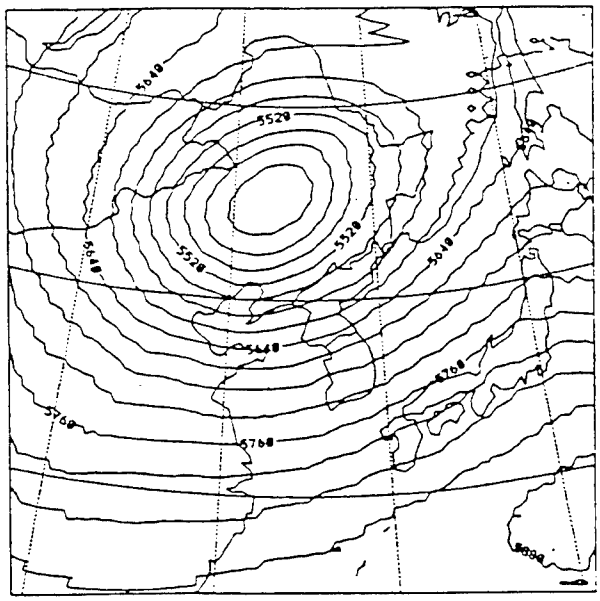

(h) RWM - no data from North Korea and China

Figure 4-34. Geopotential height - Korea. (Continued)

4.2.6 Phenomenology Results - Single Sounding Run.

As expected, the run with the single Seoul sounding showed, in a synoptically disturbed environment such as this, that a NWP model will be unable to produce a reasonable forecast if initialized from a limited observation set. If the meteorological situations were less disturbed and the main flows were physiographically forced, the NWP model would have a better chance.

RAMS was the only model that had a standard option to make a run with a single sounding. For the remaining models, we generated a horizontally homogeneous pressure data file from the Seoul sounding and allowed their regular data analysis procedure to process the data. However, this produces a large imbalance with the initial winds and pressure fields in the three models. Because RAMS has an option for this type of run, it has a feature that assumes an initial geostrophic balance between the winds and pressure. The other models spent the majority of the run attempting to adjust to the initial imbalance.

4.3 OBJECTIVE OR ENHANCED TESTS.

4.3.1 Objective.

Requirements for the TFM specify an objective resolution of 6 nmi. Forecast models are sensitive to the resolution used and should produce a "better" forecast at finer scales. These tests demonstrate each model's sensitivity to scale and indicate whether the forecasts will improve at a finer scale.

4.3.2 Description.

The objective model resolution of 6 nmi was investigated with MM5, RAMS, and NORAPS6 using the nested grid configurations of these models. For the Central America (focusing on Panama) and the Middle East (focusing on Kuwait/Iraq) regions, we configured these models in a 2-grid configuration with the finer grid spacing at approximately the 6 nmi objective. RAMS allows for a user-selectable spacing ratio between the grids, so it would be possible to take the coarse grid as the 25 nmi grid used in the threshold tests and use a 4-1 grid space ratio. However, both MM5 and NORAPS6 allowed only a 3-1 grid space ratio. Therefore, we reconfigured a coarse grid domain with an 18 nmi spacing and ran all models with a nested grid at a 3-1 grid space ratio. Because of the finer spacing, we will use approximately 98x98 grid points on the coarse grid to cover the 1500 x 1500 nmi domain. By covering the same domain as the threshold runs, we provided for an additional sensitivity comparison for these models to test a 28 percent reduction in grid spacing. Nested grids were run with 71 x 71 grid points.

4.3.3 Data Source.

This remains the same as the first period of August 94 Threshold Tests.

The main differences in a model run between 25 and 6 nmi grid spacing was the ability to resolve the physiographic forcing (topography, land-use, coastline, etc.). The August period was expected to be the best period for sea breeze formation, thus testing several aspects of the models' physics (radiation, land-use, etc.) directly without the potentially stronger synoptic forcing of the November 1994 period.

4.3.4 Phenomenology Results.

The objective runs used an 18 nmi coarse resolution domain over the same area as the threshold run for the Central American and Middle Eastern domains for the run beginning on 16 August 94 0000 UTC run. A nested grid of 6 nmi spacing was placed over Panama and the Persian Gulf regions. NORAPS6 and RAMS were run in this manner, but we were unable to successfully start a run with MM5, even after

consultation with the developers at NCAR. Therefore, the following discussion will only pertain to RAMS and NORAPS6.

4.3.4.1 Middle East. The surface flow field over the Persian Gulf was simulated quite differently with RAMS with the higher resolution grid. While the flow in the objective run was about 3 m/s from the NE, RAMS produced 2 m/s flow from the SE along the SW Gulf coast. NORAPS6 did not show this variability, producing NW winds in both runs. Figure 4-35 presents the grid relationship. Figure 4-36a is a map of the NORAPS6 predicted winds in the 25 nmi threshold calculation and Figure 4-36b is in the 6 nmi nested grid. Figures 4-36(c and d) present the same data for RAMS.

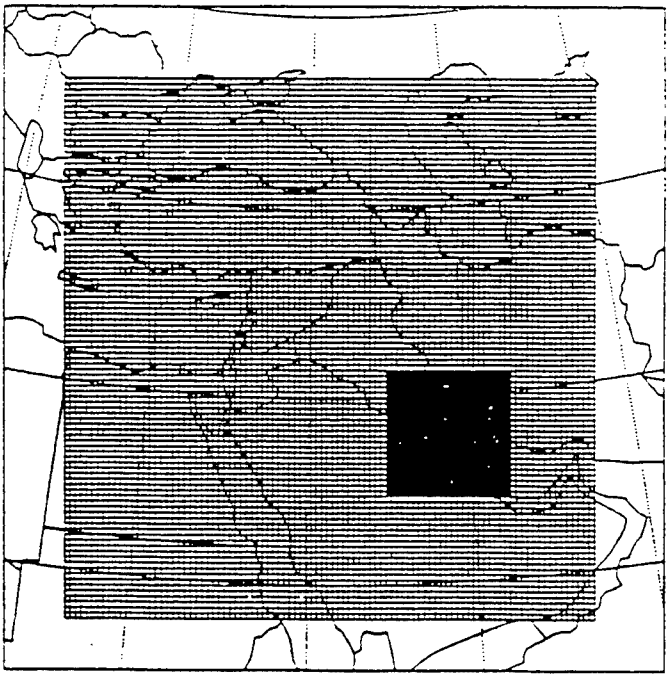

Figure 4-35. Middle East - full and nested grids.

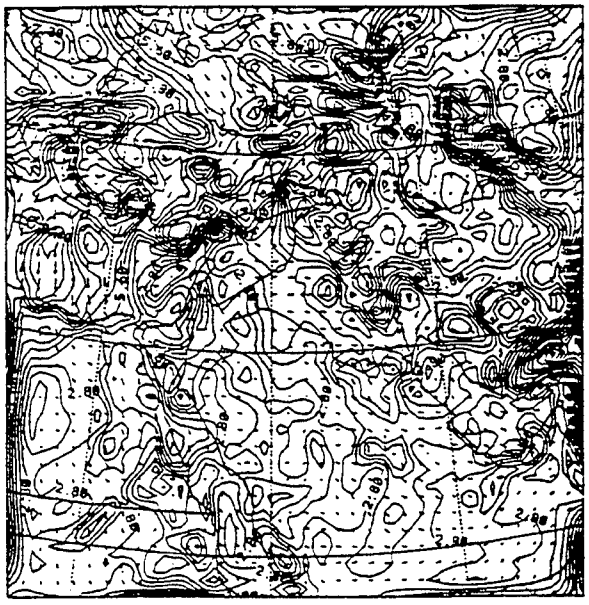

(a) NORAPS6 - 25 nmi grid spacing

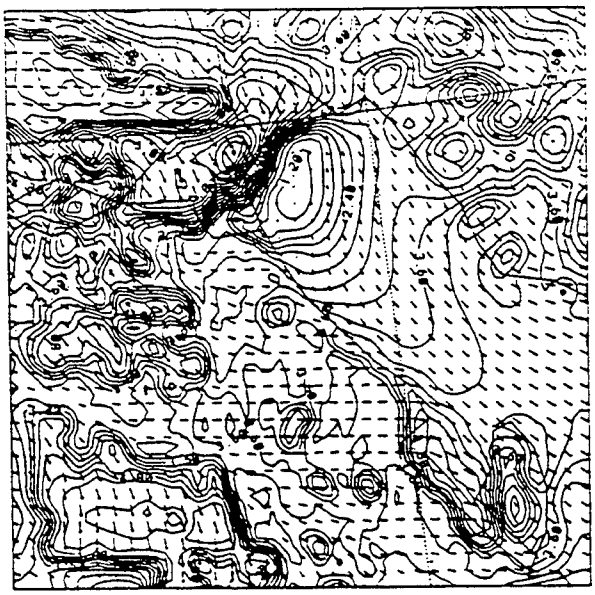

(b) NORAPS6 - 6 nmi grid spacing

Figure 4-36. Surface Winds - Middle East.

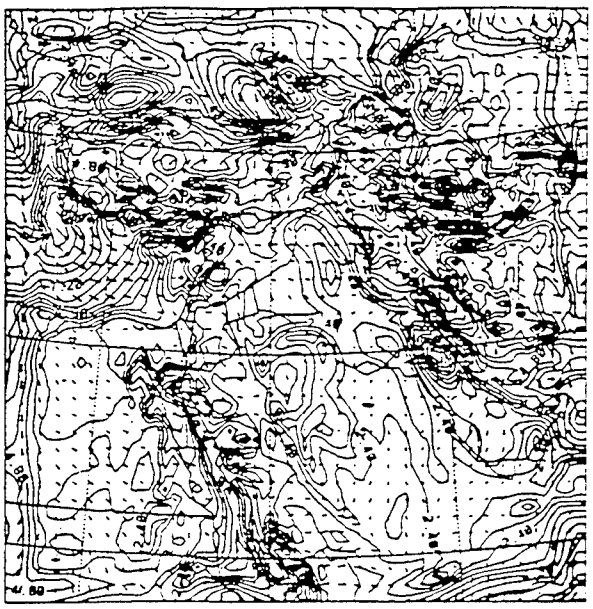

(c) RAMS - 25 nmi grid spacing

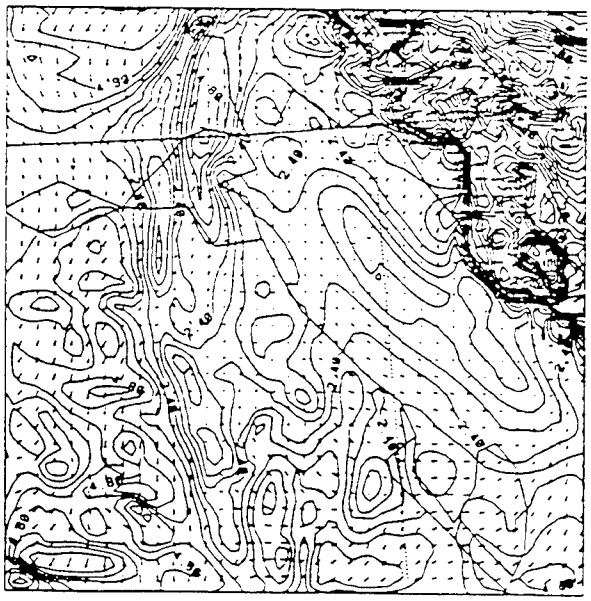

(d) RAMS - 6 nmi grid spacing

Figure 4-36. Surface Winds - M[illegible] East. (Continued)

4.3.4.2 Central America. The higher resolution of the nested grid did a much better job of capturing a sea breeze circulation than the previous coarser resolution runs. While NORAPS6 in the earlier runs did not have a sea breeze convergence zone along the southern Panama coast, the objective run produced a well-defined zone. RAMS also produced a convergence zone with slightly more local variability than NORAPS6. The coarse grid fields except in the area of the nested grid were not significantly different between the 18 nmi used here and 25 nmi runs used for the threshold tests. Figure 4-37 presents the grid relationship. Figure 4-38a is a map of the NORAPS6 predicted winds in the 25 nmi threshold calculation and Figure 4-38b in the 6 nmi nested grid. Figures 4-38(c and d) present the same data for RAMS.

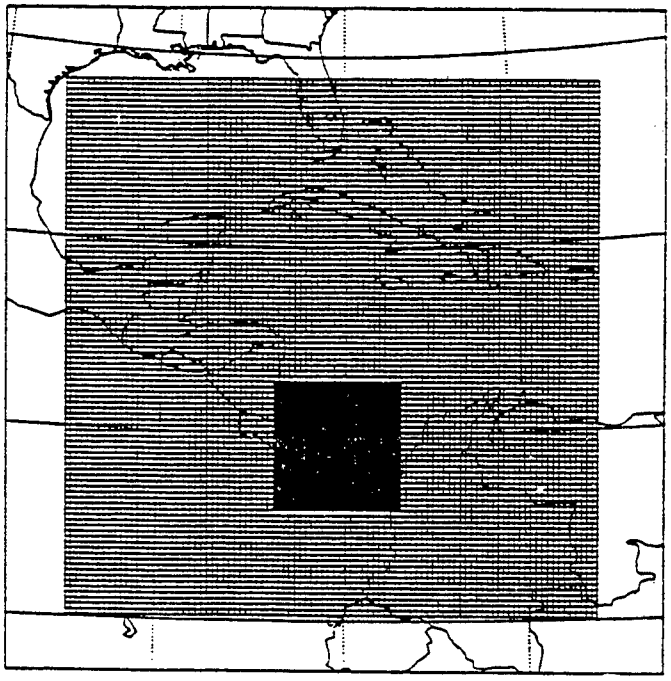

Figure 4-37. Central America - full and nested grids.

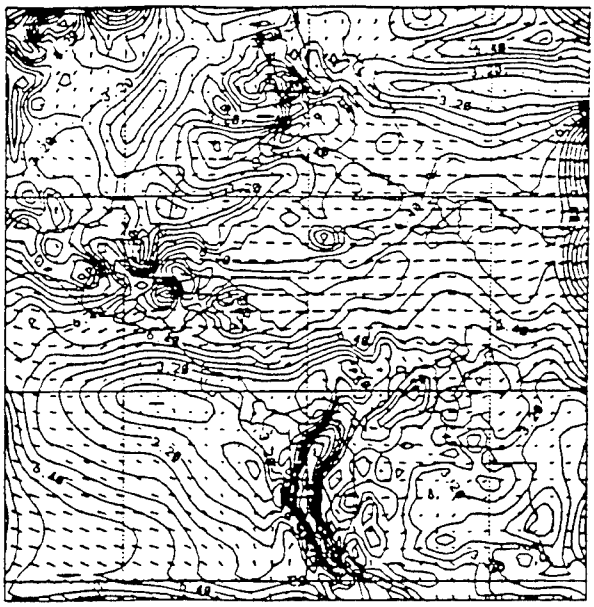

(a) NORAPS6 - 25 nmi grid spacing

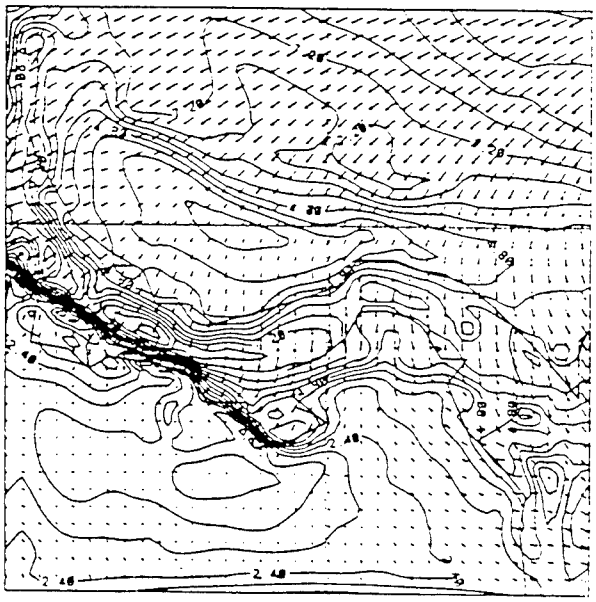

(b) NORAPS6 - 6 nmi grid spacing

Figure 4-38. Surface Winds - Central America.

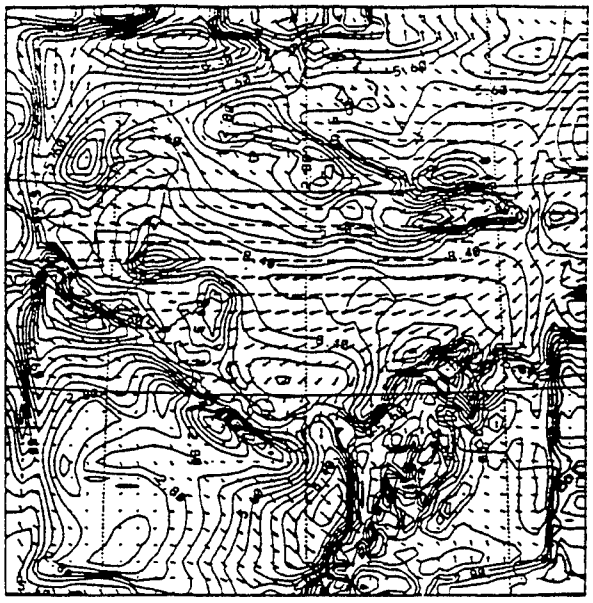

(c) RAMS - 25 nmi grid spacing

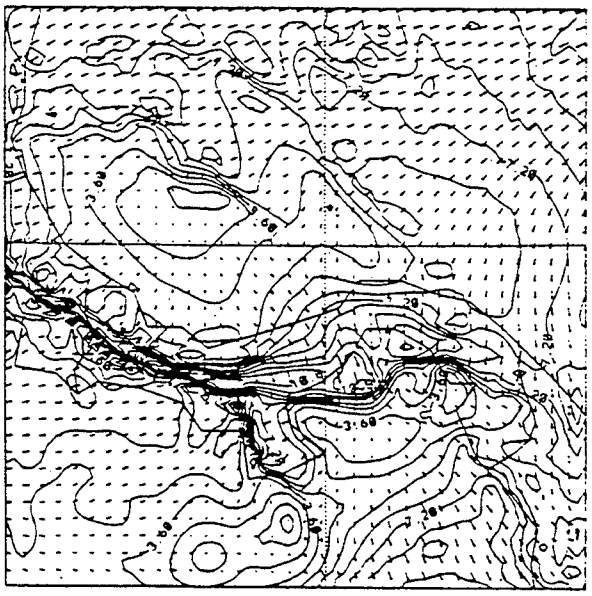

(d) RAMS - 6 nmi grid spacing

Figure 4-38. Surface Winds - Central America. (Continued).

SECTION 5
MODEL COMPARISON SUMMARY

The previous sections presented voluminous model results produced to make detailed comparisons of the four models. However, the shear volume of the data makes drawing conclusions difficult. To facilitate these comparisons several generalized procedures are developed. In this section we develop and provide this summary model comparison data.

5.1 RANK SCORING.

We have carefully reviewed the entire set of statistics. From casual inspection of those statistics it is difficult to identify a clear trend. However, we have applied a simple rank scoring methodology that does identify a clear result from the morass of detailed statistics. This rank scoring is applied to the threshold cases and not to the data denied or objective excursions. Merging the excursions into the other data would add an unnecessary level of complexity.

Rank scoring is a particularly convenient way for assessing the relative performance of each model over the diverse set of quantities that each model produces. For example, we can compare each model's predictions of surface pressures, temperatures, dew points, and wind speeds and directions with available observations and obtain quantitative error measures for each of those quantities individually. However, we also need to combine the error measures for these physically distinct quantities into a single overall measure of model performance. It is not a priori obvious, for example, how to combine an error in temperature with an error in wind direction.

Because one of our primary concerns is determining the overall performance of each model relative to all of the other models, rank scoring provides a useful and powerful tool for combining all the diverse error measures into a single performance measure for each model. We apply rank scoring by computing each model's error for each available observation. For each observation we rank all four models: the model with the smallest error is ranked 1, that with the next lowest error is ranked 2, etc. Then we examine all these accumulated rankings and, for each model, we determine how many times it ranked number 1, how many times it ranked number 2, etc.

For this model comparison, we considered only the extreme rankings: how many times each model was the best (i.e. ranked number 1) and how many times it was the worst (i.e. ranked number 4). Focusing on the extremes will help identify any model that is particularly outstanding or particularly poor. If all four models were of similar quality, we would expect the one that was best and the one that was worst for any individual observation would be largely a matter of chance. Therefore, each model would be "Best" about 25 percent of the time and "Worst" about 25 percent of the time. If a model is "Best" significantly more than 25 percent of the time or "Worst" significantly less than 25 percent of the time, then that model would be judged to be significantly better than the others. Note that rank scoring is like a zero-sum game—if one model is "Best" significantly more than 25 percent of the time then, on average, the other three models must be "Best" significantly less than 25 percent of the time.

We applied rank scoring by determining which one had the smallest RMS error for each observation. This approach rates each model's general performance without regard to the accuracy requirements for the various quantities. Our scoring system uses three of the statistics that we generated for each time, variable, and level:

1. Temperature RMSE

2. Relative humidity RMSE
3. Wind RMSVE

For each case we ran, we rank-ordered the four models from which one did best to which one did worst for each of these three statistics. Then we tabulated for each model the total number of times it gave the best result and the total number of times it gave the worst result. We combined results for verification times of 0, 12, 24, and 36 hours and two 36 hour runs for each season. This data is summarized in Table 5-1.

Table 5-1. RMS rank ordering.

Case	Theater	Scores								
		MM5		NORAPS6		RAMS		RWM		Total
		Best	Worst	Best	Worst	Best	Worst	Best	Worst	
1	Continental United States	74	21	19	86	117	7	22	118	232
2	Alaska	65	52	33	51	143	15	23	146	264
2	Korea	36	135	26	57	177	5	25	67	264
2	Middle East	22	187	34	27	168	9	40	41	264
2	Central America	29	93	27	93	169	5	39	73	264
3	Alaska	55	38	44	34	145	19	20	173	264
3	Korea	73	45	49	71	122	26	20	122	264
3	Middle East	54	46	56	39	113	25	23	136	246
3	Central America	72	40	34	45	95	37	32	111	233
	Total	490	657	322	503	1249	148	244	987	2295

5.2 SATISFYING AWS CRITERIA.

The previous comparison provides a means of comparing the model's performance but does not provide a measure of how well the predictions agreed with the observed data. This is accomplished in this section by comparing the forecast data to the observations and determining the number of times the predicted value was within the error criteria of the observed value. The previously developed weather data accuracy criteria are repeated in Table 5-2. These criteria were used as a measure of each model's forecast skill. Initially, all quantities were grouped together for each case and region to provide a net total of how often each model satisfies criteria as was done in the previous comparison.

Table 5-2. Data accuracy.

Parameter	Criteria
Temperature	2°C
Dewpoint Depression	2°C
Wind Speed	
less than 10 meters/sec	1 meter/sec
greater than 10 meters/sec	*2.5 meters/sec*
Wind Direction	30 degrees
Sea Level Pressure	1.7 millibars

5.2.1 Performance by Theater.

Table 5-3 expresses each model's performance as the percentage of times that its predicted value is within the error bounds specified.

Table 5-3. Predictions within criteria (see Table 5-2) by theater.

	Model	MM5	NORAPS6	RAMS	RWM	
Case	Theater	Percent	Percent	Percent	Percent	Observations
1	Continental United States	61	52	64	48	24971
2	Alaska	60	53	64	46	4855
2	Central America	46	44	57	48	6231
2	Korea	45	44	56	46	31427
2	Middle East	34	40	49	40	11392
3	Alaska	52	45	59	38	6056
3	Central America	48	38	58	40	4620
3	Korea	46	38	46	38	20961
3	Middle East	43	39	48	36	7114
	Total	49	44	55	43	117627

RAMS consistently produced better results for the criteria in areas other than the Continental United States. There are potentially several reasons for these differences. One reason could have been the skill of the analysis routine used to develop the initial gridded fields from the observations. The next analysis was accomplished to test this hypothesis.

5.2.2 Performance by Forecast Hour.

In this section, the relative performance by forecast hour is examined. The stratification was done only by hour, not by region/hour. The relatively large number of surface observations, compared to upper air observations was responsible for developing two tables. Table 5-4 presents the surface comparison and Table 5-5 the upper air comparison for each forecast period.

Table 5-4. Surface predictions within criteria (see Table 5-2) by forecast time.

		MM5	NORAPS6	RAMS	RWM	
Parameter	Forecast Time	%	%	%	%	Total Observations
Temperature	0 hour	65	38	66	30	3800
Dewpoint Depression	0 hour	35	9	59	21	3733
Wind Speed <10	0 hour	73	27	67	47	3735
Wind Speed >10	0 hour	88	60	100	84	129
Wind Direction	0 hour	54	35	53	39	3864
Pressure	0 hour	63	65	46	44	2080
Temperature	12 hour	32	35	42	29	3784

Table 5-4. Surface predictions within criteria (see Table 5-2) by forecast time (Continued).

Parameter	Forecast Time	MM5 %	NORAPS6 %	RAMS %	RWM %	Total Observations
Dewpoint Depression	12 hour	40	29	39	32	3722
Wind Speed <10	12 hour	24	28	41	29	3715
Wind Speed >10	12 hour	81	89	96	76	139
Wind Direction	12 hour	38	38	40	36	3854
Pressure	12 hour	47	38	42	41	2037
Temperature	24hour	31	38	44	34	3789
Dewpoint Depression	24 hour	44	33	41	38	3724
Wind Speed <10	24 hour	22	28	39	28	3696
Wind Speed >10	24 hour	82	91	97	74	146
Wind Direction	24 hour	36	36	39	34	3842
Pressure	24 hour	46	30	34	39	2078
Temperature	36 hour	29	38	42	31	3745
Dewpoint Depression	36 hour	43	37	45	38	3674
Wind Speed < 10	36 hour	26	30	37	28	3692
Wind Speed >10	36 hour	90	97	97	83	115
Wind Direction	36 hour	33	34	35	33	3807
Pressure	36 hour	34	24	34	34	2062

For the surface parameters at the analysis time (0 hour), two distinct groups appear with MM5 and RAMS with the superior scores and the other two models in the second group. (The comparison at the zero hour provides a score for the initial fields prepared by the model's analysis routine. The same data was supplied to each model.) However, by 12 hours, a significant portion of the MM5 and RAMS advantage had disappeared. These two models were still the top performers with RAMS performing better than MM5 each time for most variables.

Only in predicting sea level pressure did MM5 regularly outperform RAMS. NORAPS6 and RWM performed about the same throughout the forecast period except for dewpoint depression. NORAPS6 and RWM's predictions of dewpoint depression were very poor initially, but become competitive at later times. The poor dewpoint analysis by NORAPS6 is easily explained. NORAPS6 used the humidity data from the global gridded data and did not use the relative humidity data from the observations to generate the initial fields. Each model's skill at 12, 24, and 36 hours was relatively stable with a small degradation with time. The performance scores (Table 5-4) are lower for the surface comparisons than the corresponding upper air comparison (Table 5-5). These differences can probably be attributed to two factors. First, even though several of the models have "surface" output options there will be differences between the actual observation height and the computed height. There was no standard method used. For instance, RAMS used the lower cell parameters without correction, except for sea level pressure. This cell center is at 46 meters and velocities at this point should have a small positive bias as the observations are usually taken at 10 meters. The remaining models varied in how each computed the surface data. These output differences were probably obscured by the sub-grid variability present in the real world. Local structures, terrain features, trees, etc. affected the observed data. With a grid size in excess of 40 km, none of these local features could be modeled.

Table 5-5. Upper air predictions within criteria (see Table 5-2) by forecast time.

Parameter	Forecast Time	MM5 %	NORAPS6 %	RAMS %	RWM %	Total Observations
Temperature	0 hour	88	85	93	62	3295
Dewpoint Depression	0 hour	28	9	50	19	2455
Wind Speed <10	0 hour	80	60	82	52	1119
Wind Speed >10	0 hour	90	76	93	71	2000
Wind Direction	0 hour	90	83	94	70	3119
Temperature	12 hour	64	70	74	65	3356
Dewpoint Depression	12 hour	24	14	29	13	2509
Wind Speed <10	12 hour	48	54	61	53	1137
Wind Speed >10	12 hour	74	73	82	74	1975
Wind Direction	12 hour	72	75	80	73	3112
Temperature	24 hour	57	67	70	65	3457
Dewpoint Depression	24 hour	24	16	26	12	2599
Wind Speed <10	24 hour	50	50	63	53	1239
Wind Speed >10	24 hour	73	71	81	74	2045
Temperature	36 hour	54	63	68	63	3287
Dewpoint Depression	36 hour	22	16	24	10	2465
Wind Speed <10	36 hour	54	54	64	55	1259
Wind Speed >10	36 hour	70	72	80	75	1847
Wind Direction	36 hour	63	73	76	75	3106

A similar forecast accuracy time response can be seen in the upper air comparison, however, all the scores are higher. Sub-grid influences are much less of a factor above the surface. For each parameter and forecast time, RAMS produced the predictions that most often met the criteria. NORAPS6 often produced more accurate predictions than MM5 in the upper air calculations. However, there were cases when every model had difficulty accurately predicting a parameter; specifically, the predictions of dewpoint depression, where the highest forecast accuracy seen was 29 percent. The initialization of the dewpoint depression varied widely in accuracy and this may be reflected in these scores. This lack of consistency in upper level moisture observations is most likely the reason for this poor performance. (Dewpoint was only validated at points where relative humidity data existed. The lack of this data at some locations above 300 mb is reflected in the reduced number of observations.)

The statistical data, when depicted by forecast time (Tables 5-4 and 5-5) indicates that RAMS and MM5 have better analysis routines. However, the statistical advantage of the better analysis is not obvious by 12 hours into the forecast period. The scores at 12 through 36 hours were relatively consistent. The ranking of the models remained the same. Statistically, there appears to be no compelling reason to use a better analysis routine to initialize the forecasts. However, the largely non-linear atmospheric processes modeled by these models makes this statement somewhat risky. During a software upgrade for NORAPS6, a minimal impact in forecast accuracy was noted as a result of improving the analysis (Hodur, 1987). This somewhat corroborates the statistical results and is probably the reason NORAPS6 produces such balanced accuracy. There are more technically advanced analysis routines that all models

could use to improve the initial accuracy and potentially the overall results. The above data suggests the actual forecast model is determining the accuracy score after some start up period.

5.3 EXECUTION TIME AND HARDWARE SELECTION.

In evaluating the four candidate forecast models we emphasized each model's forecast performance and accuracy because good performance is generally more difficult and costly to achieve than is reduced run time. However, run time is important in an operational environment, and the AF requirement is to produce a 72 hour forecast in 1 hour. All tested models ran substantially slower than this on an IBM RS/6000 Model 370 workstation. Average run times for 36 hour forecasts were RWM, 2.8 hr; NORAPS6, 4.3 hr; RAMS, 8.8 hr; and MM5, ~ 18 hr. We can meet the AF's run time requirement by speeding up model execution, by using faster computers, or by a combination of both.

5.3.1 Code Improvements.

We ran each of the candidate forecast models using the best physics models each one offered. It is unrealistic to relax this choice because, even using their best physics, none of the models fully met the AF's forecast performance criteria. In fact, the converse would appear to be true: additional and better physics models must be added to improve forecast ability and to predict phenomena, such as clouds, that are not provided by current models.

In general it is more cost-effective to speed up existing physics models than to develop new models. We can improve the performance of existing detailed physical models by parameterizing their output or by approximating parts of them with analytic functions. Of the four TFM candidates, RAMS and MM5 could benefit most from this type of improvement because they already contain the most sophisticated physics models. It is difficult to accurately predict the speed improvement that can be achieved, but a factor or 2 to 4 is not unreasonable. We base this estimate on our experience with how much time is spent executing various portions of each code and realizing that some portions, such as the basic atmospheric advection, cannot be sped up significantly. The biggest improvement may be obtained by restructuring a code to take advantage of available hardware configurations, such as multiple CPUs.

5.3.2 Hardware Improvements.

Hardware improvements continue to drive the computer industry; Moore's Law—that computing power doubles every 18 months with no increase in price—has been true for the last decade and is still true today. Achieving improved execution speed through hardware selection is a viable and cost-effective supplement to code improvements. Furthermore, to achieve the required forecast performance, we must plan to incorporate more complex physical models, increasing the number of floating point operations and, hence, the demand on execution times. This increase must be accomplished within the operational constraint of one hour of execution time for a 72 hour forecast.

Two existing workstation architectures could meet the TFM run time requirement: distributed memory, parallel processor machines, such as the IBM SP-2 and CONVEX Exemplar, or a workstation cluster linked with a high speed optical network interconnect. These alternatives both use multiple CPUs linked by high-speed communications, and they differ primarily in packaging; the SP-2, for example, consists of several IBM RS/6000 CPU boards housed in a single cabinet. Using multiple, independent workstations, either in a single cabinet or free standing, also improves reliability and provides graceful degradation in a field environment—should a single workstation element fail, the remaining workstations can still produce a forecast with only minimal degradation in performance. Field maintenance can be accomplished at the same level by replacing individual workstation elements. And,

because workstations have become almost commodity items, they offer attractive, competitive pricing. Both of these architectures offer a good price/performance ratio, built-in redundancy, and easier maintenance than other potential platforms, such as specialized vector computing machines.

To operate efficiently on a distributed, multi-processor system, a numerical weather prediction model must be restructured, so it would be advantageous to choose a model that has already been modified to run on a distributed-memory architecture. RAMS and MM5 have both already been modified and are currently operational on workstation clusters; NORAPS6 and RWM have not been modified. These versions of RAMS and MM5 have been available and operating for over two years. MM5 was adapted by the Scientific Computing Division (SCD) of NCAR. We have extensive experience running the parallel version of RAMS, but not MM5. The following performance estimates are based on our experience with the single processor versions of MM5, so the actual performance of NCAR's parallel version may vary from these estimates. Using the run times listed above, we estimate the following run times for multi-processor versions.

In constructing Table 5-6, we assumed a speed ratio of 2.5 between the IBM RS/6000-370 and RS/6000-390. An SP-2 consists of several RS/6000-390s in a single cabinet. The third and fourth columns assume 11 and 14 RS/6000 elements, respectively. Our experience running RAMS on a cluster of 8 IBM RS/6000s shows that an efficiency factor of .75 can typically be achieved. We used this efficiency in estimating the run times on multiple workstation configurations. Actual efficiencies can depend on the individual codes, the number of computer elements, and the type of communication used between elements.

Table 5-6 illustrates that using an SP-2, or similar computer, the distributed architecture versions of MM5 or RAMS could meet the run time requirement. Using a single element workstation will require significant improvements in a model's performance.

Table 5-6. Approximate execution times for a 72 hour forecast without code improvements.

	RS/6000-370	RS/6000-390	11 Element SP-2	14 Element SP-2
MM5	36 hr	14.4 hr	<2 hr	<1.5 hr
NORAPS6	8.5 hr	3.4 hr	n/a	n/a
RAMS	17.5 hr	7 hr	<1 hr	<45 min.
RWM	5.5 hr	2.2 hr	n/a	n/a

SECTION 6
MODEL ADAPTATION

6.1 INTRODUCTION.

The previously described model comparison determined which mesoscale forecast model best-satisfied DSWA and AF accuracy and speed requirements under proscribed resolution constraints. For its transport and dispersion program, DSWA decided to use RAMS to provide high resolution meteorological forecasts. At the time this report is being written, the model is being run routinely on an IBM workstation at resolutions of 10 km or less. A number of changes have been made in the model as a result of adapting it to this application. The majority of these changes relate to either accepting data from DSWA or military sources or providing data in formats compatible with the dispersion models used by DSWA. These formats are adequately described in the User's Manual (Bauer et al., 1997) being delivered under this contract effort. Specific modifications have been made to RAMS to reduce execution time. Other modifications have been explored and will be used in future versions. These existing and potential changes will be discussed in this section.

6.1.1 Execution Time.

In evaluating the four candidate forecast models we emphasized each model's forecast performance and accuracy because good performance is generally more difficult and costly to achieve than is reduced run time. However, run time is important in an operational environment, and the AF desired to produce a 72 hour forecast in 1 hour. DSWA has a similar objective. All tested models ran substantially slower than this on an IBM RS/6000 Model 370 workstation. We can meet the AF's run time requirement by using faster computers, by speeding up model execution, or by a combination of both.

6.1.2 Hardware Improvements.

Hardware improvements continue to drive the computer industry; Moore's Law—that computing power doubles every 18 months with no increase in price—has been true for the last decade and is still true today. Achieving improved execution speed through hardware selection is a viable and cost-effective supplement to code improvements. Furthermore, we must anticipate the incorporation of more complex physical models, increasing the number of floating point operations and, hence, the demand on execution times. Several existing workstation architectures could meet the TFM run time requirement: distributed memory, parallel processor machines, such as the IBM SP-2 , HP Exemplar, SGI Origin or a workstation cluster linked with a high speed optical network interconnect. These alternatives all use multiple CPUs linked by high speed communications with some computer architecture differences; the SP-2, for example, consists of several IBM RS/6000 CPU boards housed in a single cabinet, while the SGI Origin 200 has two enclosures each containing two processors.

6.2 RESTRUCTURING FOR MULTIPROCESSOR SYSTEMS.

To operate efficiently on a distributed, multi-processor system, a numerical weather prediction model must be restructured. The version of RAMS distributed to the worldwide user community at the start of this effort was the single workstation version 3b, the version that was used in the previously described tests. Parallel versions of RAMS capable of operating on a parallel processor computer system were

under development at that time, and prototypes were under evaluation at Kennedy Space Center (KSC) and elsewhere.
One of the commonly available commercial parallel computer systems is the IBM SP-2. The SP-2 is a Multiple Instruction, Multiple Data (MIMD) computer system. This type of computer uses independent workstations or nodes linked by a communications interface that transfers data from one processor to another. Therefore, it is basically a workstation cluster assembled in a single cabinet with enhanced communications and operating system. There are several communication protocols that can be used to link the various workstation nodes in this cluster environment. The communication protocol between nodes used by the KSC prototype was the *Parallel Virtual Machine* (PVM). At the direction of the government, RAMS was modified to use the somewhat more recent *Message Passing Interface* (MPI) communications protocol. Essentially similar to PVM, MPI is being implemented on a number of platforms including the SP-2.

These changes have been implemented in RAMS Version 4a. The main change that characterizes Version 4a from the current release version 3b is that the RAMS code structure has be changed to allow for the parallel computation on a MIMD computer architecture, such as an IBM SP-2 or a workstation cluster. Version 4a retains the ability to operate on a single processor with the same version of the code. This is a user selectable option.

6.2.1 RAMS Parallel Version.

6.2.1.1 Parallel Design Considerations. Before beginning the modification of the RAMS code for parallel computation in 1991, we considered many issues. This section will describe some of these considerations. The following were our initial goals; we will mention if we met these goals for each point.

- We concentrated on the "large" three-dimensional computational configurations of RAMS, not the smaller two-dimensional runs that can be requested. In general, the larger the three-dimensional domain (measured in numbers of grid points), the more efficient the parallelization should become. This goal has been met; only three-dimensional runs are allowed to run in parallel.

- No compromises should be made in the physics or numerics. It would be possible to reduce numerical accuracies in some schemes such as advection to reduce the amount of communication among the processors. This goal has been met, although the sixth-order advective scheme has not been implemented yet in the newest parallel version.

- We targeted the distributed memory MIMD architecture. With Single Instruction, Multiple Data (SIMD) computers or shared-memory systems, a micro-tasking structure in which the parallelization is done on the individual loop level could be explored, which would require a distinctly different code structure than a MIMD machine. Distributed-memory architecture usually requires a much coarser-grained parallelism, since communication between processors needs to be kept to a minimum. This goal has been met. It has turned out that the MIMD parallel structure has been extremely efficient on shared memory platforms tested.

- Scalability of the parallel algorithms to massively-parallel platforms was considered. Although our initial goal was to target a workstation cluster (< 8 nodes), we have ported RAMS to massively-parallel platforms (> 64 nodes). This goal has been partially met; we are continuing to

work on the scalability.

- For ease of software maintenance, a single code version should be developed for both uniprocessor and parallel platforms. This goal has been met.
- There should not be any performance degradation for the code on uniprocessor platforms. This goal has been met and we continue to work on overall efficiency improvements such as better cache usage.

Therefore, with these requirements and considerations, the code modification has progressed. The following sections will summarize the features of the parallel RAMS and the basic techniques used in accomplishing the goals.

6.2.1.2 RAMS Parallel Version Differences. The parallel version of RAMS was designed to be very compatible with the latest single-processor version. The differences that do exist between the latest serial RAMS version (3b) and the parallel version are because of unimplemented features in the parallel version or at the code level.

- Unimplemented features: There are a number of RAMS features that have not been used very extensively in recent years, which were not chosen for implementation in the parallel version. These include:
  - Hydrostatic equation set options
  - Forward and leapfrog time differencing (only the "hybrid" scheme was implemented)
  - "Old" microphysics scheme
- Code changes: At the code level, there are a large number of changes mostly due to the modifications for the parallel execution. The major changes fall into four categories:
- Allowing the code to execute on a *sub-domain* - The serial code was generally of a structure, which executed a process or set of instructions over the full set of grid points for any grid. This had to be modified to allow it to execute these instructions over a subset of these points. Along with the considerations for parallel efficiency (such as communication/computation overlap), care needed to be taken to make sure that operations were scheduled correctly so that the boundary regions of the sub-domains had access to the correct information that is passed from adjoining nodes.
- Message passing - Code was developed to handle the passing of data (messages) between the sub-domains. Since, at different places in the execution, different amounts of data need to be passed, different sets of code were implemented to handle these tasks. Code to handle the bookkeeping chores also was developed. This includes the tasks of domain decomposition and dynamic load balancing.
- Additional C language code: Generally, the message passing libraries have been developed and written in the C language. Therefore, it is advantageous at times to interface to these libraries with C routines. A few additional RAMS code files have been rewritten in C, most notably the main program. This also allows for the capability to include standard portable command line arguments when specifying the executable name. Also, several of the FORTRAN modules are now passed through the C preprocessor to allow for conditional compilation.
- Code improvements - Several improvements to the code were made as development of version

4a progressed, either from efficiency considerations or for ease of use. Examples of these changes include a completely rewritten advection scheme (which combines the leapfrog and forward advective schemes in the same set of code) and a new method of setting up memory and output variable specifications. Because of this latter change, a new input data file is now required to set up the model variable structure.

6.2.1.3 Parallel Components and Structure. The original version of the parallel RAMS, which began its development at CSU in 1991, used the Parallel Virtual Machine (PVM) software, developed at Oak Ridge National Laboratory, for communication among the processors of the parallel computer platform (Bequelin et . al., 1991). However, since then, a consortium of industry, government, and university computer scientists has developed a new de facto standard called MPI (Message Passing Interface). RAMS has been modified to use MPI in addition to retaining the capability to execute under PVM. RAMS is structured in a standard master-node configuration, where the master process is a main controlling process handling model initialization and output while the nodes are the main workers, performing virtually all of the floating point computations needed for the model simulations.

Basic Code Structure

The basic structure of RAMS in this master-node configuration is the standard method of *domain decomposition* where each processor is given a portion of the modeling domain on which to perform the computations. Each node is given a rectangular set of grid points and a surrounding boundary region, which will be referred to as the *subdomain*. Again, all computation is done on the node processes. During each model timestep, the nodes must exchange information at the subdomain boundaries.

Domain decomposition

Domain decomposition is the process of spatially subdividing any computational grid domain in the model into two or more subdomains, each one to be handed to a separate processor for carrying out the necessary computations for time integration. There are many possible ways of decomposing a 3-D grid domain, but the following considerations point strongly to one best method.

- Some computational algorithms in the model solve tri-diagonal linear systems in the vertical, requiring simultaneous knowledge of all grid cell values in the vertical column. Thus, it is to great advantage to keep an entire column on the same processor and to decompose only in one or both horizontal directions.

- Although 1-D horizontal decomposition, i.e., grouping not only an entire column but also all columns in a given constant-x or constant-y slab into the same subdomain, is conceptually and algorithmically simpler than 2-D decomposition, it increases both the total memory requirement and, more importantly, the amount of information that must be communicated between processors. Thus, we adopted the more general approach of decomposing in both horizontal directions.

- We desire the flexibility to utilize any number of processors that may be available including prime numbers.

- Parallel efficiency dictates that all processors should perform their computational tasks in nearly the same amount of time so that no processor needs to waste time waiting for the results from another. This requirement, coupled with the facts that (1) processors may run at different speeds (e.g., in a parallel cluster of dissimilar workstations) and (2) certain regions of a model grid

require more computational steps than others (e.g., where clouds occur), dictates that model grid subdomains must be allowed to have unequal sizes in order to properly balance the computational load on each processor.

The domain decomposition algorithm in RAMS satisfies all the above requirements. The algorithm requires as input the number of grid points (vertical columns) in each horizontal direction, the number of processors to be used, the relative speed of each processor, and a set of "column work factors" or relative computational workload (CPU time) of each vertical column. Both the relative processor speeds and column work factors may be evaluated from the performance over the preceding timesteps or, at the beginning of a model run, estimated.

A diagram of grid subdomains resembles bricks laid in tiers, with straight, unbroken lines separating each tier. The lines separating the bricks in each tier generally terminate at the top and bottom of the tier but in some cases coincide with lines in adjacent tiers. The number of tiers is an integer close to the square root of the number of processors, as is the number of bricks in each tier, but adjustments are made as necessary to accommodate the exact number of processors available. Different tiers in general have different thicknesses, and bricks in a tier in general have different lengths. These dimensions, i.e., the horizontal dimensions of each subdomain, are collectively determined from the relative processor speeds and the column work factors in order to achieve precise load balancing.

An entire model grid consists of interior vertical grid columns where field variables are prognosed plus a single row of grid columns in which diagnostic lateral boundary conditions are applied forming a lateral perimeter. In the domain decomposition, each interior prognostic column is placed in only one subdomain and prognosed only in that subdomain which completely avoids repetitive prognostic computations between different processors. A single row of grid columns (the "halo" or overlap region) is added to form a perimeter around each subdomain prognostic region, which duplicates a modest number of columns comprising the entire grid. These columns are used to store field values communicated from adjacent subdomain interiors where they are prognosed.

In applications where nested grids are employed in RAMS, domain decomposition is completely independent for each grid. Thus, decomposition is based only on the grid size and work factors plus the number and speed of the processors and does not depend on where the grid is placed within its parent grid, where finer grids are placed within it, or how the finer and parent grids are decomposed.

Types of communication

There are seven distinct types of message-passing events in the RAMS structure. These are:

- Initialization: During initialization, the master process will compute the grid decomposition and send all necessary information and data to the compute nodes. The full subdomain of information is sent for almost all variables. This will also occur during the dynamic load balancing.
- Long timestep overlap region: At the beginning of a timestep, the nodes will exchange the overlap regions of the prognostic variables. We have reduced the overlap region to one row.
- Long timestep overlap region (turbulence): In order to reduce the overlap region to one row, it was necessary to add an extra communication step where the turbulence exchange coefficients in the overlap region are exchanged between nodes. This technique has added an additional 5-10% parallel efficiency, depending on the platform, to the RAMS runs.

- Small timestep overlap region: During the computation of the small acoustic timestep, the compute nodes will exchange the overlap regions of the u and v velocity components and the pressure. This is only needed for one overlap row.
- Nested grid boundaries: Nodes containing a coarse grid will send the necessary data to a fine grid node for interpolation of the nested grid boundaries.
- Nested grid feedback: The compute nodes will average their fine grid information to the coarse grid structure and transfer that data to the appropriate coarse grid nodes.
- File output: When it is time for file output, the compute nodes will send the full subdomain of the prognostic variables to the master process.

All node to node communication types package variables into a single message before sending to the receiving nodes.

Concurrent computation/communication

It is desirable that communication between each processor of the parallel system be kept to a minimum if the overhead involved in the communication between processors in a system is significant compared to the computations performed. One way of minimizing the communication cost is to "schedule" communications so that they occur concurrently with computation. The modular structure of the RAMS code is very conducive to this type of technique. The timestep computational structure has been rearranged so that many of the model computational schemes that do not require information from the subdomain boundary regions (those schemes that operate either at a single grid point or in a vertical column) are executed first during a timestep. In addition, some of the model routines compute the interior portion of subdomains first. While these are occurring, the node processes exchange the subdomain boundary information. When the node is finished with the first set of computations, the subdomain boundary information will have been received so that the node can continue with the remainder of the computations. For smaller number of nodes, the concurrent scheduling of communication and computation can even allow for reasonable efficiency in the use of a cost-effective, standard Ethernet for communication in a clustered workstation system (over a small number of nodes), rather than the more expensive optical fiber components.

Bookkeeping arrays

Once the domain decomposition is performed, all required communications between subdomain processors are determined. This involves tabulating the exact set of grid point locations for each variable to be sent and received between all relevant pairs of subdomains. In order to minimize communication, only required variables from required locations are sent and received. In some cases, only a single grid column needs to be communicated between processors while in others a rectangular block of columns must be sent. The starting and ending grid coordinates in both horizontal directions for each block are stored in a 5-D integer array. The arguments of this array are (1) the source or sending subdomain or processor, (2) the destination or receiving subdomain or processor, (3) the model grid number (since decomposition is different in general for each grid), (4) the designation of one of the four block coordinates, and (5) the type of communication.

File output

The file output of RAMS is accomplished through the master process. When the time comes to output the files, the compute processes send all necessary information back to the master, which can then write the files to local disk. Other techniques have been used where each node will output its portion of the

data, then a separate process will recombine the individual parts. The concept of the master I/O process has several advantages including:

- The transfer of data is done over the usually higher speed message passing hardware. Network File System software is not used.
- No local disk space is needed (for MIMD platforms).
- After the nodes have transferred their data, they can continue with their processing without waiting for the master process to finish writing the files.
- The output files are immediately available from the master node for other activities.

Nested grid considerations

As mentioned, RAMS contains a two-way interactive grid nesting scheme where, during a timestep, the coarser grid gives boundary information to a fine grid and a fine grid averages its domain and overlays the appropriate area of the coarse grid. Nested grids can be either telescoping or simultaneously nested within a coarser grid. There is no limit imposed in RAMS as to the number of nests or the spatial nesting ratio between nests. This situation does pose a challenge for the development of an efficient parallel version of RAMS which uses domain decomposition, dynamic load balancing, and strives to minimize communication among the nodes.

The nesting scheme has been modified to increase its scalability. The new scheme decomposes each of the nested grids independently. Then the appropriate communications are done for the two-way nesting algorithms. For the feedback process, the fine grid data is averaged on the fine grid nodes, then transferred to the coarse nodes. For the nested boundary interpolations, the coarse grid nodes send the data to the fine grid nodes where the interpolation is done. Note that in each of these schemes, only coarse grid data is transferred, thus reducing the amount of communication as much as possible.

Dynamic load balancing

With the techniques of domain decomposition, inefficiencies will arise when one processor takes much longer with its subdomain than the other processors. This can happen frequently in RAMS because of spatial differences in model physics and hence the complexity of the physical parameterizations the model has to compute. If this happens, the remainder of the processors will sit idle. However, we have implemented a technique for *dynamic load balancing,* an objective way to allow for the adjustment of the computational load among the processors as a model simulation progresses.

The dynamic balancing in RAMS is accomplished in the following manner. At the end of each timestep, the compute nodes will send the CPU time and the wall clock time from its subdomains back to the master process. The master process then can determine if imbalances are occurring. When the compute nodes have sent all the subdomain fields back to the master process, which occurs when it is time to write an output file to disk, the master process is able to basically repeat the initialization procedure. This consists of computing the work factor for each grid column, decomposing the model grids according to the work factors, and sending out new subdomain information and data to the compute processes.

6.2.1.4 Parallel Efficiency Results. Numerous tests have been run with the parallelized version RAMS on several parallel platforms. As of this writing, we have ported the code to workstation clusters, the IBM SP2, and the HP/Convex Exemplar. Other groups have ported the parallel RAMS to the CRAYJ90, T3D, and T3E and the SGI Power Challenge. Obviously, the parallel performance is dependent on the hardware characteristics including the machine architecture, speed of CPU, and type and speed of the CPU interconnect. But parallel efficiency is also dependent on the configuration of the model simulation, with such things as numbers of grid points, number of grids, and complexity of physics needing to be considered.

For the ports we have made, we will state generally some of the parallel efficiencies we have attained.

- Workstation clusters: We have run on several clusters (2-8 nodes) of IBM RS/6000 workstations using standard Ethernet as the networking hardware. Efficiencies attained have ranged from 60% to 85% depending on model configuration and number of nodes. Efficiency is defined as:

$$\frac{\text{time required for a single processor}}{(\text{time required for the parallel processor})\,(\text{number of processors})}$$

- IBM SP2: On the SP2 using the high-speed switch, efficiencies have ranged from about 90% on larger simulations using 8 nodes to about 68% using 64 nodes.
- HP/Convex Exemplar: The Exemplar (or SPP 1600) is an 8 processor, shared memory machine using a crossbar switch. For large multi-grid runs, we routinely achieve 90-95% efficiency on the 8 processors. For moderate size multi-grid runs (number of horizontal grid points: 50 by 50), we are able to get better than 100% efficiency because of better cache utilization.
- SGI Origin: We have access to a Silicon Graphics Origin 200, a 4 processor, shared memory machine. For medium-size, multi-grid runs, we have achieved 90-95% efficiency.

6.2.1.5 Future Developments. RAMS continues to be developed and capabilities expanded. Following are some of the issues we will be considering in the near future as related to the computational performance.

- *Increased serial code efficiency:* We continue to look for ways to increase the single processor performance of the code. These include better algorithmic ways to program various numerical techniques and to better utilize the CPU cache.
- *Investigate additional concurrent communication/computation possibilities:* Additional possibilities exist for overlapping the computations and communications such as computing more terms on the sub-domain interior first.
- *More complicated "work" factor:* The computation of the work factor, which is used in the domain decomposition, is not a straightforward technique, as it relies on the presence of a wide range of different variables and the knowledge of how these variables affect the computational cost. We are continuing to experiment with better algorithms to define this quantity.
- *Continue to explore shared-memory architecture considerations:* Computer manufacturers are beginning to introduce MIMD-type platforms where each node is a symmetric multi-processor. We will be looking at this architecture to determine the most efficient ways to utilize these

platforms. Also, several shared memory platforms with a moderate number of processors (8-32 CPUs) have come on to the market recently. Although our initial impression is favorable as to the efficiency of a MIMD code structure on these platforms, we will continue to investigate the code performance.

6.3 CODE IMPROVEMENTS.

We ran each of the candidate forecast models using the best physics models each one offered. It is unrealistic to relax this choice because; even using their best physics, none of the models fully met the AF's forecast performance criteria. In fact, the converse would appear to be true: additional and better physics models must be added to improve forecast ability and to predict phenomena, such as clouds, that are not provided by current models.

In general it is more cost-effective to speed up existing physics models than to develop new models. We can improve the performance of existing detailed physical models by parameterizing their output or by approximating parts of them with analytic functions. Of the four TFM candidates, RAMS and MM5 could benefit most from this type of improvement because they already contain the most sophisticated physics models. It is difficult to accurately predict the speed improvement that can be achieved, but a factor or 2 to 4 is not unreasonable. We base this estimate on our experience with how much time is spent executing various portions of each code and realizing that some portions, such as the basic atmospheric advection, cannot be sped up significantly. Speeding up individual physics models is generally a difficult and time-consuming process. However, late in the contract a technique called the Fully Equivalent Operational Model (FEOM) was identified as a potential means of improving performance significantly without laborious recoding.

6.3.1 Investigation To Reduce Physics Model Execution Time.

We investigated methods for reducing the time required to run the RAMS model would allow weather and dispersion predictions to be made quicker and updated more frequently. Traditional methods for reducing computational runtimes trade model prediction fidelity for reduced run times through model simplifications. Here we document an innovative approach to reduce RAMS runtime while preserving prediction fidelity. This involved the application of a new computational modeling tool, the Fully Equivalent Operational Model (FEOM) algorithm, to a computationally intensive radiation transport module in the RAMS code. *The FEOM algorithm produced a new module that predicts the original module's output with high precision and 10^3 times faster.* The new algorithm was developed by Dr. Jeffrey A. Shorter of Mission Research Corporation and Professor Herschel Rabitz of Princeton University.

The two modules that consume the greatest portion of computational resources in RAMS are cloud microphysics and Radiation Transport Module (RTM). The microphysics module calculates the evolution of rain, ice, and snow in the model while the RTM calculates the net amount of energy deposited into the atmosphere from solar radiation, blackbody emission from ground, and infrared emission from the atmosphere. The proof of concept for the conversion of the RTM into a FEOM has been completed and is described here. While time and effort did not allow a complete development of the RTM and its implementation into RAMS, the results are very encouraging.

6.3.1.1 Background - Radiative Transfer Module. The RTM in RAMS calculates altitude dependent atmospheric heating rates due to absorption and emission of solar and infrared energy.

The heating rate is used to predict changes to the atmospheric temperature profiles. A physics-based two-stream radiation transport model is used for the calculations. This model treats the atmosphere as a series of horizontal layers. Solar light impining from the top of the atmosphere is propagated layer by layer through the atmosphere, then reflects off the Earth's surface, and propagates up, layer by layer. In each layer, the light can pass through, be absorbed, or scattered by molecules and/or aerosols. Scattering is either in the forward or reverse direction. The infrared longwave emission from the Earth is propagated upward layer by layer and can either pass through the layer or be absorbed. Since long wavelength energy from blackbody radiation and infrared emission is not treated in the model. The infrared emission of three trace gases (H_2O, O_3 and CO_2) are treated in this model. This molecular emission is propagated both upward and downward in the atmosphere and can either pass either through the layer or be absorbed. These processes are shown schematically in Figure 6-1. The horizontal lines represent the layering of the atmosphere. The set of arrows on the left depict the solar radiation entering the atmosphere from above, propagating downward, reflecting off the surface, and propagating back upward. The middle set of arrows represents the black body emission from the Earth that is propagated upward. The set of arrows on the right depicts the infrared emission from the trace gas species in one layer going in the upward and downward directions. This light is treated similarly to the black body emission. In the first two cases, the weight of the arrows represents the magnitude of the optical intensity. As the lines narrow, the light is being absorbed by the atmosphere and transferred to heat. The RTM calculates the amount of light absorbed and converts it to a heating rate (deg/sec). The atmospheric trace gas concentrations are either prescribed by McLatchy soundings (O_3 and CO_2) or are prognostically calculated in RAMS (H_2O).

The evolution of atmospheric dynamics is very sensitive to the heating rates calculated in the RTM. As such, a first principle approach is used. This involves separating the radiation into many different

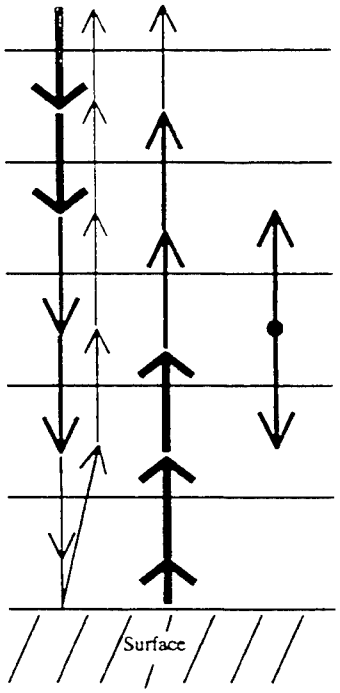

Figure 6-1. Schematic of the atmospheric representation in the radiation transport module.

wavelength bands, calculating wavelength-dependent absorption coefficients for each trace gas absorber, and coupling the downward and upward radiation fluxes. As a result, the RTM is very computationally intensive. To compensate for the RTM runtime, RAMS only calls the module every 10 to 30 time steps and/or only at specific locations in the grid space. The heating rates are assumed not to change between RTM calculations. For locations in the grid between RTM calculation points, the heating rates are interpolated. Even with this restricted utilization of the RTM, it consumes between 15-30% of the total CPU time of a simulation.

By calculating heating rates orders of magnitude faster, while maintaining accurate results, one could:

- Run the RTM more frequently to increase the temporal fidelity of the heating rate profiles;
- Run the RTM for more grid columns to increase the spatial fidelity of the heating rate profiles;
- Reduce the overall runtime of RAMS by one third (estimated).

This acceleration of the RTM has been achieved through the use of FEOMs and is discussed below.

6.3.1.2 Fully Equivalent Operational Models (FEOMs). FEOM addresses the perceived complex problem of mapping the input-output relationship behavior of complex systems. A traditional approach to a problem with n input variables $x_1,\ldots,x_n$ would consist of sampling each variable at s point to assemble an interpolated lookup table of computational effort s^n. Realistically one may expect s to be approximately 5 to 10 and n can be $10\text{-}10^2$ or larger. Viewed from this perspective, attempts at creating a lookup table would be prohibitive. However, this analysis implicitly assumes that all n variables are important and, most significantly, that there are correlations among variables to all orders (i.e., single pairs,...., up to all n variables acting in a tightly correlated fashion).

The fundamental principle underlying the FEOM representation is that output correlations between independent variables die off rapidly. This assertion does not eliminate strong variable dependence or even the possibility that all the variables are important. Various sources of information support this point. First, variables in most physical models enter as simple functions, often as additive sums of low-order multiplicative terms. This kinematic simplicity tends to survive in the output, although often scrambled in a complex fashion. Second, traditional statistical analysis of model behavior has revealed that a variance and covariance analysis of the output in relation to the input variables often adequately describes the physics (i.e., only low-order correlations describe the dynamics). Finally, these statements are also familiar from many-body physics where rarely do interactions higher than two-body play a significant role. This general observation leads to a dramatically reduced computational scaling when one seeks to map input-output relationships of complex systems. Considering this analysis, one may now argue power-law scaling to learn the input-output behavior, such as $\sim n^l$. Here, l is the highest order of significant correlation and, typically, $l \leq 3$. Polynomial growth poses a far more tractable algorithm than the often accepted view of exponential growth s^n above.

The approach to generating a FEOM is to evaluate the input-output response of the model. This is achieved by performing a hierarchical, correlated function expansion of a special mathematical structure on the model and evaluating each term of the expansion independently. This expansion is then used as the FEOM. One may show that a function, $g(\mathbf{x})\equiv g(x_1,x_2,\ldots,x_n)$ can uniquely be decomposed into summands of different dimensions:

$$g(x_1, x_2, \ldots, x_n) = f_0 + \sum_{i=1}^{n} f_i(x_i) + \sum_{1 \le i \le j \le n} f_{ij}(x_i, x_j) + \cdots + f_{1,2,3,\ldots,n}(x_1, x_2, \ldots, x_n) \qquad (6.1)$$

where f_0 is a constant, $f_i(x_i)$ is a function of one variable x_i, $f_{ij}(x_i,x_j)$ is a function of two variables, x_i, x_j, and the higher dimensions follow until $f_{1,2,3,\ldots,n}(x_1,x_2,x_3,\ldots,x_n)$ which is a function of all the variables (i.e., it is defined as being the remainder: g minus all the prior terms in the sum). The function $f_i(x_i)$ describes the independent action of the variable x_i, while $f_{ij}(x_i,x_j)$ gives the pair correlated behavior, etc.

By representing the function as a summation of terms and investigating their respective magnitudes, it is expected that many will not contribute significantly to the summation and can be removed. This is a key benefit to the FEOM approach. Furthermore, this representation makes interpolating between function values trivial since they are low dimensional interpolations. Importantly, no constraining forms are applied to the expansion functions; they are numerically represented and form an interpolate look-up table.

The individual functions are explicitly calculated by running the model a number of times with a series of judiciously chosen input sets. Special care is taken to ensure that the entire phase space of the model input is covered when generating the FEOM. The FEOM generation process is shown schematically in Figure 6-2. A series of input sets are generated and run through the model. The resulting output is then related back to the input and the input-output relationship is deduced. This is then encapsulated into the FEOM.

6.3.1.3 FEOM Construction. The proof of concept for converting the RTM into a FEOM was achieved.

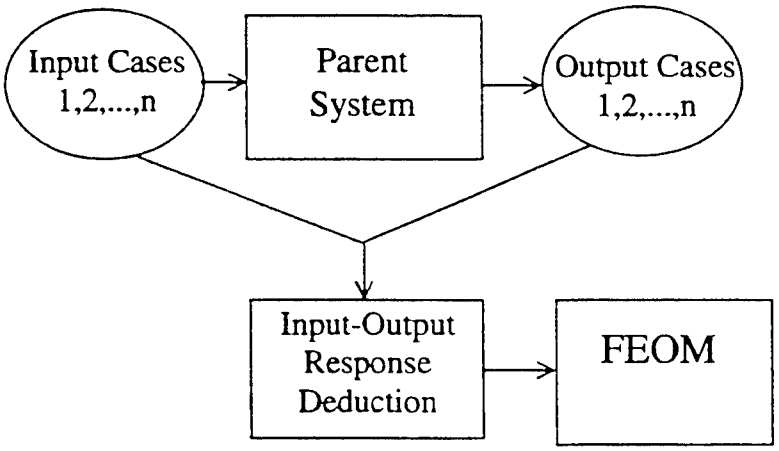

Figure 6-2. Schematic of the FEOM generation process.

The FEOM developed for the RTM calculates heating rates between 0 and 20 km altitude in 30 discrete levels. The predictions are within 0.1% of RAMS RTM calculated output values on average and the FEOM predictions are made 10^3 times faster. The inputs to the FEOM are H_2O concentrations at each level, the atmospheric temperature at each level, the surface temperature, and the surface albedo. A clear sky condition was assumed for this initial investigation and the solar input flux at the top of the atmosphere was assumed to be constant. Both of these assumptions could be incorporated with little impact on the overall FEOM runtime. A schematic of the RTM FEOM is shown in Figure 6-3. The FEOM uses the same input parameters as the RTM and predicts the same output. This makes the implementation of the FEOM transparent to RAMS. A series of discrete layers are represented in the heating rate profile output box to emphasize that the FEOM actually consists of a set of sub-FEOMs with each one predicting the heating rate in a given layer. The FEOM approach can be constructed to allow the user flexibility of defining altitude ranges and number of layers even though this particular FEOM is for a specific number of layers and altitude ranges.

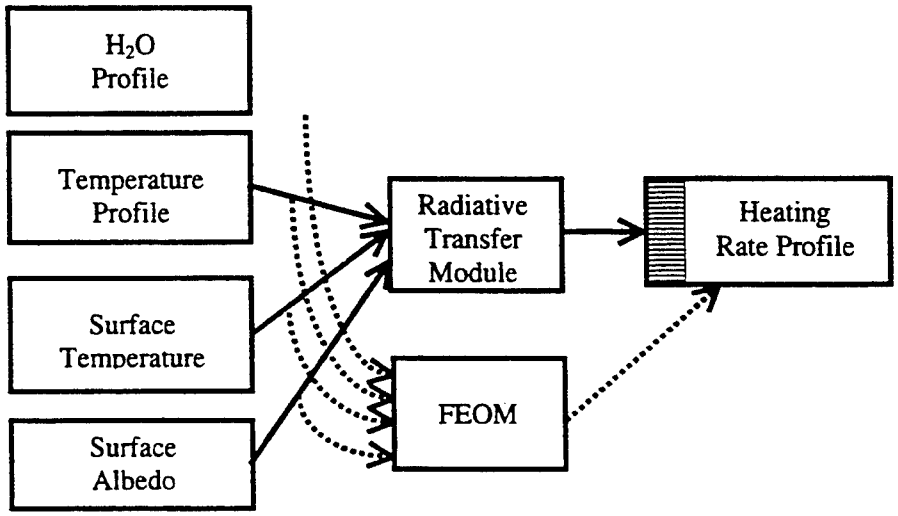

Figure 6-3. Schematic of the radiative transfer module FEOM.

Input parameter phase space.

The H_2O and air temperature profiles are represented as deviations from a reference mid-latitude summer profile. The profiles are broken into 30 discrete layers spaced 0.666 km apart and span an altitude range from 0 to 20 km. In each layer, the H_2O value can vary from 10% to 160% of the reference value. The temperature can vary ± 10% from the reference values. We emphasize that the H_2O and temperature values in each layer are treated independent of from all other layers and thus the profiles can be very structured. The H_2O and temperature ranges are shown in Figure 6-4. The surface temperature can vary from -8 to 50°C and the surface albedo can vary from 0 to 1.0.

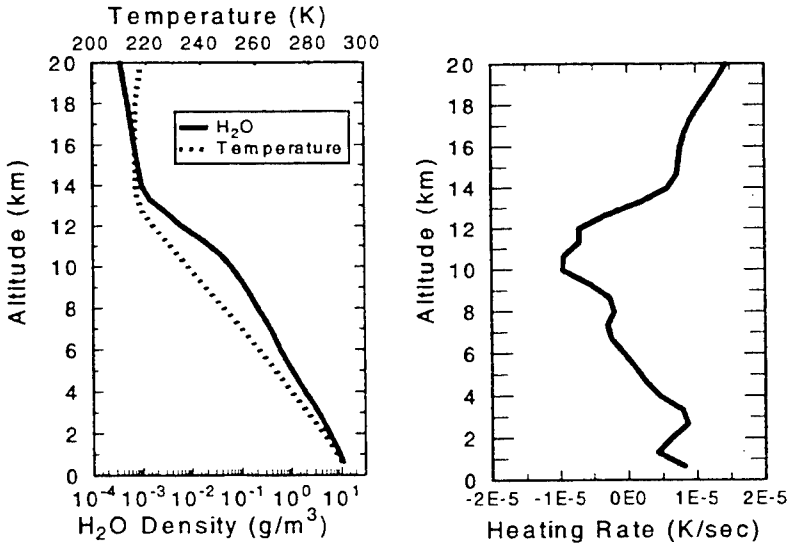

Figure 6-4. Reference input profiles for H_2O and temperature (left). The heating rate calculated using the RAMS RTM (right).

Table 6-1 summarizes the description of the parameters as well as the minimum and maximum variation.

Table 6-1. List of input parameters for the FEOM.

Parameter	*Description*	*Minimum*	*Maximum*
1-30	H_2O for Level 1 to 30	0.1	1.6
31-60	Air Temperature for Level 1 to 30	0.9	1.1
61	Surface Temperature (°C)	-8	50
62	Surface Albedo	0.0	1.0

Radiative Transfer Module Output.

The RTM calculates the altitude dependent atmospheric heating rate in degrees per second. The heating rate can be either positive, indicating that the atmospheric layer is absorbing more energy than it is emitting, or negative, indicating more optical emission than absorption. The values typically range between $\pm 4x10^{-5}$ K/sec ($\pm$ 3.5K/day). The heating rate profile for the mid-latitude reference atmosphere is shown in Figure 6-4.

Functional Representation.

A FEOM to replace the RTM will consist of a set of sub-FEOMs; one for each vertical layer in the model. Each sub-FEOM predicts the heating rate for a specified atmospheric layer. Since the atmospheric representation for this proof of principle was divided into thirty layers, thirty independent FEOMs were developed. Though each sub-FEOM only predicts the heating rate for a specified layer, it uses information from all other layers to make the prediction. This information is contained in the RTM input parameters: 30 H_2O values (one for each layer), 30 air temperatures, the surface temperature, and the surface albedo.

For each of the sub-FEOMs, the first three sets of terms of the function expansion (Equation 6.1) were calculated. There is one zeroth order term, which is determined by running the model with the nominal values of the model. There are 62 first order term functions, one for each parameter, and 1891 second order terms, one for each possible pair of parameters. Each first order function was represented with 16 points spanning the parameter phase space. Each second order function was represented by 16 points for each parameter, resulting in a 16 x 16 surface (256 points).

Once all 1,954 functions were calculated for each sub-FEOM, they were evaluated for significance. If a function is not significant, it is removed from the expansion. The ability to remove these functions is an advantage of the FEOM function expansion's special mathematical structure. A function was considered significant if the absolute magnitude of any point of the surface was greater than $1x10^{-6}$ deg/sec. This value is approximately 2% of the maximum heating rate magnitude. Using this criteria, 304 first order functions and 138 second order functions for *all* 30 sub-FEOMS were kept. That is a very small fraction of all the first and second order functions evaluated. The number of first and second order terms kept for each layer is shown in Table 6-2.

6.3.1.4 Analysis of the FEOM. The completed FEOM was evaluated for prediction accuracy and runtime relative to the original RAMS RTM. The evaluation was performed by running both models over a range of input conditions and comparing both the output results and the time required to attain the results. The input sets were generated using Monte Carlo methods such that each input parameter was assigned a random value within its phase space. This procedure produced very structured H_2O and temperature profiles and provided a rigorous test of the FEOM algorithm. Three sample H_2O and temperature profiles and their resulting heating rates are shown in Figure 6-5.

Accuracy.

The results displayed in the previous section show that the FEOM prediction agrees well with the model output. A quantitative assessment of the FEOM accuracy was calculated by averaging the absolute difference between the RTM calculated heating rate and the FEOM predicted heating rate for all 1000 input sets. This was performed for each atmospheric layer represented in the model.

The largest magnitude average error was $3x10^{-9}$ K/sec. This is 10^3 to 10^4 times smaller than typical heating rate calculated in the RTM and is smaller than the error that is incurred when the atmosphere is segmented into finite layers.

Table 6-2. The number of significant functions for each sub-FEOM layer.

Altitude level	Altitude (km)	Number of 1st order terms	Number of 2nd order terms
1	0.66	6	4
2	1.33	8	7
3	1.99	11	8
4	2.66	13	10
5	3.33	13	11
6	3.99	15	9
7	4.66	14	8
8	5.33	12	9
9	6.00	13	7
10	6.66	12	8
11	7.33	12	7
12	8.00	11	11
13	8.66	12	15
14	9.33	14	7
15	10.00	12	11
16	10.66	11	3
17	11.33	10	1
18	12.00	8	2
19	12.66	8	0
20	13.33	7	0
21	14.00	6	0
22	14.66	7	0
23	15.33	8	0
24	16.00	9	0
25	16.66	9	0
26	17.33	9	0
27	18.00	9	0
28	18.66	9	0
29	19.33	9	0
30	20.00	7	0

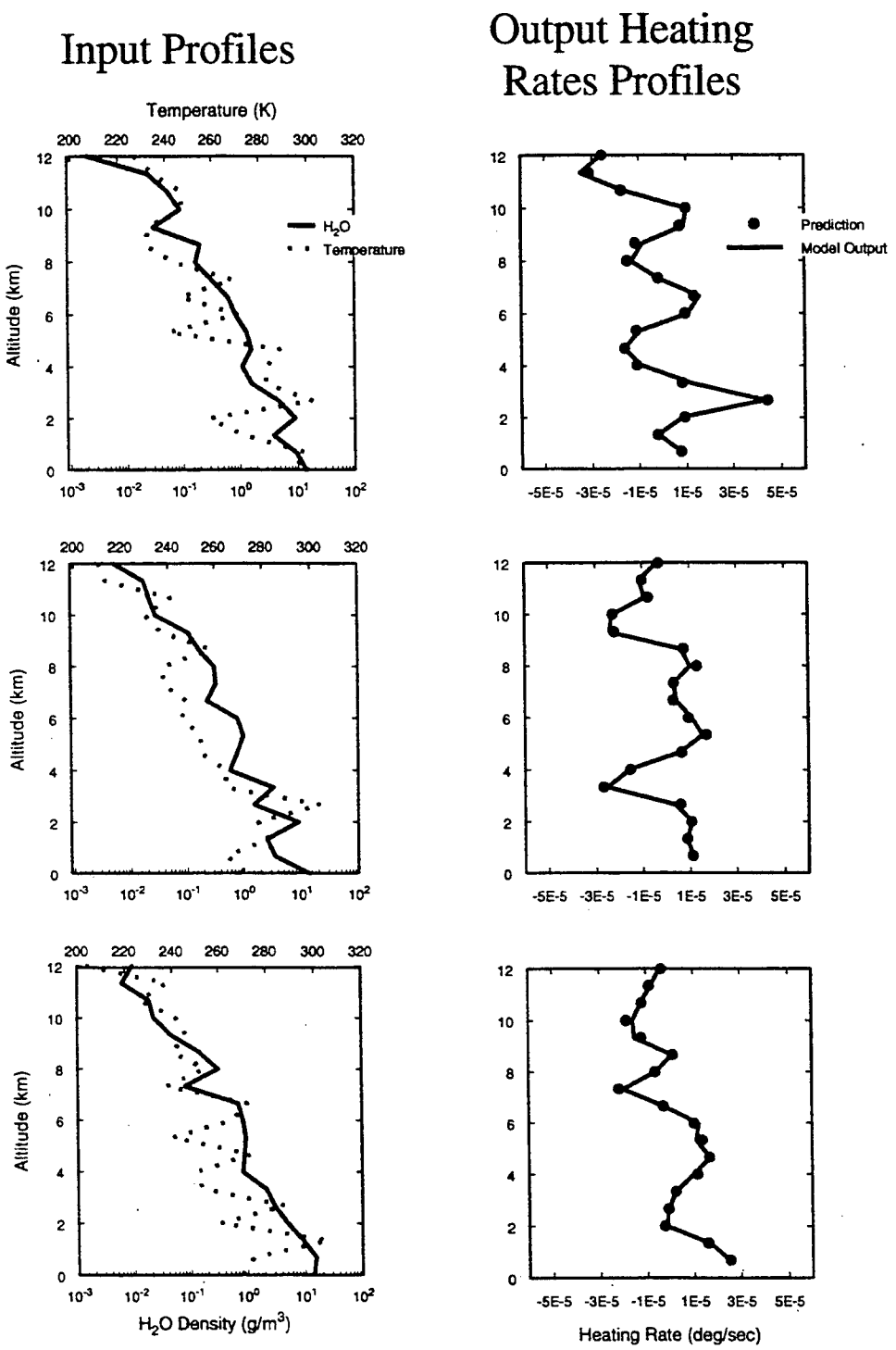

Figure 6-5. Input H_2O and temperature profiles from three of the Monte Carlo generated input sets (left) and the corresponding heating rate (right) calculated with the RTM (lines) and the FEOM(symbols).

Runtime.

The runtime was assessed by timing the execution time for RTM and FEOM calculations for 1000 input sets. The RTM required 0.48 seconds per calculation and the FEOM required 0.11 milliseconds per calculation. Thus the FEOM provides heating rate predictions 10^3 times faster than the RTM, with the same output fidelity.

6.3.1.5 Summary and Recommendations. This section described the successfully conversion of a prototype of the Radiative Transfer Module from RAMS TO A Fully Equivalent Operational Model. The *resulting* FEOM *operates 10^3 times faster* than the RTM while producing virtually identical output. Though this proof of concept was limited to clear air cases, we anticipate similar quality results and a comparable reduction in computational speed upon the inclusion of clouds and particles.

The demonstrated ability to calculated heating rates 10^3 times faster, while maintaining accurate results, could have a tremendous impact on both RAMS prediction fidelity and runtime. By completing the FEOM development and replacing the existing RTM with a FEOM, the *fidelity of* RAMS *would be improved through:*

- Improved temporal resolution of the heating rates, since the FEOM could be called on every time step instead of every 10 to 30 steps
- Improved spatial resolution of the heating rates since the FEOM could be called for every grid column instead of a small sample

Additionally, it is estimated that the *overall runtime of RAMS could be reduced by up to one third* since the computational burden of the RTM would be replaced with the ultra-fast and accurate FEOM.

In parallel with the RTM FEOM development should be the development of a FEOM for the microphysics module. This module is also very computationally intensive, and like the RTM, takes about a third of the total RAMS CPU time. There are even cases when the microphysics module has been left out of a RAMS simulation to save CPU time. We anticipate that the output of the microphysics module could be accurately predicted with similar 10^3 savings in computational time. *The impact of a microphysics FEOM would be both increased RAMS prediction fidelity and reduced run times.*

To provide DSWA with the best tools to make discussions with, we recommend:

1) Incorporating clouds and particles (rain, snow, hail, etc.) into the RTM FEOM
2) Developing logic to piece together varying vertical resolution FEOMs thus allowing user defined vertical layer structuring
3) Implementing the completed RTM FEOM into RAMS
4) Testing of the FEOM- RAMS
5) Application of FEOM to the cloud microphysics module

6.3.2 Improvements To Numerical Schemes.

6.3.2.1 Exploration of a New Scheme for Computation of Gradients. Determination of horizontal gradients in a terrain-following coordinate system has always been problematic, whether the vertical coordinate is height or pressure. All terrain-following coordinate models have this problem. NCEP's ETA model was devised because of the problem (although that type of coordinate has it's own limitations). In a signa-z coordinate model such as RAMS , the problem becomes most severe when the vertical grid spacing is small relative to the horizontal grid spacing in the presence of steep topography. If the ratio of the change in topography in one grid space divided by the minimum vetical grid spacing becomes too large (in the range of 4-5), numerical truncation can occur which can lead to non-physical results at those grid pints. Currently, in order to rectify the error in a model simulation, the following methods can be used:

- Smooth the topography so that the change of height from one grid space to the next is reduced
- Increase the vertical grid spacing
- Increase the horizontal grid resolution

In most instances, these methods are usually undesirable. Therefore, we investigated a technique to improve the accuracy of the horizontal gradients.

The determination of a horizontal gradient in a traditional terrain-following coordinate system is done by looking at the gradient along a 'sigma' or terrain following surface, and then decomposing the result into vertical and horizontal parts. This is in contrast to taking a pure Cartesian or horizontal gradient that is determined by interpolating surrounding values to the same height. When the vertical resolution is relatively coarse, the sigma gradient and the Cartesian gradient give similar results. However, when the vertical resolution increases, the Cartesian gradient in the presence of steep topography crosses several sigma surfaces and this gradient then becomes different and more accurate than a gradient determined along a sigma surface.

We have been working on a solution to this problem by specifying horizontal diffusion as a tendency that results from a 3-point smoothing operation along a Cartesian surface. This eliminates the need to determine terrain-following horizontal gradients (at least in the diffusion scheme) and will allow for the specification of the vertical resolution without regards to the horizontal resolution or topography steepness. The new code has been implemented into version 4a of RAMS, but it still needs additional testing to see how well it works in a general situation. There is also some evidence we have recently discovered that indicates similar modifications may have to be made to the advective terms and the pressure gradient term.

SECTION 7
TEST SUPPORT

7.1 INTRODUCTION.

The Hazard Assessment System for Consequence Analysis (HASCAL) is part of the Hazard Prediction and Assessment Capability (HPAC). The objective of HASCAL is to provide an automated collateral effects prediction and tracking tool for weapons of mass destruction (WMD). RAMS forecast data is one source of meteorological data available to this system. There were two main focuses of our efforts in support of HPAC. The first was to make RAMS easier to use and implement, and the second was to integrate and test RAMS' meteorological predictions with the hazardous material dispersion code (SCIPUFF) under development by DSWA. The meteorological support provided during these demonstration tests was essentially operational support for the test staff. Little meteorological data was available to validate predictions. Often the only validation was matching visually observed plume motion or deposition samples collected from the plume. This section documents the support provided and provides samples of the predicted dispersion patterns.

To test and integrate RAMS with the hazardous material dispersion codes, RAMS was used to support counterproliferation explosive testing at White Sands Missile Range (WSMR). This testing was part of the overall Counterproliferation (CP) Advanced Concept Technology Demonstration (ACTD) of which HPAC is a key element. We supported tests in the Dipole Orbit (DO), Dipole East (DE) and Dipole Tiger (DT) test series (Bradley et. al, 1996). The model interfaces to the dispersion model SCIPUFF (Sykes et. al, 1996) were refined and evaluated based on the experience gained during the support of these explosive tests. While the objectives of these test series varied, they all resulted in releases of chemical or pseudo-biological materials as a result of an explosion. Predicting the dispersion of these materials in the complex terrain associated with WSMR was a challenging task.

While the specific support plan for each test varied, the general plan did not. Initially, relatively coarse (10 km grid spacing) forecasts were produced up to 72 hours prior to the expected event. This was followed by more finely resolved forecasts (3.3 km grid spacing) for shorter periods prior to the expected event. This series of forecasts supported planning meetings that lead up to the test event. In addition, a very fine 1:1 km grid was imbedded in the 3.3 km grid for post test analysis if required, and for some backup runs made with an experimental parallel version of RAMS. The pretest forecasts were usually accomplished on an IBM RS 6000/590 located at the test site. Backup forecasts were also made on a similar workstation located at DSWA. Standard weather observations, local weather observations, and regional forecasts were used to initialize the RAMS forecasts. Figure 7-1 depicts the weather data network supporting the WSMR tests. The large round dots are National Weather Service observations sites. The "plus signs" indicate the WSMR surface observation system. These observations were used along with the gridded fields from a regional National Center for Environmental Prediction (NCEP) model (predominately ETA) to produce the initial gridded fields RAMS requires. The regional model also provides the time dependent boundary conditions.

The nested grid capability in RAMS was used to provide multiple levels of resolution. The "2 grid" forecasts used a 40 km resolution grid with a nested 10 km grid. The "3 grid" nested an additional 3.3 km resolution grid within the 10 km grid. The grid structure for the pretest forecasts is shown in Figure 7-2. Run times on the IBM RS 6000/590 were .13 times real time for the "2 grid" and .31 time real time for the "3 grid". Thus a 12-hour "3 grid" forecast would take about 4 hours to complete.

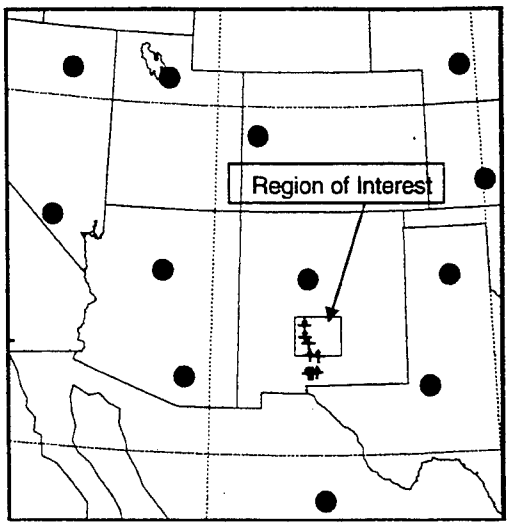

Figure 7-1. Weather Data Network

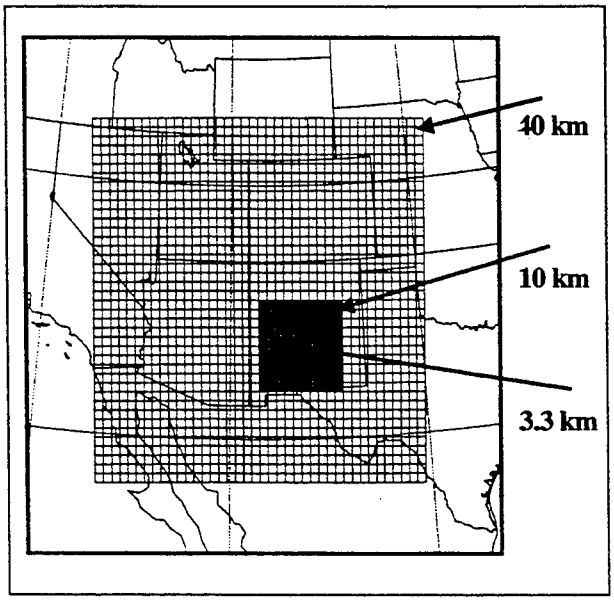

Figure 7-2. Grid Locations.

7.2 TEST SUPPORT.

As noted above test support varied from test to test depending on whether a dry run was scheduled or the test was delayed. These circumstances resulted in the complete or partial repeats of the test cycle. Current surface observations as well as gridded model and forecast analyses (ETA model for forecast up to 48 hours and MRF for forecasts of 60 or 72 hours) from NCEP's ftp server, were used to initialize

RAMS and prepare boundary conditions for forecasts ranging in length from 12 hours to 72 hours. In addition, when available, local observations from surface stations, a profiler network, and rawinsondes were included in the initial analyses. For simulations greater than 24 hours, RAMS was run with 2 grids. The second grid with grid spacing of 10 km was nested within the first grid with grid spacing of 40 km. Simulations of 24 hours or less allowed the use of a further nested third grid with a grid spacing of 3.3 km centered over the test site. Figure 7-3 shows the "normal" experiment time line. Table 7-1 provides a summary of the tests supported and forecasts produced.

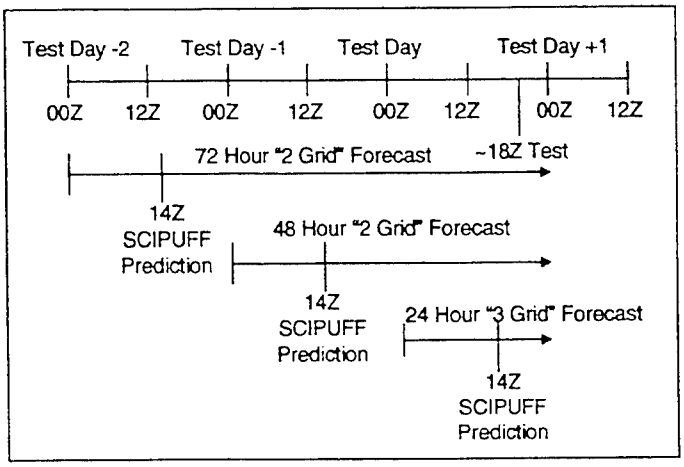

Figure 7-3. Forecast Timelines.

Table 7-1. Demonstration tests supported and forecasts produced.

Experiment Initial Date time [Z]	Simulation period [h] - No. grids	Experiment Initial Date time [Z]	Simulation period [h] - No. grids
DO-1 (3 Dec Shot)	Post test predictions only	DE-159 (20 July Shot)	
		16jul00	72 - 2 grid
DO-4 (9 April Shot)		17jul00	72 - 2 grid
5apr00	24 - 3 grid	18jul00	48 - 2 grid
5apr12	12 - 3 grid	19jul00	72 - 2 grid
7apr00	72 - 2 grid	19jul12	60 - 2 grid
8apr00	48 - 2 grid	20jul00	24 - 3 grid
8apr16	8 - 3 grid		
9apr00	24 - 3 grid	DO-3 (10 Dec Shot)	
9apr12	12 - 3 grid	9dec00	48 – 2 grid
		10dec00	12 – 3 grid and 48 – 2 grid

Table 7-1. Demonstration tests supported and forecasts produced (Continued).

Experiment Initial Date time [Z]	Simulation period [h] No. grids	Experiment Initial Date time [Z]	Simulation period [h] No. grids
DO-5 (No Shot)			
23apr00	72 - 2 grid	DO-6 (6 Feb Shot)	
24apr00	36 - 2 grid	4feb00	72 – 3 grid
25apr00	48 - 2 grid	5feb00	72 –3 grid
		6feb00	48 – 3 grid
DO-5b (11 June Shot)			
9jun12	48 - 2 grid	DT-1 (17 April Shot)	
10jun00	24 - 3 grid	15apr00	Hardware error
10jun12	36 - 2 grid	16apr00	48 – 2 grid
10jun12	24 - 3 grid	17apr00	24 – 3 grid
DE-159 (20 July Shot)		DT-2 (15 May Shot)	
16jul00	72 - 2 grid	13may00	48 – 2 grid
17jul00	72 - 2 grid	14may00	48 – 2 grid
18jul00	48 - 2 grid	15may00	24 – 3 grid
19jul00	72 - 2 grid		
19jul12	60 - 2 grid		
20jul00	24 - 3 grid		

7.2.1. Interface Development.

Enhanced interfaces were developed between SCIPUFF and RAMS. The SCIPUFF model now can run with an estimate of the surface heat flux and/or turbulent kinetic energy and the boundary layer height. These quantities are computed in RAMS. As an initial test of the impact of using RAMS predicted fields, two dimension fields of surface heat flux and boundary layer height were used. SCIPUFF was run using the predicted winds and its normal assumptions, and compared to the calculation using the additional information. The SCIPUFF predictions using the boundary layer information from RAMS matched the observed test data better. This was especially true in cases like Dipole East 159 where an observed shear layer significantly affected the predicted dispersion pattern. The default boundary layer height computed within SCIPUFF was higher than this layer causing the dispersion model to mix the plume below this height, effectively destroying the effect of the shear layer. The ability to input the heat flux and boundary layer height when a sophisticated model like RAMS is used is now a standard SCIPUFF option. The results depicted below all use this option. As noted above, the initial transfer of data from RAMS to SCIPUFF used a gridded data field option within SCIPUFF (the "MEDOC" option). A second method of transferring data involves the use of "posts". These "posts" are vertical profiles taken at a point within the grid. SCIPUFF can be used to predict the dispersion using these data posts. The use of posts allows the meteorological model to be run at one location and the dispersion model at a second location with a minimum of data transferred. (A gridded data set is actually an array of posts.) The post option in SCIPUFF also allows the boundary layer and heat flux to be specified.

7.2.2 Dipole Orbit 1.

Dipole Orbit 1 (DO1) occurred in early December 1995. We did not start providing meteorological support to the HPAC program until April 1996. However, DO1 was the first event we computed using RAMS. We initially attempted to use the data (surface observations, rawinsonde data, and gridded analysis) from the National Center for Atmospheric Research (NCAR) archives. The resulting forecasts did not match the observations at the test site. Eventually we were able to obtain the forecast output of NCEP's MRF model for the test period to replace the NCAR gridded analysis. This resulted in wind and dispersion patterns that more closely corresponded to those observed.

The best simulation resulted from a series of model runs. Initially, a 24-hour 3-grid simulation was run starting at 0Z on 3 December with a smallest grid spacing of 3.3 km. Then, the model was restarted at 12Z and a fourth grid with a smallest grid spacing of 1.1 km was added. Available meteorological was assimilated at this time. Figure 7-4 depicts the surface deposition of a simulated BG agent 5 hours after the explosion. The terrain contours are shown in this figure. Mockingbird Gap is located between the hill at top center and the ridge is near midway point on the left. As can be seen, the plume was simulated to pass through the Mockingbird Gap and continue on a south-southeast trajectory. To better reconcile the plume trajectory, another four-grid run was re-initialized at 18Z with available meteorological data. Figure 7-5 shows the modified dispersion pattern with reinitialization. Only the roads are shown in this figure. This run captured the southeast trajectory of the tail of the plume, but the initial trajectory was too far to the east. This may be explained by noting that SCIPUFF used hourly data starting from 19Z from the re-initialized run, so that the trajectory starting from 18:45Z extrapolated the model fields from 19Z and later times. It is then possible that if model results were ingested into SCIPUFF starting at shot time, the initial trajectory would be more favorable.

The SCIPUFF dispersion calculation for Figure 7-5 was initiated using 13 posts around the release point. The results reproduce a similar dispersion pattern computed using the gridded MEDOC format.

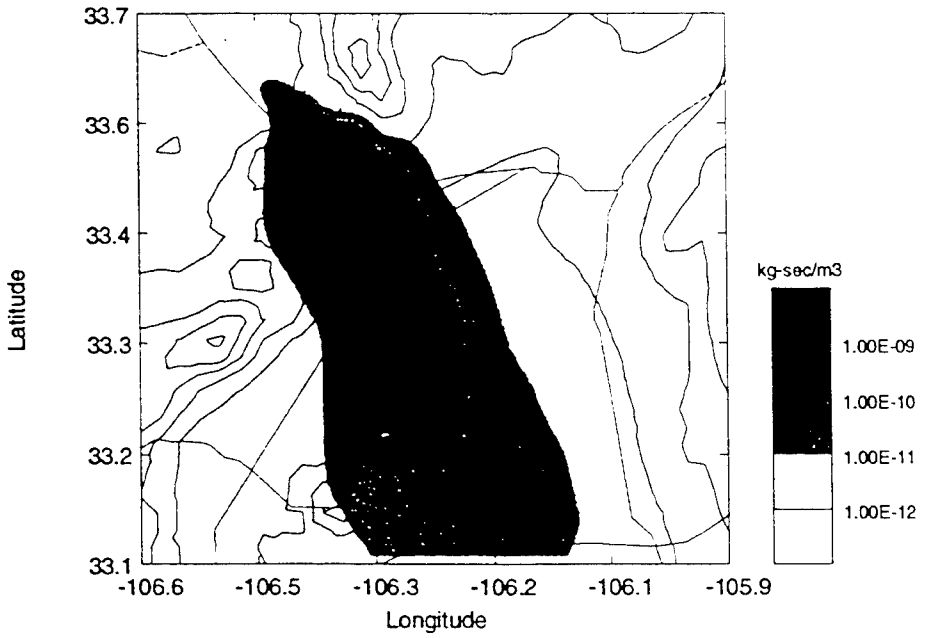

Figure 7-4. DO1 Four grid forecast at 5 hours.

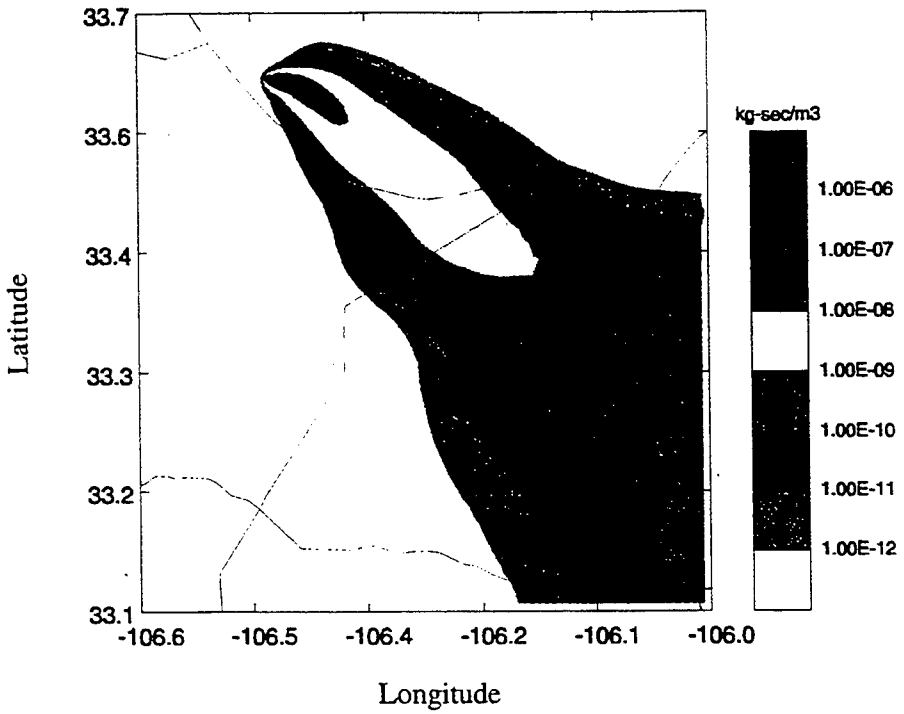

Figure 7-5. DO1 Four Grid Forecast with reinitialization

7.2.3 Dipole Orbit 4.

The first field test supported at WSMR was Dipole Orbit 4 (DO4), April 4 – 9, 1996. During this test, we installed RAMS on DSWA's IBM workstation model 590. All forecasts were available when needed. Data from the 3.3 km fine grid were used to successfully drive the SCIPUFF dispersion model. Good agreement between forecast and observation data was obtained in most cases. Time dependent boundary conditions were obtained from NCEP's ETA model for up to 48 hours and the MRF model for 60 and 72 hours. The fields predicted by MRF for 72 hours did not match those subsequently observed. They resulted in incorrect time dependent boundary conditions that were reflected in the RAMS predictions. Shorter forecasts made later allowed the use of more realistic boundary conditions. The capability of starting a RAMS forecast from previous analysis files and current WSMR data was also demonstrated during this test.

7.2.4 Dipole Orbit 6.

The test supported at WSMR, April 22 - 23, essentially duplicated the first, except the capability to include the rawinsonde data available at WSMR in the analysis was included. This test also demonstrated the ability to produce the forecast using RAMS remotely. Once the revised code had been installed and tested, we departed the site and produced the required forecasts remotely from our office in Fort Collins, Colorado.

7.2.5 Dipole Orbit 5 and 5b.

Nominal forecast support provided for the first scheduled event and the actual test event.

7.2.6 Dipole East 159.

This was the most challenging test supported. The winds were relatively light and there was a complex flow pattern observed with a shear layer approximately 6 hours prior to the test. Although there were data from balloon soundings, surface mesonet stations, mobile profiler soundings, and lidar, the data were not on a consistent enough temporal and spatial scale to fully understand the flow fields during DE-159. Unfortunately, this made model verification difficult. Although there were few actual observations against which the code could be checked, the plume tracking data compared to the RAMS-SCIPUFF predictions indicated more study was required. Figure 7-6 depicts the surface dispersion of SF6 5 hours after the explosion. Sampler data indicate that at least a portion of the plume went north and crossed highway 380 (the horizontal road north of the release point-see Figure 7-6). Application of the improved interface that used the RAMS boundary layer height resulted in flow that crossed this highway. A number of parametric runs were made to understand the reasons for the forecast results. The issue concerned the correct surface moisture. The model had made good predictions in the past at this site, but dry desert conditions were applicable for these tests. For DE159, there was rain in the area, but not necessarily at the test site, prior to the release. These wet conditions can modify the dynamics and thermodynamics and might affect the predicted results. Sensitivity simulations included allowing a moister surface layer, which lowered surface temperatures, and forcing a zero albedo, which had the effect of minimally heating the lowest model level. Compared to the limited observations, it appears that the moister model run produced superior results, moving the plume northward over Rt. 380. Increasing the surface heat flux reduced the amount of northerly flow and reasonable desert values eliminated it entirely.

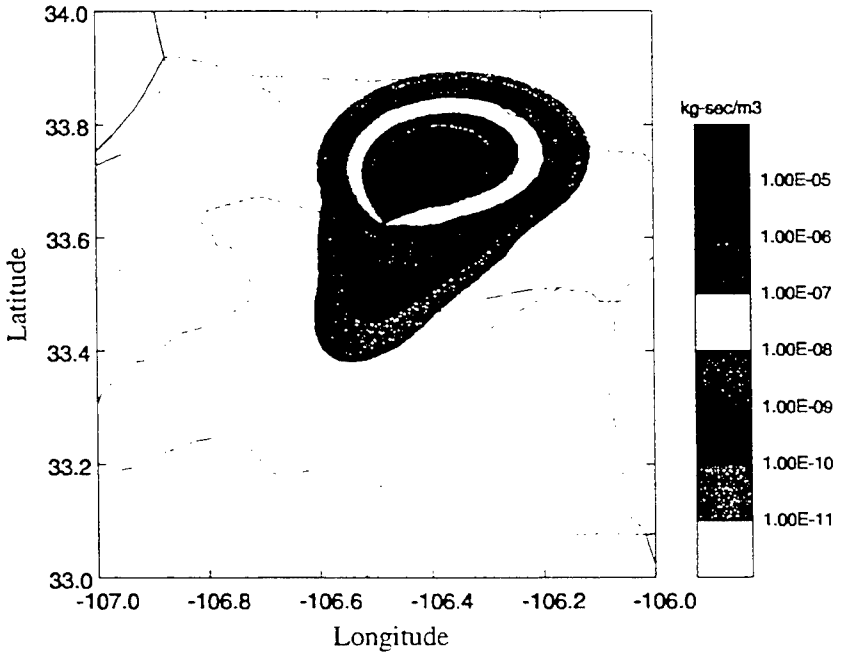

Figure 7-6. DE159 dispersion at 5 hours.

The low level atmospheric structure observed in DE 159 brought into focus a problem common to models using terrain following coordinate systems. This was discussed in Section 6.3.2.1.

7.2.7 Dipole Orbit 3.

The support for Dipole Orbit 3 was similar to the support provided for the other tests. A preliminary version of the new Graphical User Interface (GUI) was installed just prior to this test and user reaction evaluated. The GUI was determined to be a great improvement over the previous interface.

7.2.8 Dipole Orbit 6.

On site support was not provided for Dipole Orbit (DO6). The test staff at WSMR ran RAMS using the improved GUI for the experiment using mostly two grids, while the parallel version of RAMS was run at MRC for three grids with forecasts up to 72 hours. Due to the nature of the synoptic weather, it was decided to expand the RAMS coarse grid to better simulate the evolution of a large closed low near Nevada that was too close to the northern and western boundary of the original grid. Although the evolution of the upper air pattern was far superior in the expanded grid, simulated near-surface conditions were similar to those simulated with the smaller grid.

7.2.9 Dipole Tiger 1.

Support for Dipole Tiger 1 (DT-1) was provided by the DSWA test staff at WSMR with backup forecasts on the workstation at DSWA. A timely 24 hour forecast was not produced at the test site due to a computer malfunction that occurred after forecast initiation and the staff's departure for the night. The calculation was restarted the next morning after the problem had been corrected but insufficient time remained prior to the test event to produce the forecast. Forecast results were good.

7.2.10 Dipole Tiger 2.

The planned support configuration was the same as DT-1 with the primary forecast produce by the staff at WSMR and backup forecast support from the workstation at DSWA. The improved GUI allowed the DSWA WSMR test staff to run the forecast remotely, demonstrating its ease of use.

REFERENCES

Arakawa, A. and W.H. Schubert, *Interaction of a Cumulus Cloud Ensemble with the Large Scale Environment*, (Part I) Atmos. Sci., 31, 674-701, 1974 (UNCLASSIFIED).

Avissar, R. and R.A. Pielke, *A Parameterization of Heterogeneous Land Surfaces for Atmospheric Numerical Models and Its Impact on Regional Meteorology*, Mon. Wea. Rev., 117, 2113-2136, 1989 (UNCLASSIFIED).

Bames, S.L., *Mesoscale Objective Map Analysis Using Weighted Time Series Observations*, NSSL, Tech Memo NSSL-62, 1973 (UNCLASSIFIED).

Bauer, B.L., C.J. Tremback, and T. Myers, *Software User's Manual for the Regional Atmospheric Modeling System (RAMS)*, Mission Research Corp., Huntsville AL, MRC-HSV-R-97-004 (Version 1), 1997 (UNCLASSIFIED).

Bauer, B.L., T. Myers, R. Stagat, and C. Tremback, *Benchmark Report Theater Forecast Model Selection*, Mission Research Corp., Huntsville AL, 1995 (UNCLASSIFIED).

Bequelin, A., J. Dongarra, G.A. Geist, R. Manchek, and V. Sunderam, *A User's Guide to PVM-Parallel Virtual Machine*, ORNL, Knoxville TN, Tech Rpt ORNL/TM-11826, 1991 (UNCLASSIFIED).

Bradley, S., D. Bacon, B. Bauer, R. Fry, J. Hodge, A.J. Kuehn, T. Mazzola, J. McGahan, B. Morris, D. Myers, R. Newell, R. Ross, A. Sjoreen, T. Smith, J. Sontowski, D. Srinavasa, I. Sykes, L. Wittwer, and B. Worley, *Initial Verification and Validation of HPAC 1.3*, Logicon, Arlington VA, LRDA-TR-211-6261-3103-001, 1996 (UNCLASSIFIED).

Busch, N., W. Klug, R. Pearce, and P. White, *Comments on Statistical Results of Mesoscale Modeling of the Atmosphere*, Meteor. Mono., Amer. Meteor. Soc., 25, 155-156, 1994 (UNCLASSIFIED).

Businger, J.A., J.C. Wyngaard, Y. Izumi, and E.F. Bradley, *Flux-Profile Relationship in the Atmosphere Surface Layer*, J. Atmos. Sci., 28, 181-189, 1971 (UNCLASSIFIED).

Chen, S. and W.R. Cotton, *The Sensitivity of a Simulated Extratropical Mesoscale Convective System to Long Wave Radiation and Ice-Phase Microphysics*, J. Atmos. Sci., 45, 3897-3910, 1988 (UNCLASSIFIED).

Clark, T.L. and R.D. Farley, *Severe Downslope Windstorm Calculations in Two and Three Spatial Dimensions Using Anelastic Interactive Grid Nesting: A Possible Mechanism for Gustiness*, J. Atmos. Sci., 41, 329-350, 1984 (UNCLASSIFIED).

Clark, T.L. and W.D. Hall, *Multi-Domain Simulations of the Time Dependent Navier-Stokes Equations: Benchmark Error Analysis of Some Nesting Procedures*, J.Comp. Phys., 92, 456-481, 1991 (UNCLASSIFIED).

Combat Weather Systems Technical Alternatives Study, Dynamics Research Corp., Andover MA, F49650-91-D-0011, 1993 (UNCLASSIFIED).

Combat Weather Systems Technical Alternative Study Interim Report, HQ AFMC, ESC, Hanscom AFB MA, 30 Jun 93 (UNCLASSIFIED).

Conversion of Goddard Soil Types to Equivalent Clapp and Hornberger Codes for Use in RWM, AFGWC, Offutt AFB NE, p 12 fm Draft AFGWC/TN-93/XXX, 1993 (UNCLASSIFIED).

Converting Matthews' Vegetation Types to Vegetation Types Used by AFGWC, AFGWC, Offutt AFB NE (UNCLASSIFIED).

Deardoff, J.W., *Parameterization of the Planetary Boundary Layer for Use in General Circulation Models*, Mon. Wea. Rev., 100, 93-106, 192 (UNCLASSIFIED).

Dudhia, J., *Numerical Study of Convection Observed During the Winter Monsoon Experiment Using a Mesoscale Two-Dimensional Model*, J. Atmos. Sci., 46, 3077-3107, 1989 (UNCLASSIFIED).

Englehart, L.M., R.L. Hughes, and K.J. Lunn, *Functional Description AFGWS/SYSM*, AFGWC, Offutt AFB NE, 1993 (UNCLASSIFIED).

Gal-Chen, T. and R.C.J. Somerville, *On the Use of a Coordinate Transformation for the Solution of the Navier-Stokes Equations*, J. Comput. Phys., 17, 209-228, 1975 (UNCLASSIFIED).

Gill, D.O., *A User's Guide to the Penn State/NCAR Mesoscale Modeling System*, NCAR, Boulder CO, NCAR Tech Note 381+IA, 1992 (UNCLASSIFIED).

Grell, G.A., J. Dudhia, and D.R. Stauffer, *A Description of the Fifth Generation Penn State/NCAR Mesoscale Model.* NCAR, Boulder CO, NCAR Tech Note 398+IA, 1993 (UNCLASSIFIED).

Grell, G.A., Y.-H. Kuo, and R. Pasch, *Semi-Prognostic Tests of Cumulus Parameterization Schemes in the Middle Latitudes*, Mon. Wea. Rev., 119, 5-31, 1991 (UNCLASSIFIED).

Haack, James, *Computational Characteristics of the NCAR CCM1 Model*, CCM Core Group, NCAR, Boulder CO, Jan 93 (UNCLASSIFIED).

Haagenson, P.L., J. Dudhia, D.R. Stauffer, and G. Grell, *The Penn State/NCAR Mesoscale Model (MM5) Source Code Documentation*, NCAR, Boulder CO, NCAR Tech Note 392 (UNCLASSIFIED).

Hodur, R.M., *Evaluation of a Regional Model with an Update Cycle*, Mon. Wea. Rev., 115, 2707-2718, 1987 (UNCLASSIFIED).

Klemp, J.B. and D.K. Lilly, *Numerical Simulation of Hydrostatic Mountain Waves*, J. Atmos. Sci., 35, 78-107, 1978 (UNCLASSIFIED).

Klemp, J.B. and R.B. Wilhelmson, *The Simulation of Three-Dimensional Convective Storm Dynamics*, J. Atmos Sci., 35, 1070-1096, 1978 (UNCLASSIFIED).

Kopp, T.J., T.J. Neu, and J.M. Lanicci, *A Description of Air Force Global Weather Central's Surface Temperature Model*, 10th Conf. on Numerical Weather Prediction, Amer. Meteor. Soc., Boston MA, 1994 (UNCLASSIFIED).

Kuo, H.-L., *Further Studies of the Parameterization of the Effect of Cumulus Convection on Large Scale Flow*, J.Atmos. Sci., 31, 1232-1240,1974 (UNCLASSIFIED).

Kuo, H.-L., *Further Studies of the Parameterization of the Influence of Cumulus Convection on Large-Scale Flow*, J.Atmos. Sci., 31, 1232-1240, 1974 (UNCLASSIFIED).

Louis, J.F., *A Parametric Model of Vertical Eddy Fluxes in the Atmosphere*, Boundary-Layer Meteorol., 17, 187-202, 1979 (UNCLASSIFIED).

Madala, et.al., *Description of the Naval Research Laboratory Limited Area Dynamical Weather Prediction Model*, NRL, Monterey CA, NRL Memo Rpt 5992, 1987 (UNCLASSIFIED).

Mahrer, Y. and R.A. Pielke, *A Numerical Study of the Air Flow Over Irregular Terrain*, Contrib. Atmos Phys., 50, 98-113, 1977 (UNCLASSIFIED).

Manning, K.W. and Haagenson, P.L., *Data Ingest and Objective Analysis Got the PSU/NCAR Modeling System: Programs DATAGRID AND RAWINS*, NCAR, Boulder CO, NCAR Tech Note 376+IA, 1992 (UNCLASSIFIED).

Mathor, M., *A Quasi-Lagrangian Regional Model Designed for Operational Weather Predictions*, Mon. Wea. Rev., 111, 2087-2098, 1983 (UNCLASSIFIED).

Matthews, E., *Vegetation, Land Use and Seasonal Albedo Data Sets: Documentation of Archived Data Tape*, NASA Goddard Space Flight Center NY, NASA Tech Note, 1984 (UNCLASSIFIED).

Mesinger, F. and A. Arakawa, *Numerical Methods Used in Atmospheric Models*, WMO/ICSU Joint Organizing Committee, GARP Pub. Series, No. 14, 1976 (UNCLASSIFIED).

Moore, B.D., et.al., *A Worldwide Near-Real Time Diagnostic Agrometeorological Model*, 20th Conf. on Agricultural and Forest Meteorology, Amer. Meteor. Soc., Boston MA, 1991 (UNCLASSIFIED).

Operational Requirements Document (ORD) - Combat Weather System, HQ USAF, AFXOWX, USAF 211-89-I/III (UNCLASSIFIED).

Orlanski, I., *A Simple Boundary Condition for Unbounded Hyperbolic Flows*, J. Comput. Phys., 21, 251-269, 1976 (UNCLASSIFIED).

Pielke, R. and R. Pearce, Ed., *Mesoscale Modeling of the Atmosphere*, Meteor. Mono., Amer. Meteor. Soc., Vol. 25, 1994 (UNCLASSIFIED).

Relocatable Window Analysis Model Maintenance Model, File Structures, AFGWC, Offutt AFB NE, 1990 (UNCLASSIFIED).

Software User's Manual for the Navy Operational Regional Atmospheric Prediction System (NORAPS), NRL, Monterey CA, 1994 (UNCLASSIFIED).

Statement of Need (SON) - Tactical Forecast Systems (TFS), HQ USAF, USAF 212-89 (UNCLASSIFIED).

Statement of Operational Need (SON) - Tactical Weather Observing Systems (TWOS), HQ USAF, USAF-211-89 (UNCLASSIFIED).

Staub, B. and C. Rosenzweig, *Global Digital Data Sets of Soil Type, Soil Texture, Surface Slope, and Other Properties: Documentation of Archived Data Tape,* NASA Goddard Space Flight Center NY, NASA Tech Memo 100685, 1987 (UNCLASSIFIED).

Sykes, R.I., S.F. Parker, D.S. Henn, and R.S. Gabruk, *PC-SCIPUFF*, Princeton NJ, DNA-TR-96-27 (Version 0.2), 1996 (UNCLASSIFIED).

TFM Requirements, Letter, DNA, 21 Jun 94 (UNCLASSIFIED).

TFM Weather System Model Selection Program Plan: Appendix A – TFM Statement of Work, HQ DNA, Alexandria VA, (Version 1.0), Aug 94 (UNCLASSIFIED).

Tremback, C.J., *Numerical Simulation of a Mesoscale Convective Complex: Model Development and Numerical Results*, Colorado State Univ., PhD. Dissertation, 1990 (UNCLASSIFIED)

Tremback, C.J. and R. Kessler, *A Surface Temperature and Moisture Parameterization for Use in Mesoscale Numerical Models*, Preprints – 7th Conf. on Numerical Weather Prediction (17-20 Jun 85), Montreal Canada, AMS, 1985 (UNCLASSIFIED).

Tremback, C.J., and R.L. Walko, *RAMS Technical Manual (Draft)*, Mission Research Corp., ASTeR Div., Ft Collins CO, 1994 (UNCLASSIFIED).

Tremback, C.J., R.L. Walko, and R.F.A. Hertenstein, *RAMS Version 3 User's Guide*, Mission Research Corp., ASTeR Div., Ft Collins CO, 1994 (UNCLASSIFIED).

Tripoli, G.J. and W.R. Cotton, *The Colorado State University Three-Dimensional Cloud/Mesoscale Model, Part I – General Theoretical Framework and Sensitivity Experiments*, J. de Rech. Atmos., 16, 185-195, 1982 (UNCLASSIFIED).

Weather Support for Army Tactical Operations, Depts. of Army and Air Force, FM 34-81 / AFM 105-04, Aug 89 (UNCLASSIFIED).

Zhang, D.-L. and R.A. Anthes, *A High-Resolution Model of the Planetary Boundary Layer – Sensitivity Tests and Comparisons with SESAME-79 Data*, J. Appl. Meteor., 21, 1594-1609, 1982 (UNCLASSIFIED).

DISTRIBUTION LIST

DEPARTMENT OF DEFENSE

DEFENSE TECHNICAL INFORMATION CENTER
8725 JOHN J KINGMAN RD., SUITE 0944
FORT BELVOIR, VA 22060-6218
ATTN: DTIC/OCP

DEFENSE THREAT REDUCTION AGENCY
6801 TELEGRAPH ROAD
ALEXANDRIA, VA 22310-3398
ATTN: CPW, MAJ T SMITH
ATTN: CPWCT
ATTN: CPWE, DAVID MYERS
ATTN: CPWE, MAJ WELLS
ATTN: CPWT, L WITTWER

DEFENSE THREAT REDUCTION AGENCY
ALBUQUERQUE OPERATIONS
1680 TEXAS ST. SE
KIRTLAND AFB, NM 87117-5669
ATTN: CPT-D G BALADI
ATTN: CPTO
ATTN: CPX, LTC D R LITTLE

JOINT CHIEFS OF STAFF
DIRECTOR FOR FORCE STRUCTURE,
RESOURCES & ASSESSMENT (J-8)
8000 DEFENSE PENTAGON
WASHINGTON, DC 20318-8000
ATTN: J8 WAR FIGHTING DIV

DEPARTMENT OF DEFENSE CONTRACTORS

AEROSPACE CORP
P O BOX 92957
LOS ANGELES, CA 90009
ATTN: DR MIKE PLONSKI, MS M8/719

APPLIED RESEARCH ASSOCIATES, INC.
4300 SAN MATEO BLVD, NE
SUITE A220
ALBUQUERQUE, NM 87110-1260
ATTN: R NEWELL

CHARLES NEEDHAM
1424 HERTZ DR S.E.
ALBUQUERQUE, NM 87108
ATTN: C NEEDHAM

ITT INDUSTRIES
ITT SYSTEMS CORPORATION
ATTN: AODTRA/DASIAC
1680 TEXAS ST SE
KIRTLAND AFB, NM 87117-5669
ATTN: DASIAC
ATTN: DASIAC/DARE

JAYCOR
1410 SPRING HILL ROAD
SUITE 300
MCLEAN, VA 22102
ATTN: DR CYRUS P KNOWLES

LOGICON RDA
6940 S KINGS HWY
SUITE 202
ALEXANDRIA, VA 22310
ATTN: R POPE
ATTN: T MAZOLLA

MISSION RESEARCH CORP
ASTER DIVISION
2629 REDWING DRIVE, SUITE 310
FORT COLLINS, CO 80526
ATTN: CRAIG TREMBACK
ATTN: MIKE WEISSBLUTH

MISSION RESEARCH CORP
P O BOX 1257
HUNTSVILLE, AL 35807
ATTN: BRUCE BAUER

MISSION RESEARCH CORP.
6703 ODYSSEY DRIVE
SUITE 101
HUNTSVILLE, AL 35806
ATTN: BRUCE L BAUER
ATTN: JEFFREY A SHORTER
ATTN: PRECILA C IP
ATTN: THERESA CAMPBELL
ATTN: THOMAS M MYERS

PACIFIC-SIERRA RESEARCH CORP.
2901 28TH STREET
SANTA MONICA, CA 90405-2938
ATTN: H BRODE

PRINCETON UNIVERSITY
129 FRICK LAB
PRINCETON, NJ 08544
ATTN: HERSCHEL A RABITZ

SCIENCE APPLICATIONS INT'L CORP
2111 EISENHOWER AVE
SUITE 303
ALEXANDRIA, VA 22314
ATTN: J COCKAYNE

SCIENCE APPLICATIONS INTL CORP
10260 CAMPUS POINT DRIVE
SAN DIEGO, CA 92121-1578
ATTN: T JARRETT

DEPARTMENT OF DEFENSE CONTRACTORS

SCIENCE APPLICATIONS INTL CORP
1100 FIRST AVENUE
SUITE 300
KING OF PRUSSIA, PA 19406
ATTN: J SONTOWSKI

SCIENCE APPLICATIONS INTL CORP
2109 AIR PARK ROAD, SE
ALBUQUERQUE, NM 87106
ATTN: J MANSHIP

SCIENCE APPLICATIONS INTL CORP
P O BOX 1303
MCLEAN, VA 22102
ATTN: D BACON
ATTN: J MCGAGHAN

THE TITIAN CORPORATION
TITAN RESEARCH & TECHNOLOGY DIV
P O BOX 2229
PRINCETON, NJ 08543-2229
ATTN: IAN SYKES

TITAN CORPORATION (THE)
TITAN RESEARCH & TECHNOLOGY DIVSN
9410 TOPANGO CANYON BLVD
SUITE 104
CHATSWORTH, CA 91311-5771
ATTN: R ENGLAND

TRW S. I. G.
STRATEGIC SYSTEMS DIVISION
P O BOX 1310
SAN BERNARDINO, CA 92402-1310
ATTN: NORMAN LIPNER

VISIDYNE, INC.
P O BOX 1399
GOLETA, CA 93116-1399
ATTN: J DEVORE

DEPARTMENT OF ENERGY

UNIVERSITY OF CALIFORNIA
LAWRENCE LIVERMORE NATIONAL LAB
P O BOX 808
LIVERMORE, CA 94551-9900
ATTN: L-030 ALLEN KUHL

LOS ALAMOS NATIONAL LABORATORY
P O BOX 1663
LOS ALAMOS, NM 87545
ATTN: MS J514/A S MASON
ATTN: MS670 J NORMAN
ATTN: R W WHITAKER/ESS-5,MS/F665
ATTN: WX-1/B SHAFER

DEPARTMENT OF THE AIR FORCE

AF WEATHER TECHNICAL LIBRARY
151 PATTON AVE, ROOM 120
ASHEVILLE, NC 28801-5002
ATTN: KAY MARSHALL

HEADQUARTERS
AIR FORCE SPACE COMMAND
DIRECTOR OF OPERATIONS
150 VANDENBERG STREET
PETERSON AFB, CO 80914-4120
ATTN: AFSPC/DO

AIR FORCE WEATHER AGENCY/DNXM
106 PEACEKEEPER DR, SUITE 2N3
OFFUTT AFB, NE 68113-4039
ATTN: MAJ RANDY LEFEVRE

AIR UNIVERSITY LIBRARY
600 CHENNAULT CIRCLE
BLDG 1405 - ROOM 160
MAXWELL AFB, AL 36112-6424
ATTN: AUL-LSE

HQ USAF/XOWX
1490 AIR FORCE PENTAGON
WASHINGTON, DC 20330-1490
ATTN: XOWX

DEPARTMENT OF THE ARMY

DEPARTMENT OF THE ARMY
DEPUTY CHIEF OF STAFF FOR
OPERATIONS AND PLANS
PENTAGON
WASHINGTON, DC 20310-0460
ATTN: DAMO-NCZ

US ARMY RESEARCH LAB
AMSRL-SL-CS E3331
5101 HOADLEY RD
ABERDEEN PROVING GROUND, MD 21010-5423
ATTN: SLCBR-SS-T (TECH LIB)

US ARMY RESEARCH LABORATORIES
2800 POWDER MILL ROAD
ADELPHI, MD 20783-1197
ATTN: AMSRL-SL-CE
ATTN: J MARTIN
ATTN: R CIONCO

COMMANDER
WEST DESERT TEST CENTER
ATTN: STEDP-WD-M
DUGWAY, UT 84022-5000
ATTN: CHRIS BILTOFT
ATTN: JIM BOWERS

DEPARTMENT OF THE NAVY

DEPUTY CHIEF OF NAVAL OPERATIONS
(PLANS, POLICY & OPERATIONS)
2000 NAVY PENTAGON ROOM
ROOM 4E592 (N3/N5)
WASHINGTON, DC 20350-2000
ATTN: BRANCH HEAD (N514)

NAVAL RESEARCH LABORATORY
4555 OVERLOOK AVE, SW
WASHINGTON, DC 20375-5000
ATTN: CODE 5227 RESEARCH REPORT
ATTN: SIMON CHANG

COMMANDER
NAVAL SURFACE WARFARE CENTER
DAHLGREN DIVISION
17320 DAHLGREN ROAD
DAHLGREN, VA 22448-5000
ATTN: CODE BSI T. BAUER